THESIS
5
2001

This is to certify that the

dissertation entitled

Interactions of Dinuclear Transition Metal Compounds with DNA Nucleobases and Related Nitrogen Donor Ligands

presented by

Kemal V. Catalan

has been accepted towards fulfillment
of the requirements for

PhD degree in Chemistry

Major professor

Date 2/26/99

MSU is an Affirmative Action/Equal Opportunity Institution O-12771

LIBRARY
Michigan State
University

PLACE IN RETURN BOX to remove this checkout from your record.
TO AVOID FINES return on or before date due.
MAY BE RECALLED with earlier due date if requested.

DATE DUE	DATE DUE	DATE DUE

6/01 c:/CIRC/DateDue.p65-p.15

Interactions of Dinuclear Transition Metal Compounds with DNA Nucleobases and Related Nitrogen Donor Ligands

Volume I

By

Kemal V. Catalan

A Dissertation

Submitted to
Michigan State University
In partial fulfillment of the requirements
For the degree of

DOCTOR OF PHILOSPHY

Department of Chemistry

1999

The Interaction
Nucl

nuclear trans

known for th

been devoted to t

gold is the inhi

guanine bases thr

transition metal c

is attributed to

formed DNA b

thiol carboxylate

of Ru, Rh and Re

published. Rece

notes for the m

synthesis and sp

compounds with

have been perfo

indicate that the

template strand.

crystallographic

The Interactions of Dinuclear Transition metal Compounds with DNA Nucleobases and Related Nitrogen Donor Ligands

Kemal V. Catalan

Mononuclear transition metal compounds such as cisplatin, iproplatin and carboplatin are well known for their extraordinarily high carcinostatic activity. Years of research have been devoted to the elucidation of their mechanism of action. The generally accepted model is the inhibition of DNA replication by the covalent binding of two adjacent guanine bases through their respective N^7 atoms to the platinum metal center. Other transition metal compounds are known to exhibit considerable anticancer activity that is also attributed to direct metal-DNA interactions. In this vein, we are investigating the preferred DNA binding sites as well as the exact binding modes of dinuclear transition metal carboxylates of the type $M_2(O_2CR)_4$, $M_2X_4(O_2CR)_2$ and $M_2(DTolF)_2(O_2CCF_3)_2$ (M = Ru, Rh and Re; R = CH_3, CH_2CH_3, $CH_2CH_2CH_3$; DTolF = di-p-tolylformamidinate; X = halide). Recent studies in our laboratories have elucidated unprecedented bridging modes for the model nucleobases 9-ethylguanine and 9-ethyladenine. In addition, the synthesis and spectroscopic characterization of the reaction products of these metal compounds with the twelve base pair oligonucleotide, d(5'-CCT CTG GTC TCC-3'), have been performed. Other studies involving the polymerase chain reaction (PCR) indicate that the DNA replication process is inhibited by covalent metal binding to the template strand. The PCR results along with ^1H NMR spectroscopic, HPLC and X-ray crystallographic results will be presented.

Copyright
Kemal V. C
1998

Copyright by
Kemal V. Catalan
1998

LIST OF TA

LIST OF FIG

LIST OF CO

CHAPTER I

1.

2.

3.

List of F

CHAPTER I

1. Intro

2. Expe

A. P

B. S

i.

ii.

(I) M

Table of Contents

Page

LIST OF TABLES.....xi

LIST OF FIGURES.....xii

LIST OF COMPOUNDS.....xiii

CHAPTER I. INTRODUCTION.....1

1. Anticancer Activity of Cisplatin.....2

2. Dirhodium Compounds.....19

3. Reactions with Oligonucleotides.....25

List of References.....31

CHAPTER II. THE REACTIONS OF 9-ETHYLADENINE (9-EtAH) And 9-ETHYLGUANINE (9-EtGH) with $[Rh_2(DTolF)_2(CH_3CN)_6]^{2+}$.....33

1. Introduction.....34

2. Experimental Section.....40

A. Physical Measurements.....40

B. Syntheses.....41

i. Starting Materials.....41

ii. Reaction Procedures.....42

(1) Modified Preparation of $Rh_2(DTolF)_2(O_2CCF_3)_2(CH_3CN)_2$ **(1)** 42

(2) Modified Preparation of 9- Ethyladenine (9-EtAH).....42

(3) $[Rh_2(DTolF)_2(9\text{-}EtAH)_2(CH_3CN)][BF_4]_2$ **(4)**.....43

(4) NMR Scale Reaction of **(1)** with 9-EtAH.....43

(5) Preparation of $Rh_2(DTolF)_2(O_2CCH_3)_2(H_2O)$ **(6)**.....43

C. X-ray Crystallography and Structure Solution.....44

(1) $Rh_2(DTolF)_2(O_2CCF_3)_2(CH_3CN)_2$ **(1)**.....45

(2) $[Rh_2(DTolF)_2(9\text{-}EtAH)_2(CH_3CN)](BF_4)_2$ **(4)**.....46

(3) $[Rh_2(DTolF)_2(9\text{-}EtGH)_2(CH_3CN)](BF_4)_2$ **(3)**.....47

(4) $Rh_2(DTolF)_2(O_2CCH_3)_2(H_2O)$ **(6)**.....49

3. Results and Discussion.....50

A. Modified Preparation of $Rh_2(form)(O_2CCF_3)_2L_2$ **(1)**.....50

(1) Syntheses.....50

(2) Molecular Structure of **(1)**.....51

B. Reaction of $[Rh_2(DTolF)_2(CH_3CN)_6][BF_4]_2$ **(2)**

with 9-EtGH.....54

(1) Synthesis.....54

(2) Electrochemistry of **(3)**.....55

(3) Molecular Structure of **(3)**.....55

(4) ^1H NMR Spectroscopic Data of **(3)**.....62

C. Reaction of $[Rh_2(DTolF)_2(CH_3CN)_6][BF_4]_2$ **(2)** with 9-EtAH.....63

(1) Syntheses.....63

(2) Electrochemistry of **(4)**.....66

(3) ^1H NMR studies of **(4)**.....67

(4) Molecular structure of **(4)**.....71

D. Reaction of $Rh_2(DTolF)_2(O_2CCF_3)_2(CH_3CN)_2$ **(1)** with 9-EtAH.....73

(1) Synthesis.....73

(2) ^1H NMR Studies of **(5)**.....75

(3) Molecular Structure of **(5)**.....77

E. Preparation of $Rh_2(DTolF)_2(O_2CCH_3)_2(H_2O)$ **(6)**.....78

(1) Synthesis.....78

(2) Molecular Structure of **(6)**.....81

4. Conclusions.....84

5. List of References.....94

CHAPTER III. DIRHODIUM FORMAMIDINATE COMPOUNDS WITH NITROGEN CHELATES AS MIMICS FOR 9-ETHYLADENINE 96

1. Introduction.....97

2. Expe

A. P

B. S

i.

ii

(1) F

(2) F

(3) F

(4) F

(5) F

(6) F

(7) F

(8) F

C.)

(1) F

2. Experimental Section.....104

A. Physical Measurements.....104

B. Synthesis.....104

i. Starting Materials.....104

ii. Reaction Procedures.....105

(1) Preparation of $[Rh_2(DTolF)_2(bpy)(CH_3CN)_4][BF_4]_2$ **(7a, 7b)**..105

(2) Preparation of $[Rh_2(DTolF)_2(bpy)_2(CH_3CN)][BF_4]_2$ **(8)**.....106

(3) Preparation of $[Rh_2(DTolF)_2(phen)(CH_3CN)_3][BF_4]_2$ **(9)**.....107

(4) Preparation of $[Rh_2(DTolF)_2(phen)_2(CH_3CN)_2][BF_4]_2$ **(10)**.....107

(5) Preparation of the mixture of

$[Rh_2(DTolF)_2(bpy)(CH_3CN)_4][BF_4]_2$ **(7)** and

$[Rh_2(DTolF)_2(bpy)_2(CH_3CN)][BF_4]_2$ **(8)**.....107

(6) Reaction of $[Rh_2(DTolF)_2(bpy)(CH_3CN)_3][BF_4]_2$ **(7)** with 9-

ethyladenine (9-EtAH).....108

(7) Reaction of $[Rh_2(DTolF)_2(bpy)(CH_3CN)_3[BF_4]_2$ **(7)** with 9-

ethylguanine (9-EtGH).....109

(8) Reaction of $[Rh_2(DTolF)_2(bpy)_2(CH_3CN)[BF_4]_2$ **(8)**

with 9-EtAH.....109

C. X-ray Crystallography and Structure Solution.....110

(1) $[Rh_2(DTolF)_2(bpy)(CH_3CN)_3][BF_4]_2$ **(7a)**.....111

(2) $[Rh_2(DTolF)_2(bpy)(CH_3CN)_4][BF_4]_2$ **(7b)**.....112

(3) $[Rh_2(DTolF)_2(bpy)_2(CH_3CN)][BF_4]_2$ **(8a)**.....113

(4) $[Rh_2(DTolF)_2(bpy)_2(H_2O)][BF_4][BPh_4]$ **(8b)**.....114

(5) $[Rh_2(DTolF)_2(phen)(CH_3CN)_3][BF_4]_2$ **(9)**.....116

(6) $[Rh_2(DTolF)_2(phen)_2(CH_3CN)][BF_4]_2$ **(10)**.....117

3. Results and Discussion.....117

A. Reactions of $Rh_2^{II,II}$ and bpy.....117

(1) Syntheses.....117

(2) Electrochemistry of **(7)** and **(8)**.....119

(3) ^1H NMR studies of **(7)** and **(8)**.....120

(4) Molecular Structures of **(7a)** and **(7b)**.....124

(5) Molecular Structures of **(8a)** and **(8b)**.....130

B. Reactions of $Rh_2^{II,II}$ and 1,10-phenanthroline.....137

(1) Syntheses.....137

(2) Electrochemistry of **(9)** and **(10)**.....137

(3) ^1H NMR studies of **(9)** and **(10)**.....140

(4) Molecular Structures of **(9)** and **(10)**.....142

C. Reactions of **(7)**and **(8)** with 9-EtAH and 9-EtGH.....145

(1) Syntheses.....145

(2) ^1H NMR Studies of the Reaction Between (7) and 9-EtGH.....146

4. Summary.....146

5. L

Chapter I

1. In
2. E
A
B

(1

(2

(3

(4

(5)

3. Re
A.

(1)
(2)
(3)

B.

(1)
(2)
C.
(1)
D.
(1)
(2)
(3)
E.
(1) S

5. List of References.....155

Chapter IV. THE REACTIONS OF DIRHDOIUM CARBOXYLATE COMPOUNDS WITH DNA.....157
1. Introduction.....158
2. Experimental Section.....164
A. Physical Measurements.....164
B. Synthesis.....166
i. Starting Materials.....166
ii. Reaction Procedures.....167
(1) Reaction of $Rh_2(O_2CCH_3)_4(H_2O)_2$ **(11)** with 5'-pGpG-3' Dinucleotide.....167
(2) Reaction of $[Rh_2(O_2CCH_3)_2(CH_3CN)_6][BF_4]_2$ **(12)** with 5'-pGpG-3' Dinucleotide.....167
(3) Reaction of $Rh_2(DTolF)_2(O_2CCF_3)_2(H_2O)_2$ **(3)** with 5'-pGpG-3' Dinucleotide.....168
(4) Reaction of $Rh_2(O_2CCH_3)_4(H_2O)_2$ **(11)** with 5'-CCTCTGGTCTCC-3' (GG-12mer).....169
(5) Reaction of $[Rh_2(O_2CCH_3)_2(CH_3CN)_6][BF_4]_2$ **(12)** with GG-12mer.....169
3. Results and Discussion.....171
A. Reaction of $Rh_2(O_2CCH_3)_4(H_2O)_2$ **(11)** with the 5'-pGpG-3' Dinucleotide.....171
(1) Synthesis.....171
(2) HPLC Chromatography of 5'-pGpG-3'.....172
(3) ^1H NMR Spectroscopic Studies of 5'-pGpG-3' and $[Rh_2(O_2CCH_3)_2(5'\text{-pGpG-}3')(H_2O)_2$ **(13)**.....175
B. Reaction of $[Rh_2(O_2CCH_3)_2(CH_3CN)_6][BF_4]_2$ **(12)** with 5'-pGpG-3' Dinucleotide **(13)**.....181
(1) Synthesis.....181
(2) HPLC Chromatography.....181
C. Reaction of $Rh_2(DTolF)_2(O_2CCF_3)_2(H_2O)_2$ **(3)** with 5'-pGpG-3' Dinucleotide **(14)**.....184
(1) Synthesis.....184
D. Reaction of $Rh_2(O_2CCH_3)_4(H_2O)_2$ **(11)** with GG-12mer.....185
(1) Synthesis.....185
(2) HPLC Chromatography.....188
(3) ^1H NMR Spectroscopy.....188
E. $E[Rh_2(O_2CCH_3)_2(CH_3CN)_6][BF_4]_2$ **(12)** with GG-12mer.....194
(1) Synthesis.....194

(2) HPLC Chromatography....194
(3) ^{1}H NMR Spectroscopy....194

4. Summary....198
5. List of References....200
Chapter V. Inhibition of DNA Replication....202
1. Introduction....203
A. Inhibition of DNA Replication by Cisplatin....203
B. Inhibition of DNA Replication by Dirhodium Tetracarboxylates....208
2. Experimental....211
A. Synthesis....211
3. Results....212
A. Autoradiograph of the PCR Inhibition by $Rh_2(O_2CCH_3)_4(H_2O_2)$ **(11)**....212
B. Autoradiograph of the PCR Inhibition by $[Re_2(O_2CCH_2CH_3)_4][SO_4]$....219
4. Conclusions....221
5. List of References....222
Appendix....223

Table 1.1

Table 1.2

Table 1.3

Table 1.4

Table 1.5

Table 1.6

Table 2.1

Table 2.2

Table 2.3

Table 2.4

Table 2.5

Table 2.6

List of Tables

Page

Table 1.1 Comparison of A-, B-, Z-DNA.....7

Table 1.2 pKa Values for DNA Nucleobases.....12

Table 1.3 Activity of Dirhodium Compounds Against Human Oral Carcinoma KB Cells.....27

Table 1.4 Survival Studies with Swiss albino mice bearing Ehrlich ascites tumors.....28

Table 1.5 $Rh_2(O_2CEt)_4$(poly-A) against Ehrlich ascites.....29

Table 1.6 In Vivo Studies of $Rh_2(DTolF)_2(O_2CCF_3)_2(H_2O)_2$ Against Yoshida Ascites Sarcoma Cells.....30

Table 2.1 Crystallographic Data for $Rh_2(DTolF)_2(O_2CCF_3)_2(CH_3CN)$ **(1)**, $Rh_2(DTolF)_2(O_2CCH_3)_2(H_2O)$ **(6)**, $[Rh_2(DTolF)_2(9\text{-}EtAH)_2(CH_3CN)][BF_4]_2$ **(4)**, $[Rh_2(DTolF)_2(9\text{-}EtGH)_2(CH_3CN)][BF_4]_2$ **(3)**.....86

Table 2.2 Selected Bond Distances (Å) and Angles (deg) for $Rh_2(DTolF)_2(O_2CCF_3)_2(CH_3CN)_2$ **(1)**.....88

Table 2.3 Selected Bond Distances (Å) and Angles (deg) for $[Rh_2(DTolF)_2(CH_3CN)_6][BF_4]_2$ **(6)**.....89

Table 2.4 Selected Bond Distances (Å) and Angles (deg) for $[Rh_2(DTolF)_2(9\text{-}EtAH)_2(CH_3CN)][BF_4]_2$ **(4)**.....90

Table 2.5 Selected Bond Distances (Å) and Angles (deg) for $[Rh_2(DTolF)_2(9\text{-}EtGH)_2(CH_3CN)][BF_4]_2$ **(3)**.....91

Table 2.6 NMR Spectroscopic Data for **3, 4, 5, 6** and **7**.....92

Table 3.1

Table 3.2

Table 3.3

Table 5.1

Table 3.1 Crystallographic Data for $[Rh_2(DTolF)_2(bpy)(CH_3CN)_3][BF_4]_2 \cdot OC(CH_3)_2 \cdot H_2O$ **(7a)**, $[Rh_2(DTolF)_2(bpy)(CH_3CN)_4][BF_4]_2$ **(7b)**, $[Rh_2(DTolF)_2(bpy)_2(CH_3CN)][BF_4]_2$ **(8a)**, $[Rh_2(DTolF)_2(bpy)_2(H_2O)][BF_4][BPh_4] \cdot OC(CH_3)_2 \cdot 3CH_3CH_2O_2CH_2CH_3$ **(8b)**, $[Rh_2(DTolF)_2(phen)(CH_3CN)][BF_4]_2 \cdot CH_3CH_2O_2CH_2CH_3 \cdot 4H_2O$ **(9)**, $[Rh_2(DTolF)_2(phen)_2(CH_3CN)_2][BF_4]_2$ **(10)**.....148

Table 3.2 Selected Bond Distances (Å) and Angles (deg) for $[Rh_2(DTolF)_2(bpy)(CH_3CN)_3][BF_4]_2 \cdot OC(CH_3)_2 \cdot H_2O$ **(7a)**....149

Table 3.3 Selected Bond Distances (Å) and Angles (deg) for $[Rh_2(DTolF)_2(bpy)(CH_3CN)_4][BF_4]_2$ **(7b)**.....150

Table 5.1 Summary of the $Rh_2^{II,II}$ concentrations used to inhibit DNA replication by Bear and coworkers.....215

Figure 1
Figure 1
Figure 1
Figure 1
Figure 1.
Figure 1.
Figure 1.
Figure 1.8
Figure 1.9
Figure 1.1
Figure 2.1
Figure 2.2
Figure 2.3
Figure 2.4
Figure 2.5

List of Figures

Page

Figure 1.1 Anticancer active compounds.....2

Figure 1.2 The four nucleic acids and the phosphate backbone of DNA....5

Figure 1.3 The three structural types of DNA, A, B, and Z.....7

Figure 1.4 The DNA binding modes of cisplatin.....9

Figure 1.5 Distortion of deoxyribose ring of DNA due to platination.....11

Figure 1.6 Molecular structure of *cis*-$Pt(NH_3)_2$(5'-pGpG-3').....16

Figure 1.7 Structure of a double-stranded DNA molecule coordinated to cisplatin.....18

Figure 1.8 The dinuclear transition metal anticancer agents.....20

Figure 1.9 Schematic representation of the chelating possibilities for 2,2'-bipyridine, adenine, guanine and cytosine.....23

Figure 1.10 The anticancer active compound $Rh_2(DTolF)_2(O_2CCF_3)_2L_2$...24

Figure 2.1 Schematic representation of anticancer active compounds.....35

Figure 2.2 PLUTO diagram of $Rh_2(O_2CCH_3)_4$(1-methyladenosine)$_2$ replotted from X-ray coordinates.....36

Figure 2.3 Schematic representation of the H-H and H-T bridging modes of the DNA purines 9-EtGH and 9-EtAH to dinuclear transition metal centers.....38

Figure 2.4 Example of a chelating 9-EtAH ligand depicted in the ORTEP representation of $[Rh_2(O_2CCH_3)_2(bpy)(9\text{-EtA})]^{2+}$.....39

Figure 2.5 ORTEP representation of compound **(1)** drawn at the 50% probability level.....53

Figure 2.6

Figure 2.7

Figure 2.8

Figure 2.9

Figure 2.10

Figure 2.11

Figure 2.12

Figure 2.13

Figure 2.14

Figure 2.15

Figure 2.16

Figure 2.17

Figure 2.18

Figure 3.1

Figure 2.6 Cyclic voltammograms in 0.1 M eletrolyte CH_3CN at a scan rate of 200 mV/s using a Pt electrode for (a) $[Rh_2(DTolF)_2(CH_3CN)_6][BF_4]_2$ **(2)** and (b) $[Rh_2(DTolF)_2(9\text{-}EtGH)_2(CH_3CN)][BF_4]_2$ **(3)**.....58

Figure 2.7 ORTEP representation of compound **(3)** drawn at the 50% probability level.....59

Figure 2.8 Schematic representation of protonated and deprotonated 9-ethylguanine.....60

Figure 2.10 Cyclic voltammograms in 0.1 M eletrolyte CH_3CN at a scan rate of 200 mV/s using a Pt electrode for (a) $[Rh_2(DTolF)_2(9\text{-}EtAH)_2(CH_3CN)][BF_4]_2$ **(4)**.....65

Figure 2.11 Schematic representation of the tautomers of 9-EtAH.....66

Figure 2.12 ^1H NMR spectrum depicting the H8 region of $[Rh_2(DTolF)_2(9\text{-}EtAH)_2(CH_3CN)][BF_4]_2$ **(4)** in CD_3CN at 25°C and $^-$32°C.....69

Figure 2.13 ^1H NMR spectrum depicting the H8 region of $[Rh_2(DTolF)_2(9\text{-}EtAH)_2(CH_3CN)][BF_4]_2$ **(4)** in acetone-d6 at 25°C and $^-$40°C..70

Figure 2.14 ORTEP representation of compound **(4)** drawn at the 50% probability level.....74

Figure 2.15 ^1H NMR spectrum depicting the H8 region of $Rh_2(DTolF)_2(O_2CCF_3)_2$ **(1)** and 9-EtAH.....76

Figure 2.16 Proposed structure of $[Rh_2(DTolF)_2(9\text{-}EtAH)_2(O_2CCF_3)_2$ **(5)**..78

Figure 2.17 ORTEP representation of $Rh_2(O_2CCH_3)_4(HDTolF)_2$ replotted from atomic coordinates.....80

Figure 2.18 ORTEP representation of compound **(6)** drawn at the 50% probability level.....83

Figure 3.1 ORTEP representation of $[Rh_2(O_2CCH_3)_3(bpy)(9\text{-}EtA)]$.....98

Figure 3

Figure 3

Figure 3

Figure 3

Figure 3

Figure 3

Figure 3

Figure 3

Figure 3

Figure 3.

Figure 3.

Figure 3.

Figure 3.

Figure 3.

Figure 3.

Figure 4.1

Figure 4.2

Figure 3.2 ORTEP representation of the polymer $[Rh_2(O_2CCH_3)_3(bpy)(9\text{-}EtGH)_x][BF_4]_{2x}\cdot yC_5H_{10}O$.....99

Figure 3.3 Schematic representation of the way that 2,2'-bipyridine can mimic the chelating abilities of adenine.....100

Figure 3.4 Schematic representation of the two possible binding modes of bpy to a dinuclear metal center.....103

Figure 3.5 Cyclic voltammograms of compounds **(2)**, **(7)** and **(8)**.....121

Figure 3.6 2-dimensional ^1H NMR spectrum in the aromatic bipyridine region of the mixture of compounds **7** and **8**.....122

Figure 3.7 ORTEP representation of the cation of compound **7a**.....125

Figure 3.8 PLUTO representation of compound **7b**.....129

Figure 3.9 ORTEP representation of the cation of compound **8a**.....131

Figure 3.10 ORTEP representation of the cation of compound **8a** depicting the splaying of the bpy ligands.....133

Figure 3.11 ORTEP representation of the cation of compound **8b**.....135

Figure 3.12 Cyclic voltammograms of compounds **(9)** and **(10)**.....138

Figure 3.13 ^1H NMR spectra of compounds **(9)** and **(10)** depicting the aromatic region.....141

Figure 3.14 ORTEP representation of the cation of compound **9**.....143

Figure 3.15 ^1H NMR spectrum in the aromatic bpy region of the product from the reaction between $[Rh_2(DTolF)_2(bpy)(CH_3CN)_{3,4}]^{2+}$ **(7)** and 9-EtGH.....148

Figure 4.1 Molecular structure of *cis*-$Pt(NH_3)_2$(5'-pGpG-3').....159

Figure 4.2 Structure of a double-stranded DNA molecule coordinated to cisplatin.....162

Figure 4.3

Figure 4.4

Figure 4.6

Figure 4.7

Figure 4.8

Figure 4.9

Figure 4.10

Figure 4.12

Figure 4.14

Figure 4.15

Figure 4.17

Figure 4.18

Figure 4.20

Figure 4.21

Figure 4.3 Structure of $Rh_2(O_2CCH_3)_2$(5'-pGpG-3') from molecular modeling studies....163

Figure 4.4 Overlay of the sugar-phosphate backbones of *cis*-$Pt(NH_3)_2$(5'-pGpG-3') and $Rh_2(O_2CCH_3)_2$(5'-pGpG-3') from molecular modeling studies....165

Figure 4.6 Rotation around the N-glycosidic bond of guanosine....174

Figure 4.7 HPLC chromatogram of 5'-pGpG-3'....176

Figure 4.8 ^1H NMR spectrum of 5'-pGpG-3' in D_2O....177

Figure 4.9 ^1H NMR spectrum in D_2O depicting the H8 region of 5'-pGpG-3' after HPLC purification....178

Figure 4.10 ^1H NMR spectrum of the products from the reaction of **(11)** with impure 5'-pGpG-3'....179

Figure 4.12 The HPLC chromatogram of $Rh_2(O_2CCH_3)_2$(5'-pGpG-3')$(H_2O)_2$ (13)....182

Figure 4.14 HPLC chromatogram of $Rh_2(O_2CCH_3)_x$(GG-12mer)....186

Figure 4.15 ^1H NMR spectrum of ds[$Rh_2(O_2CCH_3)_x$(GG-12mer)]....189

Figure 4.17 ^1H NMR spectra depicting the imino region of ds[$Rh_2(O_2CCH_3)_x$(GG-12mer)]....192

Figure 4.18 ^1H NMR spectra of ds(GG-12mer) and ds[$RhOAc)_x$(GG-12mer)]....193

Figure 4.20 HPLC chromatogram of ss[$RhOAc)_x$(GG-12mer)] adduct...196

Figure 4.21 ^1H NMR spectra depicting the imino region of ds[$Rh_2(O_2CCH_3)_2$(GG-12mer)]....199

Figure 5.1

Figure 5.2

Figure 5.3

Figure 5.4

Figure 5.5

Figure 5.6

Figure 5.1 Schematic representation of DNA replication by DNA polymerase I.....204

Figure 5.2 Schematic representation of the DNA replication process of DNA polymerase I (pol I) inhibited by cisplatin.....207

Figure 5.3 Schematic representation of the steps of the Polymerase Chain Reaction (PCR).....213

Figure 5.4 Schematic of the inhibition of PCR by dinuclear transition metal compounds.....214

Figure 5.5 Autoradiograph of the inhibition of PCR by $Rh_2(O_2CCH_3)_4(H_2O)_2$ **(11)**.....218

Figure 5.6 Autoradiograph of the inhibition of PCR by $[Re_2(O_2CCH_2CH_3)_4(H_2O)_2][SO_4]$.....220

Å
br
β
cn
oC
d
δ
ε
λ
g
m
m
h
IF
J
k
N
N
n
n
μ
n
N
v
p

Abbreviations

Å	Angström
br	broad
β	Bohr magneton
cm^{-1}	wavenumber
^oC	degree centigrade
d	doublet (NMR), day, deuterated
δ	parts per million (ppm)
ε	molar extinction coefficient
λ	wavelength
g	gram
mol	mole
mmol	millimole
h	hour
IR	infrared
J	coupling constant (NMR)
k	Boltzmann constant
MHz	megaHertz
M	mole per liter
m	medium, multiplet
mL	milliliter
μ	bridging ligand
nm	nanometer
NMR	nuclear magnetic resonance
ν	frequency
ppm	parts per million

s

TM

UV

w

X

DN

RN

G

A

ade

d(pC

9-Et

9-Et

9-Et

9-Et

DTc

DPh

form

S

L

s	singlet, strong
TMS	tetramethylsilane
UV	ultraviolet
w	weak
X	halide
DNA	deoxyribonucleic acid
RNA	ribonucleic acid
G	guanosine
A	adenosine
ade	adenine or substituted adenine bases
d(pGpG)	dimer of DNA containing guanine
9-EtGH	9-ethylguanine
9-EtAH	9-ethyladenine
9-EtG$^-$	9-ethylguanine deprotonated at the N1 position
9-EtA$^-$	9-ethlyadenine deprotonated at the N6 position
DTolF$^-$	N,N'-p-tolyformamidinate
DPhF$^-$	N,N'-diphenylformamidinate
form	both DTolF$^-$ and DPhF$^-$
S	donor solvent
L	ligands

Chapter I

Introduction

1. **Anti**

Inorg

Metal com

arthritic ac

developme

chemothera

tumors of

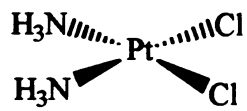
activity of

H_3

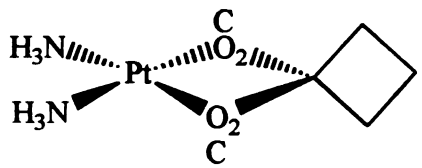
H_3

1. Anticancer Activity of Cisplatin

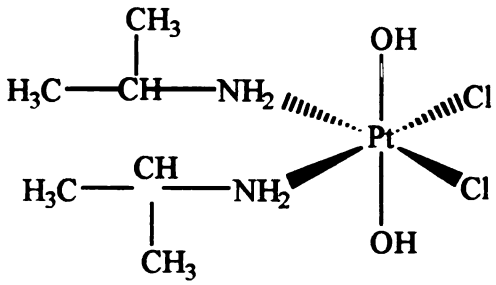
Inorganic compounds have been used medicinally since ancient times. Metal compounds that exhibit antiviral, anti-bacterial, anticancer and anti-arthritic activity to name a few, are in frequent clinical use today.[1a-d,3] The development of cisplatin (*cis*-DDP) and related complexes (Figure 1) for the chemotherapeutic treatment of testicular and ovarian cancers as well as tumors of the head and neck has stimulated investigation of the antitumor activity of a wide range of transition metal complexes.[2]



Cisplatin



Iproplatin



Carboplatin

Figure 1. Anticancer active platinum compounds.

The r

clinical use

century with

use due to t

anti-bacteria

compounds

patients wh

side effects

peripheral

dangerous t

An even m

related con

carcinogeni

unknown.[3]

therapeutic

iproplatin (

States as a

cancer and

been approv

and design

The medical community initially opposed FDA approval for the clinical use of cisplatin. This is not surprising, as the early part of this century witnessed the exclusion of heavy metal compounds from therapeutic use due to the replacement of highly toxic arsenic, antimony and mercury anti-bacterial agents with organic compounds. Although the platinum compounds currently in clinical use are effective against key deadly tumors, patients who are administered cisplatin are threatened by a range of toxic side effects including nephrotoxicity, myelosuppression, ototoxicity, nausea, peripheral neuropathies and cardiac abnormalities. Obviously, less dangerous treatments are sought so that such health risks can be minimized. An even more compelling reason for further research into cisplatin and related compounds is the recent findings that cisplatin itself exhibits carcinogenic effects, although the extent of carcinogencity in humans is unknown.[3] Second generation drugs have been developed that exhibit high therapeutic activity with reduced toxicity; these include carboplatin and iproplatin (Figure 1). Carboplatin has recently been approved in the United States as a much less toxic alternative to cisplatin in the treatment of ovarian cancer and small lung cancers, and an oral analogue of cisplatin has recently been approved for use.[3] The challenge now faced by researchers is to tailor and design inorganic complexes with improved biological activity and

resistance to

toxic side ef

Befor

description

material of a

namely, d

monophosph

deoxycytidir

are linked to

of DNA is

strands run

stabilize the

each other in

B, C, and Z

of the three

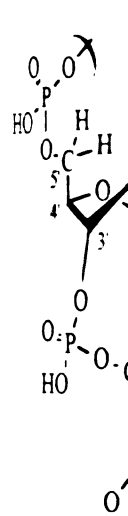
structure of

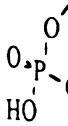
right-handed

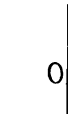
strands run

resistance to physiological decomposition, with concomitant reduction of toxic side effects.

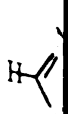
Before proceeding further with this discussion, however, a general description of DNA structure should be presented. DNA is the genetic material of all living entities on Earth. It is composed of four nucleic acids, namely, deoxyadenosine monophosphate (dAMP), deoxythymidine monophosphate (dTMP), deoxyguanosine monophosphate (dGMP), and deoxycytidine monophosphate (dCMP) (Figure 2).[4] The four nucleic acids are linked together through a sugar-phosphate backbone. Each single strand of DNA is base-paired to another single strand of DNA such that the two strands run anti-parallel to each other. Base stacking and base pairing stabilize the duplex structure of DNA. The two strands are coiled around each other into a helix. DNA exists in several types of structural families: A, B, C, and Z (Figure 3). Table 1 summarizes pertinent structural information of the three major types of DNA structures. B-DNA which is an average structure of DNA, is the most common and stable form. It consists of two right-handed polynucleotide chains coiled about a common axis. The two strands run anti-parallel with respect to each other (5' to 3' and 3' to 5'). The











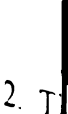




Figure 2. T

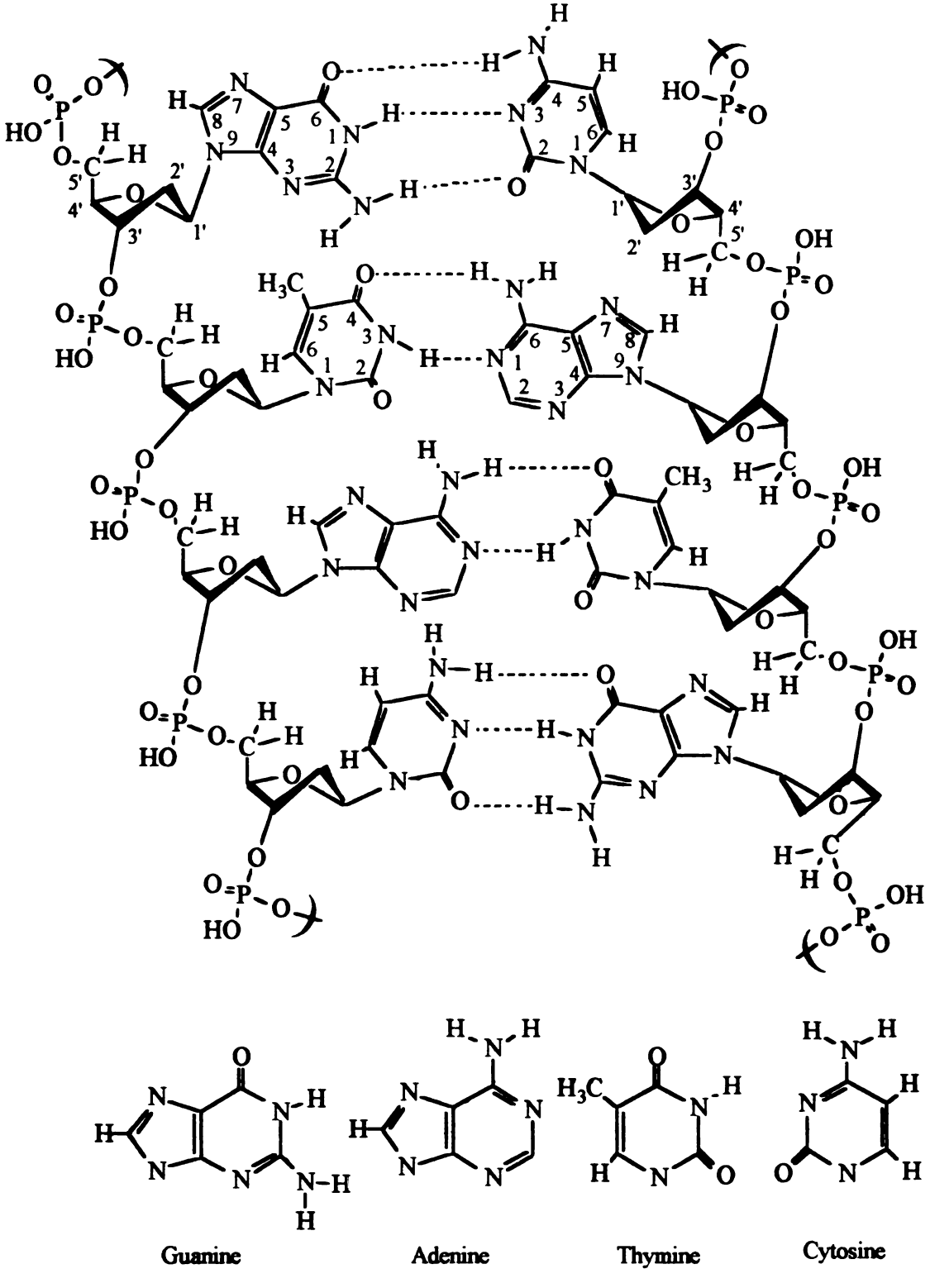


Figure 2. The four nucleic acids and the phosphate backbone of DNA.

bases are bas

cytosine. Th

bases are ins

The sugar-ph

the helix. Th

the helix dian

between base

DNA is pre

bacterial spo

of DNA stru

diameter is i

OH group.

sequence-sp

anti-conform

Z-DNA diff

phosphate b

diameter is n

reported in c

bases are base-paired such that adenine pairs with thymine, and guanine with cytosine. The bases are stacked such that the hydrophobic groups of the bases are inside the helix, which imparts stability by the exclusion of water. The sugar-phosphate backbone is hydrophilic and is found on the outside of the helix. The planes of the bases are perpendicular to the helical axis, and the helix diameter is approximately 24 Å. B-DNA has a vertical rise of 3.4 Å between bases. Approximately 10.4 bases are present per helical turn. A-DNA is preferred for DNA/RNA hybrids, RNA hairpins, and in some bacterial spores (Figure 3). In comparison to B-DNA, the most common type of DNA structure, A-DNA is wider and more vertically compact. The diameter is important since RNA needs to be wider to accommodate the 2'-OH group. Z-DNA is transiently adopted by short stretches of B-DNA in a sequence-specific fashion (poly-G). The guanine bases of Z-DNA are in the anti-conformation while all other bases are in a syn-conformation (Figure 3). Z-DNA differs from A and B-DNA in that is left-handed, and the sugar phosphate backbone is present in a zig-zag repeating unit. The helix diameter is narrower and longer than the other forms. C-DNA has only been reported in crystal structures, and will not be described.



A-DN

Shape	
Rise Base Pair	
Helix Diameter	
Screw Sense	
Glycosidic Bon	
Base Pairs Helical	
Pitch Helical Turn	
Tilt of Base Pa	
Major Groove	
Minor Groove	

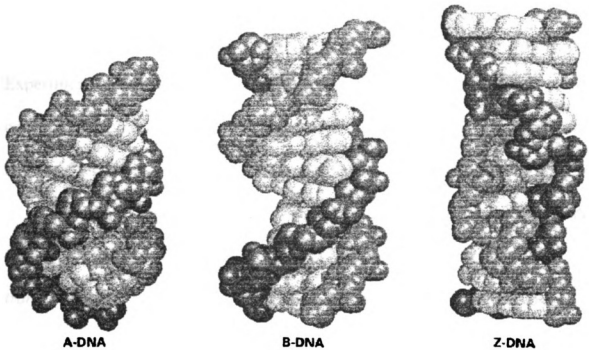


Figure 3. The three structural types of DNA, A, B and Z.

	A	B	Z
Shape	Broadest	Intermediate	Narrowest
Rise/Base Pair	2.3 Å	3.4 Å	3.8 Å
Helix Diameter	25.5 Å	23.7 Å	18.4 Å
Screw Sense	Right-handed	Right-handed	Left-handed
Glycosidic Bond	*anti*	*anti*	*anti* for C, T *syn* for G
Base Pairs/Helical Turn	11 10.4	12	
Pitch/Helical Turn 25.3 Å	35.4 Å45.6 Å		
Tilt of Base Pairs	19°	1°	9°
Major Groove	Narrow & Deep	Wide & Deep	Flat
Minor Groove	Broad & Shallow	Narrow & Deep	Narrow & Deep

Table 1. Comparison of A-, B-, and Z-DNA.

After many y

coordination

Experiments

cells reveale

modes of Pt

The r

adduct of

trans-(NH_3)

and N is a

intrastrand

~90% of all

cisplatin fro

and is thoug

studies also

platinum ch

G-G bases

After many years of research on the subject, researchers generally agree that coordination of Pt to DNA is a major factor in cisplatin's anticancer activity. Experiments measuring the rates of biomolecule syntheses in cisplatin treated cells revealed that DNA replication is preferentially inhibited.[5] Coordination modes of Pt(II) to DNA bases have been elucidated by enzymatic studies.

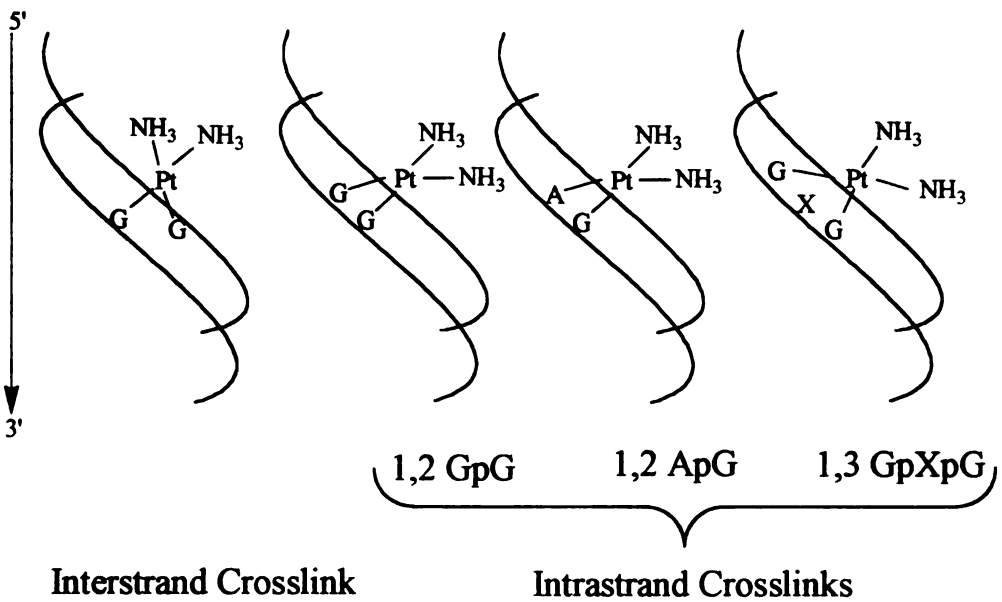
The most common DNA platinum species is a bifunctional DNA adduct of general formulae *cis*-$(NH_3)_2$Pt(XpX), *cis*-(NH_3)Pt(XpNpX) or *trans*-(NH_3)Pt(XpNpX) where X is either guanosine (G) or adenosine (A), and N is any of the other DNA nucleosides.[1c,3c-e] These 1,2 and 1,3 intrastrand cross-links, where d(XpX) is either GpG or ApG account for ~90% of all platinum/DNA binding modes (Figure 4). Migration of bound cisplatin from one nucleobase to another has been found to be uncommon, and is thought to be an unlikely event under ambient conditions.[6] Previous studies also suggest that a shortening and unwinding of DNA occurs after the platinum chelation of a G-G sequence. This chelation causes a tilting of the G-G bases out of their parallel alignment, and instigates a kink in the helix of



Interstr

(= gu
A = ad
X = cy

F



G = guanine
A = adenine
X = cytosine (C), thymine (T), adenine (A)

Figure 4. The DNA binding modes of cisplatin.

about 40°

which und

ring pucke

intrastrand

found to a

double-stra

important

The

dependent

being the

of guanine

to be th

compound

been obse

positions

compound

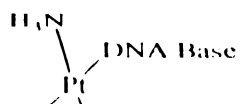
observed

exposed i

bonding.

about 40° - 70°. Additional distortion occurs at the 5'-deoxyribose ring, which undergoes a conformational change from a C2'-endo to a C3'-endo ring puckering to accommodate the strain caused by the cisplatin 1,2-intrastrand binding (Figure 5). Although inter-strand cross-links have been found to account for less than 1% of the total amount of platinum bound to double-stranded DNA, this mode of binding cannot be ruled out as an important binding mode for antitumor compounds.[6]

The observed coordination modes for Pt(II) to DNA bases are pH dependent, with the N7 position of guanine and the N3 position of adenine being the preferred binding sites at neutral pH (Table 2).[7] The N7 position of guanine has been determined by X-ray crystallographic and NMR studies to be the most likely site of coordination for platinum anticancer compounds. Likewise, both the N7 and N1 positions of adenine have also been observed, leading researchers in the field to believe that the purine N7 positions are the active coordination sites for cisplatin and related compounds. The main rationale for purine N7 positions being the frequently observed coordination sites in double helical DNA is that this position is exposed in the major groove, and is not involved in Watson-Crick hydrogen bonding.[7]


DNA Base

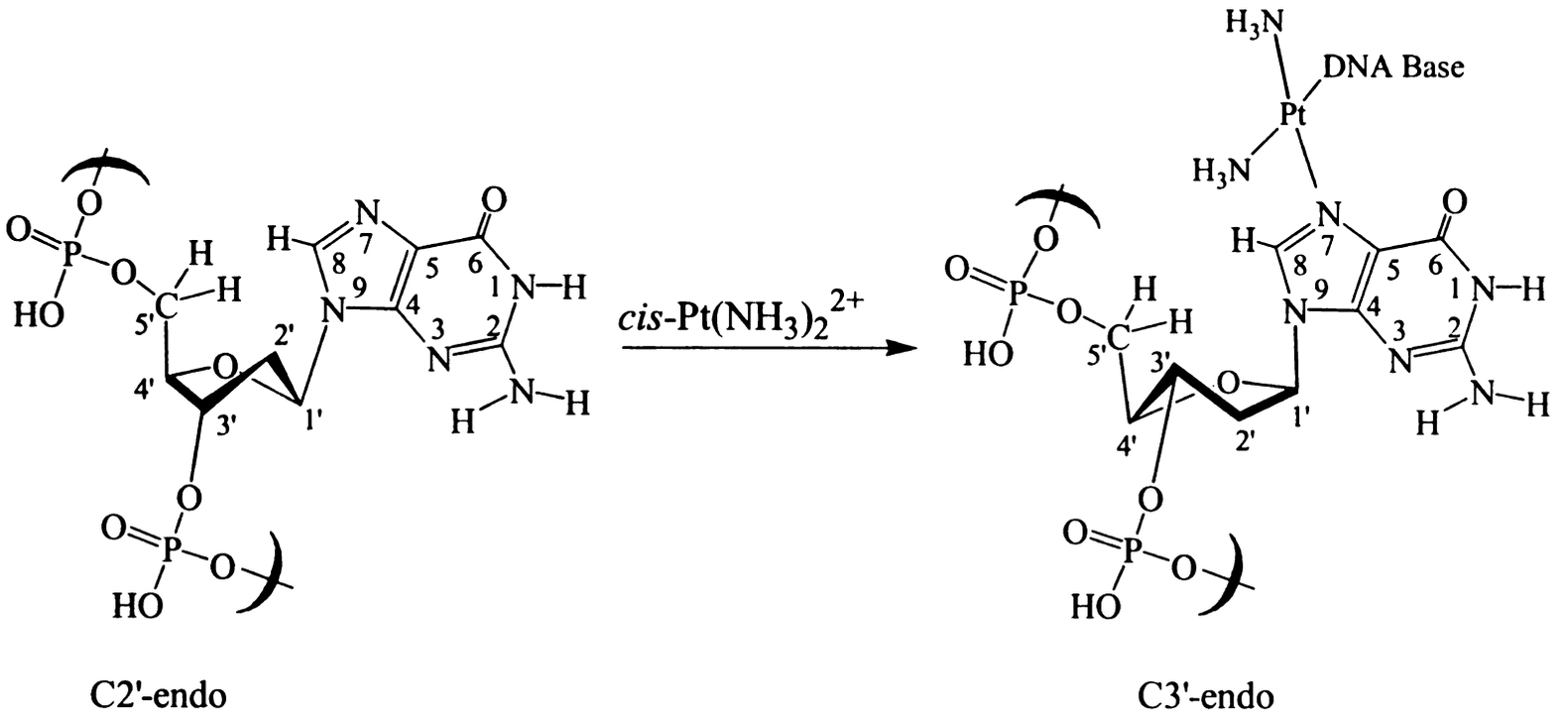


Figure 5. Distortion of deoxribose ring of DNA due to platination.

Pu
G
G
G
A
A
A
C
C
U
T

Both
replication
compounds
both 1,2-int
Transplatin
intrastrand
and interstr
more transp
in vivo.[5]

Table 2[7]

Purine	Site	pK_a Range
Guanine	N7	2.3
Guanine	N1	9.3
Guanine	N3	?
Adenine	N7	-1.5
Adenine	N1	3.7
Adenine	N6[a]	?
Cytosine	N3	4.4
Cytosine	N4	?
Uracil	N3	9.5
Thymine	N3	9.5

[a] = N6 is the exocyclic nitrogen after deprotonation

Both cisplatin and its *trans* isomer are known to inhibit DNA replication to the same extent *in vitro*.[5] Both of these platinum(II) compounds bind to DNA, but in different ways. Cisplatin binds to DNA *via* both 1,2-intrastand crosslinks and 1,3-intrastrand crosslinks described above. Transplatin, on the other hand, is geometrically unable to make 1,2-intrastrand crosslinks to DNA, and thus binds *via* 1,3-intrastrand crosslinks and interstrand crosslinks. Cellular uptake of both isomers is equal, but more transplatin than cisplatin is needed in order to inhibit DNA replication *in vivo*.[5] Time evolved studies revealed that cisplatin bound to DNA

accumulat

that the D

Stuc

responsibl

revealed tl

excision a

by a diff

damage re

sides of th

damaged D

intrastrand

intrastrand

mammalia

by revealir

DNA, and

these prot

Recognitio

large numb

mobility gr

six HMG d

accumulates in a cell, whereas transplatin does not. These results suggest that the DNA adducts of the two isomers are processed differently in cells.

Studies designed to determine what DNA repair mechanism is responsible for the repair of platinated DNA was performed.[5] These studies revealed that cisplatin modified DNA were repaired by a combination of excision and recombination processes, whereas the *trans* isomer is repaired by a different cellular mechanism. Excision repair processes involve damage recognition by a protein, incision of the damaged DNA on both sides of the error, removal of the damaged sequence, and replacement of the damaged DNA by polymerase and ligase. The studies also showed that 1,3-intrastrand adducts were repaired at a higher efficiency than the 1,2-intrastrand adducts of AG and GG sequences. Gel mobility shift assays in mammalian cellular extracts supported the difference in repair recognition, by revealing that certain cellular proteins bind specifically to platinated DNA, and can distinguish between 1,2 and 1,3-intrastrand adducts. One of these proteins was cloned and expressed.[5] The Structure Specific Recognition Protein 1 (SSRP1) is ~80 kDa, and was determined to contain a large number of charged residues and a DNA binding region called a high mobility group (HMG) domain. HMG proteins, in general, contain one to six HMG domains. The HMG domains of SSRP1 were identified to be

similar to

domains of

residue as

bases. Th

towards the

are very sim

contains thr

residues lo

which is a

hydrophobi

specifically

further bend

85°.[5] The

the protein

Sever

the discover

adducts.[5] O

repair, and

damaged D

transcription

similar to the human cellular proteins HMG1 and HMG2. The HMG domains of HMG1 are responsible for binding to DNA using a hydrophobic residue as an intercalative wedge in order to locally destack several of the bases. This intercalation causes unwinding and bending of the DNA towards the major groove. The structural changes induced by HMG proteins are very similar to those observed when cisplatin binds to DNA. The protein contains three domains, the HMG domains A (N-terminus) and B are ~80 residues long, positively charged, and homologous. The third domain, which is at the C-terminus, is ~30 residues long, acidic, and lacks hydrophobic side chains. The A and B domains of HMG2, like HMG1, bind specifically to platinated DNA. These HMG proteins have been shown to further bend cisplatin-DNA adducts at or near the platinated site by 70° – 85°.[5] The variability of the bends is dependent on the specific contacts of the protein with the DNA.

Several models for cisplatin's cytotoxicity were postulated based upon the discovery of the specific binding of the HMG domains to cisplatin-DNA adducts.[5] One of these hypotheses is that the HMG proteins signal normal repair, and Pt-DNA adducts rob the cell of these proteins, leaving other damaged DNA that would normally be repaired available for use in transcription. Another theory of SSRP is that these proteins regulate gene

expression
DNA migh
from their
cellular fun
vivo as we
adduct shie
the cell. O
HMG dom
binding site

The
domains of
the coordin
anticancer
characterize
6).[5a,8] The
coordinated
the dinucle
coordination
solution stru
same. Many

expression necessary for cancer cell growth. The binding of cisplatin to DNA might afford a structure that mimics the recognition signal of SSRP from their natural binding sites, causing changes in the regulation of other cellular functions. Yet another theory, which is supported experimentally *in vivo* as well as *in vitro*, is that the binding of an SSRP to a cisplatin-DNA adduct shields the platinated DNA from the excision repair mechanisms of the cell. Overall, cisplatin-DNA adducts in the cell divert the function of the HMG domain proteins either by removing them from their natural DNA binding sites or depleting the pool of these proteins.

The findings that cisplatin is specifically recognized by the HMG domains of SSRPs suggests that the alteration of DNA structure induced by the coordination of cisplatin to DNA plays an important role in cisplatin's anticancer activity. The cisplatin DNA adduct that was structurally characterized by X-ray crystallography is *cis*-[$Pt(NH_3)_2${d(pGpG)}] (Figure 6).[6a,8] The molecule is composed of a square-planar platinum atom coordinated to two NH_3 ligands and the N7 atoms of the guanine bases of the dinucleotide. The base stacking of the guanines is disrupted by the coordination. The solid state structure was compared to previously reported solution structures, and it was found that the structures are essentially the same. Many years later, the structure of a much longer piece of platinated

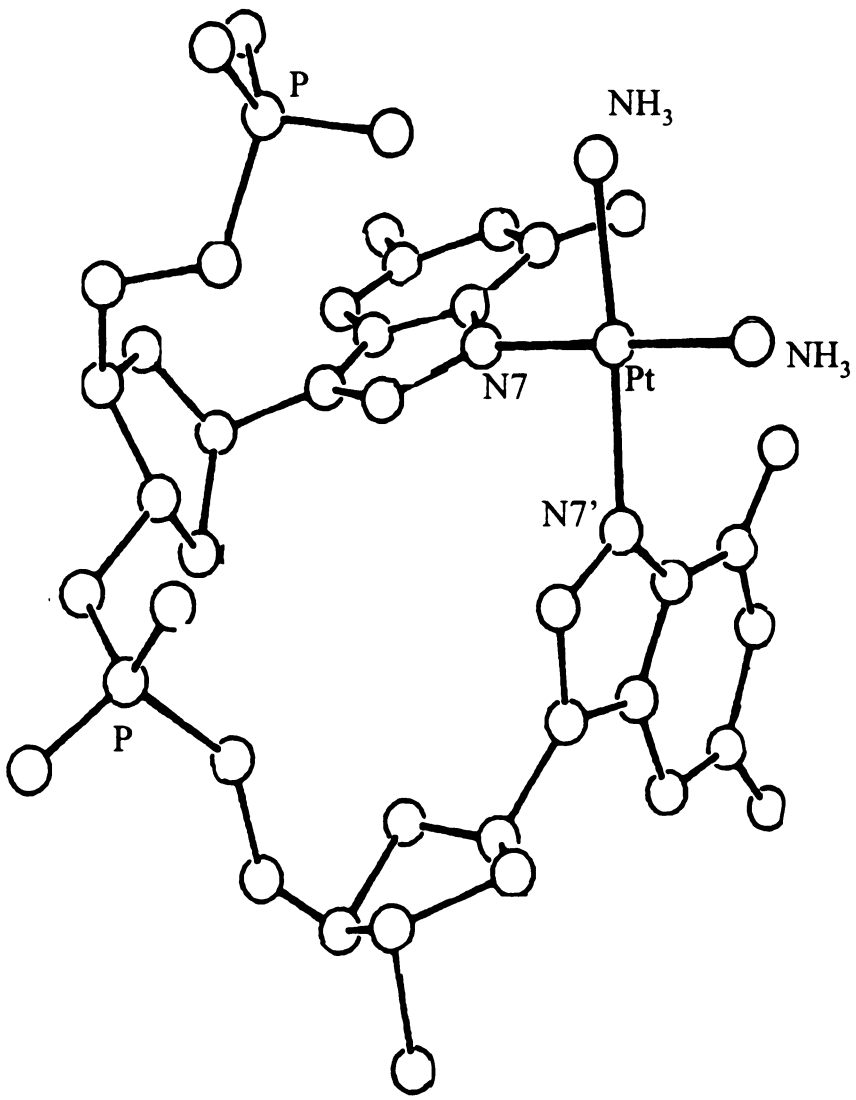


Figure 6. Molecular structure of *cis*-$Pt(NH_3)_2$(5'-pGpG-3').[3]

DNA was

Namely,

(CCTCTG

$(NH_3)Pt$

$[Pt(NH_3)_2$

to have the

to a square

A-DNA fr

3' end of

change in

packing fo

destacks th

Whi

inhibits D

other trans

the nucleic

carcinosta

elucidating

of the mec

DNA was also subjected to X-ray crystallographic determination. cisplatin-Namely, the 12 base-pair (bp) double strand sequence (CCTCTGGTCTCC)·(GGAGACCAGAGG) was crystallized with a $(NH_3)Pt$ moiety coordinated.[9] The structure of *cis*-$[Pt(NH_3)_2\{d(CCTCTG*G*TCTCC)\cdot(GGAGACCAGAGG)\}]$ was reported to have the same type of coordination through the N7 atoms of the guanines to a square planar Pt atom (Figure 7). The DNA in this structure resembles A-DNA from the 5' end to the coordinated Pt atom. From the Pt atom to the 3' end of the dodecamer DNA the biomolecule resembles B-DNA. This change in the DNA structural form is thought to be influenced by crystal packing forces. As can be seen in Figure 7, coordination of Pt to the DNA destacks the bases analogous to the dinucleotide structure.

While it is not safe to assume that the mechanism whereby cisplatin inhibits DNA replication is applicable to the antitumor activity observed for other transition metal compounds, it is nonetheless important to extrapolate the nucleic acid chemistry of cisplatin in order to recognize key patterns for carcinostatic behavior. From the extensive mechanistic studies aimed at elucidating the effect of cisplatin DNA replication, and the collective studies of the mechanisms of similar platinum complexes, fundamental trends have

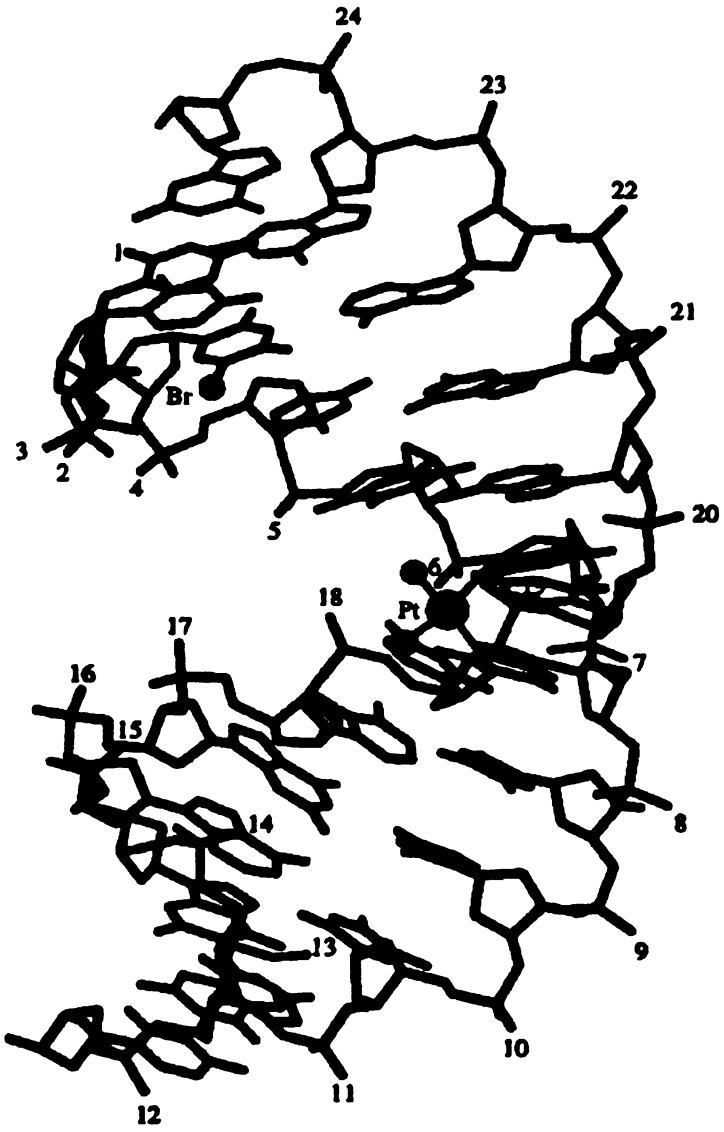


Figure 7. Structure of a double-stranded DNA molecule coordinated to cisplatin.[6]

emerged re

designed su

with biolog

square plan

compounds

Å apart on

the remaini

robust, and

DNA.[1]

2. Dirhodiu

One

structures a

for anticanc

rhodium, rh

with bridgi

activity ag

ensuing.[1a,1

these comp

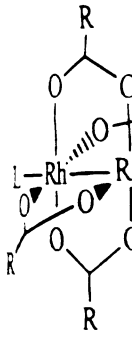
their speci

physiologic

emerged regarding their activity. For example, the complexes should be designed such that two *cis*, rather than *trans*, ligands substitute in reactions with biological molecules.[1] The geometry of the complexes should be square planar or octahedral as in the case of active platinum antitumor compounds. Another prevailing tendency is that the leaving groups are ~3.4 Å apart on the molecule (the Watson-Crick ladder spacing). Furthermore, the remaining groups *trans* to the leaving groups, such as amines, should be robust, and preferably capable of participating in hydrogen-bonding with DNA.[1]

2. Dirhodium Compounds

One entirely different class of antitumor active compounds whose structures and reactivities do not closely adhere to the cisplatin guidelines for anticancer compounds are dinuclear transition metal complexes of rhodium, rhenium and ruthenium (Figure 8). Compounds of these metals with bridging carboxylate ligands have been studied as to their antitumor activity against various tumor cell lines with very promising results ensuing.[1a,10,11] To date, however, no major advances in the development of these compounds for pharmaceutical use have been made, most likely due to their specialized nature and their purported facile decomposition under physiological conditions. The so-called "lantern" structures of these



$Rh_2(O_2CR$

Figur

compounds

(eq) and ax

Amo

active, the

CH_2CH_2C

Researche

carcinosta

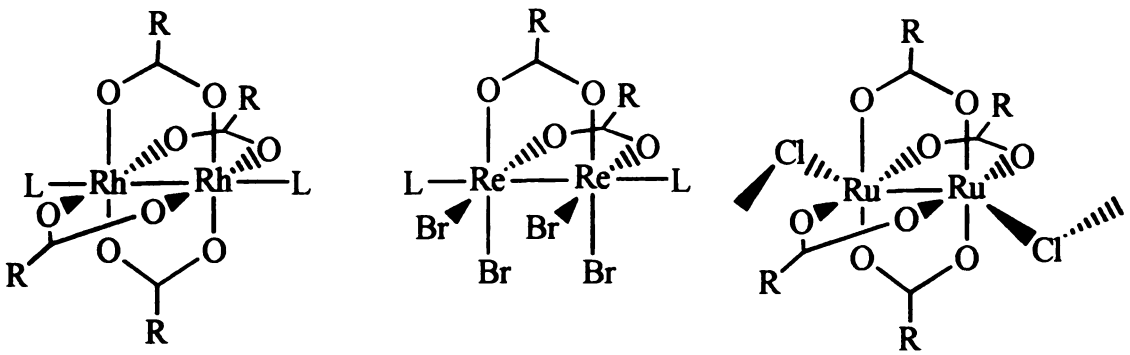
vivo.[11b]

compound

inhibit D

most pote

bind to



$Rh_2(O_2CR)_4L_2$ $Re_2(O_2CR)_2Br_4L_2$ $Rh_2(O_2CR)_4L_2$

Figure 8. The dinuclear transition metal anticancer agents.

compounds allow for two possible types of binding sites, namely equatorial (eq) and axial (ax).

Among the dinuclear compounds that have been found to be antitumor active, the dirhodium compounds $Rh_2(O_2CR)_4L_2$ (R = CH_3, CH_2CH_3, $CH_2CH_2CH_3$; L = solvent) have been studied the most extensively. Researchers have shown that these compounds exhibit significant carcinostatic activity against Erlich ascites and leukemia L1210 tumors *in* vivo.[11b] A summary of the observed antitcancer activity of dirhodium compounds is presented in Tables 3 - 7. These complexes were found to inhibit DNA but not RNA synthesis with $Rh_2(O_2CCH_2CH_2CH_3)_4L_2$ being the most potent inhibitor.[11] Model DNA studies indicated that these complexes bind to single-stranded (ss) DNA and ds(poly-A) (ds = double-stranded)

with no sig

preferences

molecules t

solvent mo

bridging ca

guanine to

In c

that guanin

and in an

performed

adenine g

these co

carboxyla

building

unpreced

prevent D

Pre

X-ray str

(9-EtG =

in our la

with no significant binding being reported for ds(poly-G). These binding preferences to adenine were postulated to be related to the fact that these molecules typically react with neutral bases by *trans* substitution of the axial solvent molecules. It has been argued that steric repulsions between the bridging carboxylate ligands and the O6 atom prevents the axial binding of guanine to the dimetal unit.[12]

In contrast to the earlier studies, very recent findings have established that guanine bases do in fact bind to $Rh_2(O_2(CCH_3)_4$ and related molecules and in an unprecedented fashion. Single crystal X-ray studies have been performed on several compounds that possess novel, *bridging* guanine and adenine groups.[13] These results support an alternate substitution pathway for these compounds that involves displacement of equatorial bridging carboxylate ligands rather than mere axial substitution. The discovery that a building block of DNA can act as a bridge between two metal centers is unprecedented and may play an important role in how dinuclear complexes prevent DNA replication in tumors.

Previous research in our laboratories led to the determination of the X-ray structures of compounds of the type $Rh_2(O_2CCH_3)_2(9\text{-EtG})_2(CH_3OH)_2$ (9-EtG = deprotonated 9-ethylguanine).[13] Related compounds synthesized in our laboratories were found to exhibit similar structures. Diruthenium as

well as dim

structure as

dimetal uni

either the h

In addition,

mode throu

structure of

Early

sought to u

biologically

9). During

such as F

bipyridine;

cells as Hu

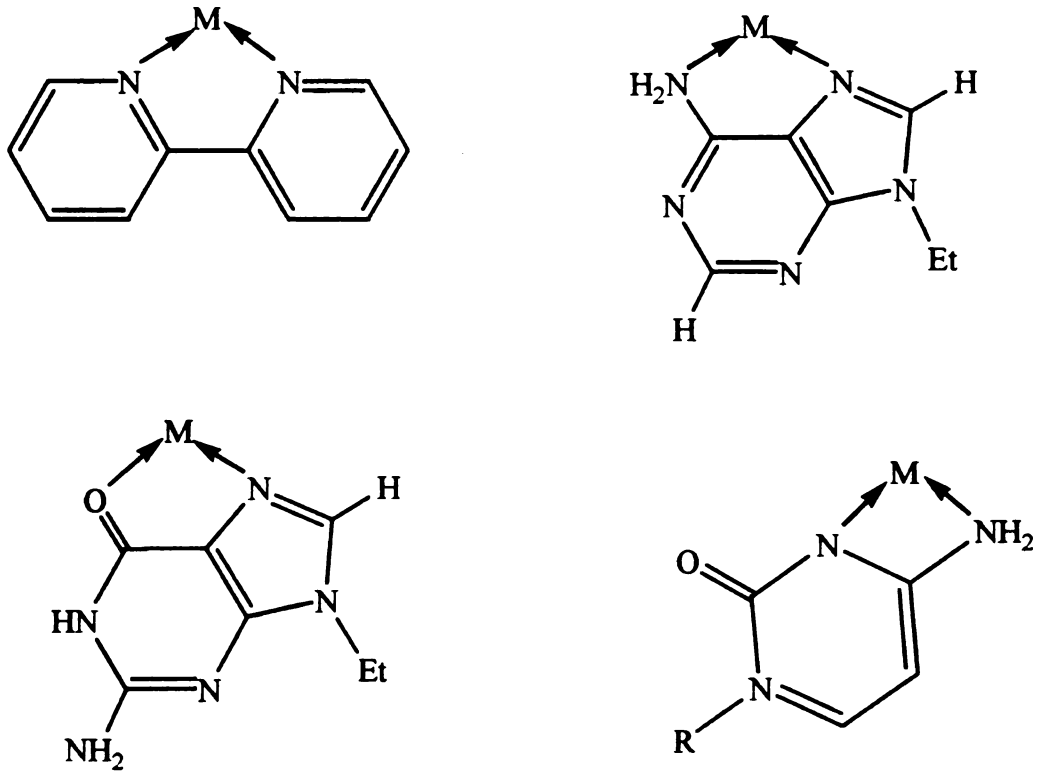
the mono-b

and 9-EtAl

by their X-

well as dimolybdenum tetra-carboxylate compounds adopt the same types of structure as dirhodium compounds in that the two guanine bases bridge the dimetal units in a *cis* disposition. Furthermore, the guanines are arranged in either the head-to-head or head-to-tail orientations of the N7 and O6 atoms. In addition, the modified purine, 9-EtAH (9-ethyladenine) adopts a bridging mode through the N7 and N6 atoms as observed in the X-ray crystal structure of $[Mo_2(O_2CCH_2F)_2(9\text{-EtAH})_2(CH_3CN)_2][BF_4]_2$.[13c]

Early in our research of purine reactions with dinuclear complexes we sought to use the chelating properties of 2,2'-bipyridine as a mimic for the biologically relevant nitrogen ligands, adenine, guanine and cytosine (Figure 9). During this time we learned that compounds containing N-N chelates such as $Rh_2(O_2CH)_4(bpy)_2Cl_2$ and $Rh_2(O_2CH)_4(phen)_2Cl_2$ (bpy = 2,2'-bipyridine; phen = 1,10-phenanthroline) were active against such cancer cells as Human Oral Carcinomas (Table 3). Studies in our laboratories with the mono-bpy compound $[Rh_2(O_2CCH_3)_2(bpy)(CH_3CN)_4][BF_4]_2$ and 9-EtGH and 9-EtAH afforded compounds containing chelating purines as determined by their X-ray structures.[14]



R = deoxyribose or ethyl

Figure 9. Schematic representation of the chelating possibilities for 2,2'-bipyridine, adenine, guanine and cytosine.

Ano

structure c

observed

Rh_2(DTolF

10).[15] Th

tumor cell

activity bu

researchers

bridging tr

Figure 10.

leads to th

solvent) w

active co

Another dirhodium compound that possesses the same "lantern" structure of the dirhodium(II) tetra-carboxylates and which has also been observed to exhibit carcinostatic activity is the mixed-ligand compound $Rh_2(DTolF)_2(O_2CCF_3)_2(H_2O)_2$ (DTolF = N,N'-p-tolylformamidinate) (Figure 10).[15] The antitumor activity of this complex was tested against various tumor cell lines, and the compound was found to exhibit equal antitumor activity but with a lower toxicity than $Rh_2(O_2CR)_4L_2$ (Table 5). The researchers who performed this study postulated that the lability of the bridging trifluoroacetate ligands and the axial water molecules in solution

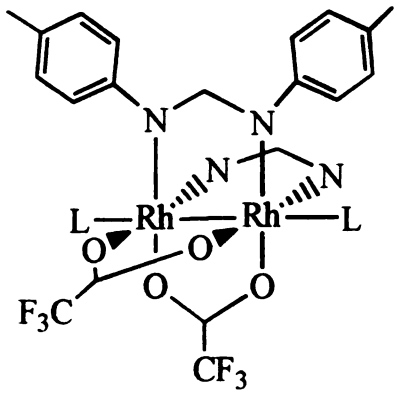


Figure 10. The anticancer active compound $Rh_2(DTolF)_2(O_2CCF_3)_2L_2$.

leads to the formation of the charged solvated cation $[Rh_2(DTolF)_2S_6]^{2+}$ (S = solvent) which is suspected to be the important physiological form of the active compound.[15] Although their preliminary work did not include

verification

concluded th

DNA inter

researchers

contrast, ou

dirhodium

tetra-carbo

Reactions

In ar

reactions

CTCTCAA

with one e

complimer

spectrosco

its stabilit

results co

DNA by

and Rh

(Chapter

verification of structures by X-ray crystallography, the researchers also concluded that axial substitution analogous to the previous postulations of the DNA interactions of $Rh_2(O_2CR)_4L_2$, was taking place.[15] The same researchers also concluded that no reactions with guanine would occur. In contrast, our work in our laboratories regarding the reactivity of this class of dirhodium compounds revealed that they display similar reactivities to the tetra-carboxylate classes of compounds (Chapter II and Chapter III).

Reactions with Oligonucleotides

In an attempt to obtain preliminary results of dirhodium-DNA binding, reactions of $Rh_2(O_2CCH_3)_2(H_2O)_2$ with the 12 bp sequence d(5'-CTCTCAACTTCC-3') (d(AA)).[16] The dirhdodium compounds was reacted with one equivalent of the DNA strand. The product was purified, and the complimentary strand was annealed to the modified d(AA) strand. ^1H NMR spectroscopic studies revealed that the duplex DNA strand was formed, and its stability was quite different from the unmetallated duplex DNA. These results coupled with the published X-ray structure of the platinated 12 bp DNA by Lippard led us to investigate the reactions of $Rh_2(O_2CCH_3)_4(H_2O)_2$ and $Rh_2(O_2CCH_3)_2(CH_3CN)_6][BF_4]_2$ with d(5'-CCTCTGGTCTCC-3') (Chapter IV). In addition, we performed studies to prove that dinuclear

transition me

early literatu

transition metal compounds react with double-stranded DNA, contrary to the early literature (Chapter V).

In vitro
Activity of D
Cells.[a]

$Rh_2(OAc)_4$–H
$Rh_2(OAc)_4$(H
$Rh_2(OAc)_4$–H
Rh_2(PhCHO
Rh_2(PhCHO
$Na_4Rh_2(CO_3$
$Na_4Rh_2(CO_3$
$Na_4Rh_2(CO_3$
$Na_4Rh_2(CO_3$
$Na_4Rh_2(CO_3$
$Na_4Rh_2(CO_3$
$Rh_2(O_2CH)_4$
$Rh_2(O_2CH)_4$
$Rh_2(O_2CH)_4$

Concentrati
[a][MeCHOH
ED_{5} = effe

Table 3

In vitro

Activity of Dirhodium Compounds Against Human Oral Carcinoma KB Cells.[17]

		Ligand	ED_{50} 106
$Rh_2(OAc)_4(H_2O)_2$			30
$Rh_2(OAc)_4(H_2O)_2$	+	2,2'-bpy	60
$Rh_2(OAc)_4(H_2O)_2$	+	1,10-phen	85
$Rh_2(PhCHOHCOO)_4(H_2O)_2$	+	2,2'-bpy	>100
$Rh_2(PhCHOHCOO)_4(H_2O)_2$	+	1,10-phen	8
$Na_4Rh_2(CO_3)_4 \cdot 2.5H_2O$	+	lactic acid*	15
$Na_4Rh_2(CO_3)_4 \cdot 2.5H_2O$	+	lactic acid + 2,2'-bpy	53
$Na_4Rh_2(CO_3)_4 \cdot 2.5H_2O$	+	lactic acid + 1,10-phen	8
$Na_4Rh_2(CO_3)_4 \cdot 2.5H_2O$	+	tartaric acid	55
$Na_4Rh_2(CO_3)_4 \cdot 2.5H_2O$	+	citric acid	>100
$Na_4Rh_2(CO_3)_4 \cdot 2.5H_2O$	+	malic acid	>100
$Rh_2(O_2CH)_4(H_2O)_2$	+	2,2'-bpy	>100
$Rh_2(O_2CH)_4(bpy)_2Cl_2$			>100
$Rh_2(O_2CH)_4(phen)_2Cl_2$			>100

Concentrations: [Rh] = 10^{-3} mol;[ligand] =2 x $1O^{-3}$ mol·dm^{-3}.
*[MeCHOHCOOH] =4 x 10^{-3} mol·dm^{-3}.
ED_{50} = effective dose to kill 50%.

In Vivo

Survival Stu

Control
$Rh_2(OAc)_4$(

$Rh_2(O_2CEt)$

$Rh_2(O_2CPr$

[a]Dosage of
[b]Therapeut
increased l

Table 4

In Vivo

Survival Studies with Swiss albino mice bearing Ehrlich ascites tumors.[11b]

	Doses[a]	%ILS[b]	$LD10^{TI}$/ILS40[c]
Control	Saline	-----	-----
$Rh_2(OAc)_4(H_2O)_2$	6.78×10^{-5}	78	
	3.39×10^{-5}	88	1.8
	2.26×10^{-5}	44	
$Rh_2(O_2CEt)_4(H_2O)_2$	8.04×10^{-4}		
	5.02×10^{-4}	143	4.2
	2.01×10^{-4}	149	
	1.00×10^{-4}	17	
$Rh_2(O_2CPr)_4(H_2O)_2$	3.61×10^{-4}		
	1.80×10^{-4}	132	
	1.08×10^{-4}	197	4.7
	5.40×10^{-7}	173	
	1.80×10^{-7}	3	

[a]Dosage of drug (mol/Kg/day x 6 days. [b]ILS = increased life span.
[c]Therapeutic indices where LD10 = lethal dose of 10% and ILS40 = increased life span 40%.

Table 5

In vivo

$Rh(O_2CEt)_4$(poly-A) against Ehrlich ascites.[11e]

poly-A:Rh	Survival time[a]	%ILS[b]	survivors[c]
0:1	37.0	190	2
10:1	45.1	279	5
20:1	45.2	280	5
40:1	39.7	212	1
60:1	38.3	201	2
SalineControls	12.9		0
Saline/poly-A	12.7		0

[a]Mean survival time (days). [b]%ILS = increased life span. [c]Number of survivors at day 50.

In Vivo S
sarcor

cells day 0[a]

10^5

10^6

10^7

10^8

[a]The numb
(mmol x 1
survival tir
dead total

Table 6

In Vivo Studies of $Rh_2(DTolF)_2(O_2CCF_3)_2(H_2O)_2$ against Yoshida ascites sarcoma cells.[15c]

cells day 0[a]	Drug ILS%[f]	Dose[b] D/T[g]	Dose[c] LTS > 60 days[h]	Avg. life span[d]	time[e]
10^6	Rh(II) acetate	3	6.78	17.2 ± 4.18	
	17.2/10.7	60.7	6/10	4	
10^6	Rh(II) form	3	3.27	18.5 ± 5.74	
	18.5/11.4	62.3	5/10	5	
10^6	cisplatin	5	16.6	18.7 ± 10.4	
	18.7/10.7	74.8	4/20	16	
10^6	Rh(II) form	5	5.46	19.0 ± 4.24	
	19.0/11.4	66.7	2/18	16	

[a]The number of tumor cells at day 0. [b]Drug dose (mg/Kg). [c]Drug dose (mmol x 10^{-3}/Kg. [d]Average life span in days ± standard deviation. [e]Median survival time (treated/control). [f]ILS = increased life span. [g]D/T = dead/total. [h]LTS = long term survivors.

1. (a) Kep
Inorg.
D. in
Studies
York,
A. *Scie*
Rev. **19**
42, 71
Psychi
2. (a) Ros
Proce
Coord
Ed.; S
34, 15
615. (
1333.
Howe
Perez-
3. (a) Ro
York,
Lippa
New
Lippa
J. *Coo*
4. (a) Ba
Editio
1995.
5. White
Intera
Const
1996,
6. (a) Sl
Chem
Graaf
109, 4
7. Lippa
8. Sherm
230, 4

List of References

1. (a) Keppler, B. K. *New J. Chem.* **1990**, *14*, 389. (b) Sadler, P. *J. Adv. Inorg. Chem.* **1991**, *36*, 1. (c) McAuliffe, C. A.; Sharma, H. L.; Tinker, N. D. in *Chemistry of the Platinum Group Metals Recent Developments, Studies in Inorganic Chemistry 11*, Hartley, F. R., Ed.; Oxford, New York, **1991**, Ch. 16 and references therein. (d) Abrams, M. J.; Murrer, B. A. *Science*, **1993**, *261*, 725. (e) Brow, D. H.; Smith, W. E. *Chem. Soc. Rev.* **1980**, *9*, 217. (f) Silver, S.; Misra, T. K. *Annu. Rev. Microbiol.* **1988**, *42*, 717. (g) Birch, N. J., Ed.; *"Lithium: Inorganic Pharmacology and Psychiatric Use."* IRL Press, Oxford, **1988**, 11-39.
2. (a) Rosenberg, B.; VanCamp, L. *Nature*, **1969**, *222*, 385. (b) Thomson, A. *Proceedings of the Second International Symposium on Platinum Coordination Complexes in Cancer Chemotherapy*, Connors and Roberts, Ed.; Springer-Verlag, Berlin, **1974**. (c) Eastman, A. *Pharma. Ther.* **1987**, *34*, 155. (d) Pasini, A.; Zunino, F. *Angew. Chem. Int. Ed. Engl.* **1987**, *26*, 615. (e) Frey, U.; Ranford, J. D.; Sadler, P. J. *Inorg. Chem.* **1993**, *32*, 1333. (f) *Platinum and Other Metal Complexes in Cancer Chemotherapy*, Howell, S. B., Ed.; Plenum Press, New York, **1991**. (g) Baker, S. A. B.; Perez-Soler, R.; Khokhar, A. R. *J. Coord. Chem.* **1993**, *29*, 1
3. (a) Rosenberg, B.; in *Metal Ions in Biology*, Spiro, T. G., Ed.; Wiley, New York, **1980**, *1*, 1. (b) Umapathy, P. *Coord. Chem. Rev.* **1989**, *95*, 129. (c) Lippard B. Chapter 1 in *Prog. Inorg. Chem.* Lippard, S. J., Ed.; Wiley, New York, **1989**, *37*, 1, and references therein. (d) Sherman, S. E.; Lippard, S. J. *Chem. Rev.* **1987**, *87*, 1153. (e) Sundquist, W. I.; Lippard, S. J. *Coord. Chem. Rev.* **1990**, *100*, 293, and references therein..
4. (a) Baker, T. A.; Kornberg, A. *DNA Replication*, Freeman and Co. 2nd Edition, **1992**. (b) Stryer, L. *Biochemistry*, Freeman and Co. 4th Edition, **1995**. (c) Lewin, B. *Genes V*, Oxford University Press, **1994**.
5. Whitehead, J. P.; Lippard, S. J. in *Metal Ions in Biological Systems, Interactions of Metal Ions with Nucleotides, Nucleic Acids, and Their Constituents 32*. Sigel, A.; Sigel, H., Ed.; Marcel Dekker, Inc. New York, **1996**, Ch. 20 and references therein.
6. (a) Sherman, S. E.; Gibson, D.; Wang, A. H. J.; Lippard, S. J. *J. Am. Chem. Soc.* **1988**, *110*, 7368. (b) Admiraal, G.; van der Veer, J. L.; de Graaf, R. A. G.; den Hartog, J. H. J.; Reedijk, J. *J. Am. Chem. Soc.* **1987**, *109*, 592.
7. Lippard, S. J. *Pure & Appl. Chem.* **1987**, *59*, 731.
8. Sherman, S. E.; Gibson, D.; Wang, A. H. J.; Lippard, S. J. *Science*, **1985**, *230*, 412.

9. Takahara
Nature.
10.(a) Dmi
Cong. (
G.; Thor
11.(a) Erck
36, 220
Chemot
Bear, J.
Chem. 1
Chemot
12.(a) Pne
Rainen.
1975, *1*
B. S.; (
Haromy
Waysbo
13.(a) Du
Christo
Crawfo
Soc. **19**
Folting
1996, 1
14.Christo
results
15.(a) Pira
101. (b
Pirain
(c) Fin
2, 319
al. Ino
16.Dunba
17.Pruchn

9. Takahara, P. M.; Rosenzweig, A. C.; Frederick, C. A.; Lippard, S. J. *Nature*, **1995**, *377*, 649.
10. (a) Dmitrov, N. V.; Eastwood, G. W. *Current Chemother. Proc. Int. Cong. Chemother. 10th 1977*. **1978**, *2*, 1319. (b) Eastland, G. W.; Yang, G.; Thompson, T. *Meth. and Find. Exptl. Clin. Biochem.* **1989**, *10*, 41.
11. (a) Erck, A.; Sherwood, E.; Bear, J. L.; Kimball, A. P. *Cancer Res.* **1976**, *36*, 2204. (b) Bear, J. L.; Gray, Jr., H. B.; Rainen, L., et. al. *Cancer Chemotherapy Reports* **1975**, *59*, 611. (c) Howard, R. A.; Spring, T. G.; Bear, J. L. *Cancer Res.* **1976**, *36*, 4402. (d) Chen, J.; Kostic, N. M. *Inorg. Chem.* **1988**, *27*, 2862. (e) Bear, J. L.; Howard, R. A.; Dennis, A. M. *Curr. Chemother. Proc. Int. Congress Chemother. 10th Meeting*, **1977**, *vol 2*.
12. (a) Pneumatikakis, G.; Hadjiliadis, N. *J. C. S. Dalton* **1979**, 596. (b) Rainen, L.; Howard, R. A.; Kimball, A. P.; Bear, J. L. *J. Inorg. Chem.* **1975**, *11*, 2752. (c) Farrell, N. *J. Inorg. Biochem.* **1981**, *14*, 261. (d) Yu, B. S.; Choo, S. Y. *J. Pharm. Soc. Kor.* **1975**, *19*, 215. (e) Rubin, J. R.; Haromy, T. P.; Sundaralingam, M. *Acta Cryst.* **1991**, *C47*, 1712. (f) Waysbort, D.; Tarien, E.; Eichorn, G. L. *Inorg. Chem.* **1993**, *32*, 4774.
13. (a) Dunbar, K. R.; Matonic, J. H., Saharan, V. P.; Crawford, C. A.; Christou, G. J. *J. Am. Chem. Soc.* **1994**, *116*, 2201. (b) Day, E. F.; Crawford, C. A.; Folting, K.; Dunbar, K. R.; Christou, G. *J. Am. Chem. Soc.* **1994**, *116*, 9339. (c) Crawford, C. A.; Day, E. F.; Saharan, V. P.; Folting, K.; Huffman, J. C.; Dunbar, K. R.; Christou, G. *Chem. Commun.* **1996**, 1113.
14. Christou, G. J.; Crawford, C. A.; Dunbar, K. R.; Folting, K. unpublished results.
15. (a) Piraino, P.; Tresoldi, G.; Schiavo, S. L. *Inorg. Chim. Acta* **1993**, *203*, 101. (b) Schiavo, S. L.; Sinicropi, M. S.; Tresoldi, G.; Arena, C. G.; Piraino, P. *J. Chem. Soc. Dalton Trans.* **1994**, 1517 and references therein. (c) Fimiani, V.; Ainis, T.; Cavallaro, A.; Piraino, P. *J. Chemother.* **1990**, *2*, 319 and references therein. (d) Piraino, P.; Bruno, G.; Tresoldi, G.; *et al. Inorg. Chem.* **1987**, *26*, 91.
16. Dunbar, K. R.; Chifotides, H., T. Patel, D. unpublished results.
17. Pruchnik, F.; Dus, D. *J. Inorg. Biochem.* **1996**, *61*, 55.

Reaction

Chapter II
Reactions of Substituted DNA Purines with Dirhodium Complexes that Contain Formamidinate Ligands.

1. Introduc

Sinc

effective a

metal com

1). Of the

= Me, Et

Human O

performed

the antitu

The inhib

thought t

Ea

preferen

favorabl

stabilize

group a

X-ray st

2).[e] B

atom at

lone pa

1. Introduction

Since the discovery of cisplatin, *cis*-$PtCl_2(NH_3)_2$ or *cis*-DDP, as an effective antitumor agent, similar investigations of other platinum group metal complexes have unearthed a variety of active metal complexes (Figure 1). Of these compounds, the dirhodium tetracarboxylates, $Rh_2(O_2CR)_4L_2$ (R = Me, Et Ph or CF_3; L = donor solvent), are active against such tumors as Human Oral Carcinoma, Ehrlich ascites, L1210 and P388.[1] Early studies performed by Bear and coworkers pointed to DNA binding as the origin of the antitumor activity of these compounds, in a manner akin to cisplatin. The inhibition of DNA synthesis as a result of Pt-DNA interactions is thought to be a major factor that contributes to cisplatin's antitumor activity.

Early studies of $Rh_2(OAc)_4$ with DNA nucleobases revealed a strong preference for adenine over guanine which was said to be due to the favorable axial ligation of adenine.[2],[3] This axial interaction is thought to be stabilized by hydrogen binding interactions between the exocyclic amine group and a carboxylate oxygen atom which is observed in a single-crystal X-ray structure of the bis(1-methyladenosine) adduct of $Rh_2(OAc)_4$ (Figure 2).[2e] By employing similar arguments, researchers suggested that the O atom at position 6 of guanine would result in a repulsive interaction with the lone pairs on the carboxylate oxygen atoms, thus the binding of the

dirhodium

study. per

interaction

than σ-bon

explain th

Regardles

conclusion

carboxyla

positions

bridge dir

also to fo

(Figure 4

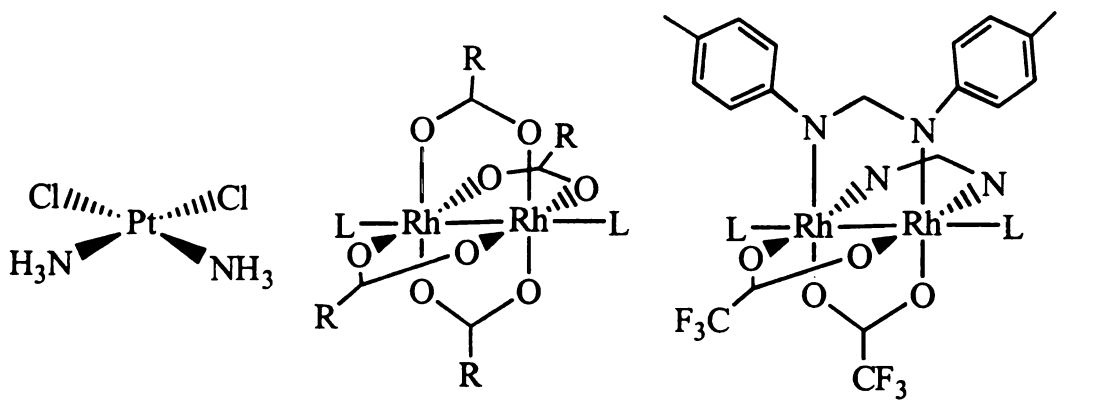
actual DX



Ci

Figure
that ex

dirhodium carboxylates to guanine would be disfavored. In a quite different study, performed by Eichorn and coworkers, NMR data indicated that interactions between the dirhodium carboxylates and adenosine is π- rather than σ-bonded in the axial positions, which these researchers claimed would explain the specificity of adenosine over the poorer π-acceptor guanosine.[2f] Regardless of these earlier conclusions, work in our laboratories supports the conclusion that guanine does, in fact, bind to dinuclear transition metal carboxylate compounds via bridging interactions involving the N7 and O6 positions (Figure 3).[4] In addition, adenine has been observed not only to bridge dinuclear transition metal centers in a similar manner to guanine, but also to form chelates at of the metal centers through the N7 and N6 positions (Figure 4). The existence of these bridging or chelating interactions in actual DNA treated with dirhodium tetracarboxylate compounds remains to



Cisplatin $Rh_2(O_2CR)_4L_2$ $Rh_2(DTolF)_2(O_2CCF_3)_2L_2$

Figure 1. Structures of dinuclear transition metal anticancer compounds that exhibit antitumor activity.

replotted from X-ray coordinates.

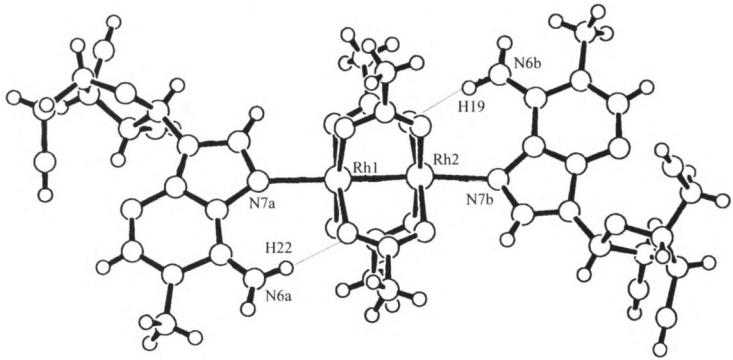


Figure 2. PLUTO diagram of $Rh_2(O_2CCH_3)_4$(1-methyladenosine)$_2$ replotted from X-ray coordinates.[2e]

be determi

The

tetracarbo

Rh_2(DTolF

prepared b

sarcoma c

antitumor

inhibition

Rh_2(DTol

react wit

coworker

earlier su

prompted

core to d

purines.

mixed-lig

formami

9- EtG

$EtGH)_2$(

of 9-ethy

be determined.

The antitumor activity of dirhodium compounds is not limited to the tetracarboxylate compounds. For example, the mixed-ligand compound, $Rh_2(DTolF)_2(O_2CCF_3)_2(H_2O)_2$ (DTolF = N,N'-*p*-tolylformamidinate), first prepared by Piraino and coworkers, is active against Yoshida ascites and T8 sarcoma cells *in vivo* (Figure 1).[5] Like tetracarboxylate compounds, the antitumor activity of this compound is thought to be the result of the inhibition of DNA synthesis. Furthermore, Piraino reports that $Rh_2(DTolF)_2(O_2CCF_3)_2(H_2O)_2$ has a high affinity for adenine, but does not react with guanine which is the same conclusion drawn by Bear and coworkers for $Rh_2(O_2CR)_4$ reactions. All of these facts combined with our earlier success with the purine reactions of dirhodium tetracarboxylates prompted us to investigate the nucleobase chemistry of the $[Rh_2(DTolF)_2]^{2+}$ core to determine the mode of binding to the dirhodium unit adopted by the purines. Contrary to the literature report concerning the reactivity of the mixed-ligand compound, $Rh_2(DTolF)_2(O_2CCF_3)_2(H_2O)_2$, we found that the formamidinate compounds do in fact react with guanine bases, in this case, 9- EtGH.[6] Herein we report the structure of $[Rh_2(DTolF)_2(9\text{-}EtGH)_2(CH_3CN)_2][BF_4]_2$. In addition, the reaction between two equivalents of 9-ethyladenine (9-EtAH) and $[Rh_2(DTolF)_2(CH_3CN)_6][BF_4]_2$ **(2)** to form

$[Rh_2(DTolF)_2(9\text{-}EtAH)_2(CH_3CN)][BF_4]_2$ **(4)** is also presented. The structure of the acetonitrile adduct of the anticancer active compound $Rh_2(DTolF)_2(O_2CCF_3)_2(CH_3CN)_2$ **(1)** as well as the analogous reaction with 9-EtAH is discussed along with the structure of the bis-acetate derivative of compound **(1)**.

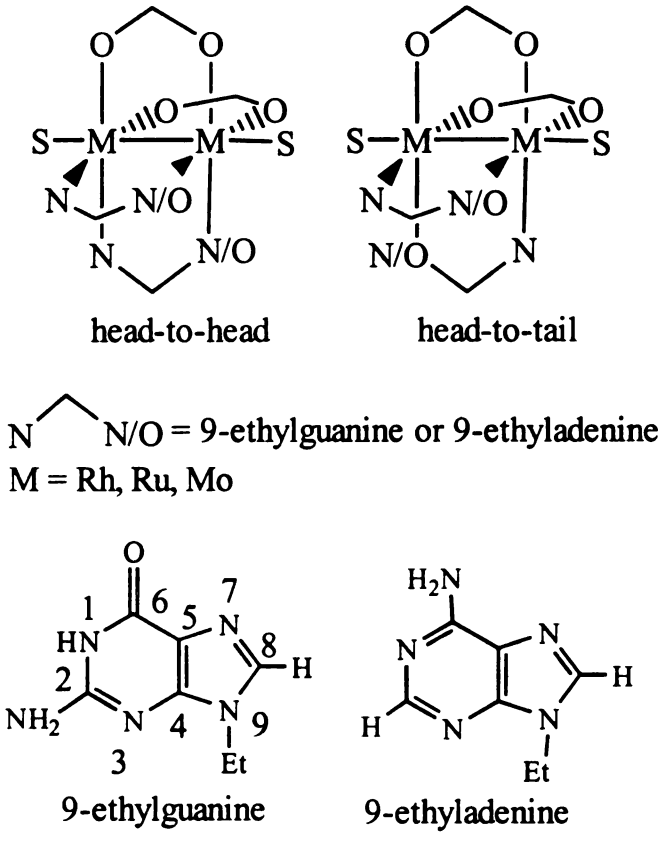


Figure 3. Schematic representation of the H-H and H-T bridging modes of the DNA purines 9-EtGH and 9-EtAH to dinuclear transition metal centers.

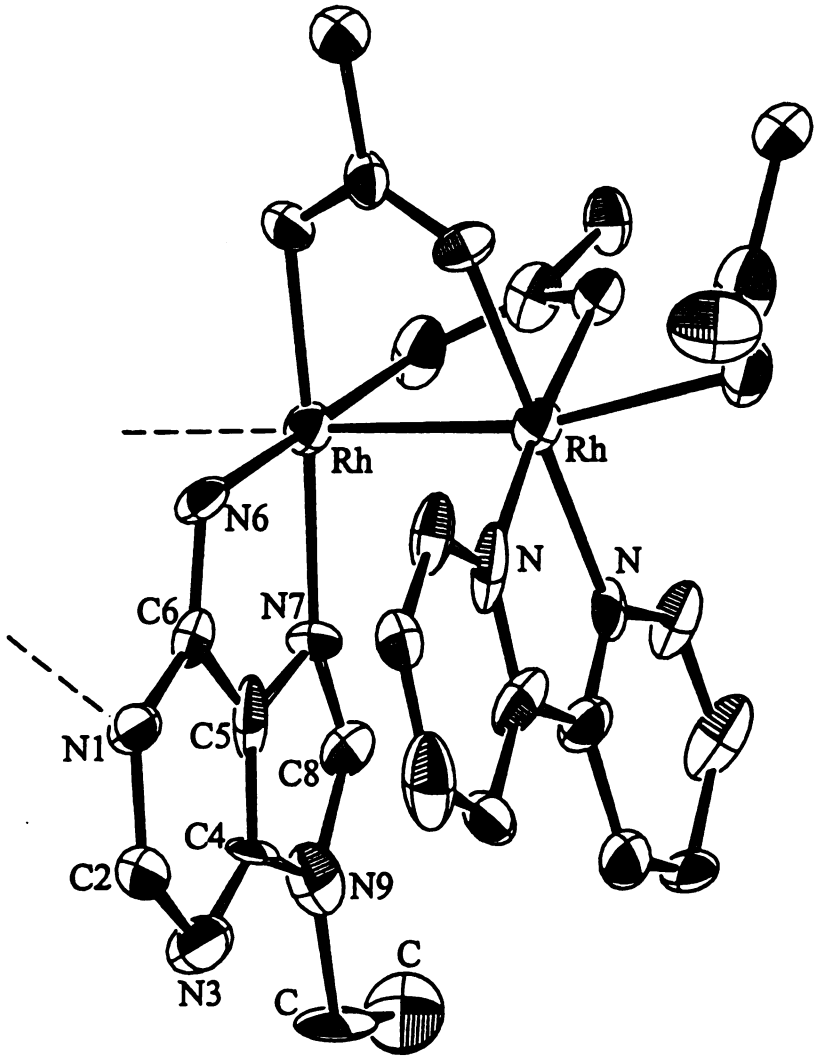


Figure 4. Example of a chelating 9-EtAH ligand depicted in the ORTEP representation of $[Rh_2(O_2CCH_3)_2(bpy)(9\text{-EtA})]^{2+}$.[4d]

2. Experim

A. Physica

The in

spectropho

dimensiona

Varian Sp

residual

measurem

Research

Model VI

[Rh_2(DTc

containin

supportin

with 0.

supportin

reference

potentia

and E

(4), resp

2. Experimental Section

A. Physical Measurements.

The infrared spectra were collected on a Nicolet 740 FT-IR spectrophotometer. All ^1H NMR spectroscopic data including the 2-dimensional experiments were collected on either a 300 or a 500 MHz-Varian Spectrometer. Chemical shifts were referenced relative to the residual proton impurities of the solvents used. Electrochemical measurements were performed by using an EG&G Princeton Applied Research Model 362 scanning potentiostat in conjunction with a Soltec Model VP-6424S X-Y recorder. The cyclic voltammetric experiments for $[Rh_2(DTolF)_2(CH_3CN)_6][BF_4]_2$ **(4)** were carried out at r.t. in acetonitrile containing 0.1 M tetra-*n*-butylammonium hexafluorophosphate, $TBAPF_6$, as supporting electrolyte while the experiments for **(3)** and **(4)** were performed with 0.1 M tetra-*n*-butylammonium tetrafluoroborate, $TBABF_4$, as supporting electrolyte. $E_{1/2}$ values, determined as $(E_{p,a} + E_{p,c})/2$, were referenced to the Ag/AgCl electrode without correction for junction potentials. The Cp_2Fe/Cp_2Fe^+ couple occurs at $E_{1/2} = {}^+0.46$ V, $E_{1/2} = {}^+0.53$ V and $E_{1/2} = {}^+0.45$ V for the cyclic voltammograms of compounds **(2)**, **(3)** and **(4)**, respectively, under the same experimental conditions in acetonitrile.

B. Syntheses

i. Starting Materials

The compounds, $[Rh(DTolF)(cod)]_2$ (cod = 1,4-cyclooctadiene) and $[Rh_2(DTolF)_2(CH_3CN)_6][BF_4]_2$ **(2)**, were prepared according to the literature procedures.[6,7a] $Rh_2(DTolF)_2(O_2CCF_3)_2(CH_3CN)_2$ **(1)**, 9-ethyladenine (9-EtAH) and $[Rh_2(DTolF)_2(9\text{-}EtGH)_2(CH_3CN)][BF_4]_2$ **(3)** were prepared using modified literature procedures.[6,7b,8] 9-Ethylguanine was purchased from Sigma whereas $AgBF_4$ NaO_2CCH_3, and $NaO_2CCH_3 \cdot 7H_2O$ were purchased from Aldrich. In all cases, commercial reagents were used without further purification. The ligand 9-EtAH was prepared by a modification of the literature procedure.[8] Prior to distillation under a nitrogen atmosphere, all solvents were predried from 4 Å molecular sieves with the exception of acetone and acetonitrile, which were predried with 3 Å molecular sieves. Diethyl ether was distilled from sodium/potassium benzophenone ketyl radical whereas toluene was also distilled from Na/K drying agent with no indicator. Acetone and acetonitrile were distilled from 3 Å molecular sieves while methylene chloride was distilled from P_2O_5. The acetonitrile used for the electrochemical measurements was further purified by passing it through an activated alumina column further purified.

ii. Rea

inert atmosp

otherwise sta

(1) Modifie

slurry of [R

methanol an

AgO_2CCF_3

allowed to s

crystallizatio

by filtration.

(2) Modifie

adenine (8

tetraethylam

bottomed fl

The reactio

evaporated

205 °C usin

further puri

of purified

spectroscop

ii. Reaction Procedures. All manipulations were performed under inert atmospheric conditions using standard Schlenk techniques unless otherwise stated.

(1) Modified Preparation of $Rh_2(DTolF)_2(O_2CCF_3)_2(CH_3CN)_2$ (1). A slurry of $[Rh(DTolF)(cod)]_2$ (157 mg, 0.32 mmol) and a 1:1 mixture of methanol and methylene chloride (7 mL) was treated with 3 mL of a AgO_2CCF_3 (281 mg, 1.3 mmol) methanol solution. The mixture was allowed to stir for 24 h at r.t., and then treated with diethyl ether to induce crystallization of the product. The green crystalline material was collected by filtration, and dried in air (204 mg, 69% yield).

(2) Modified Preparation of 9-ethyladenine (9-EtAH). An amount of adenine (828 mg, 6.13 mmol) and 2.58 g of 35% aqueous tetraethylammonium hydroxide were placed into a long neck 50 mL round-bottomed flask equipped with an internal condensor and a Schlenk adapter. The reaction mixture was stirrred for ½ h at r.t. and the water was evaporated to yield an off-white residue. The residue was sublimed at 200 – 205 °C using the internal condensor to collect the 9-EtAH. The purine was further purifed by recrystallization from methyl ethyl ketone to yield 800 mg of purified material (80% yield). Purity was confirmed by ^1H NMR spectroscopy in D_2O, CD_3CN and CD_3OD.

(3) [Rh_2(D

0.0556 mm

solution (3

for ~2 days

with dieth

$C_6H_5CH_3$ in

(4) **NMR**

Rh_2(DTolF

After obtai

added to th

for 72 h du

spectrum o

72 h period

(5) **Prepa**

compound

NaO_2CCH_3

stirred at r.t

turned ligh

material, a

through a f

(3) $[Rh_2(DTolF)_2(9\text{-}EtAH)_2(CH_3CN)][BF_4]_2$ (4). Compound **(2)** (60.3 mg, 0.0556 mmol) was dissolved in CH_3CN (2 mL) and treated with a CH_3CN solution (3 mL) of 9-EtAH (18.2 mg, 0.112 mmol). The mixture was stirred for ~2 days and the resulting green product was precipitated from solution with diethyl ether; single crystals were grown from the diffusion of $C_6H_5CH_3$ into a solution of CH_3CN **(4)**.

(4) NMR Tube Reaction of (1) with 9-EtAH. An NMR sample of $Rh_2(DTolF)_2(O_2CCF_3)_2(CH_3CN)_2$ **(1)** was prepared in CD_3CN (0.4 mL). After obtaining the ^1H NMR spectrum of the starting material, 9-EtAH was added to the red-violet dirhodium solution. The mixture was stirred at r.t. for 72 h during which time the solution color turned green. The ^1H NMR spectrum of the reaction mixture was monitored at various times during the 72 h period.

(5) Preparation of $Rh_2(DTolF)_2(O_2CCH_3)_2(H_2O)$ (6). An amount of compound **(2)** (97 mg, 0.0089 mmol) was dissolved in acetonitrile (5 mL), $NaO_2CCH_3 \cdot 4H_2O$ (17 mg, 0.021 mmol) was added, and the mixture was stirred at r.t. for 2 days. During this time, the color of the reaction mixture turned light green compared to the dark orange-red color of the starting material, and a white precipitate formed. The mixture was filtered in air through a frit covered with Celite, and treated with diethyl ether (~ 20 mL),

but this did

the solutio

produced gr

C. X-ray C

compound

diffractome

Mo Kα (w

corrected fo

structure so

Silicon Grap

Chemistry a

of the Mole

data for con

diffractome

average λ_{α}

polarization

computer.

package, a

program.[10]

using the S

but this did not serve to bring the compound out of solution. Consequently, the solution was allowed to slowly evaporate in air, which eventually produced green crystals that were suitable for a single crystal X-ray study.

C. X-ray Crystallography and Structure Solution. A quadrant of data for compound **(4)** were collected at 173 ± 2 K on a Nicolet P3/V diffractometer upgraded to a Siemens P3/F with graphite monochromated Mo Kα (with average $\lambda_\alpha = 0.71073$ Å) radiation; the reflections were corrected for Lorentz and polarization effects. All calculations for the structure solution and the refinement of compound **(4)** were performed with Silicon Graphics computers on a cluster network within the Department of Chemistry at Michigan State University using the Texsan software package of the Molecular Structure Corporation.[9] A hemisphere of crystallographic data for compounds **(1)**, **(3)**, and **(6)** was collected on a Siemens SMART diffractometer at 173 ± 2 K with graphite monochromated Mo Kα (with average $\lambda_\alpha = 0.71073$ Å) radiation and were corrected for Lorentz and polarization effects. Calculations were performed on a Silicon Graphics computer. The frames were integrated with the Siemens SAINT software package, and the data were corrected for absorption using the SADABS program.[10] The structures of **(1)**, **(3)** and **(6)** were solved by direct methods using the SHELXS program in the Siemens SHELXTL v. 5.05 software.[11a]

Refinements were carried out by full-matrix least-squares calculations on F^2 using the SHELXL-97 program.[11b] All relevant crystallographic values and other pertinent information for compounds **(1)**, **(3)**, **(4)** and **(6)** are listed in Tables 12 - 15.

(1) $Rh_2(DTolF)_2(O_2CCF_3)_2(CH_3CN)_2$ (1). A orange-red rectangular platelet having dimensions 0.31 x 0.11 x 0.10 mm^3 was obtained from the evaporation of an acetonitrile solution of **(1)**, and mounted on the tip of a glass fiber with Dow Corning grease. Indexing and refinement of 59 reflections selected from a total of 45 frames with an exposure time of 10 sec/frame gave unit cell parameters for a monoclinic unit cell. A total of 1,321 frames were collected with a scan width of 0.3° in ω and an exposure time of 30 sec/frame. The total data collection time was 13.5 h. The integration of the frame data using a monoclinic B-centered unit cell constraint yielded reflections totaling 25,160 in the range $h = 14 \rightarrow {}^{-}14$, $k = 27 \rightarrow {}^{-}28$, $l = 23 \rightarrow {}^{-}15$ with a maximum 2θ angle of 56.78°. Of the 10,101 unique reflections, a total of 3,761 reflections remained with $I > 2\sigma(I)$ and $R_{int} = 0.1177$ and $R_{sig} = 0.1912$ after data reduction. The positions of all of the non-hydrogen atoms were located by direct methods. All non-hydrogen atoms were refined anisotropically while the hydrogen atoms were

calculated a

restraints ga

of-fit param

the final c

respectively

(2) [Rh_2(D

(4) were gro

toluene. A

0.31 x 0.23

Corning gre

obtained fro

$2\theta < 21°$.

maximum 2

that were co

the data co

significant

correction v

near 90°.

program, a

carbon ato

calculated at fixed positions. Final refinement of 506 parameters and 31 restraints gave residuals of R1 = 0.0451 and wR2 = 0.0904. The goodness-of-fit parameter was 0.992 with the maximum and minimum peak heights in the final difference Fourier map being 0.649 e/Å^3 and –0.994 e/Å^3, respectively.

(2) $[Rh_2(DTolF)_2(9\text{-}EtAH)_2(CH_3CN)](BF_4)_2$ (4). X-ray quality crystals of **(4)** were grown from the slow diffusion of an acetonitrile solution of **(4)** into toluene. A green rectangular crystal having the approximate dimensions 0.31 x 0.23 x 0.18 mm^3 was mounted on the tip of a glass fiber with Dow Corning grease. Cell constants for the monoclinic space group $P2_1/c$ were obtained from a least-squares refinement of 25 reflections in the range $15 < 2\theta < 21°$. The data were collected using the ω-2θ scan technique to a maximum 2θ value of 45° in the range $4 < 2\theta < 45°$. Of the 7,151 reflections that were collected, 6,841 were unique with $R_{int} = 0.119$. Over the course of the data collection, standards collected every 150 reflections revealed no significant decrease in diffraction intensity. An empirical absorption correction was applied on the basis of azimuthal scans of 3 reflections with χ near 90°. The structure was solved by direct methods using the MITHRIL program, and expanded using difference Fourier techniques. The ethyl carbon atoms of the 9-EtAH molecules and the aromatic carbon atoms of the

DTolF gro

atoms wer

fixed posi

2.240 obse

and R_w = (

revealed t

be ~0.65 e

(3) [Rh_2(I

having ap

the evapor

which was

fiber with

a scan wi

107 reflec

refined to

were integ

reflections

maximum

reflections

DTolF groups were refined isotropically while the remaining non-hydrogen atoms were refined anisotropically. All hydrogen atoms were calculated at fixed positions. The final least-squares refinement of 503 parameters on 2,240 observed reflections ($I > 3.00\sigma(I)$) resulted in residuals of $R_1 = 0.063$, and $R_w = 0.073$ and a goodness-of-fit = 1.30. A final difference Fourier map revealed the highest peak to be 0.75 $e^-/Å^3$ and the minimum peak height to be $^-0.65$ $e^-/Å^3$.

(3) $[Rh_2(DTolF)_2(9\text{-}EtGH)_2(CH_3CN)](BF_4)_2$ (3). A green prismatic platelet having approximate dimensions 0.10 x 0.08 x 0.06 mm^3 was obtained from the evaporation of a methylene chloride solution of **(3)**. The selected crystal, which was quite small and soft, was carefully mounted on the tip of a glass fiber with Dow Corning grease. A total of 1,321 frames were collected with a scan width of 0.3° in ω and an exposure time of 44 sec/frame. A total of 107 reflections were indexed from 15 of these frames. The reflections were refined to give unit cell parameters for a triclinic unit cell. The data collected were integrated using a triclinic unit cell constraint to yield a total of 31,002 reflections in the range $h = 13 \rightarrow ^-14$, $k = 24 \rightarrow ^-27$, $l = 19 \rightarrow ^-29$ with a maximum 2θ angle of 56.68°. After data reduction of the 12,287 unique reflections, 4,834 reflections remained with $I > 2\sigma(I)$. The R_{int} and R_{sig}

values w

indicative

were loca

located

difference

positions.

the $[BF_4]$

disordered

refined iso

The hydrog

least-square

e Å^3 and -0

wR2 = 0.01

fit parameter

(4) $Rh_2(DT$

dimensions

acetonitrile

on the tip

refinement

values were 0.1480 and 0.2539, respectively. These fairly high residuals are indicative of the low quality of the crystal. The positions of the Rh atoms were located by direct methods. The remaining non-hydrogen atoms were located through successive cycles of least-squares refinements and difference Fourier maps. A disordered $[BF_4]^-$ anion was modeled over two positions. All of the non-hydrogen atoms of the cationic complex and one of the $[BF_4]^-$ anions were refined anisotropically. The F atoms of the disordered $[BF_4]^-$ anion were refined anisotropically while the B atom was refined isotropically with a constraint on the isothermal temperature factor. The hydrogen atoms were refined at fixed positions. The final full-matrix-least-squares on F^2 revealed maximum and minimum peak heights of 1.43 e/Å^3 and -0.732 e/Å^3, respectively, with final residuals of R1 = 0.0898 and wR2 = 0.01484 for 694 parameters and 95 restraints. The final goodness-of-fit parameter was 0.974.

(4) $Rh_2(DTolF)_2(O_2CCH_3)_2(H_2O)$ (6). A green prismatic platelet having dimensions 0.62 x 0.23 x 0.13 mm^3 was obtained from the evaporation of an acetonitrile/diethyl ether solution of **(6)**. The selected crystal was mounted on the tip of a glass fiber with Dow Corning grease. Indexing and refinement of 30 reflections selected from a total of 45 frames with an

exposure ti

cell. A tot

and an exp

unit cell p

integrated

reflections

maximum

reflections.

values were

were locat

were locat

difference

anisotropic

Final refine

= 0.1101.

minimum

and -0.623

exposure time of 10 sec/frame gave unit cell parameters for a triclinic unit cell. A total of 1,321 frames were collected with a scan width of 0.3° in ω and an exposure time of 30 sec/frame. The reflections were refined to give unit cell parameters for a triclinic unit cell. The data collected were integrated using a triclinic unit cell constraint to yield a total of 14,683 reflections in the range h = 14 → -14, k = 13 → -16, l = 17 → -19 with a maximum 2θ angle of 56.50°. After data reduction of the 8,033 unique reflections, 4,413 reflections remained with $I > 2\sigma(I)$. The R_{int} and R_{sig} values were 0.0577 and 0.1333, respectively. The positions of the Rh atoms were located by direct methods, and the remaining non-hydrogen atoms were located through successive cycles of least-squares refinements and difference Fourier maps. All non-hydrogen atoms were refined anisotropically while the hydrogen atoms were calculated at fixed positions. Final refinement of 422 parameters gave residuals of R1 = 0.0628 and wR2 = 0.1101. The goodness-of-fit parameter was 1.081 with the maximum and minimum peak heights in the final difference Fourier map being 1.021 e/Å^3 and -0.623 e/Å^3, respectively.

3. Results

A. Modifie

(1)

Rh_2(DTolF

for the a

Rh_2(DTolF

greater yie

more pure.

acetonitrile

[Rh(DTolF

(2) M

Rh_2(DTolF

lantern stru

Rh_2(DTolF

dirhodium

$[O_2CCF_3]$

the Rh a

3. Results and Discussion.

A. Modified Preparation of $Rh_2(form)_2(O_2CCF_3)_2L_2$ (1)

(1) Syntheses. The synthesis of the antitumor active compound $Rh_2(DTolF)_2(O_2CCF_3)_2(H_2O)_2$ was modified by excluding water as a solvent for the addition of AgO_2CCF_3 which leads to the isolation of $Rh_2(DTolF)(O_2CCF_3)_2L_2$ **(1)** (L = CH_3CN or CH_3OH). This occurs in greater yields than the corresponding aqueous reaction, and the product is more pure.[7b] Contrary to the literature report, we did not observe the red bis-acetonitrile adduct rapidly convert to the green water adduct in air.[7b]

$$[Rh(DTolF)(cod)]_2 \xrightarrow[4(AgO_2CCF_3)]{CH_3CN/\ CH_2Cl_2} \underset{\mathbf{1}}{Rh_2(DTol)_2(O_2CCF_3)_2(CH_3CN)_2} \quad (1)$$

(2) Molecular Structure of (1). Substitution of the axial water in $Rh_2(DTolF)_2(O_2CCF_3)_2$ with acetonitrile results in subtle changes in the lantern structure of the mixed-ligand complex. An ORTEP representation of $Rh_2(DTolF)_2(O_2CCF_3)_2(CH_3CN)_2$ **(1)** is presented in Figure 5. The dirhodium core consists of two *cis* bridging $[DTolF]^-$ ligands, two bridging $[O_2CCF_3]^-$ ligands and two axial CH_3CN molecules. The geometry around the Rh atoms is essentially octahedral with a Rh-Rh bond length of

2.4743(5) Å. This is longer than the Rh-Rh bond length of the bis-water adduct for which Rh-Rh = 2.425(1) Å.[7b] The lengthening of the metal-metal bond can be attributed to the increased interaction of the axial acetonitrile molecules which are coordinated at Rh-N bond distances of 2.267(5) Å and 2.265(5) Å for Rh(1)-N(3) and Rh(2)-N(4), respectively. Interestingly, both axial acetonitriles are coordinated at angles significantly less than 180°, with the Rh(1)-Rh(2)-N(4) angle being 172.37(11)° and the Rh(2)-Rh(1)-N(3) angle being 168.88(11)°. The bis-water adduct exhibits similar bends for the axial waters (average Rh-Rh-O angle of 168.6[1]°). A comparable bend was also observed in the compound $[Rh_2(DTolF)_2(bpy)(CH_3CN)_4][BF_4]_2$ **(7)** where one of the axial acetonitrile ligands is coordinated at the acute angle of 161.9(26)° (Chapter 2).[14] The average Rh-O bond distance of the coordinated trifluoroacetate groups of 2.098[3] Å is slightly longer than the average Rh-O distance of 2.083[3] Å in the bis-water adduct. The O-C-O angles of the trifluoroacetate groups are 129.7(5)° and 131.4(5)° for O(1)-C(28)-O(3) and O(2)-C(31)-O(4), respectively. The $[O_2CCF_3]^-$ groups are twisted by 5.32(13)° and 6.03(14)° from the eclipsed orientation in comparison to the 8.0(1)° and 8.3(1)° twists of the $[O_2CCF_3]^-$ in the bis-water adduct. The $[DTolF]^-$ groups are coordinated at an average Rh-N distance of 2.011[4] Å, and are within normal ranges. Likewise, the N-C-N

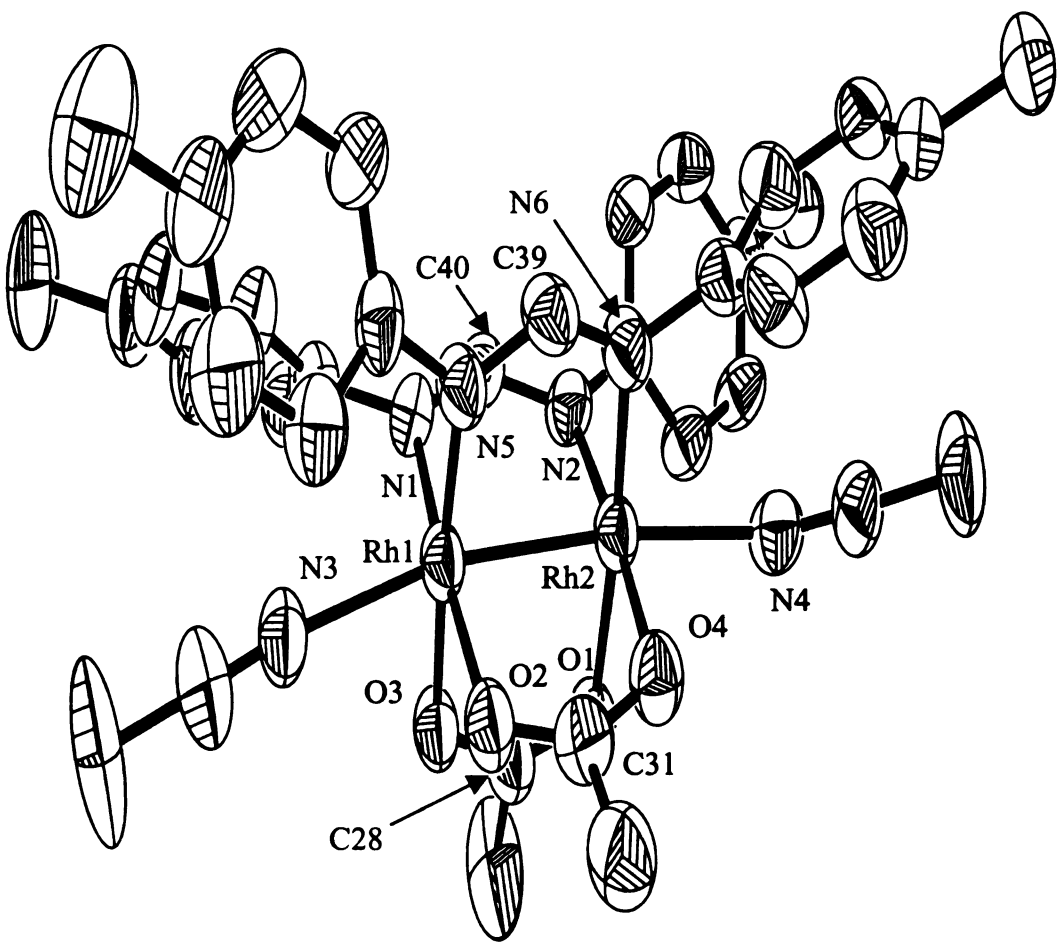


Figure 5. ORTEP representation of compound **(1)** drawn at the 50% probability level. H and F atoms are omitted for clarity.

angles of the bridgehead C atoms of 124.4(5)° and 125.8(5)° are within normal ranges. The [DTolF]$^-$ groups are slightly twisted from the eclipsed orientation by 5.4(2)° and 5.6(2)° in comparison to the larger twists reported for the bis-water adduct of 9.4(2)° and 9.5(2)°.

B. Reaction of $[Rh_2(DTolF)_2(CH_3CN)_6][BF_4]_2$ (2) with 9-EtGH

(1) Synthesis. The partially solvated compound, $[Rh_2(DTolF)_2(CH_3CN)_6][BF_4]_2$ **(2),** reacts with two equivalents of 9-EtGH in methanol/acetonitrile and also in methanol/methylene chloride mixtures under refluxing conditions to yield $[Rh_2(DTolF)_2(9\text{-}EtGH)_2(CH_3CN)][BF_4]_2$ **(3)** (Equation 2). Similar to the 9-EtGH reactions with the dirhodium bis- and tetracarboxylate compounds with this purine, two isomers are formed as judged by the ^1H NMR spectrum which will be discussed later in this chapter. Similar products are obtained for the reaction between compound **(1)** and 9-EtGH.

$$\underset{\mathbf{5}}{[Rh_2(DTolF)_2(CH_3CN)_6][BF_4]_2} + 2(9\text{-}EtGH) \xrightarrow[\text{reflux 2h}]{CH_3OH/CH_3CN} \underset{\mathbf{7}}{[Rh_2(DTolF)_2(9\text{-}EtGH)_2(CH_3CN)][BF_4]_2} \quad (2)$$

(2) Electrochemistry of (3). A cyclic voltammogram of crystals of $[Rh_2(DTolF)_2(9\text{-}EtGH)_2(CH_3CN)][BF_4]_2$ **(3)** dissolved in CH_3CN exhibits two reversible oxidations at $^{+}0.67$ V and $^{+}2.63$ V and one irreversible reduction at $^{-}1.31$ V (Figure 6). The cyclic voltammogram of compound **(2)** exhibits one reversible oxidation at $E_{1/2} = {}^{+}1.02$ V and one quasi-reversible oxidation at $E_{p,a} = {}^{+}1.55$ V (return wave at $E_{p,c} = {}^{+}1.40$ V) (Figure 2.6). Two irreversible reductions are observed at $E_{p,c} = {}^{-}0.51$ V and $^{-}1.34$ V in comparison to the bis-trifluoroacetate adduct, which exhibits only two reversible oxidation processes at $^{+}0.52$ V and $^{+}1.41$ V, and the free formamidinate ligand which exhibits an irreversible oxidation at $^{+}0.95$ V.[7b]

(3) Molecular Structure of (3). The compound $[Rh_2(DTolF)_2(9\text{-}EtGH)_2(CH_3CN)][BF_4]_2$ **(3)** crystallizes in the monoclinic space group $P2_1/n$. The ORTEP diagram of the cation, displayed in Figure 7, consists of two neutral 9-EtGH groups bridging the dinuclear unit in a head-to-head arrangement, two *cis* $[DTolF]^{-}$ bridges, and a single axial acetonitrile molecule. The structures of dirhodium compounds with bridging 9-EtGH molecules, namely, $[Rh_2(O_2CCH_3)_2(9\text{-}EtGH)_2((CH_3)_2O)(H_2O)][BF_4]_2$,

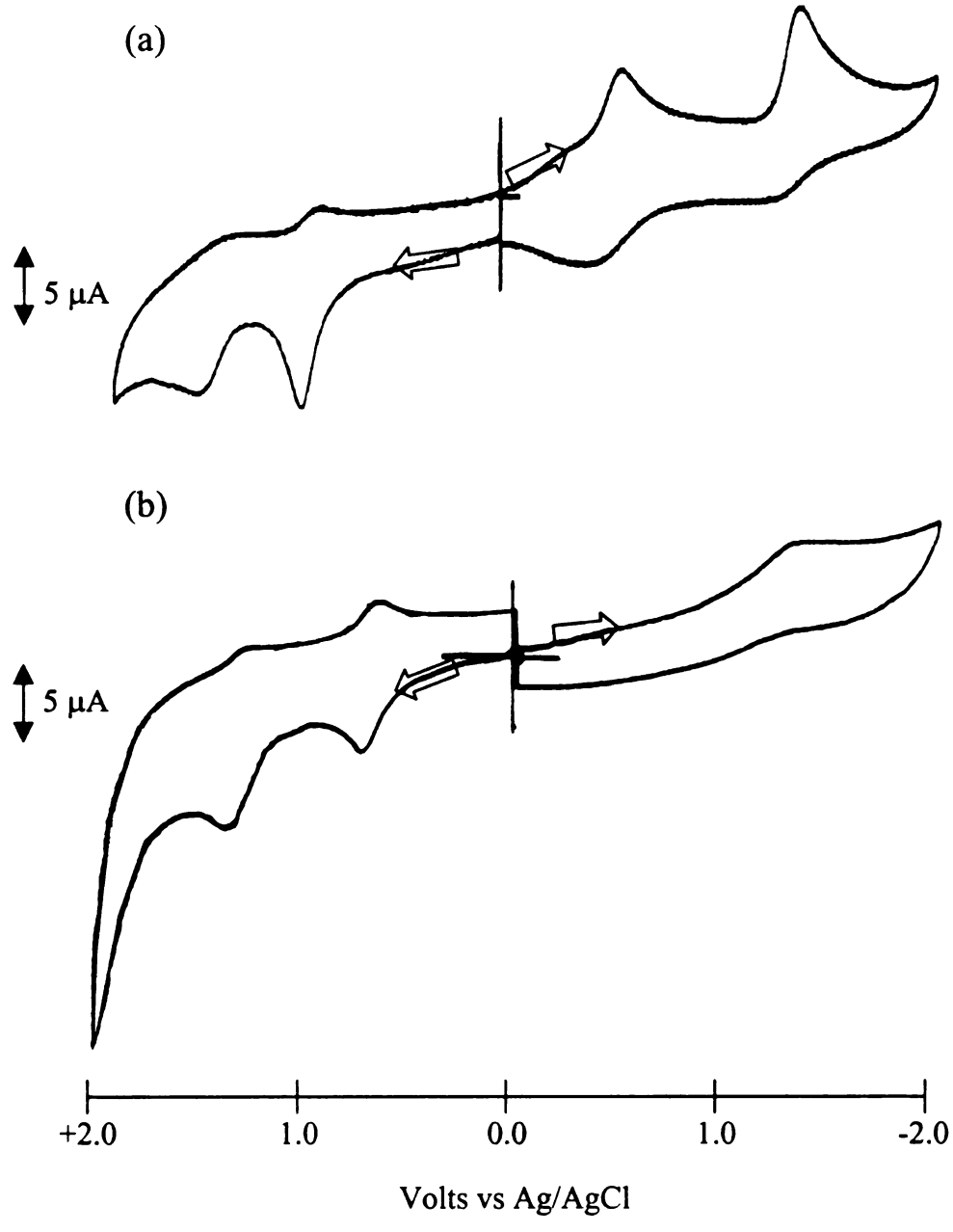


Figure 6. Cyclic voltammograms in 0.1 M electrolyte-CH_3CN at a scan rate of 200 mV/s using a Pt electrode for (a) $[Rh_2(DTolF)_2(CH_3CN)_6][BF_4]_2$ **(2)** and (b) $[Rh_2(DTolF)_2(9\text{-}EtGH)_2(CH_3CN)][BF_4]_2$ **(3)**.

$Rh_2(O_2CCH_3)_2(9\text{-}EtG)_2(CH_3OH)_2$ and $[Rh_2(O_2CCF_3)_2(9\text{-}EtGH)_2((CH_3)_2O)_2][O_2CCF_3]_2$, have revealed two types of bridging guanine ligands: (i) 9-EtGH, the neutral ligand form and (ii) $9\text{-}EtG^-$, the anionic or deprotonated form, where the purine is deprotonated at the N1 position (Figure 8). It has been documented that the pk_a of the N1 position is lowered by 1.5 - 2.0 pk_a units upon coordination to platinum complexes (from ~9.4 to 8.0).[4c,18] The anionic ligand, $9\text{-}EtG^-$, has also been observed to form *in situ* in acidic media.[18] The deprotonation of N1-H in guanine has been mainly observed in reactions with metal complexes containing basic leaving groups such as $[O_2CCH_3]^-$ ($pk_b = 9.25$). The much lower basicity of the trifluoroacetate leaving groups of **(1)** ($pk_b > 13$) was reported to allow the coordination of the neutral 9-EtGH species to the dinuclear center (Figure 8).[6b] Thus, the presence of acetonitrile as a leaving group would allow the coordination of the neutral form of the purine.

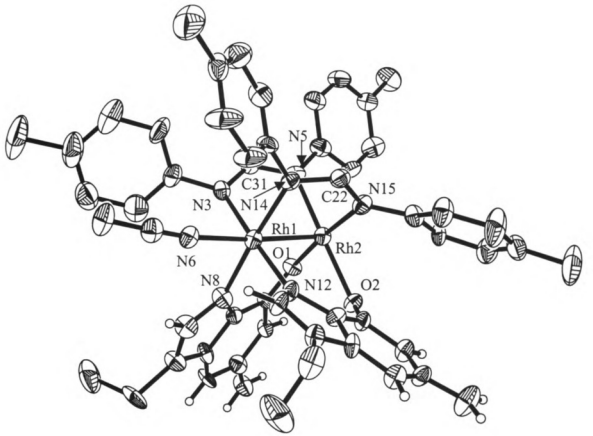
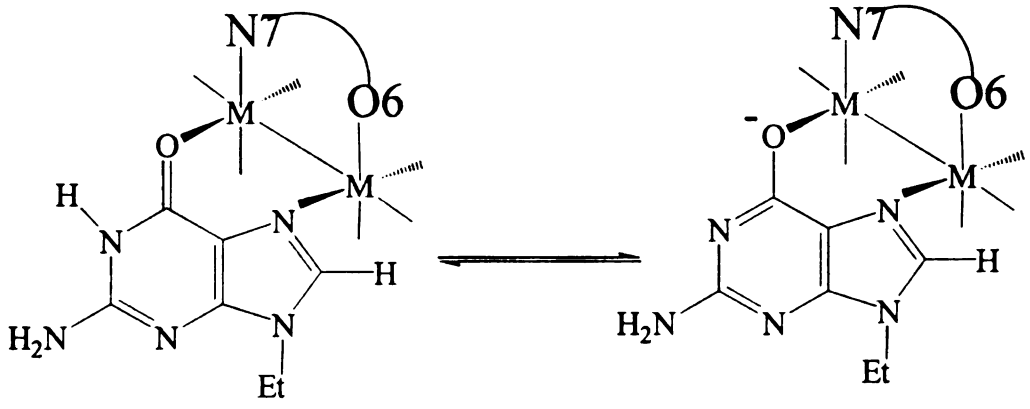


Figure 7. ORTEP representation of compound **(3)** drawn at the 50% probability level. H atoms, except for those of 9-EtGH are omitted for clarity.



9-EtGH
Ketone form

9-EtG$^-$
Enolate form

Figure 8. Schematic representation of protonated and deprotonated 9-ethylguanine.

The Rh-Rh bond length of 2.5410(10) Å is comparable to that of the related complex $[Rh_2(O_2CCH_3)_2(9\text{-EtGH})_2((CH_3)_2O)(H_2O)][BF_4]_2$ which has a metal-metal bond distance of 2.5119(19) Å.[4c] In comparison to the other two known dirhodium structures containing bridging 9-EtGH molecules, $Rh_2(O_2CCH_3)_2(9\text{-EtG})_2(CH_3OH)_2$ (Rh-Rh = 2.483(2) Å) and $[Rh_2(O_2CCF_3)_2(9\text{-EtGH})_2((CH_3)_2O)_2][O_2CCF_3]_2$ (Rh-Rh = 2.520(5) Å), the Rh-Rh bond distance of **(3)** is the longest of the group.[4c] The Rh-O bond distances to the 9-EtGH molecules are 2.070(5) Å and 2.062(6) Å for Rh(2)-O(1) and Rh(2)-O(2), respectively. The metal-nitrogen distances to the purine of Rh(1)-N(3) and Rh(1)-N(12) are 2.076(7) Å and 2.080(7) Å, respectively. The Rh-O and Rh-N distances to the purine in compound **(3)** are slightly longer than the other structurally characterized dirhodium compounds containing bridging 9-EtGH (Rh-O ~2.03 Å and Rh-N ~2.0 Å.[4] The 9-EtGH molecules of **(3)** are twisted from the eclipsed orientation by 24.3(3)° and 26.8(2)° (Figure 9).

Differences in the Rh-N bond distances between each Rh atom and the $[DTolF]^-$ ligands can be attributed to the combination of the *trans* head-to-head 9-EtGH groups and the one axial acetonitrile molecule resulting in a different electronic environment for each Rh atom. It can be observed in

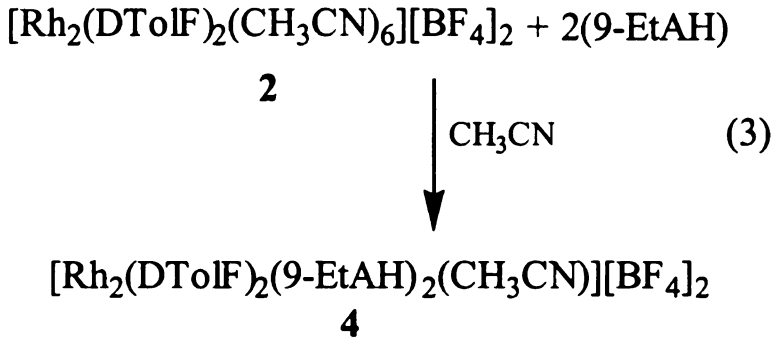
figure 7 that Rh(1) is bound to the N7 position of the 9-EtGH molecule while Rh(2) is bound to the O6 position. In addition, Rh(1) also possesses an axial acetonitrile molecule coordinated with a Rh-N bond distance of 2.142(8) Å for Rh(1)-N(6) whereas the axial position of Rh(2) is vacant. The N atoms coordinated at Rh(1), N(3) and N(14), are coordinated at distances of 2.046(7) Å and 2.042(7) Å, respectively. In contrast, Rh(2) has noticeably shorter Rh-N bond distances to the $[DTolF]^-$ groups (Rh(2)-N(5) = 2.006(7) Å and Rh(2)-N(15) =2.007(7) Å). The angles subtended by the N-C-N bridgehead are 121.8(8)° and 123.5(8)°, and are within the normal ranges. In comparison to the bridging 9-EtGH groups, the bridging $[DTolF]^-$ ligands are twisted from the eclipsed orientation by 20.2(3)° and 23.5(3)°. The twists of the anionic bridging ligands are smaller than those observed for compound **(4)** which are ~30°.

(4) ^{1}H NMR Spectroscopic Data of (3). As observed in the ^{1}H NMR spectrum of $Rh_2(DTolF)_2(9\text{-}EtGH)_2(O_2CCF_3)_2$, formed from the reaction between $Rh_2(DTolF)_2(O_2CCF_3)_2(CH_3CN)_2$ **(1)** and 9-EtGH, $[Rh_2(DTolF)_2(9\text{-}EtGH)_2(CH_3CN)][BF_4]_2$ **(3)** was reported to exhibit two H8 ^{1}H NMR resonances in a 1:1 ratio both in CD_3OD at δ = 8.32 and 8.35 ppm.[6b] A ^{1}H NMR spectrum of the crystals of **(3)** exhibited one H8 signal at 8.34 ppm. A ^{1}H NMR spectrum of the crystallizing solution after harvesting the crystals

did not exhibit signals in the H8 region that can be attributed to the H-T isomer. The X-ray structure of compound **(3)** is in accord with the ^{1}H NMR spectrum.

C. Reaction of $[Rh_2(DTolF)_2(CH_3CN)_6][BF_4]_2$ (2) with 9-EtAH

(1) Syntheses. It has been reported that $Rh_2^{II,II}$ tetracarboxylate compounds have a preference for adenine bases over guanine.[3] Piraino reports similar preferences for the antitumor active $Rh_2(DTolF)_2(O_2CCF_3)_2(H_2O)$.[12b] Reports that the bridging trifluoroacetate groups of $Rh_2(DTolF)_2(O_2CCF_3)_2(H_2O)_2$ exhibit increased lability due to the strong *trans* effects of the $[DTolF]^-$ ligands prompted us to investigate the isolation of the partially solvated cation $[Rh_2(DTolF)_2(CH_3CN)_6]^{2+}$ **(2)**.[12] Furthermore, ^{19}F NMR spectroscopy of compound **(1)** in donating solvents such as acetonitrile showed evidence that the trifluoroacetate molecules were uncoordinated. It has also been observed that the reaction between 9-EtGH and the partially solvated carboxylate complex, $[Rh_2(DTolF)_2(CH_3CN)_6]^{2+}$, yields similar products observed when $Rh_2(DTolF)_2(O_2CCF_3)(CH_3CN)$ **(1)** is reacted with 9-EtGH.[6] We have observed that compound **(2)** reacts with two equivalents of 9-EtAH in acetonitrile at r.t. (Equation 3). Unlike the reactions with 9-EtGH, only one isomer, $Rh_2(DTolF)_2(9\text{-}EtAH)_2(CH_3CN)][BF_4]_2$ **(4)**, is formed as judged by ^{1}H NMR spectroscopy.


[Rh2(DTolF)2(CH3CN)6][BF4]2 + 2(9-EtAH)
2
CH3CN
(3)
[Rh2(DTolF)2(9-EtAH)2(CH3CN)][BF4]2
4

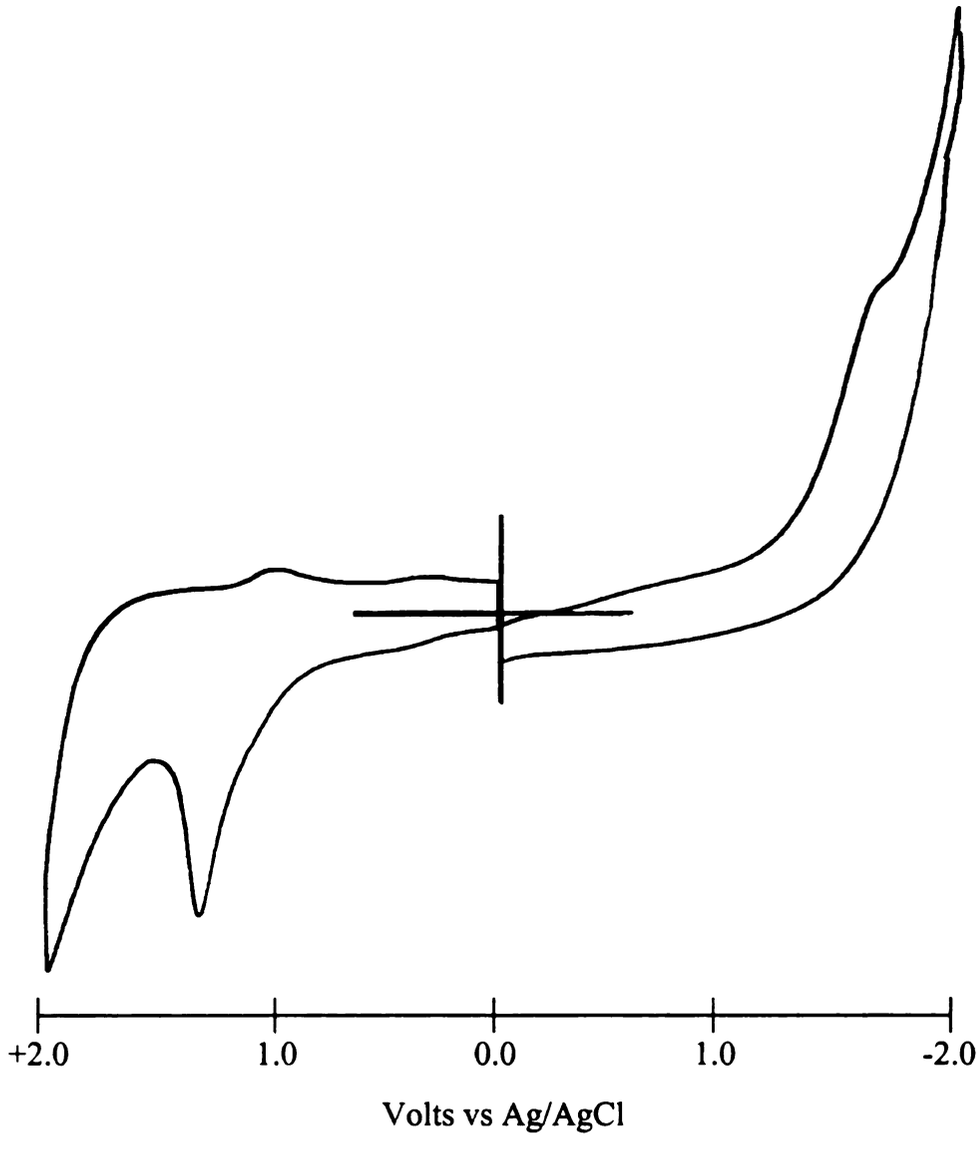


Figure 10. Cyclic voltammograms in 0.1 M electrolyte-CH_3CN at a scan rate of 200 mV/s using a Pt electrode for $[Rh_2(DTolF)_2(9\text{-}EtAH)_2(CH_3CN)][BF_4]_2$ **(4)**.

(2) Electrochemistry of (4). The redox properties of $[Rh_2(DTolF)_2(9\text{-}EtAH)_2(CH_3CN)][BF_4]_2$ **(4)** are quite different from the electrochemistry exhibited by $[Rh_2(DTolF)_2(9\text{-}EtGH)_2(CH_3CN)][BF_4]_2$ **(3).** The cyclic voltammogram of $[Rh_2(DTolF)_2(9\text{-}EtAH)_2(CH_3CN)][BF_4]_2$ **(4)** possesses one quasi-reversible anodic process at $E_{p,a}$ and $E_{p,c}$ values of $^{+}0.93$ V and $^{+}0.72$ V, respectively (Figure 10). The i_{pc}/i_{pa} ratio is 0.17, thus the process is fairly irreversible. Furthermore, only one irreversible reduction process is observed at $^{-}1.14$ V, and is masked by the reduction of the acetonitrile.

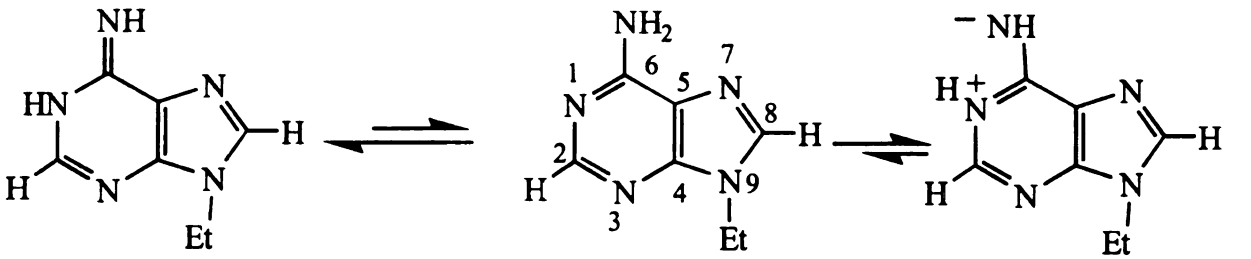


Figure 11. Schematic representation of the tautomers of 9-EtAH.

(3) ^{1}H NMR studies of (4). The ^{1}H NMR spectrum of $[Rh_2(DTolF)_2(9\text{-}EtAH)_2(CH_3CN)][BF_4]_2$ **(4)** proved to be useful in resolving

the question as to whether the N6 positions of the purines were amino (NH_2) or NH groups. The latter situation, although unusual, arises from a prototopic shift from the N6 amino group to the N1 position of the purine (Figure 11). A prototopic shift of an N6 proton to the N1 position was observed for the Mo_2 compound, $[Mo_2(O_2CCHF_2)_2(9\text{-}EtAH)_2(CH_3CN)_2][BF_4]_2$.[4b] A prototopic shift in 9-EtAH is easily recognizable by ^1H NMR spectroscopy, since three resonances would be expected for the common adenine tautomer, whereas four resonances would be expected for the adenine that had undergone the prototopic shift. The ^1H NMR spectrum in CD_3CN exhibits two singlets assignable to the H2 (8.06 ppm) and H8 (7.68 ppm) protons in the aromatic region (Figure 12). Upon lowering the temperature to $^-32$ °C, an additional singlet appears at 6.46 ppm that can be assigned to the H6 protons. Selective decoupling experiments performed on each the three resonances proved that none the resonances were coupled to each other. These assignments initially led us to conclude that the 9-EtAH ligands coordinated to the dirhodium core were neutral with the two protons of the exocyclic NH_2 group intact. Thus the N6 nitrogen atoms would be four-coordinate; a bonding situation which prompted us to question these spectroscopic data. Repeating the NMR experiment in acetone-d6 allowed for a different more reasonable interpretation (Figure

13). The room temperature ^{1}H NMR spectrum exhibits singlets at 7.94, 8.63 and 11.35 ppm that are assignable to the H2, H8 and H6 protons, respectively. At $^{-}41$ °C the resonance at 7.94 is resolved into a doublet, and the H1 proton is apparent at 7.20 ppm among the aromatic resonances of the [DTolF]$^{-}$ groups. The integration of the four resonances is 1:1:1:1, with the definitive assignments of the H1 and H2 protons being achieved by selective decoupling experiments. The H8 signal is observed in the aromatic region as expected. The solution behavior in acetone is in accord with a prototopic shift from the N6 position to the N1 position, and supports the X-ray structure of **(4)**.

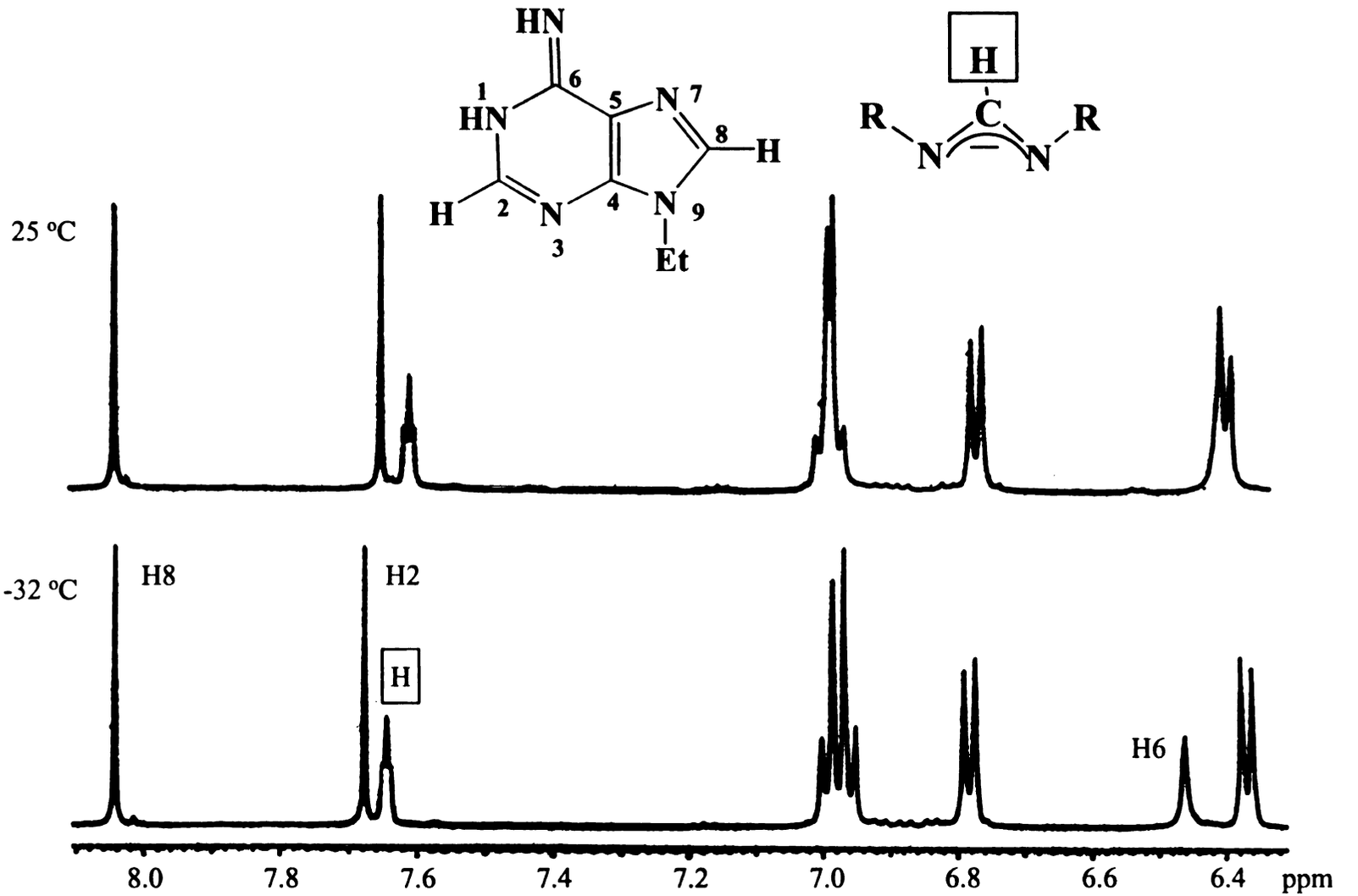


Figure 12. ^{1}H NMR spectrum depicting the H8 region of $[Rh_2(DTolF)_2(9\text{-}EtAH)_2(CH_3CN)][BF_4]_2$ **(4)** in CD_3CN at 25 °C and -32 °C.

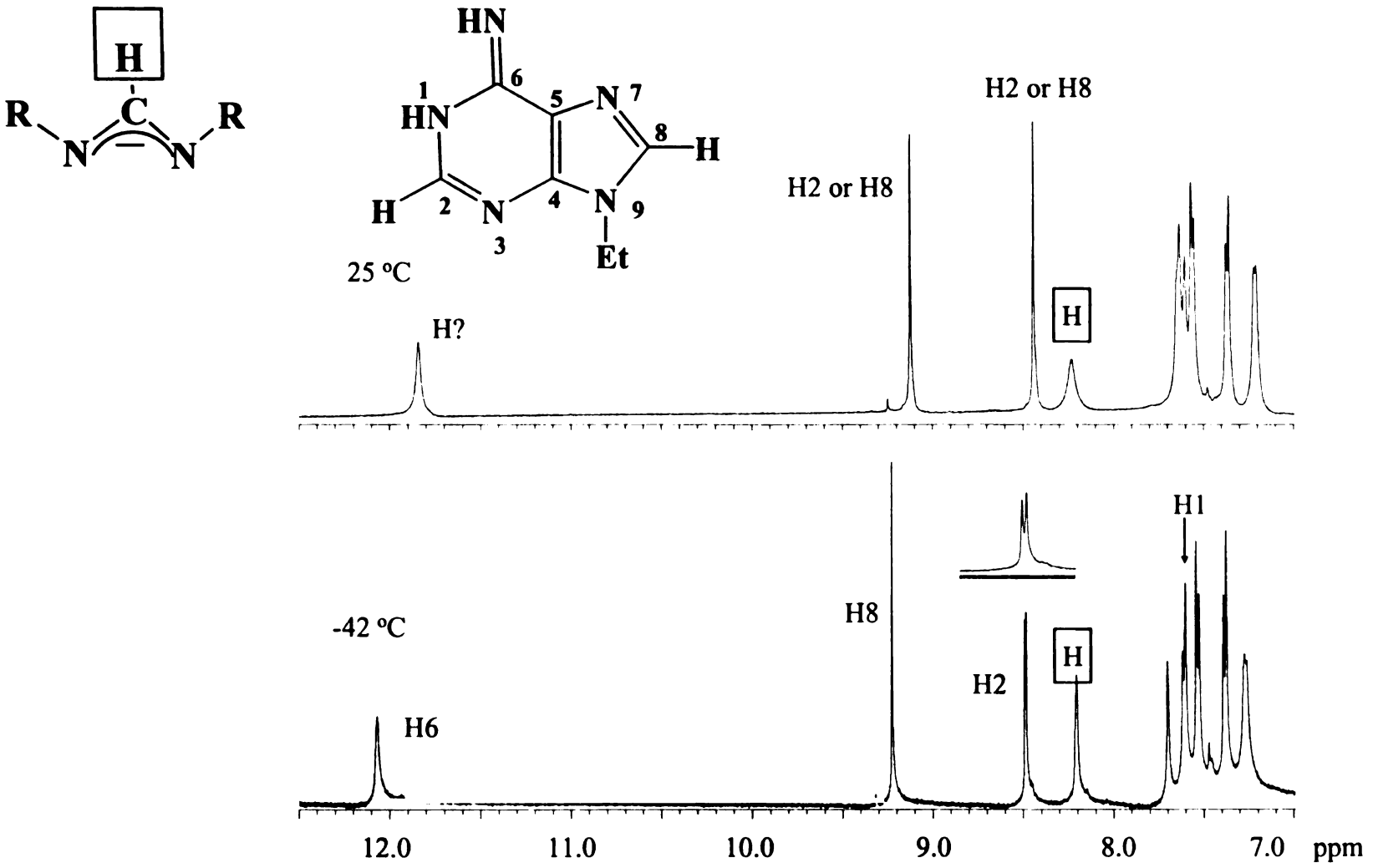


Figure 13. ^{1}H NMR spectrum depicting the H8 region of $[Rh_2(DTolF)_2(9\text{-}EtAH)_2(CH_3CN)][BF_4]_2$ **(4)** in acetone-d6 at 25 °C and -42 °C.

(4) Molecular structure of (4). The reaction with two equivalents of 9-EtAH and compound **(2)** yields the compound $[Rh_2(DTolF)_2(9\text{-}EtAH)_2(CH_3CN)][BF_4]_2$ **(4)**. Compound **(4)** crystallizes in the monoclinic space group $P2_1/c$ with the asymmetric unit consisting of the entire cation and two $[BF_4]^-$ anions (Figure 14). The cation consists of one axial acetonitrile molecule, two bridging $[DTolF]^-$ anions and two *cis* 9-EtAH ligands coordinated in a head-to-tail bridging orientation through the N7 and N6 positions of the purine. Compound **(4)** is the second compound possessing a bridging adenine in this manner. The first reported compound with a bridging 9-EtAH ligand, $[Mo_2(O_2CCHF_2)_2(9\text{-}EtAH)_2(CH_3CN)_2][BF_4]_2$, also contains the adenine ligand in a head-to-tail arrangement.[4b] The unusual monoaxial acetonitrile has a fairly short Rh-N bond distance of 2.06(2) Å in comparison to other monoaxial acetonitrile containing compounds that have been recently observed in our laboratories. The N-chelate compounds $[Rh_2(DTolF)_2(bpy)(CH_3CN)_3]^{2+}$ **(7)**, $[Rh_2(DTolF)_2(bpy)_2(CH_3CN)]^{2+}$ **(8)** and $[Rh_2(DTolF)_2(phen)(CH_3CN)_3]^{2+}$ **(9)**, which are presented in chapter 2, all possess one axial acetonitrile ligand coordinated at Rh-N bond distances of 2.101(4) Å, 2.115(4) Å and 2.126(3) Å, respectively.[14] As a consequence of the coordination by the axial

acetonitrile, the N7 and N6 positions of the purines are not related by symmetry. Thus, the metal-nitrogen distances involving these groups are slightly different from each other, *viz.*, Rh(1)-N(4) = 1.99(2) Å and Rh(2)-N(6) = 2.03(2) Å; Rh(1)-N(2) = 2.04(2) Å and Rh(2)-N(8) = 2.03(2) Å, but in the range expected for eq Rh-N bond distances. The fact that two outer-sphere $[BF_4]^-$ anions are present in the structure requires the 9-EtAH molecules to be neutral, but does not resolve the question as to whether the N6 positions are amino (NH_2) or NH groups. This question was previously addressed.

The bridging $[DTolF]^-$ ligands of $[Rh_2(DTolF)_2(9\text{-}EtAH)_2(CH_3CN)][BF_4]_2$ **(4)** are twisted from the eclipsed orientation by ~30°, which is nearly 10° more than the torsion observed for the precursor $[Rh_2(DTolF)_2(CH_3CN)_6][BF_4]_2$ **(2)**, and more than 20° greater than the bis-trifluoroacetate derivatives. The Rh-Rh bond length of 2.510(3) Å in **(4)** is slightly shorter than that of the parent complex $[Rh_2(DTolF)_2(CH_3CN)_6][BF_4]_2$ **(2)**, but longer than that observed for $Rh_2(DTolF)_2(O_2CCF_3)_2(CH_3CN)_2$ **(1)**. This may be attributed to the addition of the bridging 9-EtAH ligands to the Rh_2^{2+} core. The Mo-Mo bond length in $[Mo_2(O_2CCHF_2)_2(9\text{-}EtAH)_2(CH_3CN)_2][BF_4]_2$ of 2.1436(17) Å is significantly shorter than the Rh-Rh distance in compound **(4)**, and indicates

that the 9-ethyladenine ligand can bridge a wide range dimetal bond distances.

D. Reaction of $Rh_2(DTolF)_2(O_2CCF_3)_2(CH_3CN)_2$ (1) with 9-EtAH

(1) Synthesis. Since we had already established that $[Rh_2(DTolF)_2(CH_3CN)_6]^{2+}$ **(2)** reacts with 9-EtAH, we wanted to confirm that a reaction leading to similar products would take place with the antitumor active bis-trifluoroacetate compound. Analogous to the reaction between $[Rh_2(DTolF)_2(CH_3CN)_6]^{2+}$ **(2)** and 9-EtAH, the NMR scale reaction between compound **(1)** and 9-EtAH forms only one isomer, $Rh_2(DTolF)_2(9\text{-}EtAH)_2(O_2CCF_3)_2$ **(5)**, as determined by ^1H NMR spectroscopy.

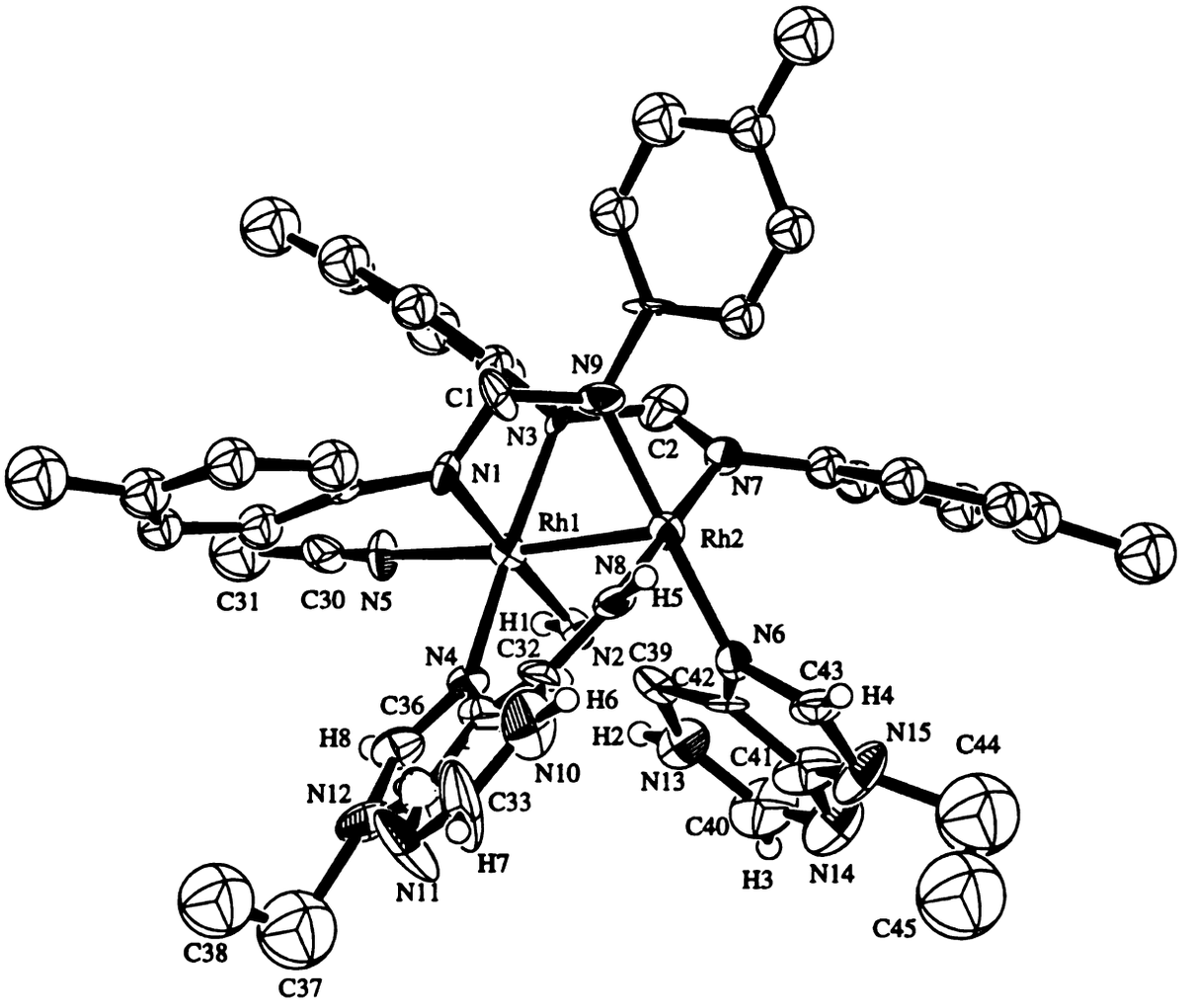


Figure 14. ORTEP representation of compound **(4)** drawn at the 50% probability level. H atoms except for the 9-EtAH ligands are omitted for clarity.

(2) ^{1}H NMR Studies of (5). The ^{1}H NMR spectrum of compound **(5)** in the H8 region of the purine suggests the presence of two compounds after 72 h (Figure 15). One of the compounds can be identified as the starting compound, $Rh_2(DTolF)_2(O_2CCF_3)_2(CH_3CN)_2$ **(1)**, and the other one as the product, $Rh_2(DTolF)_2(9\text{-}EtAH)_2(O_2CCF_3)_2$ **(5)**. The three singlets at 8.24, 8.05 and 8.00 ppm can be attributed to the H8, H1, and H2 protons of a coordinated 9-EtAH molecule. Likewise, the broad resonance at 7.80 ppm can also be attributed to a coordinated 9-EtAH. The breadth of this signal suggests that this resonance is the H6 proton. Selective decoupling experiments were inconclusive since the signals for the protons at 7.80, 8.00 and 8.05 ppm are too close together such that selective irradiation of any of these protons results in the loss of all of these signals. Selective decoupling did prove, however, that the resonance at 8.24 ppm is not coupled to any of the other resonances, suggesting that the assignment of this resonance is the H8 proton. Although these assignments are not definitive, they do prove that a reaction did take place as the protons for the free purine in CD_3CN resonate at 8.21, 7.89 and 5.90 ppm for the H2, H8 and H6 protons, respectively (Table 16). The resonance at 7.63 ppm can be assigned to the

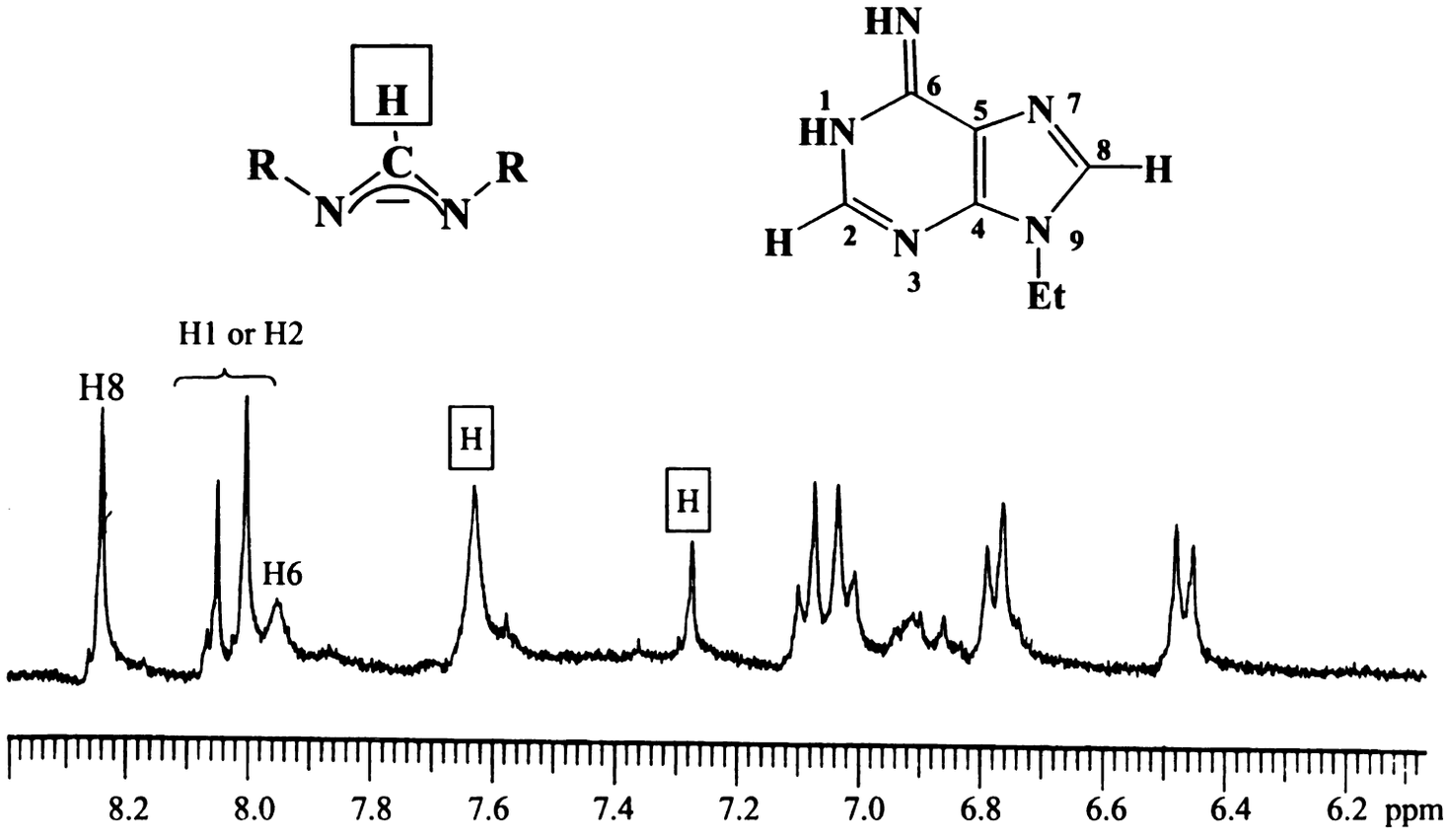


Figure 15. ^{1}H NMR spectrum depicting the H8 region of the NMR scale reaction between $Rh_2(DTolF)_2(O_2CCF_3)_2$ **(1)** and 9-EtAH.

methylene protons of the $[DTolF]^-$ groups, as this is the same region these protons are observed in the related compound $[Rh_2(DTolF)_2(9\text{-}EtAH)_2(CH_3CN)][BF_4]_2$ **(4)**. The resonance at 7.27 ppm can be attributed to the methylene protons of the $[DTolF]^-$ groups of the starting material.

(3) Molecular Structure of (5). The structure of compound **(5)** is thought to be quite similar to that of $[Rh_2(DTolF)_2(9\text{-}EtAH)_2(CH_3CN)][BF_4]_2$ **(4)** (Figure 14). The ^1H NMR spectrum suggests that the 9-EtAH groups are bridging the dimetal centers, and are neutral after having undergone a prototopic shift of an N6 proton to the N1 position (Figure 16). Whether the purine is bridging in the head-to-head or head-to-tail bridging mode remains undetermined. The trifluoroacetate groups are displaced from the bridging equatorial positions to the axial positions. The fact that the axial trifluoroacetate groups would be in exchange with the donor solvent would account for the differences in the ^1H NMR spectra between $Rh_2(DTolF)_2(9\text{-}EtAH)_2(O_2CCF_3)_2$ **(5)** and $[Rh_2(DTolF)_2(9\text{-}EtAH)_2(CH_3CN)][BF_4]$ **(4)**.

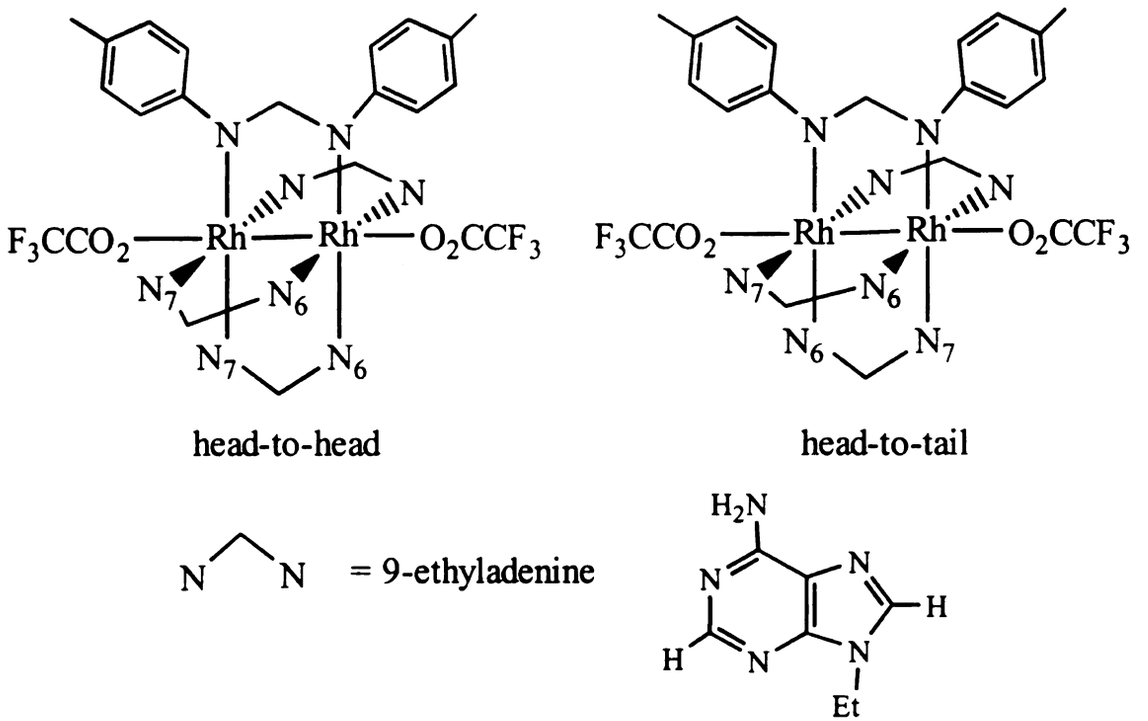


Figure 16. Proposed structure of $Rh_2(DTolF)_2(9\text{-}EtAH)_2(O_2CCF_3)_2$ **(5)**

E. Preparation of $Rh_2(DTolF)_2(O_2CCH_3)_2(H_2O)$ (6)

(1) Synthesis. In an attempt to modify the $[Rh_2(DTolF)_2]^{2+}$ core for future reactivity studies with DNA nucleobases we decided to substitute the bridging trifluoroacetate groups for the less electron withdrawing acetate groups. The differences between the effects on 9-EtGH by acetate and trifluoroacetate groups were previously discussed. A previous attempt to synthesize $Rh_2(DTolF)_2(O_2CCH_3)_2L_2$ (L = donor solvent) was performed by Piraino and coworkers.[20] The researchers attempted to isolate this compound by the chemical oxidation of $[Rh(DTolF)(cod)]_2$ with AgO_2CCF_3. This synthetic procedure was successful in the synthesis of

$Rh_2(DTolF)_2(O_2CCF_3)_2L_2$ **(1)**. Unfortunately, this procedure does not work with AgO_2CCH_3. Piraino took note that $Rh_2(O_2CCH_3)_4L_2$ reacts with excess HDTolF to form the dirhodium tetra-formamidinate compound, $Rh_2(DTolF)_4$.[20a] A different reaction takes place when the stociometry of HDTolF is controlled. The reaction between $Rh_2(O_2CCH_3)_4L_2$ and two equivalents of HDTolF leads to the formation of $Rh_2(O_2CCH_3)_4(HDTolF)_2$, which has been structurally characterized. The formamidinate molecules are neutral and coordinated in the axial positions of the dirhodium compound (Figure 17).[20b] Attempts to deprotonate the HDTolF ligand in hopes that the ligands would swing into a bridging equatorial mode failed.

Although the previous attempts were not promising, we decided to advantage of the substitution chemistry of the partially solvated compound, $[Rh_2(DTolF)_2(CH_3CN)_6][BF_4]_2$ **(2)**. The addition of two equivalents of $NaO_2CCH_3 \cdot 7H_2O$ in acetonitrile leads to the precipitation of $NaBF_4$, and the

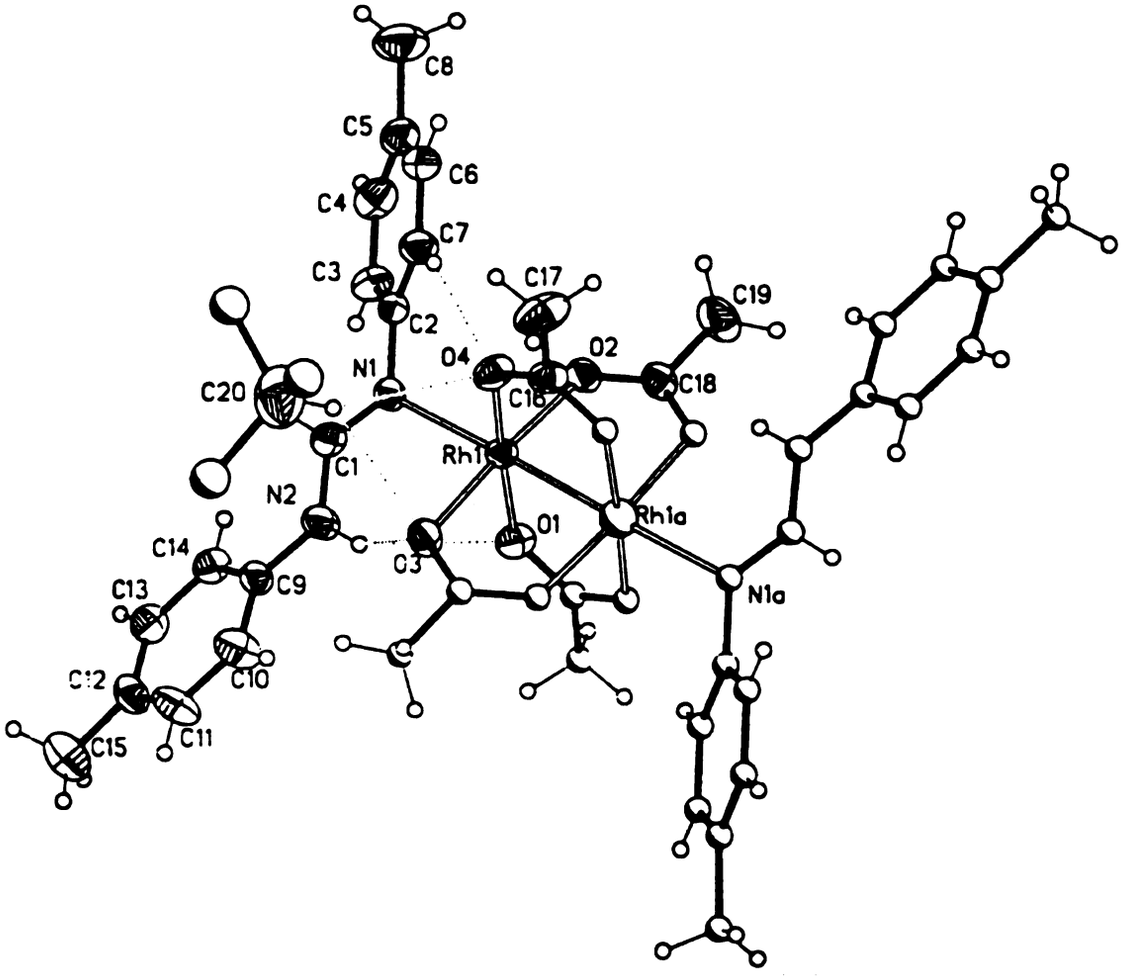


Figure 17. ORTEP representation of $Rh_2(O_2CCH_3)_4(HDTolF)_2$ replotted from atomic coordinates.[20b]

formation of $Rh_2(DTolF)_2(O_2CCH_3)_2(H_2O)$ **(6)** as determined by X-ray crystallography (Equation 4).

$$[Rh_2(DTolF)_2(CH_3CN)_6][BF_4]_2 + 2(NaO_2CCH_3 \cdot 7H_2O \xrightarrow{CH_3CN} Rh_2(DTolF)_2(O_2CCH_3)_2(H_2O) + NaBF_4 \quad (4)$$

(2) Molecular Structure of (6). An ORTEP representation of $Rh_2(DTolF)_2(O_2CCH_3)_2(H_2O)$ **(6)**, which crystallizes in the triclinic space group P-1 is presented in Figure 18. Unlike the solid-state structures of $Rh_2(DTolF)_2(O_2CCF_3)_2(CH_3CN)_2$ **(1)** and $Rh_2(DTolF)_2(O_2CCF_3)_2(H_2O)_2$, the X-ray structure of $Rh_2(DTolF)_2(O_2CCH_3)_2(H_2O)$ **(6)** possesses only one axial solvent molecule, namely, water. Compound **(6)** also possesses two *cis* bridging $[DTolF]^-$ groups as well as two bridging $[O_2CCH_3]^-$ groups. The neutral compound also crystallizes with four interstitial water molecules in the interstices. The Rh-Rh bond length of 2.4171(7) Å is slightly shorter than the metal-metal bond distance of compound **(1)**, which is observed to be 2.4743(5) Å. The bis-water adduct, on the other hand, has a very similar

Rh-Rh bond distance of 2.425(1) Å.[7b] In a similar fashion to the trifluoroacetate derivatives, the axial water molecule is coordinated at an angle significantly less than 180°. The O(5)-Rh(1)-Rh(2) angle is 171.24(11)°. The axial solvents of $Rh_2(DTolF)_2(O_2CCF_3)_2(CH_3CN)_2$ **(1)** and $Rh_2(DTolF)_2(O_2CCF_3)_2(H_2O)_2$ are coordinated at an average angle of 170°. Th Rh(1)-O(5) bond distance of 2.250(4) Å is shorter than axial water molecules in $Rh_2(DTolF)_2(O_2CCF_3)_2(H_2O)_2$ (2.311(3) Å and 2.319(3) Å). The average Rh-O bond distance to the bridging acetate ligands of 2.072[4] Å is within in the normal range. The O-C-O angles of the acetate groups are 124.6(6)° and 124.2(6)° for the O(1)-C(30)-O(2) and O(3)-C(32)-O(4) angles. These angles are within the expected ranges, but are smaller than angles observed in compound **(1)** (129.7(5)° and 131.4(5)°). The angles subtended by the N-C-N bridgehead of the $[DTolF]^-$ groups are 124.2(6)° and 122.4(6)°, and are within the expected ranges. The Rh-N distances of to the $[DTolF]^-$ ligands coordinated at Rh(1) of 2.024(5) Å and 2.026(5) Å are slightly longer than the Rh-N distances between Rh(2) and the $[DTolF]^-$ groups (2.002(5) Å and 2.006(5) Å). A more dramatic difference in these

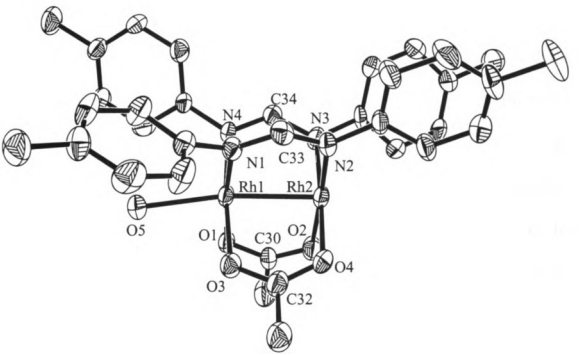


Figure 18. ORTEP representation of compound **(6)** drawn at the 50% probability level. H atoms are omitted for clarity.

bond lengths are observed for other compounds presented in chapter 2 where only one metal atom possesses an axial solvent molecule. A similar bonding situation was also previously discussed for compound **(3)**. The bridging formamidinate ligands are slightly twisted from the eclipsed orientation by 4.8(2)° and 5.7(2)°.

4. Conclusions.

Recent developments in our laboratories in the chemistry of dirhodium tetracarboxylate compounds with DNA purines opened the question of the possible involvement of the O6 position in the observed DNA binding of this class of compounds. Investigations of the purine reactions of $Rh_2(DTolF)_2(O_2CCF_3)_2(CH_3CN)_2$ **(1)** $[Rh_2(DTolF)_2(CH_3CN)_6]^{2+}$ **(2)** have been explored. The products with 9-EtGH formed from the reactions with $Rh_2(DTolF)_2(O_2CCF_3)_2(CH_3CN)_2$ **(1)** and $[Rh_2(DTolF)_2(CH_3CN)_6]^{2+}$ **(2)** show little or no preference for the formation of the head-to-head isomer over the head-to-tail isomer as determined by ^1H NMR spectroscopy. Single crystal X-ray crystallographic studies performed on $[Rh_2(DTolF)_2(9\text{-}EtGH)_2(CH_3CN)]^{2+}$ **(3)** showed that a preference for crystallizing the head-to-head isomer. Conversely, the reactions between 9-EtAH $[Rh_2(DTolF)_2(CH_3CN)_6]^{2+}$ **(2)** shows a preference for the formation of the head-to-tail isomer over the head-to-head isomer as elucidated from ^1H

NMR spectroscopy and single crystal X-ray diffraction studies.. The compounds containing the $[DTolF]^-$ bridging groups and the purines also exhibit very rich redox chemistry. From these studies we expect that the dirhodium formamidinate compounds will react with DNA similarly to the dirhodium tetracarboxylate compounds under current investigation in our laboratories. The new compound $Rh_2(DTolF)_2(O_2CCH_3)_2(H_2O)$ **(6)** shows little or no differences to the lantern structure to the trifluoroacetate derivatives. We are confident that this compound will exhibit similar reactivities with the DNA nucleobases to compounds **(1)** and **(2)**.

Table 1. Crystallographic Data for $Rh_2(DTolF)_2(O_2CCF_3)_2(CH_3CN)$ **(1)**, $Rh_2(DTolF)_2(O_2CCH_3)_2(H_2O)$ **(6)**, $[Rh_2(DTolF)_2(9\text{-}EtAH)_2(CH_3CN)][BF_4]_2$ **(4)**, $[Rh_2(DTolF)_2(9\text{-}EtGH)_2(CH_3CN)][BF_4]_2$ **(3)**

	1	6	4	3
Formula[a]	$C_{38}H_{36}F_6N_6O_4Rh_2$ $C_{46}H_{53}B_2F_4N_{15}O_2Rh_2$	$C_{37}H_{37}O_6N_4Rh_2$	$C_{46}H_{48}B_2F_8N_{15}Rh_2$	
Fw, g/mol	960.55	839.53	1190.40	1227.47
Space group	$P2_1/n$	P-1	$P2_1/c$	$P2_1/n$
a, Å	10.8495(3)	11.1110(2)	15.648(8)	11.3612(9)
b, Å	21.4349(6) 20.8031(16)	12.5251(2)	16.515(5)	
c, Å	18.6766(3) 22.6171(18)	14.4516(1)	20.026(8)	
α, deg	90	69.904(1)	90	90
β, deg	90.059(1)	74.237(1)	105.17(4)	100.021(2)
γ, deg	90	87.173(1)	90	90
V, $Å^3$	4340.6(2)	1815.55(5)	4994(6)	5264.0(7)
Z	*4*	*2*	*4*	*4*
T, K	173	173	173	173
Radiation[b]	MoKα	MoKα	MoKα	MoKα
ρ_{calc}, g/cm^3	1.470	1.536	1.583	1.549
μ, cm^{-3}	0.829	0.959	7.40[j]	0.709
Unique data	10101	8033	6841	12287
Obsd data[c]	3761	4413	2240[g]	4834
R_{int} (R_{sig}) (0.2539)	0.1177 (0.1912)	0.0577(0.1333)	0.119	0.1480
R_1 (wR_2) (0.1484)	0.0449 (0.0898)	0.0628 (0.1101)	0.063[h] (0.073)[i]	0.0898
GooF[f]	0.985	1.081	1.30	0.974

[a]Including solvent molecules. [b]Graphite monochromator. [c]$I > 2\sigma(I)$. [d]$R_{int} = \Sigma|F_o^2 - F_{o(mean)}^2|/\Sigma[F_o^2]$; $R_{sigma} = \Sigma[\sigma(F_o^2)]/[F_o^2]$. [e]$R1 = \Sigma||F_o|-|F_c||/\Sigma|F_o|$; $wR2 = [\Sigma[w(F_o^2-F_c^2)^2]/\Sigma[w(F_o^2)^2]]^{1/2}$. [f]Goodness-of-Fit = $S = [\Sigma[w(F_o^2-F_c^2)^2]/(n-p)]^{1/2}$. [g]$F_o^2 > 3\sigma(F_o)^2$. [h]$R = \Sigma||F_o|-|F_c||/\Sigma|F_o|$. [i]$R_w = [\Sigma w(|F_o|-|F_c|^2/\Sigma w|F_o|^2]^{1/2}$; $w = 1/\sigma^2(|F_o|)$.

Table 2. Selected Bond Distances (Å) and Angles (deg) for $Rh_2(DTolF)_2(O_2CCF_3)_2(CH_3CN)_2$ **(1)**.

(a) Bonds

Rh(1)-Rh(2)	2.4745 (5)	Rh(1)-N(3)	2.266 (5)
Rh(1)-N(1)	2.007 (4)	Rh(2)-N(6)	2.012 (4)
Rh(1)-N(5)	2.015 (4)	Rh(2)-N(2)	2.008 (4)
Rh(1)-O(3)	2.095 (3)	Rh(2)-O(1)	2.098 (3)
Rh(1)-O(2)	2.102 (3)	Rh(2)-O(4)	2.100 (3)
Rh(2)-N(4)	2.269(5)		

(b) Angles

N(1)-Rh(1)-N(5)	91.6 (2)	N(1)-Rh(1)-O(3)	87.89 (14)
N(5)-Rh(1)-O(3)	175.16 (15)	N(1)-Rh(1)-O(2)	175.3 (2)
N(5)-Rh(1)-O(2)	88.14 (15)	O(3)-Rh(1)-O(2)	91.95 (13)
N(1)-Rh(1)-N(3)	97.1 (2)	N(5)-Rh(1)-N(3)	101.2 (2)
O(3)-Rh(1)-N(3)	83.62 (14)	O(2)-Rh(1)-N(3)	87.6 (2)
N(6)-Rh(2)-N(2)	91.8 (2)	N(6)-Rh(2)-O(1)	174.84 (15)
N(2)-Rh(2)-O(1)	88.41 (14)	N(6)-Rh(2)-O(4)	88.18 (15)
N(2)-Rh(2)-O(4)	175.1 (2)	O(1)-Rh(2)-O(4)	91.20 (13)
N(6)-Rh(2)-N(4)	93.8 (2)	N(2)-Rh(2)-N(4)	99.2 (2)
O(1)-Rh(2)-N(4)	91.28 (14)	O(4)-Rh(2)-N(4)	85.66 (14)
N(2)-C(40)-N(1)	124.4 (5)	N(5)-C(39)-N(6)	125.9 (5)
O(1)-C(28)-O(3)	129.9 (5)	O(2)-C(31)-O(4)	131.2 (5)
N(4)-Rh(2)-Rh(1)	172.37 (11)	N(3)-Rh(1)-Rh(2)	168.87 (11)
N(2)-Rh(2)-Rh(1)-N(1)	5.6 (2)	O(2)-Rh(1)-Rh(2)-O(4)	5.33 (13)
N(5)-Rh(1)-Rh(2)-N(6)	5.4 (2)	O(3)-Rh(1)-Rh(2)-O(1)	6.08 (13)

Table 3. Selected Bond Distances (Å) and Angles (deg) for

$[Rh_2(DTolF)_2(CH_3CN)_6][BF_4]_2$ **(6)**

(a) Bonds			
Rh(1)-Rh(2)	2.4171 (7)	Rh(2)-N(2)	2.006 (5)
Rh(1)-N(1)	2.026 (5)	Rh(2)-N(3)	2.002 (5)
Rh(1)-O(3)	2.073 (4)	Rh(2)-O(4)	2.055 (4)
Rh(1)-O(1)	2.091 (4)	Rh(2)-O(2)	2.070 (4)
Rh(1)-O(5)	2.250 (4)		
Rh(1)-N(4)	2.024 (5)		
(b) Angles			
N(4)-Rh(1)-N(1)	90.5 (2)	O(5)-Rh(1)-Rh(2)	171.24 (11)
N(4)-Rh(1)-O(3)	175.0 (2)	N(3)-Rh(2)-N(2)	89.7 (2)
N(1)-Rh(1)-O(3)	88.7 (2)	N(3)-Rh(2)-O(4)	177.2 (2)
N(4)-Rh(1)-O(1)	91.0 (2)	N(2)-Rh(2)-O(4)	89.5 (2)
N(1)-Rh(1)-O(1)	174.9 (2)	N(3)-Rh(2)-O(2)	91.2 (2)
O(3)-Rh(1)-O(1)	89.3 (2)	O(4)-Rh(2)-O(2)	89.4 (2)
N(4)-Rh(1)-O(5)	100.4 (2)	O(2)-C(30)-O(1)	124.6 (6)
N(1)-Rh(1)-O(5)	94.2 (2)	O(3)-C(32)-O(4)	124.2 (6)
N(1)-C(33)-N(2)	124.2 (6)	N(3)-C(34)-N(4)	122.4 (6)
N(4)-Rh(1)-Rh(2)-N(3)	4.8 (2)	N(1)-Rh(1)-Rh(2)-N(2)	5.7(2)
O(3)-Rh(1)-Rh(2)-O(4)	5.0 (2)	O(1)-Rh(1)-Rh(2)-O(2)	5.1 (2)

Table 4. Selected Bond Distances (Å) and Angles (deg) for

$[Rh_2(DTolF)_2(9\text{-}EtAH)_2(CH_3CN)][BF_4]_2$ **(4)**

	(a) Bonds		
Rh(1)-Rh(2)	2.510 (3)	Rh(1)-N(1)	2.04 (2)
Rh(1)-N(2)	2.04 (2)	Rh(1)-N(3)	2.07 (2)
Rh(1)-N(4)	1.99 (2)	Rh(1)-N(5)	2.06 (2)
Rh(2)-N(6)	2.03 (2)	Rh(2)-N(7)	2.00 (2)
Rh(2)-N(8)	2.03 (2)	Rh(2)-N(9)	2.03 (2)
	(b) Angles		
N(1)-Rh(1)-N(2)	177.7 (8)	N(1)-Rh(1)-N(3)	92.1 (7)
N(1)-Rh(1)-N(4)	88.6 (7)	N(1)-Rh(1)-N(5)	98.9 (8)
N(2)-Rh(1)-N(3)	87.1 (7)	N(2)-Rh(1)-N(4)	92.1 (7)
N(2)-Rh(1)-N(5)	83.2 (8)	N(3)-Rh(1)-N(4)	176.4 (8)
N(3)-Rh(2)-N(5)	90.1 (7)	N(4)-Rh(2)-N(5)	93.3 (8)
N(6)-Rh(2)-N(7)	89.5 (8)	N(6)-Rh(2)-N(8)	91.8 (7)
N(6)-Rh(2)-N(9)	179.0 (7)	N(7)-Rh(2)-N(8)	176.5 (7)
N(7)-Rh(2)-N(9)	89.6 (7)	N(8)-Rh(2)-N(9)	89.2 (7)
N(1)-C(1)-N(9)	116 (2)	N(3)-C(2)-N(7)	118 (2)
N(1)-Rh(1)-Rh(2)-N(9)	30.2 (7)	N(3)-Rh(1)-Rh(2)-N(7)	27.1 (7)
N(4)-Rh(1)-Rh(2)-N(8)	29.9 (7)	N(2)-Rh(1)-Rh(2)-N(6)	29.8 (7)
N(4)-C(35)-C(32)-N(8)	6 (4)	N(2)-C(39)-C(42)-N(6)	6 (4)

Table 5. Selected Bond Distances (Å) and Angles (deg) for

$[Rh_2(DTolF)_2(9\text{-}EtGH)_2(CH_3CN)][BF_4]_2$ **(3)**.

	(a) Bonds		
Rh(1)-Rh(2)	2.5140 (10)	Rh(1)-N(14)	2.042 (7)
Rh(1)-N(3)	2.046 (7)	Rh(1)-N(8)	2.076 (7)
Rh(1)-N(12)	2.080 (7)	Rh(1)-N(6)	2.142 (8)
Rh(2)-N(5)	2.006 (7)	Rh(2)-N(15)	2.007 (7)
Rh(2)-O(2)	2.062 (6)	Rh(2)-O(1)	2.070 (8)
	(b) Angles		
N(14)-Rh(1)-N(3)	89.3 (3)	N(14)-Rh(1)-N(8)	176.1 (3)
N(3)-Rh(1)-N(8)	92.4 (3)	N(14)-Rh(1)-N(12)	89.0 (3)
N(3)-Rh(1)-N(12)	177.8 (3)	N(8)-Rh(1)-N(12)	89.2 (3)
N(14)-Rh(1)-N(6)	93.5 (3)	N(3)-Rh(1)-N(6)	91.3 (3)
N(8)-Rh(1)-N(6)	89.9 (3)	N(12)-Rh(1)-N(6)	90.2 (3)
N(5)-Rh(2)-N(15)	92.8 (3)	N(5)-Rh(2)-O(2)	171.9 (2)
N(15)-Rh(2)-O(2)	92.8 (3)	N(5)-Rh(2)-O(1)	89.0 (3)
N(15)-Rh(2)-O(1)	172.6 (3)	O(2)-Rh(2)-O(1)	84.7 (2)
N(6)-Rh(1)-N(2)	176.0 (2)	N(5)-C(31)-N(3)	123.5 (8)
N(15)-C(22)-N(14)	121.8 (8)	N(14)-Rh(1)-Rh(2)-N(15)	23.5 (3)
N(3)-Rh(1)-Rh(2)-N(5)	20.2 (3)	N(8)-Rh(1)-Rh(2)-O(1)	24.2 (3)
N(12)-Rh(1)-Rh(2)-O(2)	26.8 (2)	N(8)-C(19)-C(36)-O(1)	0.2 (17)
N(12)-C(7)-C(34)-O(2)	0.4 (17)		

Table 6. NMR Spectroscopic Data for **3**, **4**, **5**, **6** and **7**.

compound	NMR spectra, ppm
3 $Rh_2(DTolF)_2(9\text{-}EtGH)_2(O_2CCF_3)_2$	^1H NMR (CD_3CN) δ ppm: 1.35-1.37 (m, CH_3), 1.95 (s, CH_3CN), 2.15 broad (s, H_2O), 2.23 (s, CH_3), 4.05 (m, CH_2), 6.80 (d, phenyl), 6.89 (d, phenyl), 7.03-7.19 broad (m, phenyl), 7.55 (m, NCHN), 7.99 (s, H8), 8.02 (s, H8). ^{19}F NMR (both CD_3CN and acetone-d6) δ ppm: -12.49 referenced to $C_6H_5CF_3$ (s, O_2CCF_3).
4 $Rh_2(DPhF)_2(9\text{-}EtGH)_2(O_2CCF_3)_2$	^1H NMR (CD_3CN) δ ppm: 1.35-1.38 (m, CH_3), 1.95 (s, CH_3CN), 2.21 broad (s, H_2O), 4.04-4.07 broad (m, CH_2), 6.82 (d, phenyl), 6.89 (d, phenyl), 7.04-7.20 broad (m, phenyl), 7.55 (m, NCHN), 7.93 (s, H8), 8.03 (s, H8). ^{19}F NMR (both CD_3CN, acetone-d6) δ ppm: -12.47 referenced to $C_6H_5CF_3$ (s, O_2CCF_3). ^{103}Rh NMR (CD_3CN) δ ppm: 5551.98.
5 $[Rh_2(DTolF)_2(CH_3CN)_6][BF_4]_2$	^1H NMR spectrum in CD_3CN: δ = 7.51 (t, $^3J_{Rh\text{-}H}$ = 4 Hz, NCHN), 6.99 (m, Ph), 2.27 (s, $\underline{CH_3}$-Ph), 2.49 (s, *eq*-CH_3CN), and 1.96 (s, *ax*-CH_3CN). ^{103}Rh NMR spectrum in CD_3CN:δ = 4648.

6 $[Rh_2(DTolF)_2(9\text{-}EtAH)_2(CH_3CN)][BF_4]_2$	^1H NMR spectrum in CD_3CN at 25 °C: δ = 1.25 (t, CH_3), 1.95 (s, CH_3CN), 2.25 (s, CH_3), 2.33 (s, CH_3), 3.98-4.11 (m, CH_2), 6.46 (d, phenyl), 6.76 (d, phenyl), 7.02 (d, phenyl), 7.09 (d, phenyl), 7.26 (s, NCHN), 7.68 (s, H2 or H8), 8.06 (s, H2 or H8), 8.63 (s, H6). ^1H NMR spectrum at -32 °C: δ = 1.28 (t, CH_3), 1.95 (s, CH_3CN), 2.13 (s, H_2O), 2.23 (s, CH_3), 4.08 (m, CH_2), 6.36 (d, phenyl), 6.46 (s, H6), 6.78 (d, phenyl), 6.96 (d, phenyl), 6.99 (d, phenyl), 7.65 (t, NCHN), 7.68 (s, H2 or H8), 8.04 (s, H2 or H8). ^1H NMR spectrum in acetone-d6 at 25 °C: δ = 1.30 (t, CH_3-9-EtAH), 1.88 (s, *ax*-CH_3CN), 2.14 (s, H_2O), 2.24 (s, $\underline{CH_3}$-Ph), 4.15-4.19 (m, CH_2-9-EtAH), 6.71 (d, Ph), 6.86 (d, Ph), 7.06 (d, Ph), 7.12 (d, Ph), 7.73 (bs, NCHN), 8.63 (s, H8), 11.35 (s, H6). ^1H NMR spectrum at -41 °C: δ = 1.27 (t, CH_2-9-EtAH), 1.84 (s, *ax*-CH_3CN), 2.13 (s, H_2O), 2.20 (s, $\underline{CH_3}$-Ph), 4.17 (m, CH_2-9-EtAH), 6.76 (d, H6), 6.88 (d, Ph), 7.03 (d, Ph), 7.11 (d, Ph), 7.20 (s, H2), 7.71 (bs, NCHN), 7.99 (d, H1), 8.73 (s, H8), 7.94 (s, H1), 11.57 (s, H6).
7 $[Rh_2(DTolF)_2(9\text{-}EtGH)_2(CH_3CN)][BF_4]_2$	^1H NMR (CD_3OD) δ ppm: 1.36 (t, CH_3), 1.40 (t, CH_3), 1.92 (s, CH_3CN), 2.23 (s, CH_3), 3.98 (q, CH_2), 4.05 (q, CH_2), 6.80 (m, phenyl), 6.89 (m, phenyl), 7.00 (m, phenyl), 7.50 (t, NCHN), 7.55 (t, NCHN), 8.32 (s, H8), 8.35 (s, H8).

List of References

1. (a) Pruchnik, F.; Dus, D. *J. Inorg. Biochem.* **1996**, *61*, 55. (b) Bear, J. L.; Gray, H. B.; *et al. Cancer Chemother. Rep.* **1975**, *59*, 611. (c) Bear, J. L.; Howard, R. A.; Dennis, A. M. *Curr. Chemother. Proc. Int. Congress Chemother. 10th Meeting.* **1977**, *vol. 2.*
2. (a) Pneumatikakis, G.; Hadjiliadis, N. *J. C. S. Dalton* **1979**, 596. (b) Rainen, L.; Howard, R. A.; Kimball, A. P.; Bear, J. L. *J. Inorg. Chem.* **1975**, *11*, 2752. (c) Farrell, N. *J. Inorg. Biochem.* **1981**, *14*, 261. (d) Yu, B. S.; Choo, S. Y. *J. Pharm. Soc. Kor.* **1975**, *19*, 215. (e) Rubin, J. R.; Haromy, T. P.; Sundaralingam, M. *Acta Cryst.* **1991**, *C47*, 1712. (f) Waysbort, D.; Tarien, E.; Eichorn, G. L. *Inorg. Chem.* **1993**, *32*, 4774.
3. Bear, J. L.; Gray, Jr. H. B.; Rainen, L.; Chang, I. M.; Howard, R.; Serio, S.; Kimball, A. P. *Cancer Chemother. Rep. Part 1.* **1975**, *59*, 611.
4. (a) Dunbar, K. R.; Matonic, J. H., Saharan, V. P.; Crawford, C. A.; Christou, G. J. *J. Am. Chem. Soc.* **1994**, *116*, 2201. (b) Day, E. F.; Crawford, C. A.; Folting, K.; Dunbar, K. R.; Christou, G. *J. Am. Chem. Soc.* **1994**, *116*, 9339. (c) Crawford, C. A.; Day, E. F.; Saharan, V. P.; Folting, K.; Huffman, J. C.; Dunbar, K. R.; Christou, G. *Chem. Commun.* **1996**, 1113.
5. Fimiani, V.; Ainis, T.; Cavallaro, A.; Piraino, P. *J. of Chemother. 2*, **1990**, 319.
6. (a) Catalan, K. V.; Mindiola, D. J.; Ward, D. L.; Dunbar, K. R. *Inorg. Chem.* **1997**, *36*, 2458. (b) Catalan, K. *Master's Thesis.*
7. (a) Piraino, P.; Tresoldi, G.; Faraone, F. *J. Organomet. Chem.* **1982**, *224*, 305. (b) Piraino, P.; Bruno, G.; Tresoldi, G.; *et al. Inorg. Chem.* **1987**, *26*, 91.
8. Myers & Zeleznick, *J. Org. Chem.* **1963**, *28*, 2087.
9. (a) TEXSAN-TEXRAY Structure Analysis package, Molecular Structure Corporation, 1985. (b) MITHRIL: Integrated Direct Methods Computer Program, Gilmore, C. J. *J. Appl. Cryst.* **1984**, *17*, 42. (c) DIRDIF: Direct Methods for Difference Structures, An Automatic Procedure for Phase Extension; Refinement of Difference Structure Factors. Beurskens, P. T. Technical Report, **1984**.
10. SAINT & SADABS refs
11. (a) Sheldrick, G. *SHELXS-97*, **1990**. (b) Sheldrick, G. *SHELXL-97*. **1997**.
12. (a) Piraino, P.; Tresoldi, G.; Schiavo, S. L. *Inorg. Chim. Acta* **1993**, *203*, 101. (b) Schiavo, S. L.; Sinicropi, M. S.; Tresoldi, G.; Arena, C. G.;

Piraino, P. *J. Chem. Soc. Dalton Trans.* **1994**, 1517 and references therein.
13. Dunbar, K. R.; Majors, S. O.; Sun, R.-S. *Inorg. Chim. Acta* **1995**, *229*, 373.
14. Catalan, K. V.; Dunbar, K. R.; Maloney, M. M. manuscript in preparation.
15. Cotton, F. A. and Walton, R. A. *Multiple Bonds Between Metal Atoms*. Oxford Press, 2nd ed. **1993**, and references therein.
16. Pimblett, G.; Garner, C. D.; Clegg, W. *J. Chem. Soc. Dalton Trans.* **1986**, 1257.
17. (a) Burgess, J. *Trans. Met. Chem.* **1993**, *18*, 439. (b) Hollis, L. S.; Amundsen, A. R.; Stern, E. W. *J. Med. Chem.* **1989**, *32*, 136. (c) Allesio, E.; Balducci, G.; Calligaris, M.; Costa, G.; Attia, W. M.; Mestroni, G. *Inorg. Chem.* **1991**, *30*, 609.
18. Lippard, S. J. *Pure & Appl. Chem.* 1987, *59*, 731.
19. (a) Webb, G. A. *Annu. Rep. on NMR Spect.* **1983**, 14. (b) Garner, C. D.; Hughes, B. *Adv. in Inorg. and Radiochem.* **1975**, *17*, 1. (c) Matonic J. H.; Chen, S. J.; Pence, L. E.; Dunbar, K. R. *Polyhedron* **1992**, *11*, 541.
20. (a) Bear, J. L.; Yao, C.-L.; Lifsey, R. S.; Korp, J. D.; Kadish, K. M. *Inorg. Chem.* **1991**, *30*, 336. (b) Nicolò, F.; Bruno, G.; Schiavo, S. L.; Sinicropi, M. S.; Piraino, P. *Inorg. Chim. Acta.* **1994**, *223*, 145.

Chapter III

Dirhodium Formamidinate Compounds with Nitrogen Chelates As Mimics for 9-Ethyladenine

1. Introduction

Modified dirhodium carboxylate compounds of the type, $[Rh_2(O_2CMe)_2(N\text{-}N)_2H_2O]^{2+}$ (N-N = 2,2'-bpyridine (bpy) or 1-10-phenanthroline (phen)), exhibit higher carcinostatic activity against human oral carcinoma KB cells *in vitro* than the dirhodium tetracarboxylates.[1] Additionally, these compounds have been reported to influence the growth of the alga known as *Chlorella vulgaris* by inhibition of DNA, but not RNA synthesis.[1b] These compounds constitute yet another interesting class of dinuclear transition metal compounds for biological studies. Before embarking on reactions with biomolecules, however, we thought it would be instructive to explore general reactions of these compounds with nitrogen donor ligands.

The focus of chapter II was to demonstrate the ability of the modified purines 9-EtGH and 9-EtAH to bridge dinuclear transition metals, but there is increasing evidence that these purines can also chelate transition metals through the N6/O6 and N7 positions.[12] The compound of general formula $[Rh_2(O_2CCH_3)_3(bpy)(9\text{-}EtA)]$ is formed when one equivalent of $[Rh_2(O_2CCH_3)_4(bpy)$ or $[Rh_2(O_2CCH_3)_3(bpy)][O_2CCH_3]$ is reacted with equimolar amounts of 9-EtAH. The structure of this compound (Figure 1) revealed the presence a chelating, deprotonated $9\text{-}EtA^-$ ligand. The

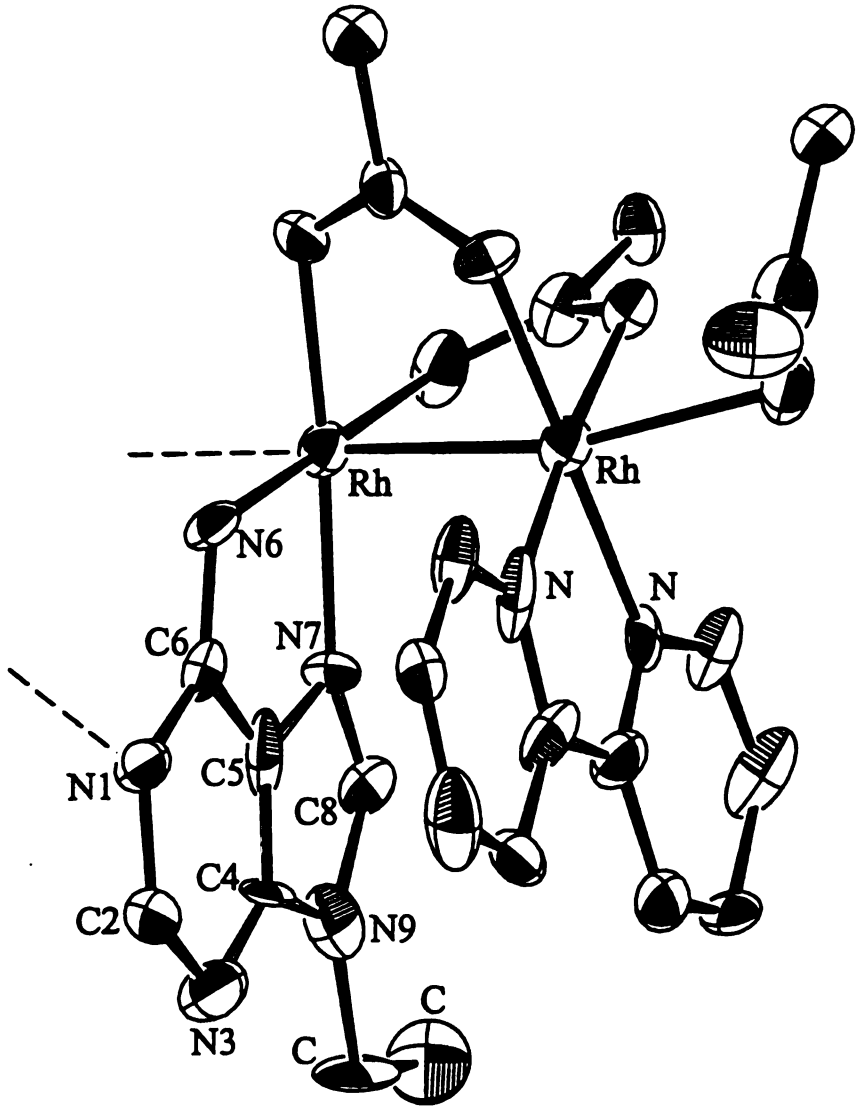


Figure 1. ORTEP representation of $[Rh_2(O_2CCH_3)_3(bpy)(9\text{-EtA})]$.[12]

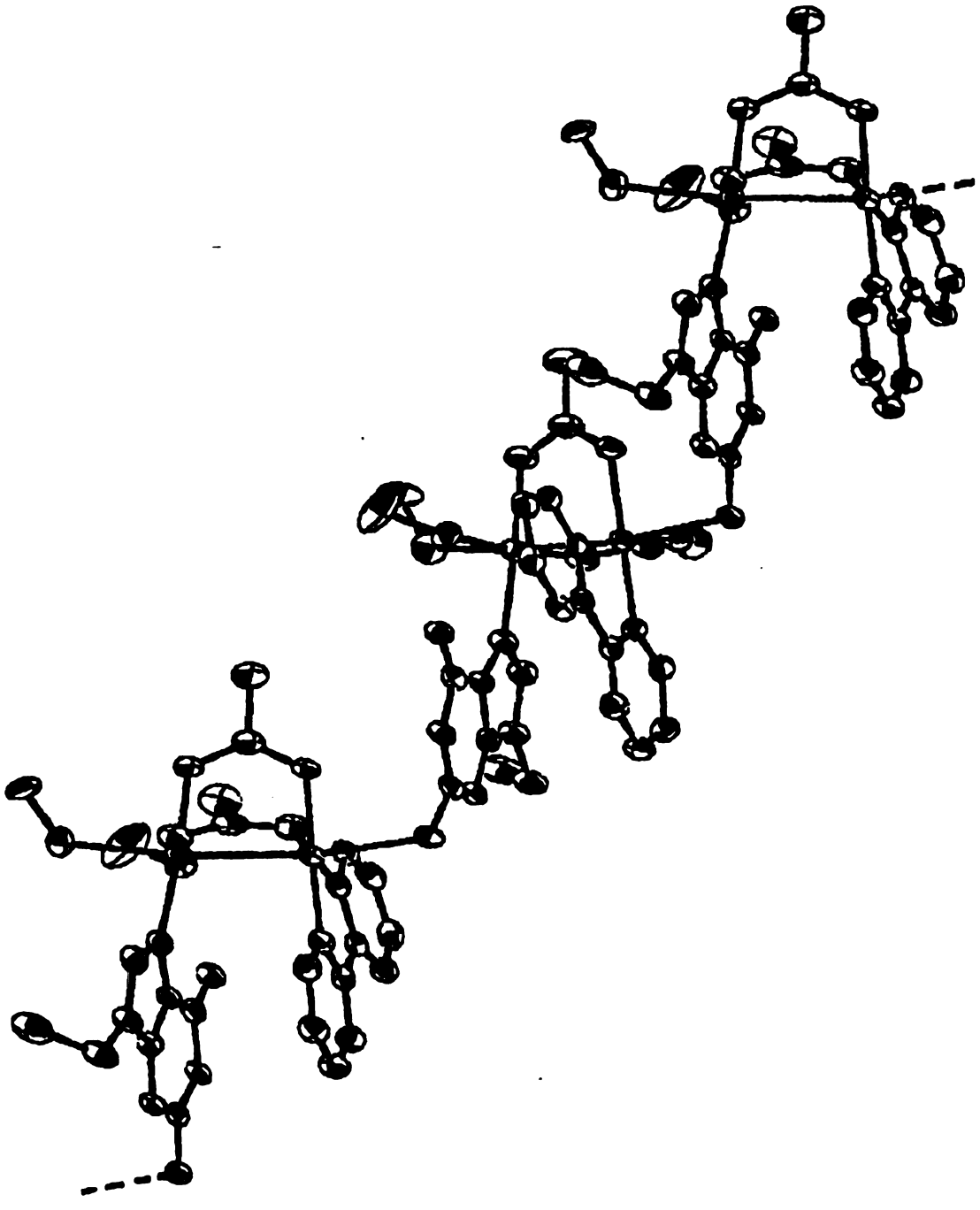
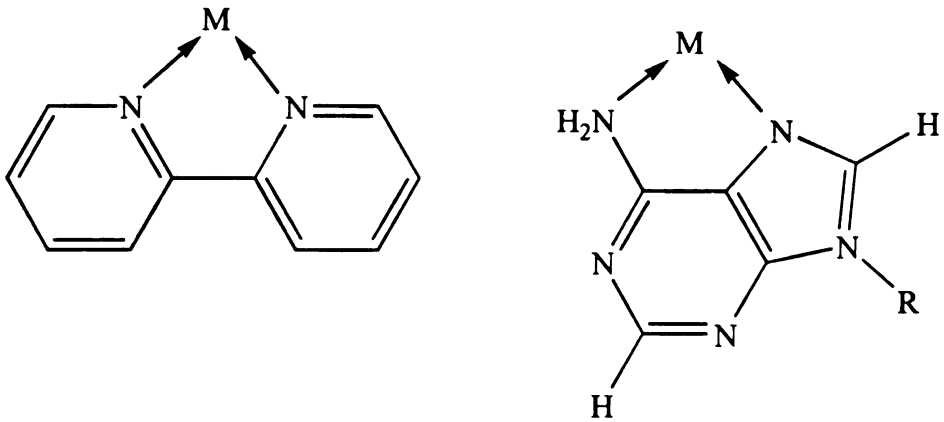


Figure 2. ORTEP representation of the polymer $[Rh_2(O_2CCH_3)_2(bpy)(9\text{-EtGH})]_x[BF_4]_{2x}\cdot yC_5H_{10}O$. The Rh2-N2' bond distance is 2.341(5) Å.[12]

dirhodium compound depicted in Figure 2 was heated in the presence of



R = deoxyribose or, ethyl

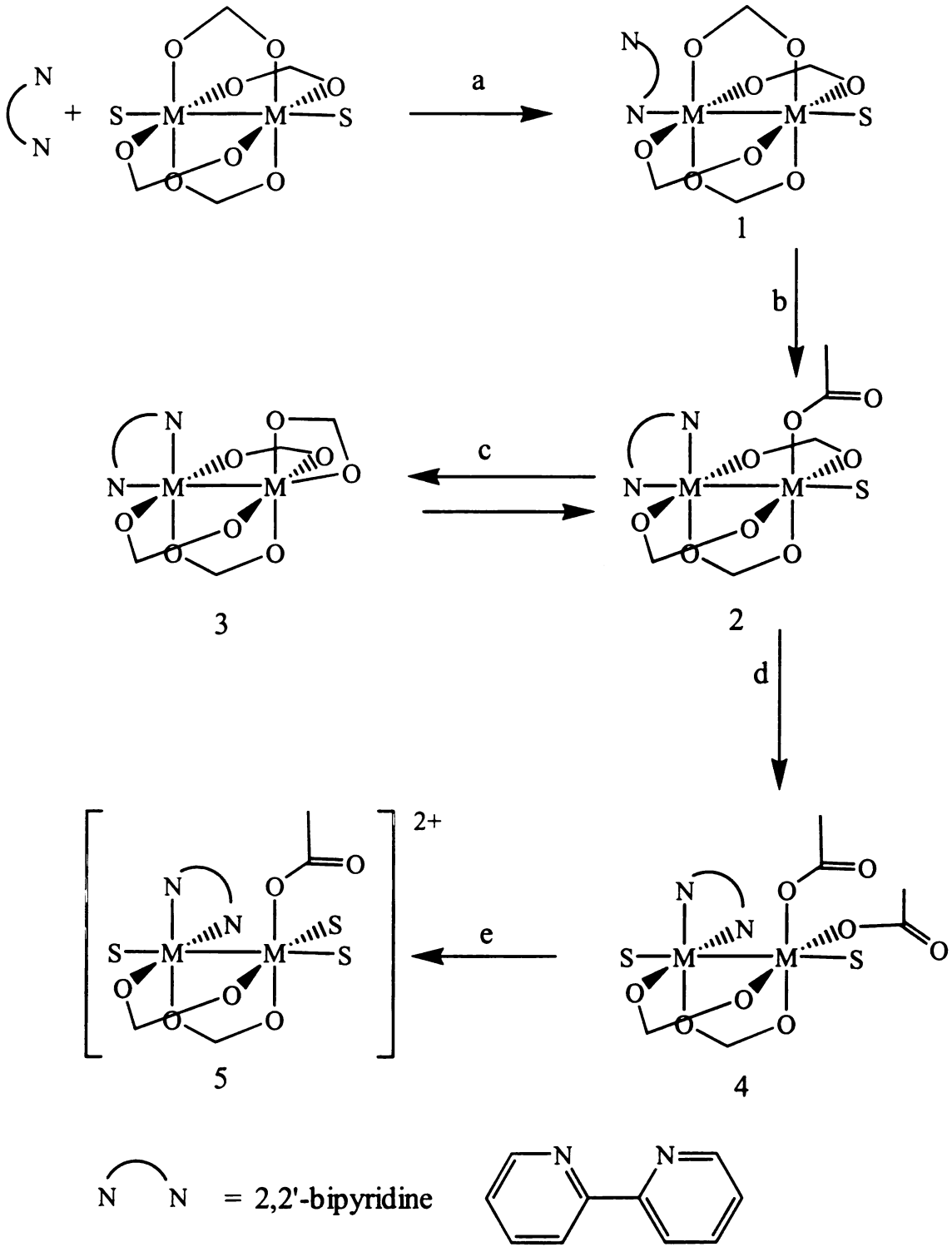
Figure 3. Schematic representation of the way that 2,2'-bipyridine can mimic the chelating abilities of adenine.

pyridine to yield a compound with a similar structure with chelating 9-EtG$^-$ in the ax-eq positions.[12]

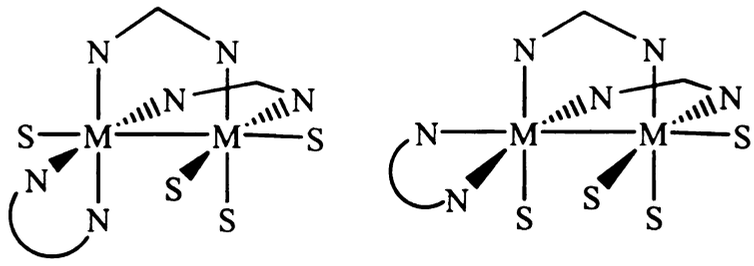
Prior to the discovery of dirhodium compounds that contain chelating 9-EtG$^-$ or 9-EtA$^-$ ligands, attempts to mimic the addition of a purine molecule to the dirhodium core were made by reacting $Rh_2(O_2CR)_4L_2$ (R = Me, Et, Ph or CF_3; L = donor solvent) with 2,2'-bipyridine (bpy) (Figure 3). These studies demonstrated the ability of a single N-N chelate ligand to interact with the Rh_2^{4+} core. The two major binding modes were found to be axial-equatorial (ax-eq) and equatorial-equatorial (eq-eq) (Figure 4).[5a-c]

Although no solid-state structures were reported, related studies

involving reactions of $Rh_2(DTolF)_2(O_2CCF_3)_2(H_2O)_2$ with bpy as well as 1,10-phenanthroline led researchers to conclude that similar binding modes for N-N chelates were possible in these compounds.[6] From a combination of structural information gathered on compounds in the solid-state and in solution, we have proposed a pathway whereby bpy enters the coordination sphere of the lantern structure of $Rh_2^{II,II}$ compounds (Scheme 1).[5c] As shown in scheme 1, the initial step involves a nucleophilic attack of the bpy at an axial site on the dirhodium unit. The axially-bound monodentate bpy (step a) rapidly undergoes chelate ring formation by displacement of an oxygen of a bridging carboxylate group (step b) to give an ax,eq chelate which is most stable as compound 3 whose single crystal X-ray structure was determined. X-ray crystallography also supports the conversion from the ax-eq chelating mode of the bpy to an eq-eq mode (step d). Compound 5 was not detected, but the structure of the cationic product of step e was verified by ^1H NMR spectroscopy.[5c]



Scheme 1



eq-eq ax-eq

Figure 4. Schematic representation of the two possible binding modes of bpy to a dinuclear metal center.

In the present chapter, we describe the syntheses and full characterization, including the single crystal X-ray structures, of compounds with one or two 2,2'-bpy or 1,10-phen ligands coordinated to a cis-$[Rh_2(DTolF)_2]^{2+}$ core. Reactions of these compounds with one equivalent each of 9-EtGH and 9-EtAH are also discussed. These investigations led to the surprising observation that certain dirhodium (II,II) compounds crystallize with vacant axial coordination sites even in the excess of donor solvent ligands. Solution structures as deduced from ^1H NMR spectroscopy and cyclic voltammetry are in accord with the solid-state structures determined by single crystal X-ray diffraction studies.

2. Experimental Section

A. Physical Measurements

^{1}H NMR spectroscopic data, including 2-dimensional experiments, were collected on a either a 300 or a 500 MHz-Varian Spectrometer. Chemical shifts were referenced relative to the residual proton impurities of the deuterated solvents. Electrochemical measurements were performed by using an EG&G Princeton Applied Research Model 362 scanning potentiostat in conjunction with a Soltec Model VP-6424S X-Y recorder. Cyclic voltammetric experiments for **(7)**, **(8)**, **(9)** and **(10)** were carried out at r.t. in acetonitrile containing 0.1 M tetra-*n*-butylammonium tetrafluoroborate as the supporting electrolyte. $E_{1/2}$ values, determined as $(E_{p,a} + E_{p,c})/2$, were referenced to the Ag/AgCl electrode without correction for junction potentials. The $Cp_2Fe/[Cp_2Fe]^+$ couple occurs at $E_{1/2} = {}^+0.45$ V for the cyclic voltammograms of compounds **(7)** and **(8)** and at $E_{1/2} = {}^+0.47$ V for compound **(10)** under the same experimental conditions in acetonitrile.

B. Synthesis.

i. Starting Materials

The partially solvated compound, $[Rh_2(DTolF)_2(CH_3CN)_6][BF_4]_2$ **(2)**, was prepared by literature procedures.[3a] The reagents 2,2'-bipyridine (bpy) and 1,10-phenanthroline (phen) were purchased from Aldrich Chemical

Company and recrystallized from anhydrous diethyl ether. $NaBPh_4$ and 9-ethylguanine were purchased from Sigma and used without further purification. The 9-ethyladenine was prepared by literature procedures.[3a] Prior to distillation under a nitrogen atmosphere, all solvents were predried from 4 Å molecular sieves with the exception of acetone and acetonitrile which were predried with 3 Å molecular sieves. Diethyl ether was distilled from Na/K benzophenone ketyl radical whereas toluene was distilled from Na/K drying agent with no indicator. Acetone and acetonitrile were distilled from 3 Å molecular sieves, and ethyl acetate was distilled from 4 Å molecular sieves while methylene chloride was distilled from P_2O_5. Acetonitrile was passed through an activated alumina column to further dry it for the electrochemical measurements.

ii. **Reaction Procedures.** All manipulations were performed under inert atmospheric conditions using standard Schlenk techniques unless otherwise stated.

(1) Preparation of $[Rh_2(DTolF)_2(bpy)(CH_3CN)_{3,4}][BF_4]_2$ (7a, 7b)

$[Rh_2(DTolF)_2(CH_3CN)_6][BF_4]_2$ **(2)** (93 mg, 0.0857 mmol) was dissolved in acetone (5 mL) to yield a green solution which was treated with a solution of bpy (13.4 mg, 0.0858 mmol) in acetone (2 mL). The reaction mixture was allowed to stir at r.t. for ~24 h, after which time the volume of

the reaction solvent was reduced to one-half of its original volume under reduced pressure. The product was precipitated from solution by the addition of diethyl ether (~10 mL), and collected by filtration in air to give 88 mg (0.0767 mmol), 89.5% yield. Single crystals of one morphology were grown from a CH_3CN solution of the compound layered with diethyl ether. A second morphology of single crystals was grown from an acetone solution layered with ethyl acetate.

(2) Preparation of $[Rh_2(DTolF)_2(bpy)_2(CH_3CN)][BF_4]_2$ (8)

A solution of **(2)** (105, mg, 0.0968 mmol) in CH_3CN (7 mL) was treated with bpy (30.24 mg, 0.0282 mmol), and refluxed for ~48 h. The reaction mixture was cooled to r.t., and diethyl ether (15 mL) was added to yield microcrystals (31 mg, 0.0181 mmol, 64%) which were collected by filtration in air. X-ray quality single crystals, **(8a)**, were grown from the careful layering of an acetone solution of **(8)** in ethyl acetate. A second morphology, **(8b)**, was prepared by treating an acetone solution of the compound with an equimolar quantity of $NaBPh_4$ (15.65 mg, 45.7 mmol) which led to the precipitation of $NaBF_4$. The solution was filtered to remove the by-product salt, and the filtrate was layered with ethyl acetate (6 mL).

(3) Preparation of $[Rh_2(DTolF)_2(phen)(CH_3CN)_3][BF_4]_2$ (9)

A mixture of **(2)** (100 mg, 0.0934 mmol) and 1,10-phenanthroline

(18.3 mg, 0.0921 mmol) in CH_2Cl_2 (5 mL) was stirred for ~72 h at r.t. The mixture was filtered through Celite in air to remove any undissolved materials, and concentrated to one-half of its original volume. The green product was isolated after the addition of diethyl ether, dried *in vacuo*, and recrystallized from methylene chloride and diethyl ether (94 mg, 89% yield).

(4) Preparation of $[Rh_2(DTolF)_2(phen)_2(CH_3CN)_2][BF_4]_2$ (10)

A mixture of **(2)** (75.0 mg, 0.0701 mmol) and 1,10-phenanthroline (13.8 mg, 0.0696 mmol) in CH_3CN (10 mL) was heated to reflux for ~64 h. The green solution was concentrated to one-half of its original volume, and the product was isolated as microcrystals after the addition of diethyl ether. The microcrystals were collected by filtration in air, and dried *in vacuo* (60 mg, 57% yield). X-ray quality single crystals were grown from the careful layering of an acetone solution of **(10)** with ethyl acetate.

(5) Preparation of the mixture of $[Rh_2(DTolF)_2(bpy)(CH_3CN)_4][BF_4]_2$ (7) and $[Rh_2(DTolF)_2(bpy)_2(CH_3CN)][BF_4]_2$ (8)

A dark orange-red solution of $[Rh_2(DTolF)_2(CH_3CN)_6][BF_4]_2$ **(2)** (75.0 mg, 0.0692 mmol) in acetone (4 mL) was added via a cannula to a solution of bpy (10.8 mg, 0.0691 mmol) in acetone (5 mL). The mixture was allowed to stir for 24 h at r.t. after which time the brown-green solution was concentrated to ~4 mL under reduced pressure, and the products precipitated

by the addition of hexanes (1 mL) and diethyl ether (5 mL). The resulting microcrystalline material was collected by suction filtration in air, and dried *in vacuo*. The product was identified as a mixture by ^{1}H NMR spectroscopy (*vide infra*).

(6) Reaction of $[Rh_2(DTolF)_2(bpy)(CH_3CN)_3][BF_4]_2$ (7) with 9-ethyladenine (9-EtAH)

A green acetone solution of **(7)** (44 mg, 0.0406 mmol, 3mL) was treated with one equivalent of 9-EtAH (6.6 mg, 0.0406 mmol) dissolved in 2 mL of acetone. The resulting mixture was allowed to stir at r.t. for ~48 h. The addition of diethyl ether (10 mL) resulted in the precipitation of a green microcrystalline solid. The product was redissolved in acetonitrile and carefully layered with diethyl ether which produced large X-ray quality crystals of the previously reported compound $[Rh_2(DTolF)_2(9\text{-}EtAH)_2(CH_3CN)][BF4]_2$.[3a]

(7) Reaction of $[Rh_2(DTolF)_2(bpy)(CH_3CN)_3[BF_4]_2$ (7) with 9-ethylguanine (9-EtGH)

A green methanol solution of **(7)** (24.3 mg, 0.022 mmol, 6 mL) was treated with 9-EtGH (4.1 mg, 0.023 mmol), and allowed to stir at r.t. for 24 h. The resulting green-brown solution was treated with diethyl ether (15 mL) which led to the precipitation of unreacted 9-EtGH. The diethyl ether was evaporated under reduced pressure, and the resulting methanol mixture was allowed to stir under refluxing conditions for ~1 h. The precipitation of a green product was induced by the addition of diethyl ether (15 mL). The green product was characterized by ^1H NMR spectroscopy as a mixture of compound **(8)** and the known compound $[Rh_2(DTolF)_2(9\text{-}EtGH)_2(CH_3CN)_2][BF_4]_2$.[13]

(8) Reaction of $[Rh_2(DTolF)_2(bpy)_2(CH_3CN)[BF_4]_2$ (8) with 9-EtAH

A green acetone solution of **(7)** (44 mg, 0.0406 mmol, 3 mL) was treated with one equivalent of 9-EtAH (6.6 mg, 0.0405 mmol). The resulting mixture was allowed to stir at r.t. for ~48 h. The addition of diethyl ether (10 mL) resulted in the precipitation of a green microcrystalline solid. The product was redissolved in acetone and carefully layered with ethyl acetate to produce large green single crystals. A unit cell

determination of the crystals revealed the compound to be crystals of **(8)**.

C. X-ray Crystallography and Structure Solution

A hemisphere of crystallographic data were collected for **(7b)**, **(8a)**, **(8b)**, **(9)** and **(10)** on a Siemens SMART diffractometer at 293(2) K with graphite monochromated Mo Kα (average λ_α = 0.71073 Å) radiation and corrected for Lorentz and polarization effects. A total of ¼ of a sphere of crystallographic data were collected for **(7a)** on the same instrument. Calculations were performed on a cluster network of Silicon Graphics computers in the visualization facility in the Department of Chemistry at Michigan State University. The frames were integrated with the Siemens SAINT software package, and the data were corrected for absorption using the SADABS program. The structures of **(7b)**, **(8b)** and **(9)** were solved by Patterson methods using the SHELXS program in the Siemens SHELXTL v. 5.05 software. The structure of compound **(7a)** was solved by direct methods using the same software package.[10] The structure of **(8a)** was solved by Patterson methods using the SHELXS-86 program in the Texsan software package.[11] The structure of compound **(10)** was not determined due to an unresolved twinning problem. All of the structures were refined by full-matrix least-squares calculations on F^2 using the SHELXL program in the SHELXTL software package. Relevant crystallographic data and

other pertinent information are listed in Tables 17 - 22.

(1) $[Rh_2(DTolF)_2(bpy)(CH_3CN)_3][BF_4]_2$ (7a). Single crystals of **(7a)** were grown by the careful layering of an acetone solution of $[Rh_2(DTolF)_2(bpy)(CH_3CN)_{3,4}][BF_4]_2$ **(7)** in ethyl acetate. A green rectangular crystal with approximate dimensions 0. 39 x 0.39 x 0.31 mm^3 was mounted on the tip of a glass fiber with Dow Corning grease. Indexing and refinement of 133 reflections selected from a total of 45 frames with an exposure time of 10 sec/frame gave unit cell parameters for a monoclinic unit cell. A total of 1,321 frames were collected with a scan width of 0.3° in ω and an exposure time of 30 sec/frame. The total data collection time was 13.5 h. The integration of the frame data using a monoclinic B-centered unit cell yielded a total of 14,297 reflections in the range h = 13 → -13, k = 26 → -30, l = 23 → -17 with a maximum 2θ angle of 55.04°. Of the 5,450 unique reflections a total of 4,269 remained with $I > 2\sigma(I)$ and $R_{int} = 0.0341$ and $R_{sig} = 0.0499$ after data reduction. The positions of the Rh atoms were located by direct methods. The remaining non-hydrogen atoms were located through successive cycles of least-squares refinements and difference Fourier maps. Atoms C(47A) and C(48A) of a disordered axial acetonitrile ligand were located by an electron density difference map, and refined

isotropically. All non-hydrogen atoms were refined anisotropically while the hydrogen atoms were calculated at fixed positions. Final refinement of 720 parameters gave residuals of R1 = 0.0462 and wR2 = 0.1134 for 5,450 reflections. The goodness-of-fit = 0.944, and the maximum and minimum peaks in the final difference Fourier map were 1.113 $e^-/Å^3$ and $^-0.363$ $e^-/Å^3$, respectively.

(2) $[Rh_2(DTolF)_2(bpy)(CH_3CN)_4][BF_4]_2$ (7b). Orange-red rectangular crystals of **(7b)** were grown from the slow diffusion of diethyl ether into an acetonitrile solution of $[Rh_2(DTolF)_2(bpy)(CH_3CN)_{3,4}][BF_4]_2$ **(7)**. A crystal of dimensions 0.31 x 0.26 x 0.21 mm^3 was mounted on the tip of a glass fiber with epoxy cement. The cell parameters of a monoclinic crystal system were refined from a fit of 82 reflections selected from 45 frames with 10 sec/frame exposure time. A total of 1,321 frames with 30 sec/frame exposure time were collected at a scan width of 0.3° in ω. The integration of the frames using a monoclinic B-centered unit cell yielded 27,163 reflections in the range h = 17 → $^-16$, k = 23 → $^-15$, l = 26 → $^-26$ with a maximum 2θ angle of 55.32°. Of the total data collected, 10,679 reflections were unique with 6,834 reflections with $I > 2\sigma(I)$ remaining after data reduction. The R_{int} was 0.0595 and the R_{sig} was 0.0945. The positions of the

Rh atoms were located by Patterson methods while the remaining non-hydrogen atoms were located through successive cycles of least-squares refinements and difference Fourier maps. All remaining non-hydrogen atoms were refined anisotropically by full-matrix least-squares calculations on F^2 while the hydrogen atoms were calculated at fixed positions. The final refinement of 654 parameters revealed maximum and minimum peak heights of 0.855 $e^-/Å^3$ and −0.497 $e^-/Å^3$, respectively in the final difference Fourier map. Final anisotropic full-matrix least-squares refinement on F^2 converged at R1 = 0.0539 and wR2 = 0.1012 and a goodness-of-fit of 1.111.

(3) $[Rh_2(DTolF)_2(bpy)_2(CH_3CN)][BF_4]_2$ (8a). A green rhombohedral crystal of **(8a)** having dimensions 0.13 x 0.13 x 0.10 mm^3 obtained by the slow diffusion of an acetonitrile solution of **(8)** into ethyl acetate was mounted on the tip of a glass fiber with Dow Corning grease. Refinement of 33 reflections indexed from 45 frames collected with an exposure time of 10 sec/frame gave unit cell parameters for a monoclinic unit cell. A total of 1,621 frames were collected with a scan width of 0.3° in ω. The exposure time for each frame was 30 sec/frame. The frames were integrated using a B-centered monoclinic unit cell to yield a total of 36,549 reflections in the range h = 25 → -22, k = 17 → -18, l = 25 → -26 with a maximum 2θ angle

of 56.58°. After data reduction, of the 11,838 unique reflections, 7,092 reflections remained with $I > 2\sigma(I)$. The data set gave a $R_{int} = 0.0767$ and $R_{sig} = 0.1018$. The positions of the Rh atoms were located by Patterson methods, and the remaining non-hydrogen atoms were located through successive cycles of least-squares refinements and difference Fourier maps. The final least squares refinement included all non-hydrogen atoms as anisotropic and hydrogen atoms at calculated positions. The final difference Fourier map revealed maximum and minimum peak heights of 0.492 $e^-/Å^3$ and -0.520 $e^-/Å^3$, respectively. The final full-matrix least-squares refinement converged at R1 = 0.0600 and wR2 = 0.0891 for 668 parameters and 11,837 reflections with a goodness-of-fit of 1.140.

(4) $[Rh_2(DTolF)_2(bpy)_2(H_2O)][BF_4][BPh_4]$ (8b). X-ray quality single crystals of **(8b)** were grown by the careful layering of an acetone solution of **(8)** in ethyl acetate, that was not predried nor distilled. Green rectangular crystals grew at the diffusion layer, but unfortunately, all of the crystals were very soft and exhibited only weak X-ray diffraction patterns even at low temperatures. In spite of this, a crystal of dimensions 0.46 x 0.36 x 0.18 mm^3 was mounted on a glass fiber with Dow Corning grease and subjected to an X-ray experiment on a CCD diffractometer. Refinement of 54 reflections that were indexed from 45 frames with an exposure time of 10

sec/frame gave unit cell parameters for a monoclinic unit cell. A total of 1,321 frames were collected with a scan width of 0.3° in ω and an exposure time of 30 sec/frame. The data were integrated using a B-centered monoclinic unit cell to yield a total of 47,533 reflections in the range h = 24 $\rightarrow$ -30, k = 10 $\rightarrow$-18, l = 36 $\rightarrow$ -36 with a maximum 2θ angle of 56.40°. After data reduction of the 19,084 unique reflections, 8,190 reflections remained with $I > 2\sigma(I)$. The high $R_{int} = 0.1321$ and $R_{sig} = 0.2235$ of the data is an indication of the poor quality of the data due to the small number of reflections observed at higher 2θ angles. The positions of the Rh atoms were located by Patterson methods and the remaining non-hydrogen atoms were located from successive cycles of least-squares refinements and difference Fourier maps. The final full-matrix least-squares refinement included all the non-hydrogen atoms as anisotropic and all of the hydrogen atoms at fixed positions. The final difference Fourier map contained maximum and minimum peak heights of 1.19 $e^-/Å^3$ and $^-0.824$ $e^-/Å^3$, respectively. The final R1 was 0.1093 with the wR2 = 0.2155 for 1,013 parameters and 19,079 reflections and a goodness-of-fit of 1.132. The high R factors are an indication of the rather poor quality of the data set which had a large mosaic spread.

(5) $[Rh_2(DTolF)_2(phen)(CH_3CN)_3][BF_4]_2$ **(9).** A green prismatic platelet of dimensions 0.31 x 0.23 x 0.13 mm^3 was obtained from the careful layering of a methylene chloride solution of **(9)** with ethyl acetate. The selected crystal was mounted on the tip of a glass fiber with Dow Corning grease. A total of 1,321 reflections were collected with a scan width of 0.3° in ω and an exposure time 30 sec/frame. A total of 107 reflections were indexed from 15 of these frames. The reflections were refined to give unit cell parameters for a triclinic unit cell. The data were integrated using a triclinic unit cell to yield a total of 17,899 reflections in the range h = 16 → -8, k = 17 → -18, l = 24 → -25 with a maximum 2θ angle of 56.48°. After data reduction of the 12,465 unique reflections, 9,752 reflections remained with $I > 2\sigma(I)$. The R_{int} and R_{sig} were 0.0167 and 0.0423, respectively. The positions of the Rh atoms were located by direct methods and the remaining non-hydrogen atoms were located from successive cycles of least-squares refinements and difference Fourier maps. Restraints were used to solve disordered ethyl acetate and water molecules that were located in the interstices. The final full-matrix least-squares on F^2 for all atoms non-hydrogen atoms as anisotropic revealed maximum and minimum peak heights of 1.097 $e^-/Å^3$ and -1.134 $e^-/Å^3$ with final residuals of R1 = 0.0449

and wR2 = 0.1250 for 708 parameters and 12,465 reflections. The final goodness-of-fit was 1.039.

(6) $[Rh_2(DTolF)_2(phen)_2(CH_3CN)][BF_4]_2$ (10). A green rectangular platelet having dimensions 0.26 x 0.21 x 0.10 mm^3 was coated in paratone oil to prevent the loss of solvent from the crystal and mounted on the tip of a glass fiber with Dow Corning grease. A total of 56 reflections were indexed from 45 frames collected at an exposure time of 20 sec/frame. The reflections were refined to give unit cell parameters for an orthorhombic unit cell. A total of 60,391 reflections were collected with a scan width of 0.3° in ω and an exposure time 60 sec/frame. The data were integrated using an orthorhombic unit cell to yield a total of 23,860 reflections in the range h = $17 \rightarrow {}^{-}17$ k = $48 \rightarrow {}^{-}50$, l = $13 \rightarrow {}^{-}26$ with a maximum 2θ angle of 84.58°. After data reduction of the 23,860 unique reflections, only 9,028 reflections remained with $I > 2\sigma(I)$. The R_{int} and R_{sig} values were 0.1624 and 0.2831, respectively. Because of the weak diffraction patterns and the inherent twinning problems with these crystals, it was not possible to solve the X-ray structure of this compound.

3. Results and Discussion

A. Reactions of $Rh_2^{II,II}$ and bpy

(1) Syntheses. Reports in the literature of reactions between

$$[Rh_2(DTolF)_2(CH_3CN)_6][BF_4]_2 \quad (\mathbf{2}) + 1\text{bpy} \xrightarrow{CH_3CN} [Rh_2(DTolF)_2(bpy)(CH_3CN)_4][BF_4]_2 \quad (\mathbf{7}) + [Rh_2(DTolF)_2(bpy)_2(CH_3CN)_2][BF_4]_2 \quad (\mathbf{8}) \qquad (1)$$

$$[Rh_2(DTolF)_2(CH_3CN)_6][BF_4]_2 \quad (\mathbf{2}) + 1\text{bpy} \xrightarrow{\text{acetone}} [Rh_2(DTolF)_2(bpy)(CH_3CN)_4][BF_4]_2 \quad (\mathbf{7}) \qquad (2)$$

$$[Rh_2(DTolF)_2(CH_3CN)_6][BF_4]_2 \quad (\mathbf{2}) + 2\text{bpy} \xrightarrow[\text{reflux}]{\text{acetone}} \mathbf{7} \qquad (3a)$$

$$[Rh_2(DTolF)_2(CH_3CN)_6][BF_4]_2 \quad (\mathbf{2}) + 2\text{bpy} \xrightarrow[\text{reflux}]{CH_3CN} [Rh_2(DTolF)_2(bpy)_2(CH_3CN)_2][BF_4]_2 \quad (\mathbf{8}) \qquad (3b)$$

$Rh_2(DTolF)_2(O_2CCF_3)_2(CH_3OH)_2$ and nitrogen-chelates revealed that the bridging trifluoroacetate ligands are substitutionally labile.[6] No products were characterized by X-ray crystallography, however, thus we investigated the related chemistry of $[Rh_2(DTolF)_2(CH_3CN)_6][BF_4]_2$ **(2)**. Compound **(2)** reacts with 1 equivalent of bpy in CH_3CN to yield a mixture of products (Equation 1) as discerned by ^1H NMR spectroscopy. Due to this situation, we set out to design a series of reactions that would preferentially yield only one of the products. This was achieved by using acetone instead of CH_3CN as the solvent (Equation 2). The product,

$[Rh_2(DTolF)_2(bpy)(CH_3CN)_{3,4}][BF_4]_2$ **(7)**, accounts for one set of bpy resonances observed in the ^1H NMR spectrum of the solid isolated from CH_3CN. Under refluxing conditions in acetone where axial CH_3CN exchange is presumably not favored, compound **(7)** is formed (Equation 3a). Thus, by replacing the coordinating solvent CH_3CN with acetone, one can effect the coordination of two bpy ligands to a single dirhodium core instead of only one. The result is the formation of $[Rh_2(DTolF)_2(bpy)_2(CH_3CN)][BF_4]_2$ **(8a)** (Equation 3b).

(2) Electrochemistry of 7 and 8. The cyclic voltammogram of $[Rh_2(DTolF)_2(bpy)(CH_3CN)_3]^{2+}$ **(7)** shows one reversible oxidation at $E_{1/2}$ = $^+1.0$ V and one reversible reduction at $E_{1/2}$ = $^-0.44$ V in acetonitrile (Figure 5). A quasi-reversible reduction process occurs at $E_{p,c}$ = $^-1.19$ V with an associated return wave of $E_{p,a}$ = $^-1.15$ V (i_{pc}/i_{pa} = 0.75). The electrochemical properties of **(7)** are somewhat different from those of the parent compound $[Rh_2(DTolF)_2(CH_3CN)_6]^{2+}$ **(2)** which exhibits a reversible oxidation at $^+1.0$ V and a quasi-reversible oxidation process at $^+1.55$ V. Two irreversible cathodic processes are also observed for compound **(7)** at $^-0.51$ V and $^-1.34$ V.[3e] The electrochemical behavior of $[Rh_2(DTolF)_2(bpy)_2(CH_3CN)_2]^{2+}$ **(8)** in acetonitrile is very similar to that of the mono-bpy compound **(7)**.

Compound **(8)** exhibits two quasi-reversible reductions at $E_{p,c} = {}^{-}0.50$ V and $^{-}1.3$ V. The associated return waves for the reductions occur at $E_{p,a} = {}^{-}0.37$ V (i_{pc}/i_{pa} = 0.5) and $^{-}1.2$ V (i_{pc}/i_{pa} = 0.4), respectively. The reversible anodic process at $E_{1/2} = {}^{+}1.02$ V for **(8)** is at nearly the same potential as the process observed for **(7)**, but is somewhat masked by the reduction of the solvent (Figure 5).

$[Rh_2(O_2CR)_2(bpy)_2CH_3CN)_2]^{2+}$ (R = Me, Et, Ph) do not undergo oxidation processes.[5a] These compounds do, however, exhibit a one-electron reduction process occurring at $\sim{}^{-}0.9$ V.

(3) ^{1}H NMR studies of (7) and (8). As previously mentioned, the original syntheses of compounds **(7)** and **(8)** involved their isolation as a mixture from CH_3CN. A ^{1}H NMR spectrum of the mixture initially prompted us to postulate that we had obtained two different mono-bpy isomers, namely those with the bpy groups arranged in either the eq-eq or ax-eq binding modes (Figure 4). Figure 6 depicts an expansion of the aromatic region in the 2-D COSY NMR spectrum of the mixture.

The 2D ^{1}H NMR spectrum of the mixture in CD_3CN depicts two independent sets of four coupled protons which can be attributed to bpy based protons. Each of these sets is shifted from the resonances observed for the free ligand. Also present in the 2D spectrum are two triplets that are not coupled to any of the protons in the sample. These two triplets can be

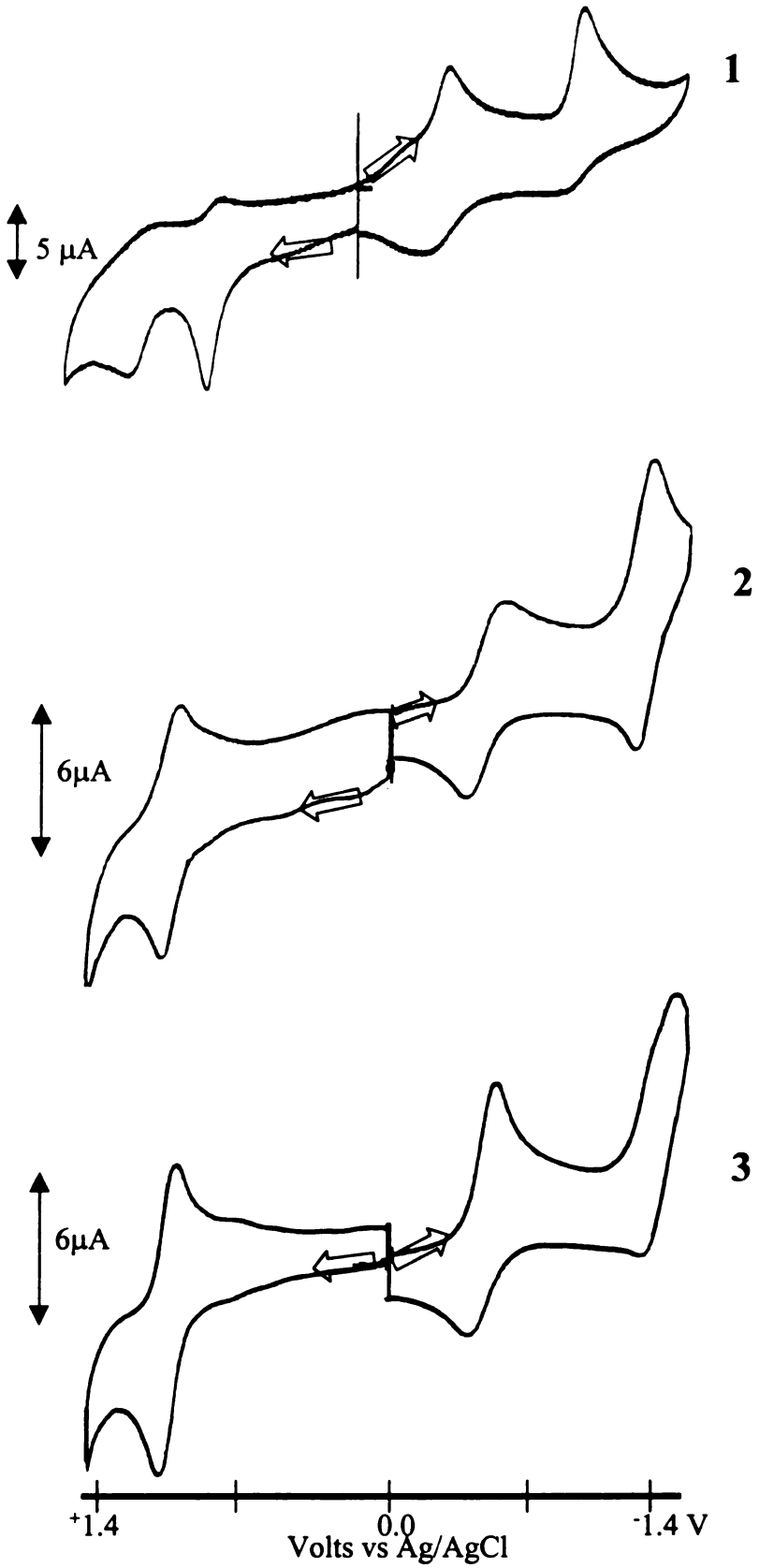


Figure 5. Cyclic voltammograms of compounds **(2)**, **(7)** and **(8)**.

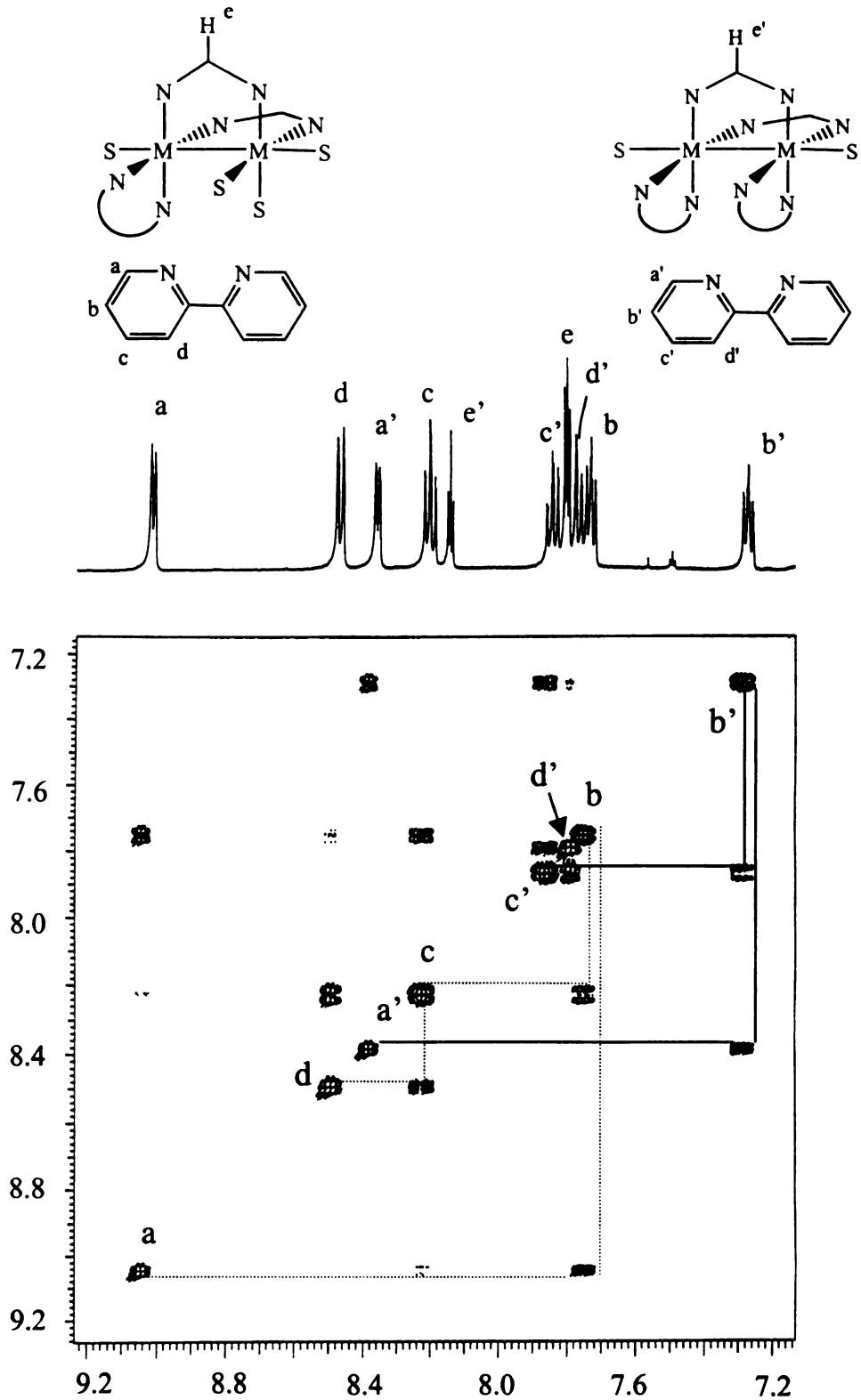


Figure 6. 2-dimensional ^{1}H NMR spectrum in the aromatic bipyridine region of the mixture of compounds **7** and **8**.

assigned to the ^{103}Rh coupled methylene protons of the $[DTolF]^-$ groups. The ^1H NMR spectra of authentic crystals of compounds **(7a)** and **(7b)** allowed us to definitively assign the 2D spectrum. One of the sets of four bpy resonances *a*, *b*, *c* and *d* at 7.75, 8.24, 8.53 and 9.04 ppm, respectively belong to the aromatic bpy protons of $[Rh_2(DTolF)_2(bpy)(CH_3CN)_{2,3}][BF_4]_2$ **(7)** (Table 23). The triplet labeled *e* at 7.82 ppm in Figure 6 is assigned to the hydrogen on the methylene carbon of the $[DTolF]^-$ groups, and is in a 1:1 ratio with each of the bpy resonances. The methyl protons of the $[DTolF]^-$ groups resonate at 2.22 ppm while the resonances for the equatorial coordinated acetonitrile groups occur at 2.25 ppm. A simulation of the ^1H NMR spectrum of compound **(7)** is in excellent agreement with the experimental spectrum.

The ^1H NMR spectrum of the bis-bpy compound $[Rh_2(DTolF)_2(bpy)_2(CH_3CN)][BF_4]_2$ **(8a)** is identical to the ^1H NMR spectrum of $[Rh_2(DTolF)_2(bpy)_2(H_2O)][BF_4][BPh_4]$ **(8b)**, and accounts for the remaining set of four bpy resonances *a'*, *b'*, *c'* and *d'* at 7.29, 7.79, 7.86 and 8.38 ppm, respectively (Table 23). The triplet at 8.17 ppm labeled *e'* is assigned to the hydrogen atom of the methylene carbon of $[DTolF]^-$, and is in a 1:2 ratio with the bpy resonances. The $[DTolF]^-$ methyl protons are observed as a singlet at 2.23 ppm. The axial CH_3CN ligands for both **(7)**

and **(8)** are in rapid exchange with CD_3CN on the NMR time scale, and are observed at the chemical shift for free CH_3CN, which is at 1.95 ppm (Table 23).

(4) Molecular Structures of (7a) and (7b). The compound $[Rh_2(DTolF)_2(bpy)(CH_3CN)_3][BF_4]_2$ **(7a)** crystallizes in the monoclinic space group $P2_1/n$ with two $[BF]_4^-$ anions, and one molecule each of interstitial acetone and water. The most notable feature of compound **(7a)** is that only one of the Rh atoms possesses an axial CH_3CN molecule, namely, Rh1 with a Rh-N bond distance of 2.101(4) Å (Figure 7). The axial position of Rh2 is vacant. Although this is an unusual result, it is not entirely unprecedented for dirhodium compounds containing formamidinate ligands to possess only one axial solvent molecule. A similar observation was made in our laboratories for the compound $[Rh_2(DTolF)_2(9\text{-}EtAH)_2(CH_3CN)][BF_4]_2$.[3a] This compound was observed to possess only one axial solvent in the coordination sphere due to a $[BF_4]^-$ anion located in close proximity to the vacant site, thus preventing the coordination of a donor solvent molecule in the solid state. It is important to note that the tetra-formamidinate compound $Rh_2(DPhF)_4$ itself can crystallize with or without the presence of axial ligands depending on the

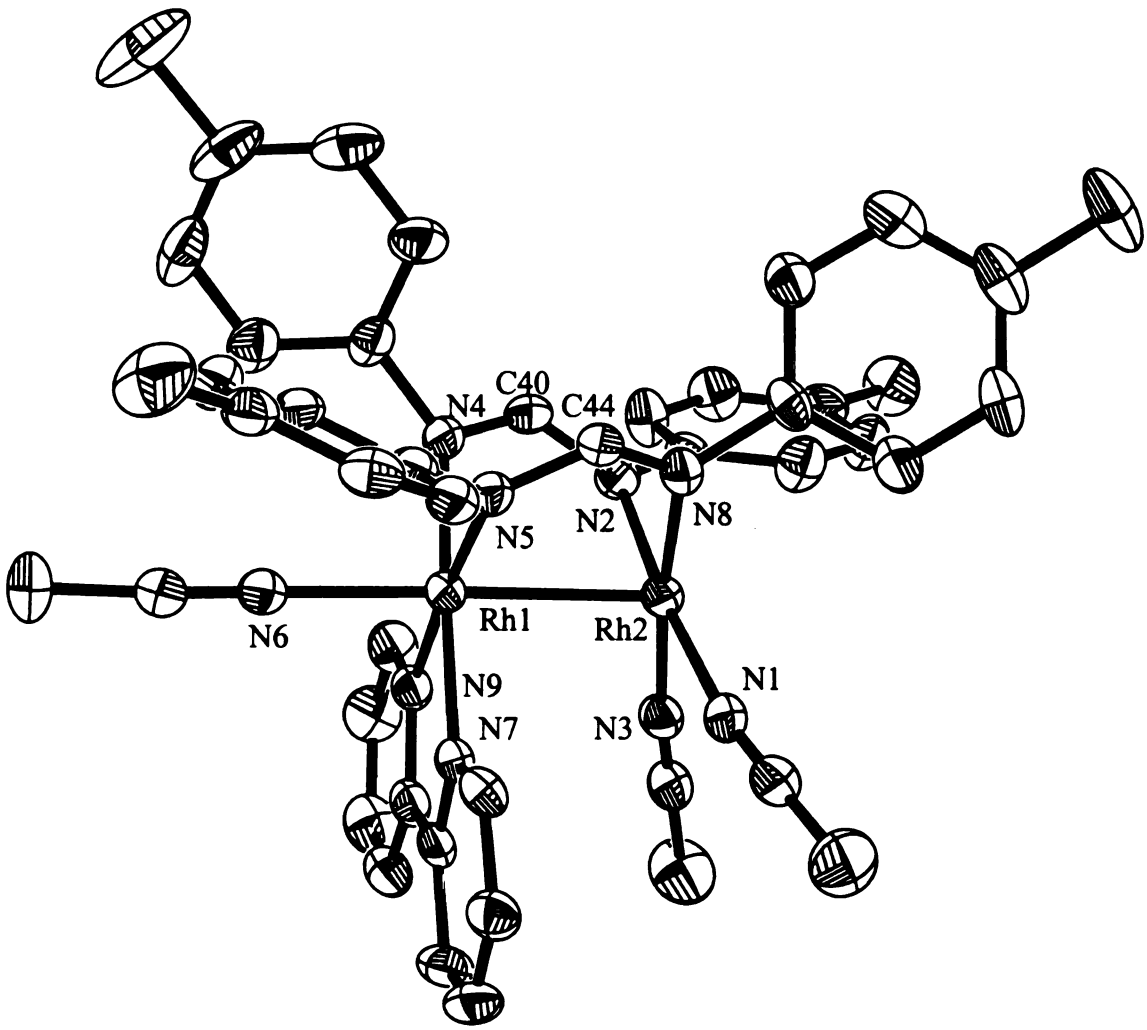


Figure 7. ORTEP representation of the cation of compound **7a** with thermal ellipsoids drawn at the 50% probability level. H atoms are omitted for clarity.

solvent of crystallization.[8a] The mono-axial compound $Rh_2(DPhF)_4(CH_3CN)$ was grown from a solution of $Rh_2(DPhF)_4$ in CH_3CN, thus the fact that one axial site is vacant must be dictated by the presence of bridging formamidinates. Mono-axial coordination is also observed in the compound $[Rh_2(DTolF)_4(H_2O)]^+$ which was synthesized from the one electron oxidation of $Rh_2(DTolF)_4$ with $AgNO_3$ in CH_3Cl_3.[8b]

The Rh-Rh bond length in $[Rh_2(DTolF)_2(bpy)(CH_3CN)_3][BF_4]_2$ **(7a)** is 2.5780(5) Å which is slightly shorter than the corresponding bond distance in

the parent compound $[Rh_2(DTolF)_2(CH_3CN)_6][BF_4]_2$ **(2)** (2.5594(8) Å).[3a] The Rh-Rh bond distance in the related compound $[Rh_2(OAc)_2(bpy)(CH_3CN)_4]^{2+}$ is very similar 2.5395(8) Å.[5c] The bpy ligand in compound **(7)** is bound in the eq-eq fashion with Rh-N bond distances of 2.034(4) Å and 2.053(4) Å. These are over 0.03 Å longer than that reported for compound $[Rh_2(OAc)_2(bpy)(CH_3CN)_4]^{2+}$, 2.001[6] Å, which is presumably a reflection of the stronger *trans* influence of the formamidinate ligands in **(7a)** versus acetate ligands in $[Rh_2(OAc)_2(bpy)(CH_3CN)_4]^{2+}$.[5c] The

pyridyl rings are slightly twisted by 2.9(6)° and the two $[DTolF]^-$ ligands are twisted by 13.28(14)° and 16.7(2)° from the eclipsed orientation as compared to 19° for $[Rh_2(DTolF)_2(CH_3CN)_6]^{2+}$ **(2)**.[3a] The N-C-N bridgehead angles of 124.1(4)° and 123.2(4)° are within normal ranges. The Rh-N distances of 2.057(4) Å and 2.066(4) Å for the $[DTolF]^-$ anions coordinated at Rh(1) are longer than the Rh-N distances for Rh(2) (2.001(4) Å and 2.020(4) Å. Similar differences in the Rh-N bond lengths were observed in the compound $Rh_2(DPhF)_4$.[8a] Likewise, the compounds $[Rh_2(OAc)_2(bpy)(CH_3CN)_4]^{2+}$ and $Rh_2(O_2CCF_3)_4(bpy)_2$ exhibit differences in the Rh-O bond lengths 2.054[4] Å and 2.021[5] Å for the acetate cation and 2.10[3] Å and 2.06[3] Å for the trifluoroacetate compound, respectively.[5a,c] The differences in the Rh-N $[DTolF]^-$ bond lengths can be explained, in part, as a consequence of the *trans* coordinated bpy ligand and the axial acetonitrile at Rh(1). The equatorial CH_3CN ligands bound to Rh(2) exhibit Rh-N bond distances of 2.026(4) Å and 2.030(4) Å, respectively.

Compound **(7)** crystallizes in a different modification when the solvent is CH_3CN (Figure 8). $[Rh_2(DTolF)_2(bpy)(CH_3CN)_4][BF_4]_2$ **(7b)** crystallizes in the monoclinic space group $P2_1/n$ with the asymmetric unit consisting of the entire cation and two $[BF_4]^-$ anions. Both $[BF_4]^-$ anions are in very close proximity to an axial CH_3CN ligand. One of these $[BF_4]^-$

anions is disordered over two positions, and the second anion is present at full occupancy. This packing arrangement causes the axial CH_3CN ligand on Rh(1) to bend at an angle of 161.9(26)°. The unusual binding of the axial CH_3CN solvent is also reflected in the long Rh-N bond distance of 2.315(6) Å as compared to the axial CH_3CN solvent molecule on Rh(2) which is coordinated at a Rh-N distance of 2.209(22) Å. These axial solvent interactions are significantly longer than the axial CH_3CN interaction in **(7a)** (2.101(4) Å).

The cation in **(7b)** contains a single chelating eq-eq bpy ligand with the pyridyl rings twisted by 1.9(10)°. The Rh-N bonds of the bpy ligand are 2.05(2) Å and 2.06(2) Å, which are comparable to those in **(7a)**. The two

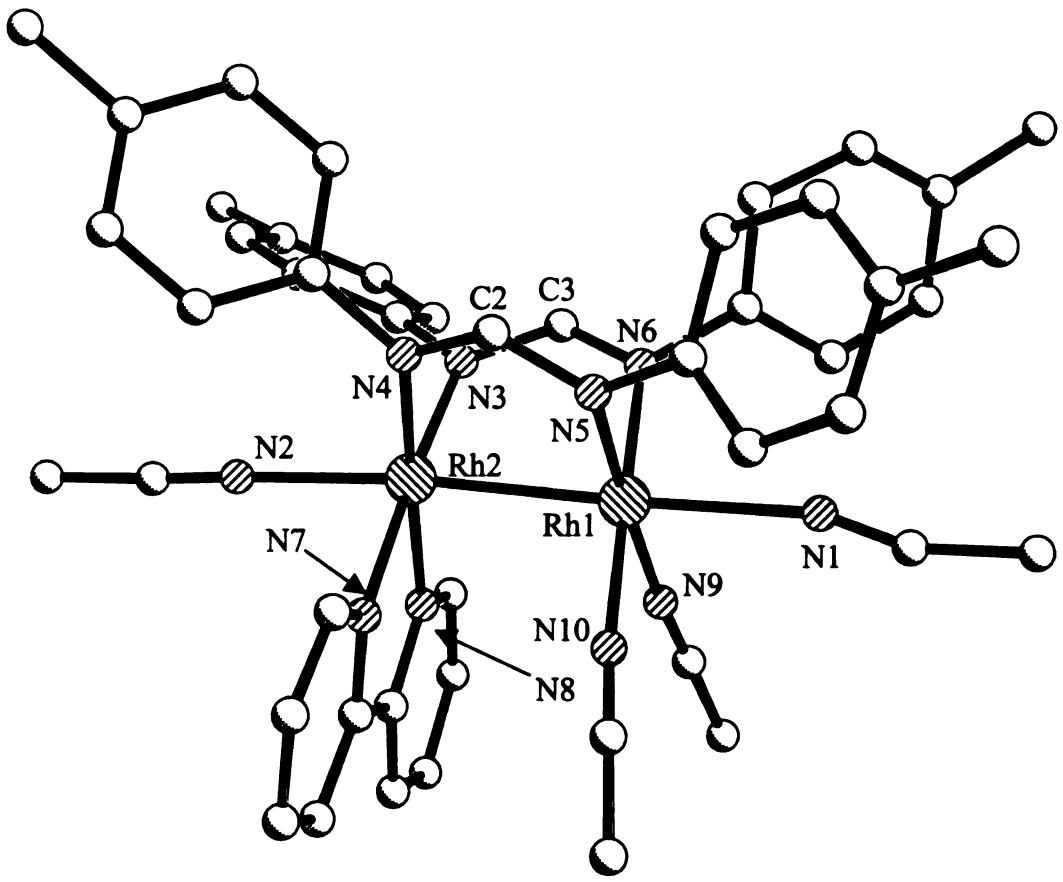


Figure 8. PLUTO representation of compound **7b**. H atoms are omitted for clarity.

equator

are

within

is 2.63

(2.578

Rh-Rh

coordi

are tw

to (7a

16.7(2

memb

distan

two R

axial

[Rh2(

spac

(7a),

mole

coor

equatorial acetonitrile Rh-N bond distances of 2.031(9) Å and 2.046(6) Å are

within normal ranges, and similar to those of **(7a)**. The Rh-Rh single bond is 2.63(2) Å which is significantly longer than the metal-metal bond in **(7a)** (2.5780(5) Å) and, indeed, in related compounds.[5a,c] The lengthening of the Rh-Rh bond can be attributed to the presence of the axial CH_3CN molecule coordinated to Rh(1), a position that is vacant in **(7a)**. The $[DTolF]^-$ groups are twisted from the eclipsed conformation by 7.7(6)° and 8.6(5)° in contrast to **(7a)** which exhibits significantly larger twist values (13.28(14)° and 16.7(2)°). The angles subtended by the N-C-N bridgehead in the five-membered rings are 124.7(7)° and 124.8(14)°. The average $[DTolF]^-$ Rh-N distances of 2.03[1] Å are within normal ranges, and are not different for the two Rh atoms as found in **(7a)**, presumably because of the presence of two axially coordinated acetonitrile ligands at Rh(1).

(5) Molecular Structures of (8a) and (8b). The bis-bpy compound, $[Rh_2(DTolF)_2(bpy)_2(CH_3CN)][BF_4]_2$ **(8a)**, crystallizes in the monoclinic space group, $P2_1/c$. As in the case of $[Rh_2(DTolF)_2(bpy)(CH_3CN)_3][BF_4]_2$ **(7a)**, the dirhodium cation in **(8a)** possesses only one axial acetonitrile molecule with a Rh-N bond distance of 2.115(4) Å (Figure 9). The vacant coordination site at Rh(1) also does not appear to be based on a steric effect.

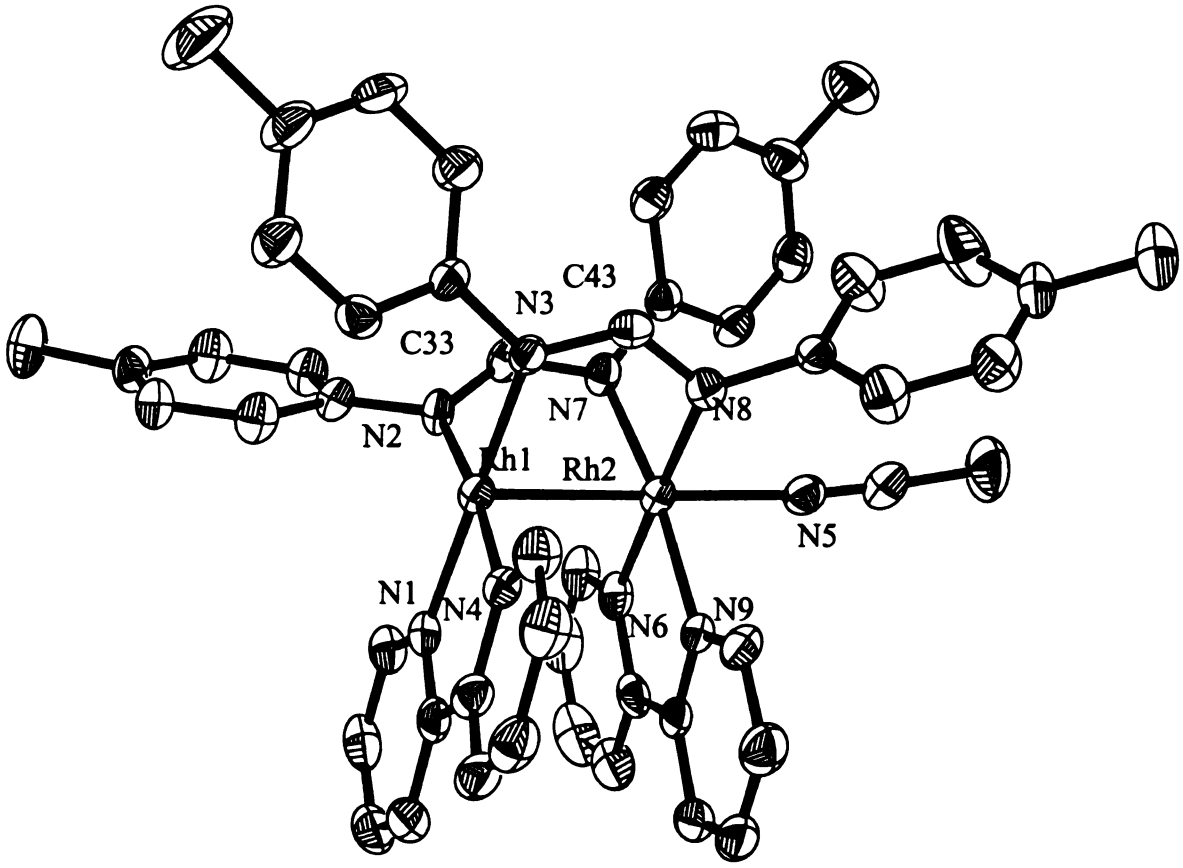


Figure 9. ORTEP representation of the cation of compound **8a** with thermal ellipsoids drawn at the 50% probability level. H atoms are omitted for clarity.

The o

two [

2.582

bpy

Rh_2(C

eq bo

distan

[Rh_2(

The p

3.5(6

(7a)

splay

in a

N(6)

copl

coor

[Rh$_2$

repo

spla

The oxidation state of each Rh atom is +2 based on the fact that there are two $[BF_4]^-$ counterions in the interstices. The Rh-Rh bond length is 2.5820(5) Å which is longer than the metal-metal bond distances of the bis-bpy compounds, $[Rh_2(OAc)_2(bpy)_2(CH_3CN)_2][PF_6]_2$ (2.548(1) Å) and $Rh_2(O_2CCF_3)_4(bpy)_2$ (2.570(6) Å).[5a,c] The average Rh-N distance for the eq-eq bound bpy groups of 2.0395[4] is comparable to the corresponding distances in **(7a)** and **(7b)**, but longer than the Rh-N bond of 1.99[1] Å in $[Rh_2(OAc)_2(bpy)_2(CH_3CN)_2][PF_6]_2$ and 1.99[3] Å in $Rh_2(O_2CCF_3)_4(bpy)_2$.[5a,c] The pyridyl rings of the bpy ligands are twisted out-of-plane by 5.9(6)° and 3.5(6)° which are slightly greater than the analogous distortions found in **(7a)** and **(7b)** (2.9(6)° and 1.9(10)°).

The unfavorably short bpy···bpy contacts in **(8a)** are alleviated by a splaying of the bpy groups away from the center of the molecule, resulting in a dihedral angle of 14.75(4)° between the N(1), N(2), N(3), N(4) and N(6), N(7), N(8), N(9) planes with the bpy planes remaining essentially coplanar with these equatorial planes (Figure 10). This distortion of the coordination environment is slightly less than that found in $[Rh_2(OAc)_2(bpy)_2(CH_3CN)_2]^{2+}$ (15.8°) and greater than the dihedral angle reported for $Rh_2(O_2CCF_3)_4(bpy)_2$ (11.7°).[5a,c] As a consequence of the splaying of the bpy groups in compound

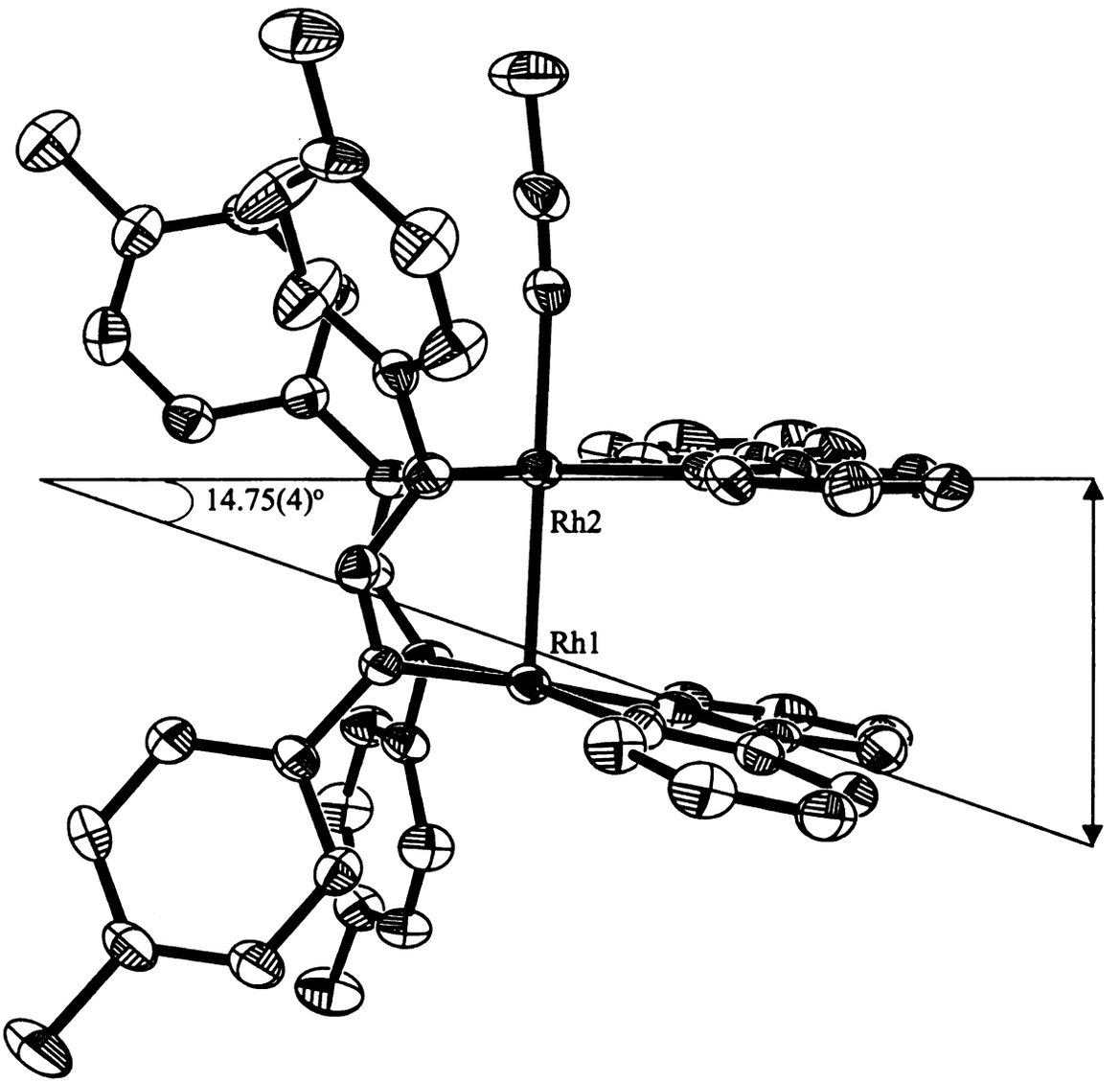


Figure 10. ORTEP representation of the cation in **8a** (with thermal ellipsoids drawn at the 50% probability level) emphasizing the splaying of the bpy ligands in the equatorial plane.

(8a).

favor

19.3

123.

the [

obse

(7a)

(9).

are

Rh(

crys

ethy

[Rh

com

mol

An

case

(8a), the distance between the two bpy planes is *ca.* 3.0 Å, which is a favorable π-stacking distance.[5a,9]

The $[DTolF]^-$ groups in compound **(8a)** are twisted by 18.12(14)° and 19.39(14)° from the eclipsed orientation. The N-C-N bridgehead angles of 123.8(4)° and 123.6(4)° are within normal ranges. The Rh-N distances of the $[DTolF]^-$ groups are different for each Rh atom similar to the differences observed in the mono-bpy compound $[Rh_2(DTolF)_2(bpy)(CH_3CN)_3][BF_4]_2$ **(7a)** and the mono-phen compound $[Rh_2(DTolF)_2(phen)(CH_3CN)_3][BF_4]_2$ **(9)**. The Rh-N distances at Rh(1) where the axial coordination site is vacant are 2.023(4) Å and 2.032(3) Å, respectively while the Rh-N distances at Rh(2) are 2.064(3) Å and 2.076(4) Å.

Compound **(8)** crystallizes in a different modification when the crystals are grown from the slow diffusion of an acetone solution of **(8)** into ethyl acetate instead of an acetonitrile solution of **(8)** into ethyl acetate. The $[Rh_2(DTolF)_2(bpy)_2(H_2O)][BF_4][BPh_4]\cdot(CH_3)_2O\cdot(CH_3CH_2O_2CCH_3)$ **(8b)** compound crystallizes in the monoclinic space group, $P2_1/n$ with one molecule of acetone and three molecules of ethyl acetate in the interstices. An ORTEP plot of the cation portion is provided in Figure 11. As was the case for **(8a)**, the dirhodium cation in **(8b)** possesses only one axial ligand,





Fig
ell
cla

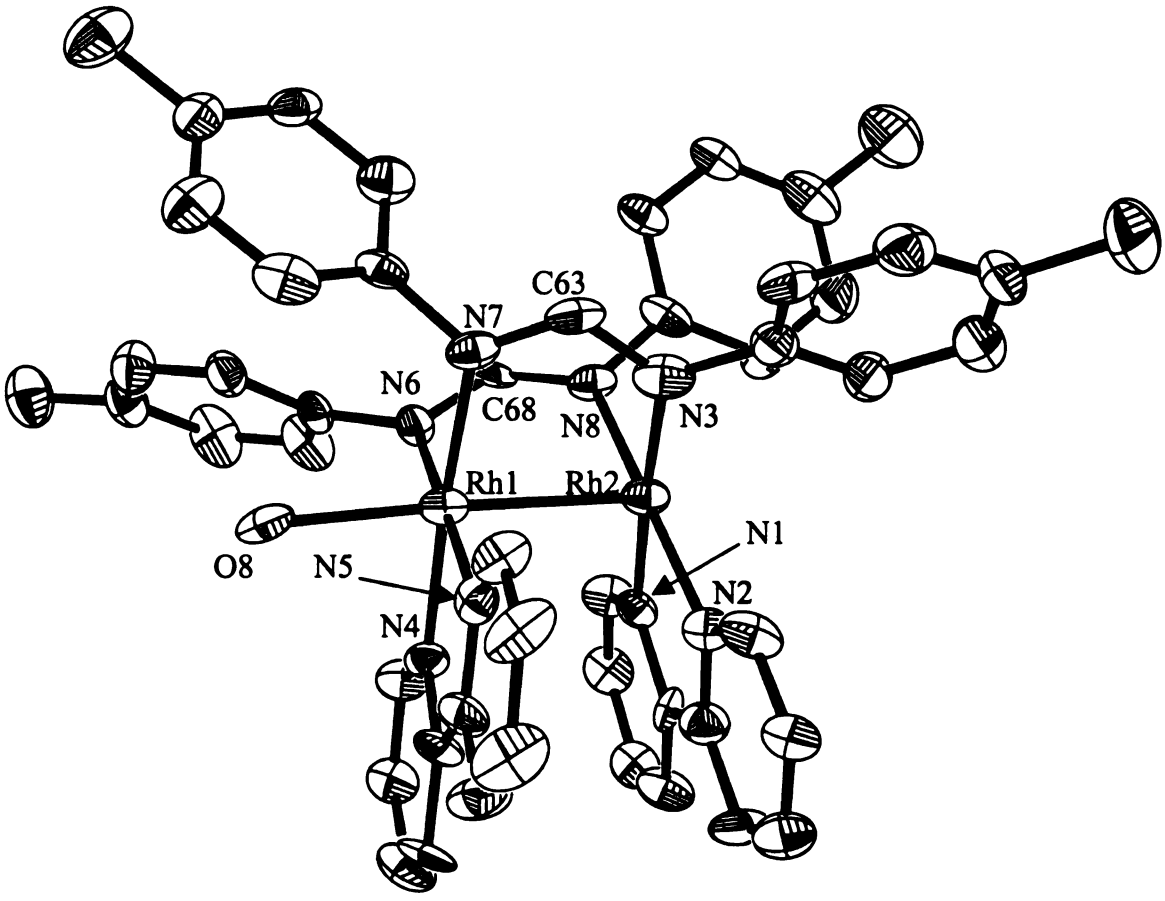


Figure 11. ORETP representation of the cation of **8b** with thermal ellipsoids drawn at the 50% probability level. H atoms are omitted for clarity.

leaving

appear

in (8b

anion

origina

rather

The F

compa

distan

the av

for [R

groups

the N-

Rh-N

signifi

avoide

molecu

N(2),

signifi

leaving an open coordination site on Rh(2) which, once again, does not appear to be based on a steric effect in the solid-state. The two counterions in **(8b)** are not the same identity, as the salt crystallized with one $[BF_4]^-$ anion and one $[BPh_4]^-$ anion. Obviously, the metathesis reaction of the original $[BF_4]^-$ salt with $NaBPh_4$ was incomplete. An axial H_2O molecule rather than acetonitrile is coordinated at an Rh-O distance of 2.221(8) Å. The Rh-Rh bond length in compound **(8b)** is 2.578(1) Å, which is comparable to that found in **(8a)** (2.5820(5) Å). The average Rh-N bond distances for the eq-eq bound bpy groups is 2.052[8] Å which is longer than the average Rh-N bpy interactions of 1.992[10] Å and 2.0395[4] reported for $[Rh_2(OAc)_2(bpy)_2(CH_3CN)_2]^{2+}$ and **(8a)**, respectively.[5a] The $[DTolF]^-$ groups are twisted by 16.9(3)° and 19.6(3)° from the eclipsed orientation and the N-C-N bridgehead angles are 123.3(10)° and 123.7(10)°. The average Rh-N distance for the formamidinate bridges is 2.064[9] Å, with no significant differences among the independent interactions.

As in **(8a)**, the unfavorably short bpy···bpy contacts in **(8b)** are avoided by a splaying of the bpy groups away from the center of the molecule, resulting in a dihedral angle of 14.25(0.45)° between the N(1), N(2), N(3), N(8) and N(4), N(5), N(6), N(7) planes.[5a,9] This is not significantly different from the dihedral angle observed for **(8a)**.

B. React

(1

[Rh_2(DT

chemistr

Equatio

chloride

second

[Rh_2(D

conditi

compou

(

[Rh_2(D

propert

[Rh_2(D

[Rh_2(D

B. Reactions of $Rh_2^{II,II}$ and 1,10-phenanthroline

(1) Syntheses. While investigating the reactions of $[Rh_2(DTolF)_2(CH_3CN)_6][BF_4]_2$ **(2)** with bpy, we sought to extend this chemistry to include other N-chelates such as 1,10-phenanthroline (phen). Equation 4 summarizes the addition of one equivalent of phen in methylene chloride to give $[Rh_2(DTolF)_2(phen)(CH_3CN)_3][BF_4]_2$ **(9)**. The addition of a second equivalent of phen to the dirhodium core to yield $[Rh_2(DTolF)_2(phen)_2(CH_3CN)_2][BF_4]_2$ **(10)** occurs only under refluxing conditions that are analogous to those required to prepare the bis-bpy compound **(8)** (Equation 5).

(2) Electrochemistry of (9) and (10). The cyclic voltammogram of $[Rh_2(DTolF)_2(phen)(CH_3CN)_3][BF_4]_2$ **(9)** reveals slightly different redox properties than the corresponding bpy compound (Figure 12).

$$\underset{\mathbf{2}}{[Rh_2(DTolF)_2(CH_3CN)_6][BF_4]_2} + 1\ \text{phen} \xrightarrow{CH_2Cl_2} \underset{\mathbf{9}}{[Rh_2(DTolF)_2(phen)(CH_3CN)_4][BF_4]_2} \quad (4)$$

$$\underset{\mathbf{2}}{[Rh_2(DTolF)_2(CH_3CN)_6][BF_4]_2} + 2\ \text{phen} \xrightarrow[\text{reflux}]{CH_3CN} \underset{\mathbf{10}}{[Rh_2(DTolF)_2(phen)_2(CH_3CN)_2][BF_4]_2} \quad (5)$$

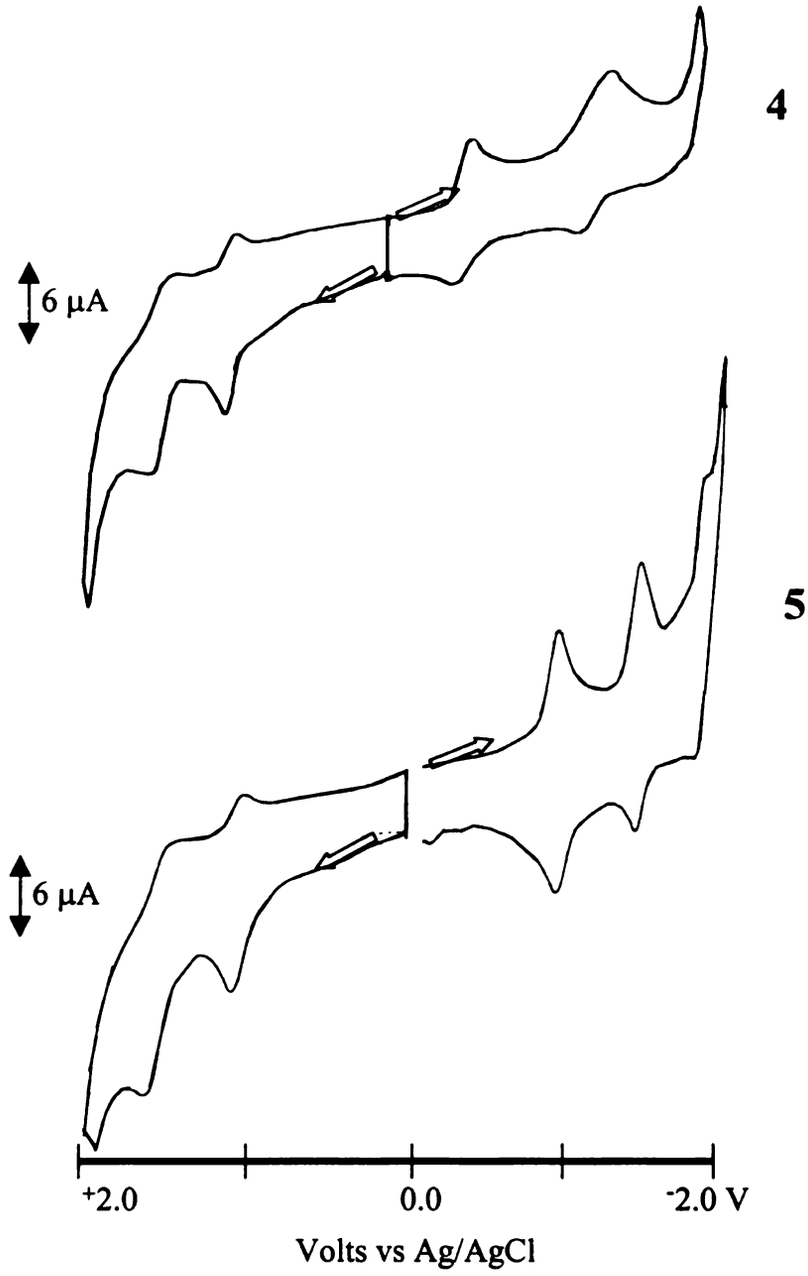


Figure 12. Cyclic voltammograms of compounds **(9)** and **(10)**.

Two rever

addition t

also detec

with thes

1.7 and 1

Th

undergoe

phen co

$E_{p,a}$ = +

+0.99 V

cathodi

irrevers

The co

-1.43 V

differe

[Rh_2(C

reducti

note,

[Rh_2(C

Two reversible anodic processes are observed at $^{+}1.07$ V and $^{+}1.50$ V. In addition to the two oxidation processes, two quasi-reversible reductions are also detected at $E_{p,c} = {}^{-}0.53$ V and $^{-}1.42$ V. The return waves associated with these processes occur at $E_{p,a} = {}^{-}0.43$ V and $^{-}1.36$ V with i_{pc}/i_{pa} ratios of 1.7 and 1.9, respectively.

The bis-phenanthroline cation, $[Rh_2(DTolF)_2(phen)_2(CH_3CN)_2]^{2+}$ **(10)**, undergoes oxidation processes in acetonitrile that are similar to the mono-phen compound **(9)** (Figure 12). Two quasi-reversible oxidations occur at $E_{p,a} = {}^{+}1.05$ V and $^{+}1.57$ V, respectively, with the return waves at $E_{p,c} = {}^{+}0.99$ V and $^{+}1.43$ V; i_{pc}/i_{pa} ratios are 1.5 and 1.8, respectively. A reversible cathodic process for compound **(10)** occurs at $E_{1/2} = {}^{-}0.91$ V, and two irreversible processes occur at $E_{p,c} = {}^{-}1.47$ V and $E_{p,c} = {}^{-}1.89$ V, respectively. The corresponding return wave for the first reduction process occurs at $E_{p,a} = {}^{-}1.43$ V with an i_{pc}/i_{pa} ratio of 0.5. The redox properties of **(10)** are very different from the behavior reported for the analogous acetate compound $[Rh_2(OAc)_2(phen)_2(CH_3CN)_2]^{2+}$, which is reported to undergo a reversible reduction at $^{-}0.83$ V with no reported oxidation processes. It is interesting to note, however, that the modified phen derivative, $[Rh_2(OAc)_2(Ph_2phen)_2(CH_3CN)_2]^{2+}$ (Ph_2phen = 4,7-diphenyl-1,10-

phenanth

-0.76 V a

(3

[Rh$_2$(DT

structure

observe

deuterat

equator

in **(9)** r

observe

protons

9.05 pp

(10) w

in dis

compo

spectru

are att

[DTol

phenanthroline), is reported to exhibit a two-electron reversible reduction at $^{-}$0.76 V and a one-electron reversible oxidation at $^{+}$0.89 V.[5a]

(3) ^{1}H NMR studies of (9) and (10). The ^{1}H NMR spectrum of $[Rh_2(DTolF)_2(phen)(CH_3CN)_3][BF_4]_2$ **(9)** is in accord with the solid-state structure (Figure 13a). The axially coordinated acetonitrile ligands are observed as free acetonitrile at 1.95 ppm due to exchange with the deuterated solvent. Unlike the mono-bpy analogue **(7)**, for which the equatorial acetonitrile protons occur at 2.25 ppm, the corresponding protons in **(9)** resonate further downfield at 2.51 ppm. The $[DTolF]^{-}$ protons are observed at 2.25 ppm for the methyl groups and 6.99 ppm for the aromatic protons. The phenanthroline protons are observed at 7.92, 8.06, 8.60 and 9.05 ppm.

Although the X-ray structure of $[Rh_2(DTolF)_2(phen)_2(CH_3CN)_2][BF_4]_2$ **(10)** was not able to be resolved, ^{1}H NMR spectroscopy proved to be useful in discerning the molecular structure. As expected, the structure of compound **(10)** closely resembles compound **(8)** as judged by its ^{1}H NMR spectrum (Figure 13b). Four resonances at 7.53, 7.63, 8.15 and 8.57 ppm are attributed to the phen ligand. A triplet at 8.30 ppm can be assigned to the $[DTolF]^{-}$ bridgehead hydrogen atom of which is in a 1:2 ratio with the four

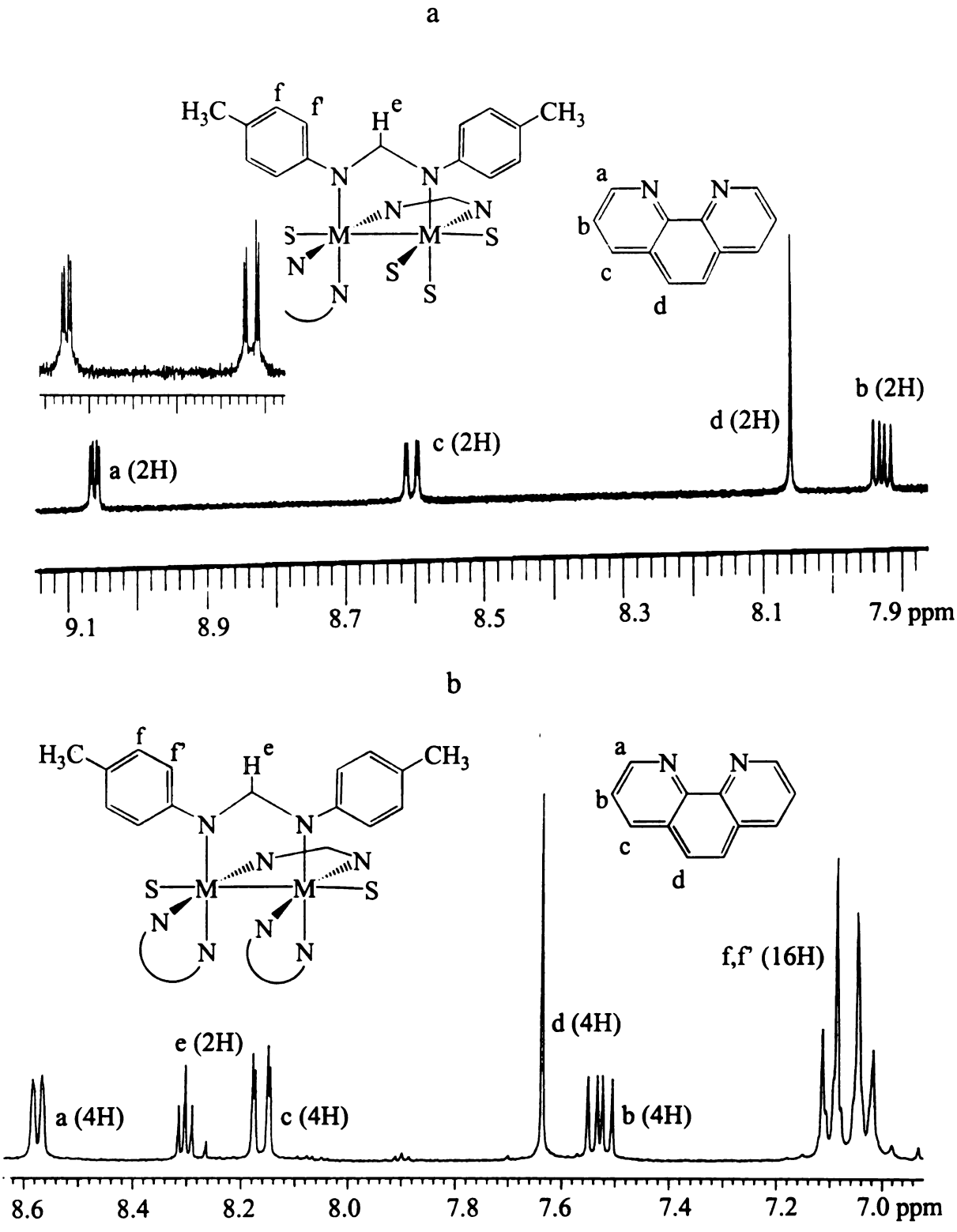


Figure 13. ^{1}H NMR spectra of compounds **9** and **10** in the aromatic region.

resonan

no dow

above

resonat

two bo

(3)

phenar

crysta

four

$Rh_2(D$

the ca

vacar

longe

eq-ec

2.06(

by 1

axial

equa

N di

resonances. The axial CH_3CN is observed as free solvent at 1.95 ppm, with no downfield resonances attributable to equatorial CH_3CN being observed above 2.0 ppm where they typically occur. The $[DTolF]^-$ methyl protons resonate at 2.24 ppm. These data are in accord with a molecule that contains two bound phen groups that are coordinated in an eq-eq mode.

(3) Molecular Structures of (9) and (10). Unlike compound **(7a)**, the phenanthroline analogue $[Rh_2(DTolF)_2(phen)(CH_3CN)_3][BF_4]_2$ **(9)** crystallizes in the P-1 crystal system with one molecule of ethyl acetate and four water molecules. The cation of **(9)** is isostructural to $Rh_2(DTolF)_2(bpy)(CH_3CN)_3][BF_4]_2$ **(7a)** (Figure 14). As was observed for the cation of **(7a)**, the axial coordination site of the solvated rhodium atom is vacant, and the Rh-Rh bond distance of 2.5804(4) Å is not appreciably longer than the metal-metal bond in **(7a)**. The phen ligand is bound in the eq-eq binding mode at Rh(1) with Rh-N distances of 2.054(3) Å and 2.060(3) Å. The pyridyl rings of the phen ligand are twisted out of the plane by 1.4(5)° in comparison to the 1.9° twist observed in compound **(7a)**. The axial acetonitrile is coordinated to Rh(1) at a distance of 2.126(3) Å. The equatorial acetonitrile molecules are coordinated to Rh(2) at an average Rh-N distance of 2.032[3] Å. The Rh-N distances of 2.064(3) Å and 2.070(3) Å

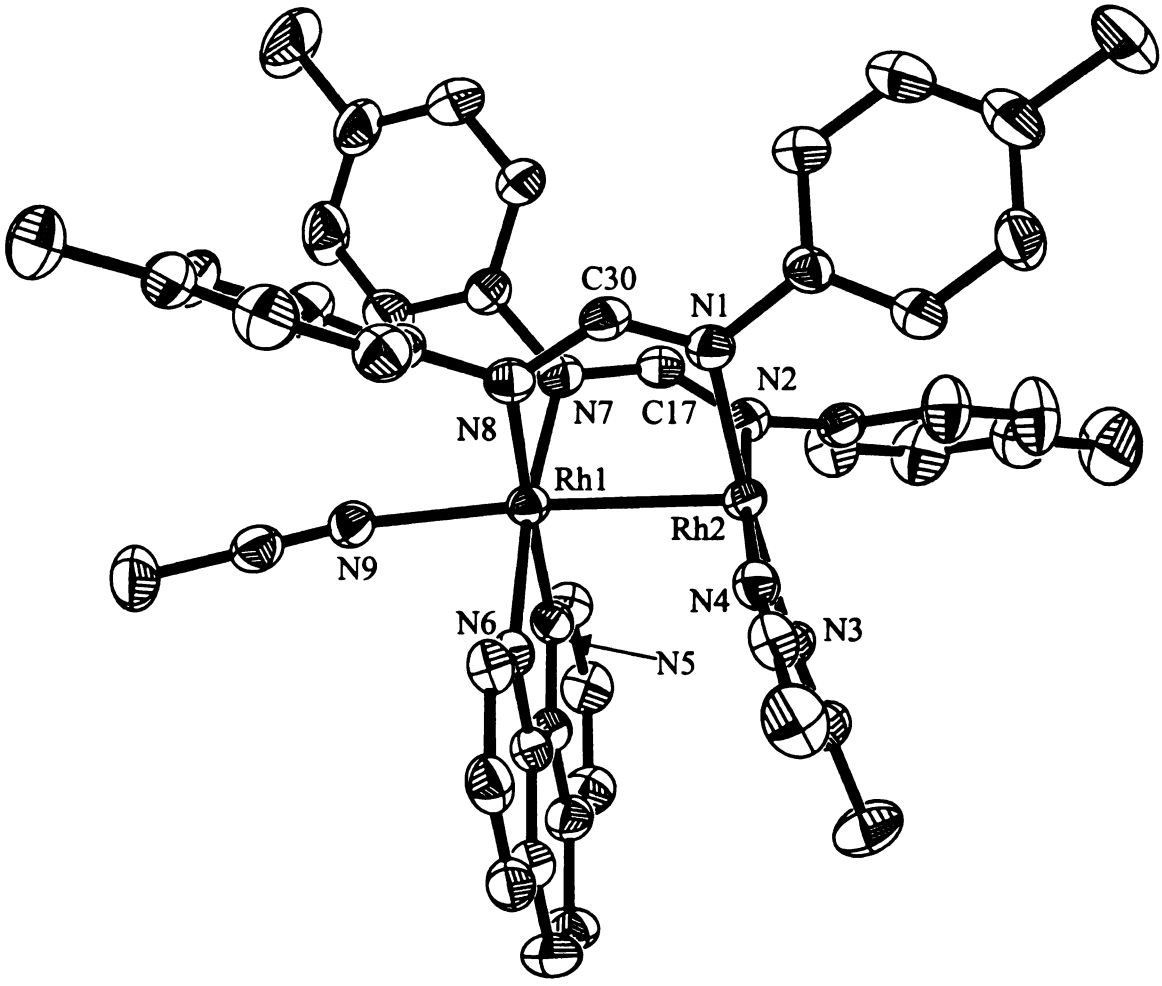


Figure 14. ORTEP representation of compound **9** with thermal ellipsoids drawn at the 50% probability level. H atoms are omitted for clarity.

for th

length

distan

The

123.5

20.4

corre

com

[Rh

The

crys

imp

eno

pre

res

and

rea

wit

pos

for the $[DTolF]^-$ ligands coordinated at Rh(1) are longer than the bond lengths for Rh(2) (2.006(3) Å and 2.015(3) Å). As in **(7a)**, the Rh-N bond distances of the $[DTolF]^-$ ligands *trans* to the N-N chelate are lengthened. The N-C-N bridgehead angles of the bridging ligands (123.5(4)° and 123.5(4)°) are within normal ranges. The $[DTolF]^-$ groups are twisted by 20.41(13)° and 16.65(13)° from the eclipsed orientation as compared to the corresponding twists of 13.28(14)° and 16.7(2)° observed in the mono-bpy complex $[Rh_2(DTolF)_2(bpy)(CH_3CN)_3][BF_4]_2$ **(7a)**.

As previously stated in the NMR section, the solid state structure of $[Rh_2(DTolF)_2(phen)_2(CH_3CN)_2][BF_4]_2$ **(10)** was not able to be determined. The crystals of **(10)** grow as severely twinned crystals regardless of the crystallization conditions that are used. Deconvolution of the twins was also impossible since the intensity of the crystal was not sufficient to allow for enough data to be collected. From the NMR data, however, it is possible to predict that the structure of $[Rh_2(DTolF)_2(phen)_2(CH_3CN)_2][BF_4]_2$ **(10)** resembles the bis-bpy compounds $Rh_2(DTolF)_2(bpy)_2(CH_3CN)][BF_4]_2$ **(8a)** and $Rh_2(DTolF)_2(bpy)_2(H_2O)][BF_4]_2$ **(8b)**. Specifically, it would be reasonable to expect that the two phen ligands are bound in an eq-eq fashion with two *cis* $[DTolF]^-$ ligands bridging the dimetal unit. Whether one axial position is vacant or not cannot be predicted.

C. Re

and

equa

[Rh

(Equ

and

with

occu

com

[Rh

(2).

for

Et(

ad

co

co

E

N

[

C. Reactions of (7)and (8) with 9-EtAH and 9-EtGH

(1) Syntheses. The reaction between the mono-bpy compound **(7)** and 9-EtAH resulted in the full substitution of the bpy ligands and the equatorial acetonitrile ligands for the purine to yield the known compound $[Rh_2(DTolF)_2(9\text{-}EtAH)_2(CH_3CN)][BF_4]_2$ as judged by X-ray crystallography (Equation 6).[3a,13] Not surprisingly, no reaction takes place between 9-EtAH and the bis-bpy compound **(8)**. When one equivalent of 9-EtGH is reacted with $[Rh_2(DTolF)_2(bpy)(CH_3CN)_{3,4}][BF_4]_2$ **(7)** at r.t. in methanol, no reaction occurs. Under refluxing conditions, however, ligands exchange occurs and compound **(7)** loses the coordinated bpy to give a mixture of $[Rh_2(DTolF)_2(bpy)_2(CH_3CN)_2][BF_4]_2$ **(8)** and $[Rh_2(DTolF)_2(CH_3CN)_6][BF_4]_2$ **(2)**.[12,13] Compound **(2)** then further reacts with the free 9-EtGH present to form the known bis-9-EtGH compound $[Rh_2(DTolF)_2(9\text{-}EtGH)_2(CH_3CN)_2][BF_4]_2$ (Equation 7).[13] The goal of these reactions was to add a chelating 9-EtAH or 9-EtGH molecule to the solvated Rh atom of compound **(7)**, but thus far we have not isolated a DTolF product that contains both bpy and a purine. It is known that the DNA nucleobases 9-EtAH and 9-EtGH can also adopt a chelating mode of binding through the N7 and N6/O6 positions when one equivalent of either purine is reacted with $[Rh_2(OAc)_2(bpy)(CH_3CN)_4][BF_4]_2$, thus it would seem that this is a feasible

goal.[12] Perhaps different reaction conditions or the use of the phen derivative will lead to one of these mixed N-N/purine compounds.

(2) ^{1}H NMR Studies of the Reaction Between (7) and 9-EtGH.

The ^{1}H NMR spectrum of the green product obtained in equation 7 is indicative of a mixture of compounds (Figure 15). The resonances at 8.37, 8.17, 7.87, 7.79 and 7.28 ppm can be attributed to the bis-bpy compound $[Rh_2(DTolF)_2(bpy)_2(CH_3CN)_2][BF_4]_2$ **(8)** as previously discussed. No other definitive assignments can be made.

4. Summary

The work described in this chapter involves the synthesis and full characterization of a series of unusual dirhodium(II,II) compounds, some of which bind only one axial solvent molecule. The vacant axial position observed in the cations $[Rh_2(DTolF)_2(bpy)(CH_3CN)_3]^{2+}$ **(7a)**, $[Rh_2(DTolF)_2(bpy)_2(CH_3CN)]^{2+}$ **(8a)**, $[Rh_2(DTolF)_2(bpy)_2(H_2O)]^{2+}$ **(8b)**, $[Rh_2(DTolF)_2(phen)(CH_3CN)_3]^{2+}$ **(9)** and the neutral compound $Rh_2(DTolF)_2(O_2CCH_3)_2(H_2O)$ **(6)** renders these compounds good candidates for further addition/substitution chemistry. A reason for the occurrence of the mono-axial compounds in this series of compounds may be the strongly donating properties of the bridging formamidinate ligands as opposed to carboxylate ligands. Apart from the axial ligation issue, the coordination of

N-chelates to $[Rh_2(DTolF)_2(CH_3CN)_6]^{2+}$ **(2)** takes place in a similar fashion to the related reactions between $[Rh_2(OAc)_2(CH_3CN)_6]^{2+}$ and N-chelates.[5] It was also observed that reactions with 9-EtAH and $[Rh_2(DTolF)_2(bpy)(CH_3CN)_{3,4}][BF_4]_2$ **(7)** result in the formation of the bis compound $[Rh_2(DTolF)_2(9\text{-}EtAH)_2(CH_3CN)[BF_4]_2$ previously prepared by a different route.[3a] Reactions with 9-EtGH revealed a preference for compound **(7)** to undergo ligand redistribution leading to the formation of $[Rh_2(DTolF)_2(bpy)_2(CH_3CN)_2]^{2+}$ **(8)** and $[Rh_2(DTolF)_2(CH_3CN)_6]^{2+}$ **(2)** in solution. Whether similar reactions with the 1,10-phenanthroline analogues will occur remains to be explained.

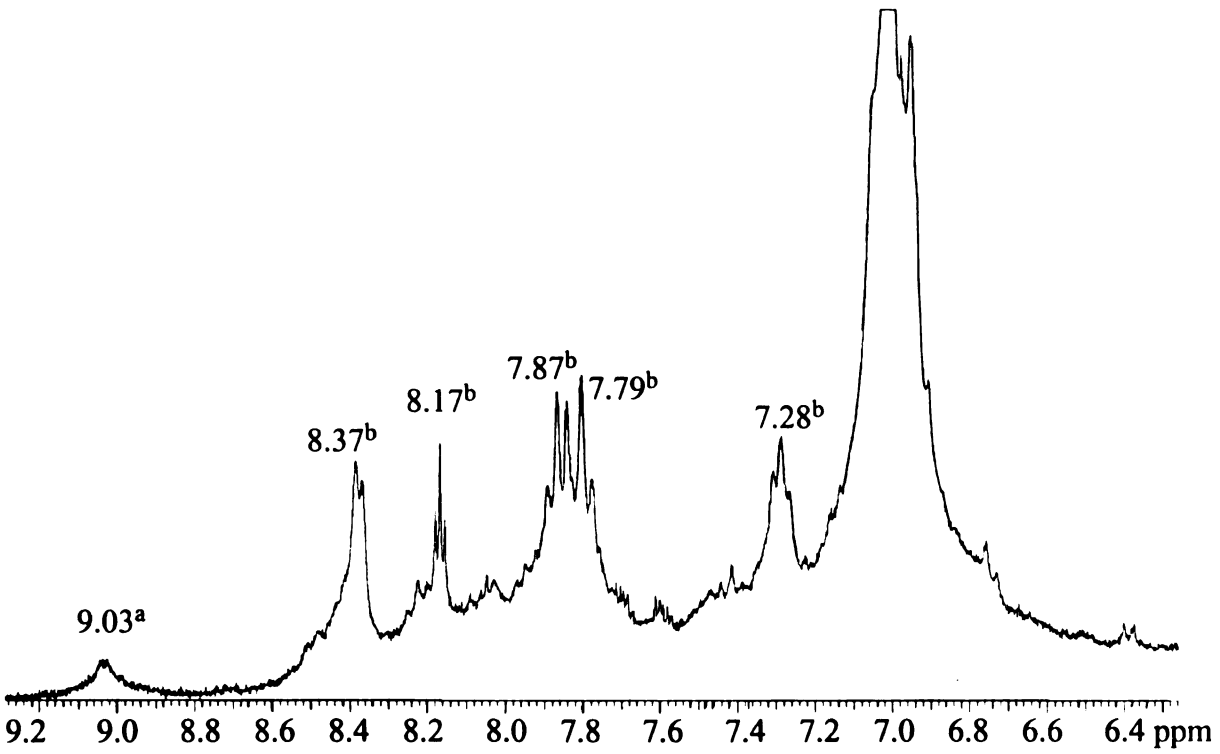


Figure 15. ^1H NMR spectrum in the aromatic bipyridine region of the product from the reaction between $[Rh_2(DTolF)_2(bpy)(CH_3CN)_{3,4}]^{2+}$ **(7)** + 1 eq 9-EtGH.

Table 1. Crystallographic Data for $[Rh_2(DTolF)_2(bpy)(CH_3CN)_3][BF_4]_2 \cdot OC(CH_3)_2 \cdot H_2O$ **(7a)**, $[Rh_2(DTolF)_2(bpy)(CH_3CN)_4][BF_4]_2$ **(7b)**, $[Rh_2(DTolF)_2(bpy)_2(CH_3CN)][BF_4]_2$ **(8a)**, $[Rh_2(DTolF)_2(bpy)_2(H_2O)][BF_4][BPh_4] \cdot OC(CH_3)_2 \cdot 3CH_3CH_2O_2CH_2CH_3$ **(8b)**, $[Rh_2(DTolF)_2(phen)(CH_3CN)][BF_4]_2 \cdot CH_3CH_2O_2CH_2CH_3 \cdot 4H_2O$ **(9)**, $[Rh_2(DTolF)_2(phen)_2(CH_3CN)_2][BF_4]_2$ **(10)**

	7a	7b	8a	8b	9	10
Formula[a]	$C_{48}H_{50}B_2F_8N_{10}Rh_2$	$C_{49}H_{53}B_2F_8N_9O_2Rh_2$	$C_{52}H_{49}B_2F_8N_9Rh_2$	$C_{89}H_{96}B_2F_4N_8O_8Rh_2$	$C_{52}H_{55}B_2F_8N_9O_6Rh_2$	$C_{54}H_{50}B_2F_8N_{10}Rh_2$
Fw, g/mol	1146.42	1179.44	1179.44	1709.18	1281.49	1132.41
Space group	$P2_1/n$	$P2_1/n$	$P2_1/c$	$P2_1/n$	P-1	$P2_12_12$
a, Å	10.9339(2)	13.586(2)	19.4534(4)	23.4894(11)	12.6346(2)	19.6939(3)
b, Å	24.48580(10)	18.0420(2)	13.8298(3)	13.5583(6)	13.5872(2)	38.7660(1)
c, Å	19.4874(3)	21.4791(3)	19.8218(5)	28.4811(13)	19.0597(3)	13.7938(2)
α, deg	90	90	90	90	71.9480(10)	90
β, deg	94.329(1)	101.044(1)	109.189(1)	114.118(1)	73.6310(10)	90
γ, deg	90	90	90	90	71.3795(7)	90
V, Å^3	5202.38(13)	5167.27(12)	5036.5(2)	8278.7(7)	2886.70(8)	10530.8(2)
Z	*4*	*4*	*4*	*4*	*2*	*8*
T, K	173	173	173	173	173	173
Radiation[b]	MoKα	MoKα	MoKα	MoKα	MoKα	MoKα
ρ_{calc}, g/cm^3	1.464	1.516	1.555	1.355	1.474	1.429
μ, cm^{-3}	0.706	0.716	0.731	0.468	0.652	0.696
Unique data	5450	10679	11838	19084	12465	23860
Obsd data[c]	4269	6834	7092	8190	9752	9028
R_{int} (R_{sig})[d]	0.0341 (0.0499)	0.0595 (0.0945)	0.0767 (0.1018)	0.1321 (0.2235)	0.0167 (0.0423)	0.1624 (0.2831)
R_1 (wR_2)[e]	0.0462 (0.1134)	0.0539 (0.1012)	0.0600 (0.0891)	0.1093 (0.2155)	0.0449 (0.125)	n/a
GoF[f]	0.988	1.111	1.140	1.132	1.039	n/a

[a]Including solvent molecules. [b]Graphite monochromator. [c]$I > 2\sigma(I)$. [d]$R_{int} = \Sigma|F_o^2-F_{o\,(mean)}^2|/\Sigma[F_o^2]$; $R_{sigma} = \Sigma[\sigma(F_o^2)]/[F_o^2]$. [e]$R1 = \Sigma||F_o|-|F_c||/\Sigma|F_o|$; $wR2 = [\Sigma[w(F_o^2-F_c^2)^2]/\Sigma[w(F_o^2)^2]]^{1/2}$. [f]Goodness-of-Fit = $S = [\Sigma[w(F_o^2-F_c^2)^2]/(n-p)]^{1/2}$.

Table 2. Selected Bond Distances (Å) and Angles (deg) for $[Rh_2(DTolF)_2(bpy)(CH_3CN)_3][BF_4]_2 \cdot OC(CH_3)_2 \cdot H_2O$ **(7a)**

(a) Bonds

Rh(1)-Rh(2)	2.5780(5)	Rh(1)-N(9)	2.034(4)
Rh(1)-N(4)	2.057(4)	Rh(2)-N(1)	2.030(4)
Rh(1)-N(5)	2.066(4)	Rh(2)-N(2)	2.020(4)
Rh(1)-N(6)	2.101(4)	Rh(2)-N(3)	2.026(4)
Rh(1)-N(7)	2.053(4)	Rh(2)-N(8)	2.001(4)

(b) Angles

N(9)-Rh(1)-N(7)	79.9(2)	N(9)-Rh(1)-N(4)	95.3(2)
N(7)-Rh(1)-N(4)	174.19(15)	N(9)-Rh(1)-N(5)	176.57(14)
N(7)-Rh(1)-N(5)	97.63(14)	N(4)-Rh(1)-N(5)	87.01(15)
N(9)-Rh(1)-N(6)	87.80(15)	N(7)-Rh(1)-N(6)	88.62(14)
N(4)-Rh(1)-N(6)	94.50(14)	N(5)-Rh(1)-N(6)	94.57(14)
N(8)-Rh(2)-N(2)	90.1(2)	N(8)-Rh(2)-N(3)	174.28(15)
N(2)-Rh(2)-N(3)	91.7(2)	N(8)-Rh(2)-N(1)	88.1(2)
N(2)-Rh(2)-N(1)	174.86(15)	N(3)-Rh(2)-N(1)	89.6(2)
N(2)-C(40)-N(4)	124.1(4)	N(5)-C(44)-N(8)	123.2(4)
N(2)-Rh(2)-Rh(1)-N(4)	16.7(2)	N(6)-Rh(1)-Rh(2)	177.83(10)
N(5)-Rh(1)-Rh(2)-N(8)	13.28(14)		
N(9)-C(29)-C(45)-N(7)	2.9(6)		

Table 3. Selected Bond Distances (Å) and Angles (deg) for $[Rh_2(DTolF)_2(bpy)(CH_3CN)_4][BF_4]_2$ **(7b)**

(a) Bonds

Rh(1)-Rh(2)	2.63(2)	Rh(2)-N(2)	2.21(2)
Rh(1)-N(1)	2.315(6)	Rh(2)-N(3)	2.04(2)
Rh(1)-N(5)	2.033(11)	Rh(2)-N(4)	2.04(2)
Rh(1)-N(6)	2.020(6)	Rh(2)-N(7)	2.05(2)
Rh(1)-N(9)	2.030(10)	Rh(2)-N(8)	2.06(2)
Rh(1)-N(10)	2.047(6)		

(b) Angles

Rh(1)-N(1)-C(47A)	161.9(26)	Rh(2)-N(2)-C(17)	173.9(8)
C(10)-N(10)-Rh(1)	170.5(6)	C(32)-N(9)-Rh(1)	175.0(9)
N(9)-Rh(1)-N(6)	178.6(3)	N(9)-Rh(1)-N(5)	92.9(4)
N(6)-Rh(1)-N(10)	92.0(2)	N(9)-Rh(1)-N(1)	85.5(3)
N(5)-Rh(1)-N(10)	177.4(3)	N(5)-Rh(1)-N(1)	93.1(3)
N(6)-Rh(1)-N(1)	93.8(2)	N(4)-Rh(2)-N(3)	87.8(10)
N(10)-Rh(1)-N(1)	84.3(2)	N(3)-Rh(2)-N(7)	96.4(4)
N(4)-Rh(2)-N(7)	174.8(14)	N(3)-Rh(2)-N(8)	175.3(16)
N(4)-Rh(2)-N(8)	96.4(3)	N(4)-Rh(2)-N(2)	99.1(13)
N(7)-Rh(2)-N(8)	79.3(9)	N(7)-Rh(2)-N(2)	83.6(2)
N(3)-Rh(2)-N(2)	95.8(11)	N(4)-C(3)-N(5)	125.0(14)
N(3)-C(2)-N(6)	125.2(6)	N(2)-C(17)-C(40)	178.0(12)
N(1)-C(47A)-C(48A)	162.0(58)	Rh(1)-Rh(2)-N(2)	177.8(6)
N(3)-Rh(2)-Rh(1)-N(6)	7.8(6)	N(4)-Rh(2)-Rh(1)-N(5)	8.5(5)

Table 4. Selected Bond Distances (Å) and Angles (deg) for $[Rh_2(DTolF)_2(bpy)_2(CH_3CN)][BF_4]_2$ **(8a)**

(a) Bonds

Rh(1)-Rh(2)	2.5820(5)	Rh(1)-N(5)	2.115(4)
Rh(1)-N(1)	2.042(3)	Rh(2)-N(6)	2.037(4)
Rh(1)-N(2)	2.023(4)	Rh(2)-N(7)	2.076(4)
Rh(1)-N(3)	2.032(3)	Rh(2)-N(8)	2.064(3)
Rh(1)-N(4)	2.032(4)	Rh(2)-N(9)	2.047(3)

(b) Angles

N(2)-Rh(1)-N(3)	88.36(14)	N(2)-Rh(1)-N(4)	174.20(14)
N(3)-Rh(1)-N(4)	94.36(14)	N(1)-Rh(1)-N(2)	96.55(15)
N(1)-Rh(1)-N(3)	174.53(14)	N(1)-Rh(1)-N(4)	80.53(14)
N(6)-Rh(2)-N(9)	79.73(15)	N(7)-Rh(2)-N(9)	172.25(14)
N(6)-Rh(2)-N(8)	178.65(15)	N(7)-Rh(2)-N(8)	87.24(14)
N(8)-Rh(2)-N(9)	99.12(14)	N(5)-Rh(2)-N(6)	89.03(14)
N(6)-Rh(2)-N(7)	93.97(15)	N(5)-Rh(2)-N(9)	87.11(14)
N(5)-Rh(2)-N(8)	90.21(15)	N(5)-Rh(2)-N(7)	97.37(15)
N(2)-C(33)-N(7)	123.8(4)	N(3)-C(43)-N(8)	123.6(4)
N(3)-Rh(1)-Rh(2)-N(8)	18.12(14)		
N(2)-Rh(1)-Rh(2)-N(7)	19.39(14)		
N(1)-C(34)-C(31)-N(4)	5.9(6)		
N(6)-C(21)-C(19)-N(9)	3.5(6)		

Table 5. Selected Bond Distances (Å) and Angles (deg) for $[Rh_2(DTolF)_2(bpy)_2(H_2O)][BF_4][BPh_4]\cdot OC(CH_3)_2\cdot 3CH_3CH_2O_2CH_2CH_3$ **(8b)**

(a) Bonds

Rh(1)-Rh(2)	2.5787(12)	Rh(1)-O(8)	2.221(8)
Rh(1)-N(4)	2.053(8)	Rh(2)-N(1)	2.040(8)
Rh(1)-N(5)	2.057(9)	Rh(2)-N(2)	2.059(9)
Rh(1)-N(6)	2.067(9)	Rh(2)-N(3)	2.078(9)
Rh(1)-N(7)	2.072(8)	Rh(2)-N(8)	2.038(8)

(b) Angles

N(4)-Rh(1)-N(5)	80.1 (3)	N(4)-Rh(1)-N(6)	97.9 (3)
N(5)-Rh(1)-N(6)	177.9(3)	N(4)-Rh(1)-N(7)	174.8(4)
N(5)-Rh(1)-N(7)	95.4(3)	N(6)-Rh(1)-N(7)	86.6(3)
N(4)-Rh(1)-O(8)	84.7(3)	N(5)-Rh(1)-O(8)	85.3(3)
N(6)-Rh(1)-O(8)	95.0(3)	N(7)-Rh(1)-O(8)	97.7(3)
N(8)-Rh(2)-N(1)	93.3(3)	N(8)-Rh(2)-N(2)	173.7(3)
N(1)-Rh(2)-N(2)	80.7(3)	N(2)-Rh(2)-N(3)	96.7(4)
N(3)-C(63)-N(7)	123.3(10)	N(6)-C(68)-N(8)	123.7(10)
N(3)-Rh(2)-Rh(1)-N(7)	19.6(3)		
N(6)-Rh(1)-Rh(2)-N(8)	16.9(3)		
N(4)-C(74)-C(70)-N(5)	3.0(15)		
N(1)-C(76)-C(61)-N(2)	3.9(13)		

Table 6. Selected Bond Distances (Å) and Angles (deg) for $[Rh_2(DTolF)_2(phen)(CH_3CN)_3][BF_4]_2$ **(9)**

(a) Bonds

Rh(1)-Rh(2)	2.5804(4)	Rh(1)-N(9)	2.126(3)
Rh(1)-N(5)	2.054(3)	Rh(2)-N(1)	2.015(3)
Rh(1)-N(6)	2.060(3)	Rh(2)-N(4)	2.029(3)
Rh(1)-N(8)	2.064(3)	Rh(2)-N(3)	2.034(3)
Rh(1)-N(7)	2.070(3)	Rh(2)-N(2)	2.006(3)

(b) Angles

N(5)-Rh(1)-N(6)	80.86(13)	N(9)-Rh(1)-N(6)	84.57(12)
N(5)-Rh(1)-N(8)	177.41(13)	N(9)-Rh(1)-N(5)	88.56(12)
N(6)-Rh(1)-N(8)	98.01(13)	N(8)-Rh(1)-N(7)	87.36(13)
N(5)-Rh(1)-N(7)	93.54(13)	N(7)-Rh(1)-N(6)	172.20(13)
N(7)-Rh(1)-N(9)	100.79(13)	N(8)-Rh(1)-N(9)	93.66(13)
N(1)-Rh(2)-N(2)	90.80(13)	N(2)-Rh(2)-N(4)	175.63(13)
N(1)-Rh(2)-N(4)	89.57(13)	N(2)-Rh(2)-N(3)	90.79(13)
N(3)-Rh(2)-N(1)	174.95(13)	N(3)-Rh(2)-N(4)	88.48(13)
N(7)-C(17)-N(2)	123.5(4)	N(1)-C(30)-N(8)	123.5(4)
N(7)-Rh(1)-Rh(2)-N(2)	20.41(13)	N(9)-Rh(1)-Rh(2)	173.97(9)
N(8)-Rh(1)-Rh(2)-N(1)	16.65(13)		
N(5)-C(21)-C(33)-N(6)	1.4(5)		

Table 7. ^{1}H NMR Spectroscopic Data for **7**, **8**, **9** and **10**.

compound	^{1}H NMR spectra,[a] ppm
7 $[Rh_2(DTolF)_2(bpy)(CH_3CN)_{3,4}][BF_4]_2$	acteone-d6: δ = 1.95 (s, *ax*-C*H*$_3$CN), 2.22 (s, C*H*$_3$), 2.25 (s, *eq*-C*H*$_3$CN), 6.95 (m, *Ph*), 7.75 (d, *bpy*), 7.82 (t, $^3J_{Rh-H}$ = 4 Hz, N-C*H*-N), 8.24, (d, *bpy*), 8.53 (d, *bpy*), 9.05 (d, *bpy*)
7 $[Rh_2(DTolF)_2(bpy)(CH_3CN)_{3,4}][BF_4]_2$	CD_3CN: δ = 1.95 (s, *ax*-C*H*$_3$CN), 2.23 (s, C*H*$_3$), 2.25 (s, *eq*-C*H*$_3$CN), 6.99 (m, *Ph*), 7.77 (d, *bpy*), 7.83 (t, $^3J_{Rh-H}$ = 4 Hz, N-C*H*-N), 8.24 (d, *bpy*), 8.53 (d, *bpy*), 9.06 (d, *bpy*)
8 $[Rh_2(DTolF)_2(bpy)_2(CH_3CN)_2][BF_4]_2$	CD_3CN: δ = 2.08 (s, *ax*-C*H*$_3$CN), 2.23 (s, C*H*$_3$), 6.99 (m, *Ph*), 7.29 (d, *bpy*), 7.79 (d, *bpy*), 7.86 (d, *bpy*), 8.17 (t, $^3J_{Rh-H}$ = 4 Hz, N-C*H*-N), 8.38 (d, *bpy*)
9 $[Rh_2(DTolF)_2(phen)(CH_3CN)_2][BF_4]_2$	CD_3CN: δ = 1.95 (s, *ax*-C*H*$_3$CN), 2.25 (s, C*H*$_3$), 2.51 (s, *eq*-C*H*$_3$CN), 6.99 (m, Ph), 7.51 (t, $^3J_{Rh-H}$ = 4 Hz, N-C*H*-N), 7.92 (q, *phen*), 8.06 (s, *phen*), 8.60 (d, *phen*), 9.05 (d, *phen*)
10 $[Rh_2(DTolF)_2(phen)_2(CH_3CN)_2][BF_4]_2$	CD_3CN: δ = 1.95 (s, *ax*-C*H*$_3$CN), 2.24 (s, C*H*$_3$), 7.05 (m, *Ph*), 7.52 (q, *phen*), 7.63 (s, *phen*), 8.16 (d, *phen*), 8.30 (t, $^3J_{Rh-H}$ = 4 Hz, N-C*H*-N), 8.57 (d, *phen*)

List of References

(1) (a) Pruchnik, F.; Dus, D. *J. Inorg. Biochem.* **1996**, *61*, 55. (b) Pruchnik, F. P.; Kluczewska, G.; Wilczok, A.; Mazurek, U.; Wilczok; *J. Inorg. Biochem.* **1997**, 25.

(2) (a) Cotton, F. A.; Walton, R. A. Multiple Bonds Between Metal Atoms, 2nd ed.; Oxford Press: New York, 1993 and references therein. (b) Felthouse, T. R. *Prog. Inorg. Chem.* **1982**, *20*, 109. (c) Boyer, E. B.; Robinson, S. D. *Coord. Chem. Rev.* **1983**, *50*, 109.

(3) (a) Catalan, K. V.; Mindiola, D. J.; Ward, D. L.; Dunbar, K. R.; *Inorg. Chem.* **1997**, *36*, 2458. (b) Dunbar, K. R.; Matonic, J. H.; Saharan, V. P., Crawford, C. A.; Christou, G. J. *J. Am. Chem. Soc.* **1994**, *116*, 2201. (c) Day, E. F.; Crawford, C. A.; Folting, K.; Dunbar, K. R.; Christou, G. J. *J. Am. Chem. Soc.* **1994**, *116*, 9339. (d) Crawford, C. A.; Day, E. F.; Saharan, V. P.; Folting, K.; Huffman, J. C.; Dunbar, K. R.; Christou, G. J. need to get IC. (e) Catalan, K. V.; Dunbar, K. R.; Mindiola, D. J.; Maloney, M.; Ward, D. L. manuscript in preparation.

(4) (a) Fimiani, V.; Ainis, T.; Cavallaro, A.; Piraino, P. *J. Chemother.* **1990**, *2*, 319. (c) Bear, J. L.; Gray, H. B.; Rainen, L.; Chang, I-M.; Howard, R.; Serio, G.; Kimball, A. P. *Cancer Chemother. Rep.* **1975**, *59*, 611. (d) Bear, J. L.; Howard, R. A.; Dennis, A. M. *Curr. Chemother. Proc. Int. Congress Chemother. 10th Meeting*, **1977**, *vol. 2.* (e) Pruchnik, F. P.; Kluczewska, G.; Wilczok, A.; Mazurek, U.; Wilczok, T. *J. Inorg. Biochem.* **1996**, *61*, 25.

(5) (a) Crawford, C. A.; Matonic, J. H.; Huffman, J. C.; Folting, K.; Dunbar, K. R.; Christou, G. *Inorg. Chem.* **1997**, *36*, 2361. (b) Perlepes, S. P.; Huffman, J. C.; Matonic, J. H.; Dunbar, K. R.; Christou, G. J. *J. Am. Chem. Soc.* **1991**, *113*, 2770. (c) Crawford, C. A.; Matonic, J. H.; Streib, W. E.; Huffman, J. C.; Dunbar, K. R.; Christou, G. J. *Inorg. Chem.* **1993**, *32*, 3125.

(6) Schiavo, S. L.; Sinicropi, M. S.; Tresoldi, G, Arena, C. G.; Piraino, P. *J. Chem. Soc. Dalton Trans.* **1994**, 1517.

(7) Piraino, P.; Bruno, G.; Tresoldi, G.; Schiavo, S. L.; Zanello, P. *Inorg. Chem.* **1987**, *26*, 91.

(8) (a) Bear, J. L.; Yao, C.-L.; Lifsey, R. S.; Korp, J. D. *Inorg. Chem.* **1991**, *30*, 336. (b) Bruno, G.; Schiavo, S. L.; Tresoldi,

G. Piraino, P. *Inorg. Chim. Acta*, **1992**, *196*, 131. (c) Piraino, P.; Bruno, G.; Schiavo, S. L.; Laschi, F.; Zanello, P. *Inorg. Chem.* **1987**, *26*, 2205.

(9) Calligaris, M.; Campana, L.; Mestroni, G.; Tornatore, M.; Alessio, E. *Inorg. Chim. Acta*, **1987**, *127*, 103.

(10) (a) Sheldrick, G. *SHELXS-97*, **1990**. (b) Sheldrick, G. *SHELXL-97*. **1997**.

(11) (a) TEXSAN-TEXRAY Structure Analysis package, Molecular Structure Corporation, 1985. (b) SHELXS-86: **1986**.

(12) Crawford, C. A.; Dunbar, K. R.; Christou, G. unpublished results.

(13) Catalan, K. V.; Dunbar, K. R.; Maloney, M. M.; Mindiola, D. J.; Ward, D. L. manuscript in preparation.


MICHIGAN STATE UNIVERSITY LIBRARIES
3 1293 02112 6440

THESIS
5
20'!

LIBRARY
Michigan State
University

PLACE IN RETURN BOX to remove this checkout from your record.
TO AVOID FINES return on or before date due.
MAY BE RECALLED with earlier due date if requested.

DATE DUE	DATE DUE	DATE DUE

6/01 c:/CIRC/DateDue.p65-p.15

Interactions of Dinuclear Transition Metal Compounds with DNA Nucleobases and Related Nitrogen Donor Ligands

Volume II

By

Kemal V. Catalan

A Dissertation

Submitted to
Michigan State University
In partial fulfillment of the requirements
For the degree of

DOCTOR OF PHILOSPHY

Department of Chemistry

1999

Chapter IV
The Reactions of Dirhodium Carboxylate Compounds with DNA

1. Introduction

The antitumor drug cisplatin, *cis*-[$PtCl_2(NH_3)_2$], is one of the leading anticancer drugs used in the routine treatment of various deadly cancers.[1] There is ample evidence that cisplatin inhibits DNA replication by forming bifunctional adducts with DNA. Extensive footprinting studies support that DNA is the primary target with regioselectivity being controlled by local sequences in which 5'-pGpG-3' and 5'-pApG-3' are found. These intrastrand adducts account for 65% and 25%, respectively, of DNA-cisplatin adducts formed.[2] Single crystal X-ray crystallography and high resolution NMR spectroscopy coupled with molecular mechanics studies support the formation and stability of these adducts in the solid-state as well as in solution.[3] Ten years ago Lippard and coworkers crystallized the dinucleotide adduct of *cis*-[$Pt(NH_3)_2$(5'-pGpG-3')] and determined its X-ray structure (Figure 1). The molecular structure of this platinated complex is in agreement with the ^1H and ^{31}P NMR spectroscopic results, and related modeling studies. Namely, the N7 atom of each guanine is coordinated to the Pt center with each purine in the head-to-head disposition, as in DNA.[4] The ribose ring of the 5' nucleoside is in the C3'-endo (A DNA) conformation while the ribose of the 3' nucleoside remains in the C2'-endo

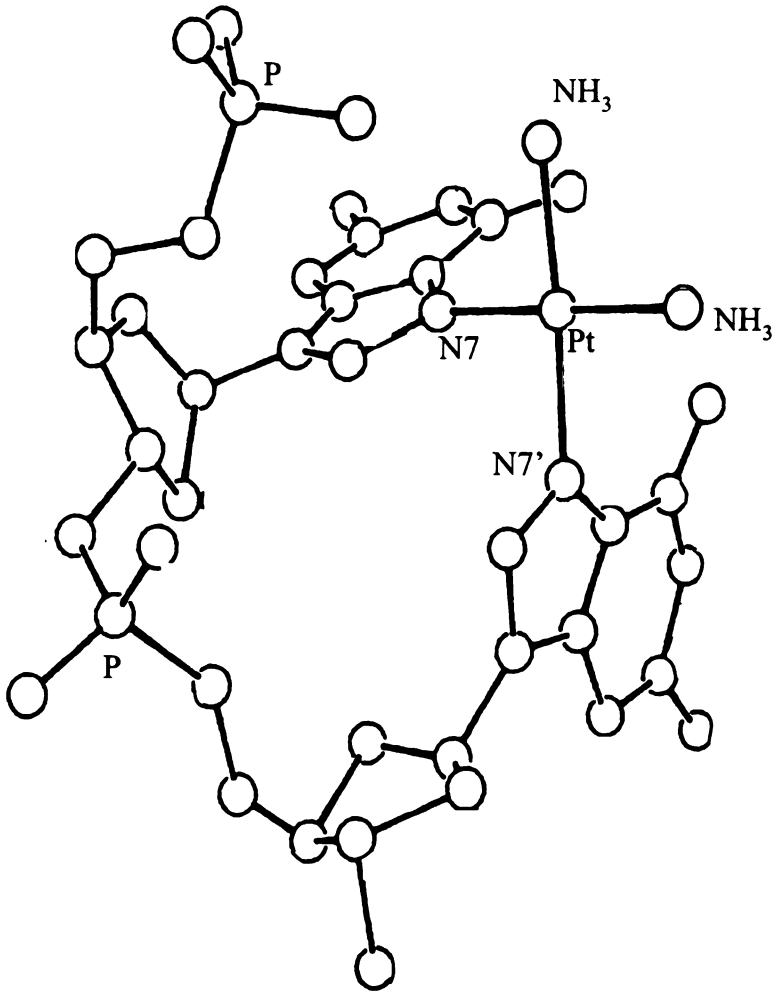


Figure 1. Molecular structure of *cis*-$Pt(NH_3)_2$(5'-pGpG-3').[3]

conformation observed in B DNA. The dihedral angle of the guanine bases in the dinucleotide structure are destacked and bent away from the helical axis by ~60°.[4]

Cisplatin reactions with short chain oligonucleotides have also been performed. For example, the NMR solution structure of the double-stranded (ds) self-complimentary DNA sequence, 5'-CATAGCTATG-3' coordinated to cisplatin shows that the two strands are actually crosslinked by the Pt atom at the GC:GC site through the N7 atoms of the guanine bases. Furthermore, the helix is unwound and bent toward the minor groove as a result of the interstrand cross-linking. The researchers supported their results with an independent gel electrophoresis bending assay.[5]

In another study, Reedijk and coworkers used ^{1}H and ^{31}P NMR spectroscopy to probe the solution structure of the decamer, 5'-TCTCGGTCTC-3' bound to cisplatin.[7] The complimentary strand was annealed to the platinated DNA, and studied under the same NMR experimental conditions.[7] This study revealed that the binding of *cis*-$[Pt(NH_3)_2]^{2+}$ to the intrastrand GG site causes an overall destabilization of the duplex as determined by the melting point of the DNA, which is lowered by 10° – 20° from the unmetallated DNA. In addition, Reedijk describes the

structure of the platinated DNA as exhibiting a kink of the double helix by $40^{\circ} - 70^{\circ}$ as determined by the collective NMR studies.

A very similar structure to the platinated DNA proposed by Reedijk was observed in the first X-ray structure of a platinated double-stranded DNA complex. The cisplatin-DNA adduct, ds[*cis*-$Pt(NH_3)_2${(5'-CCTCTG*G*TCTCC-3')·(5'-GGAGACCAGAGG-3')}], (G* designates the site of platination; ds stands for double stranded) was recently published by Lippard and coworkers (Figure 2).[6] Modeling studies predict that coordination of Pt to DNA destacks the bases and bends the DNA away from the helical axis by $39^{\circ} - 55^{\circ}$. This is comparable to the 40° - 90° bend predicted by gel electrophoresis, ^{1}H NMR spectroscopy and other modeling studies.[4]

Molecular modeling studies performed in our laboratories indicate that the models of several dinucleotide guanine and adenine adducts of the $[Rh_2(O_2CCH_3)_2]^{2+}$ fragment exhibit interesting structural features similar to those of cisplatin (Figure 3).[6] The main difference in these adducts as compared to cisplatin is that the purines bridge the dirhodium centers through the N7/N6(O6) purine positions. In order to make a comparison between the dirhodium and cisplatin structures, the molecule, *cis*-$[Pt(NH_3)_2$(5'-pGpG-3')], was modeled in the same program from the

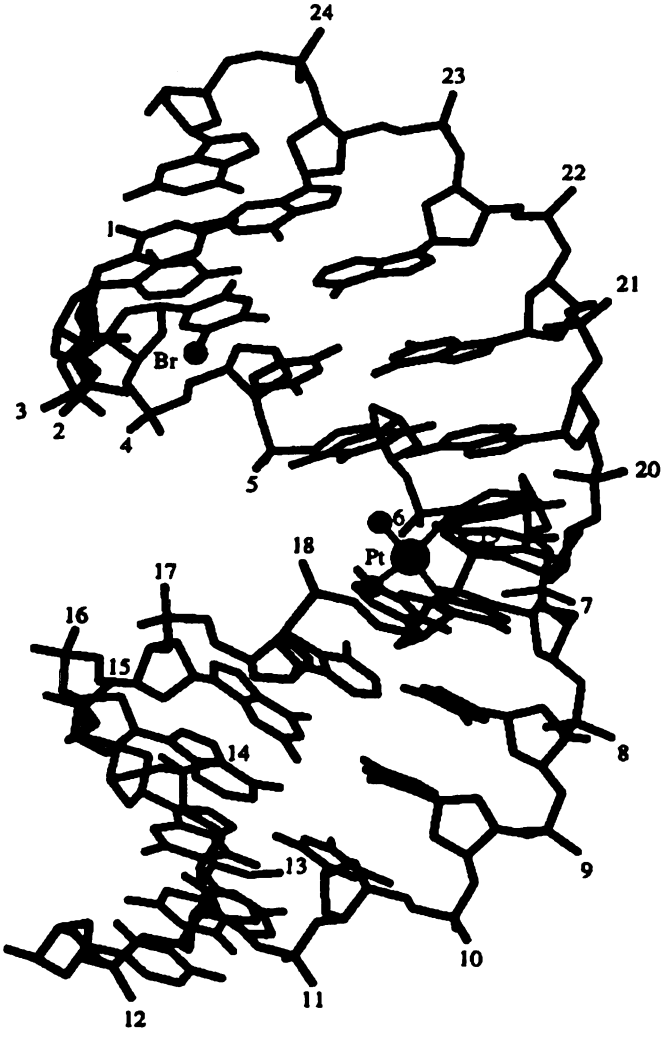


Figure 2. Structure of a double-stranded DNA molecule coordinated to cisplatin.[6]

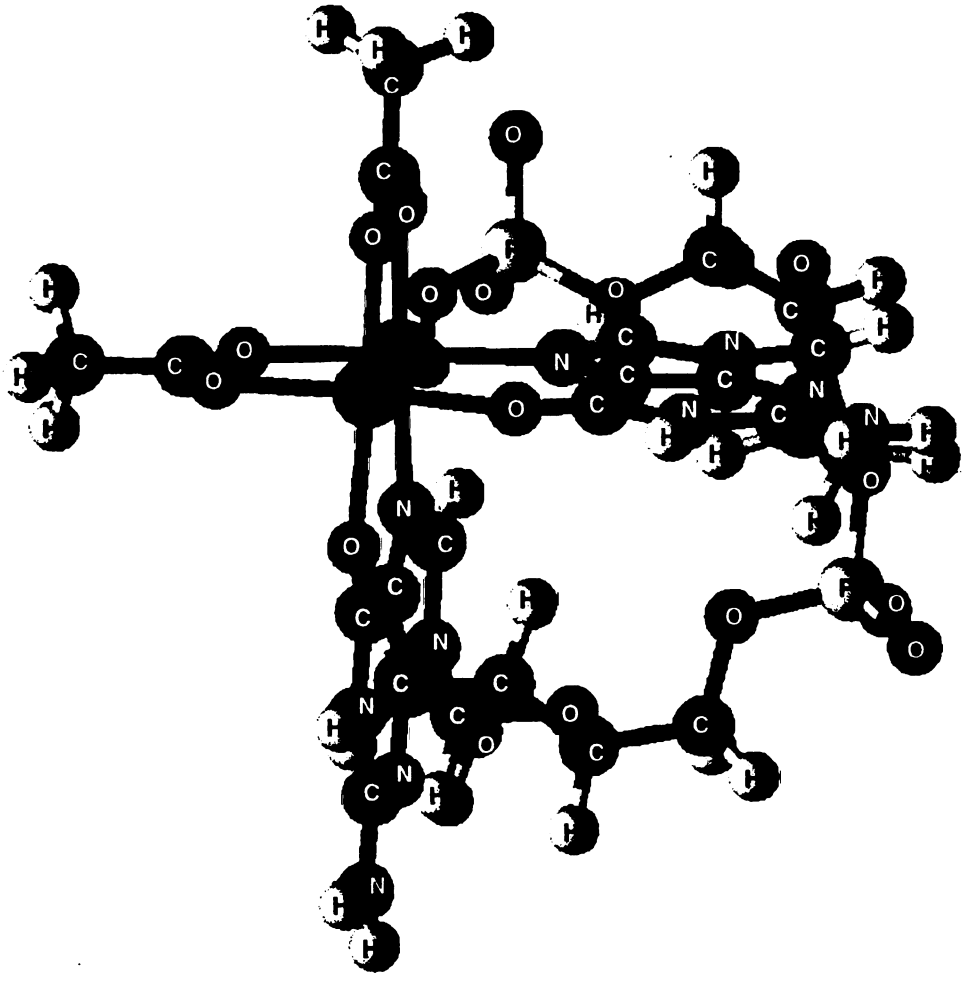


Figure 3. Structure of $Rh_2(O_2CCH_3)_2$(5'-pGpG-3') from molecular modeling studies.[6]

coordinates of the X-ray crystal structure reported by Lippard. One of the similarities observed in the structures is the conformational change in the pucker of the ribose ring in the DNA backbone, but according to this molecular mechanics calculation, the difference between the energies of the backbones of *cis*-[$Rh_2(O_2CCH_3)_2$(5'-pGpG-3')] and *cis*-[$Pt(NH_3)_2$(5'-pGpG-3')] is only 10 kcal (Figure 4).

The promising molecular modeling results prompted us to perform reactions between this dinucleotide and the dirhodium carboxylate compounds. The reactions between $Rh_2(O_2CCH_3)_4(H_2O)_2$ **(11)** and $[Rh_2(O_2CCH_3)_2(CH_3CN)_6][BF_4]_2$ **(12)** and the 12 bp DNA, ss(5'-CCTCTG*G*TCTCC-3') (single-stranded GG-12mer) have been performed. Preliminary evidence of a double-stranded DNA molecule coordinated to the $[Rh_2(O_2CCH_3)_2]^{2+}$ core was obtained and will be discussed.

2. Experimental Section

A. Physical Measurements

^{1}H NMR spectroscopic measurements were collected in collaboration with Elizabeth Lozada, on either a 500 or 600 MHz-Varian Spectrometer. Chemical shifts were referenced relative to the residual proton impurities of the deuterated solvents. Electronic absorption spectra were measured on a

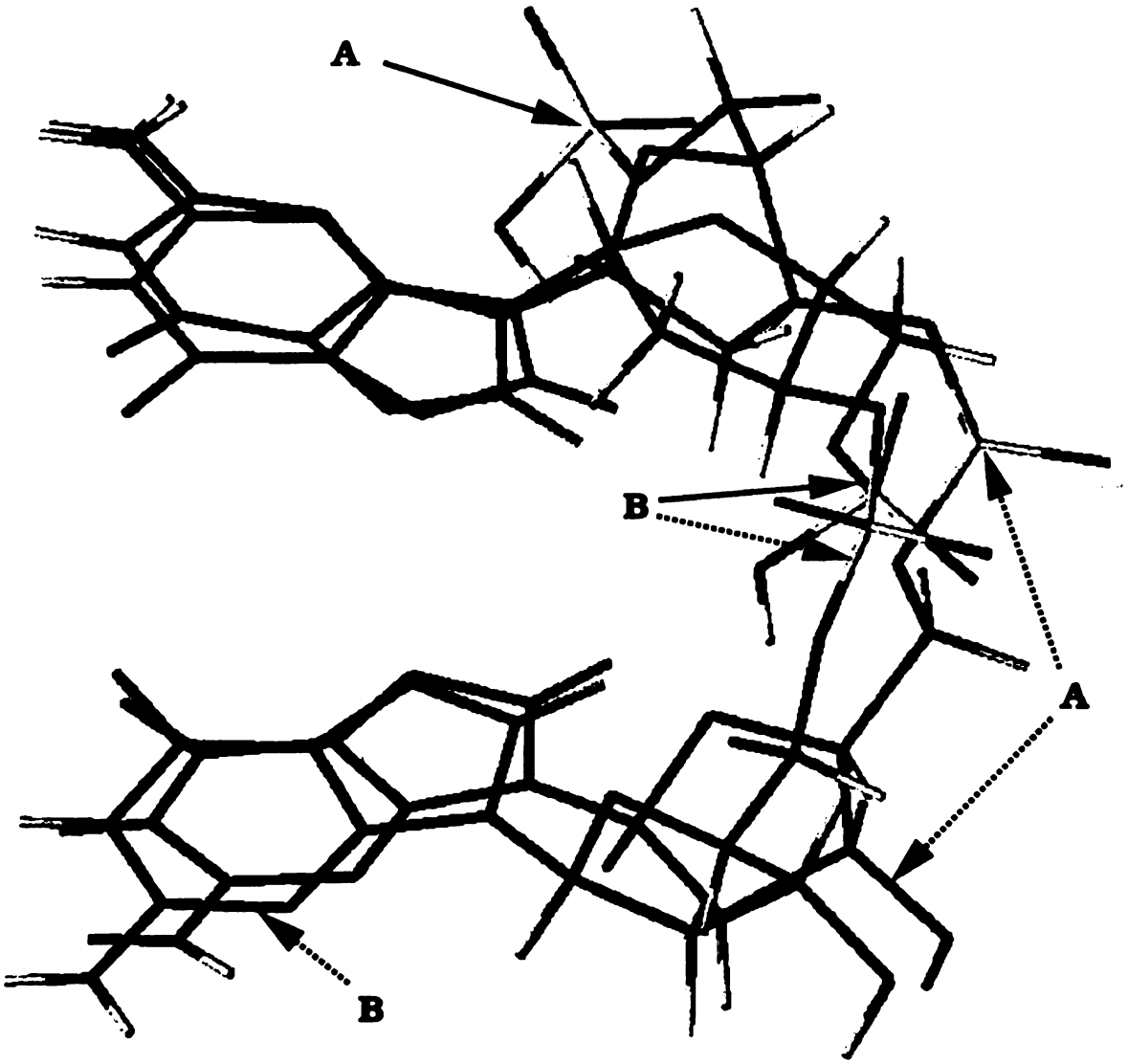


Figure 4. Overlay of the sugar-phosphate backbones of *cis*-$Pt(NH_3)2$(5'-pGpG-3') and $Rh_2(O_2CCH_3)_2$(5'-pGpG-3') from molecular modeling studies.[6]

Hitachi U-2000 spectrophotometer. HPLC chromatography was performed by anionic exchange using a Perkin Elmer LC-235 diode array detector equipped with a 20 mL Pharmacia Source Q15 Resin column.

B. Synthesis

i. Starting Materials

The compounds $Rh_2(O_2CCH_3)_4(H_2O)_2$ **(11)** and $Rh_2(DTolF)_2(O_2CCF_3)_2(H_2O)_2$ **(3)** as well as the partially solvated compound $[Rh_2(O_2CCH_3)_2(CH_3CN)_6][BF_4]_2$ **(12)** were prepared according to literature procedures.[7] The water used for the reactions was filtered through a Millipore MilliQ system. The K^+ salt of the DNA dinucleotide 5'-GG-'3 was purchased from Oligos Etc., lyophilized with H_2O, filtered through a Millipore Ultrafree-MC centrifugal unit (0.45 μ) and stored at 13 °C until use. Chelex-100 resin was purchased from Biorad. Sephadex G-10 and G-25 were purchased from Sigma. The Sephadex columns were prepared by first swelling the gel in water, and then pouring into the column. The column was rinsed with large quantities of water until the gel was firmly packed.

The DNA for the reactions with $Rh_2(O_2CCH_3)_4(H_2O)_2$ **(11)** was treated with the following protocol. After filtration through a Millipore Ultrafree-MC centrifugal unit (0.45 μ), the single strand oligonucleotide, 5'-

CCTCTGGTCTCC-3' was treated with Chelex-100 resin in a 10 mL Teflon column to remove any di-cations from the solution. Next, the GG-12mer was desalted by gel chromatography on a 70 cm x 1.5 cm G-10 or G-25 Sephadex column. After the DNA was lyophilized, it was dissolved in 122 μL H_2O for use. The complimentary strand, 5'-GGAGACCAGAGG-3' was purified by anionic exchange HPLC chromatography, treated with Chelex-100 resin, and desalted by the same procedure used for the GG-12mer.

ii. Reaction Procedures

(1) Reaction of $Rh_2(O_2CCH_3)_4(H_2O)_2$ (11) with 5'-pGpG-3' Dinucleotide.

A 162 μL aliquot of an aqueous solution of **(11)** (2 mg, 4.18 μmol, 1 mL) was added to a 2 mL aqueous solution of the 5'-pGpG-3' (0.45 mg, 0.68 μmol). The initial pH was measured to be ~5 by crude measurement using pH indicator paper. The mixture was allowed to stir at r.t. for 12 h. The blue-green color of the mixture did not change, but the pH increased to 6. The solvent was lyophilized repeatedly with D_2O, and the sample filtered through a Millipore filter unit before obtaining the ^1H NMR spectrum.

(2) Reaction of $[Rh_2(O_2CCH_3)_2(CH_3CN)_6][BF_4]_2$ (12) with 5'-pGpG-3' .

An amount of compound **(12)** (2.2 mg, 3.49 μmol) was dissolved in H_2O (200 μL). A solution of 5'-pGpG-3' (1 μmol, 300 μL) was added to the purple dirhodium solution. The 500 μL reaction mixture was separated into

two equal portions and the original reaction vessel rinsed with H_2O (2 x 5 μL) to give a total of two 260 μL reaction mixtures. Each mixture was heated at 70° C in a thermal cycle for 50 h, during which time the color of the mixture became green. Anionic exchange HPLC chromatography was used to characterize the products.

(3) Reaction of $Rh_2(DTolF)_2(O_2CCF_3)_2(H_2O)_2$ (3) with 5'-pGpG-3' Dinucleotide (14)

An amount of 5'-pGpG-3' (0.45 mg, 0.68 μmol) was dissolved in H_2O (600 μL) and an aliquot of $Rh_2(DTolF)_2(O_2CCF_3)_2(H_2O)_2$ **(3)** in CH_3CN (62.4 μL, 10.9 μM) was added. An immediate precipitation of an orange-red solid occurred which is presumably the starting material. The solid was redissolved upon the addition of 200 μL acetonitrile with heating to 70 °C, but problems with precipitation continued. The solvent was evaporated under reduced pressure, and the residue redissolved in DMSO and H_2O (20 μL and 80 μL, respectively) with heating to 70 °C. In this manner, a reaction was effected and the product was subjected to HPLC chromatography.

(4) Reaction of $Rh_2(O_2CCH_3)_4(H_2O)_2$ (11) with 5'-CCTCTGGTCTCC-3' (GG-12mer)

An amount of $Rh_2(OAc)_4(H_2O)_2$ **(11)** (0.90 μmol, 428 μL, 2092 μM) was added to a 1.5 mL microtube containing the GG-12mer (0.89 μmol, 162 μL) which effected a color change from blue-green to pink. The reaction mixture was heated at 70 °C for 16 h in a thermocycle, then cooled to room temperature. During this time the color of the reaction solution had turned green. The product was purified by anion exchange HPLC chromatography, treated with Chelex-100 resin and desalted on a G-25 Sephadex column. The complimentary strand (1 μmol, 200 μL) was added, the mixture was placed in the refrigerator at 13 °C for 24 h and then filtered through a Centricon-3. The water was evaporated under reduced pressure, and the residue redissolved in 400 μL H_2O. UV-vis spectroscopy indicated that ~5.2 mg of product was collected.

(5) Reaction of $[Rh_2(O_2CCH_3)_2(CH_3CN)_6][BF_4]_2$ (12) with the GG-12mer to prepare ds$[Rh_2(O_2CCH_3)_2$(GG-12mer·CC-12mer)$(H_2O)_2]$ (16)

An amount of $[Rh_2(O_2CCH_3)_2(CH_3CN)_6][BF_4]_2$ **(12)** (1.2 mg, 1.9 μmol) was dissolved in 100 μL of H_2O, and filtered through a Millipore Ultrafree-MC centrifugal unit (0.45 μ). A solution of the GG-12mer (1 μmol, 500 μl) was added to the purple dirhodium solution. The color

immediately changed from purple to orange. A 1 μL aliquot of the orange mixture was chromatographed by anionic exchange HPLC chromatography. The remaining reaction mixture was heated at 70° C for 50 h during which time aliquots from the reaction mixture were periodically analyzed by anion exchange HPLC chromatography. The complimentary strand, the CC-12mer, was added after treating both compound **(15)** and the CC-12mer with Chelex-100 resin, and desalting on a Sephadex G-25 column (75 cm x 1.5 cm). The double-strand product, ds[$Rh_2(O_2CCH_3)_2$(GG-12mer·CC-12mer)$(H_2O)_2$] **(16)**, was filtered through a Centricon-3 to remove any single-strand impurities.

iii. **High Performance Liquid Column Chromatography (HPLC).**

(1) HPLC chromatography for 5'-pGpG-3' and $Rh_2(O_2CCH_3)_2$(5'-pGpG-3')$(H_2O)_2$ **(13)** was performed using the following protocol and a 200 μL sample loop.

Time (min)	Flow rate (mL/min)	%A	%B
8	0.75	100	0
20	0.75	55	45
30	0.75	10	90
10	0.75	0	100

(2) The HPLC protocol used for the separations of the GG-12mer, CC-12mer and $Rh_2(O_2CCH_3)_2$(GG-12mer)$(H_2O)_2$ **(15)** is presented in the following table.

Time (min)	Flow (mL/min)	%A	%B
5	4.0	70	30
60	4.0	65	35
5	4.0	0	100
5	4.0	100	0

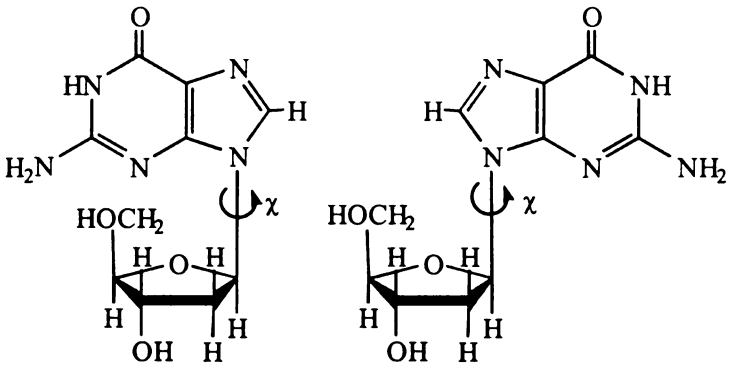
2. Results and Discussion

A. Reaction of $Rh_2(O_2CCH_3)_4(H_2O)_2$ (11) with the 5'-pGpG-3' Dinucleotide

Synthesis. Numerous studies have been performed to obtain structural information about the reaction products of cisplatin with DNA, but no such investigations involving dirhodium compounds have been performed. When we embarked on these studies we were surprised to learn that the dinucleotide starting materials are not easily obtained, especially in the purified quantities needed in order to perform reactions and structural characterization. The 5'-pGpG-3' obtained from Oligos Etc. contained a

mononucleotide (pG) impurity (see ^{1}H NMR section below). Attempts to purify the dinucleotide were unsuccessful, thus we set out to perform the reaction in the hopes that purification of the products would be possible. The products that were obtained from the reaction of a 1:1 ratio of $Rh_2(O_2CCH_3)_4(H_2O)_2$ **(11)** and 5'-pGpG-3' that contains the mononucleotide impurity are depicted in Figure 5. It is reasonable to expect that compound **(11)** will react with the dinucleotide to form head-to-head and head-to-tail isomers. The head-to-tail isomer of the dinucleotide product, $Rh_2(O_2CCH_3)_2$(5'-pGpG-3')$(H_2O)_2$ **(13)**, is possible since it is known that free rotation about the glycosidic bond allows the guanine bases in DNA to be stable in the *syn* conformation (Figure 6).[8] Two more possible products are the head-to-head and head-to-tail isomers of the bis-dinucleotide formed from the reaction of the $Rh_2(O_2CCH_3)_4(H_2O)_2$ **(11)** and two equivalents of the mononucleotide impurity, guanosine monophosphate. Unfortunately, it was not possible to purify the sample due to the low concentration of the sample. Typical concentrations of DNA di- and trinucleotide solutions studied by Lippard and others in the field are an order of magnitude greater than the amounts used in the present study.[4,9]

(1) HPLC Chromatography of 5'-pGpG-3'. The chromatogram of the free dinucleotide initially revealed that the DNA starting material was



syn guanosine *anti* guanosine

Figure 6. Rotation around the N-glycosidic bond of guanosine.

impure (Figure 7). Attempts to purify the dinucleotide were performed by HPLC, and a product that eluted at 28 minutes was collected. No attempts were made to collect other aliquots. After HPLC chromatography, we attempted to remove the salts, NaO_2CCH_3 and KCl during the purification, but desalting on a G-10 Sephadex column failed to yield good separations since the dinucleotide elutes at approximately the same rate.

(2) ^{1}H NMR Spectroscopic Studies of 5'-pGpG-3' and $[Rh_2(O_2CCH_3)_2(5'\text{-}pGpG\text{-}3')(H_2O)_2$ (13). The ^{1}H NMR spectrum of the free dinucleotide is in accord with the chromatogram shown in Figure 7 (Figure 8). The ^{1}H NMR spectrum exhibits two H8 resonances in a 1:2 ratio. The resonance at 7.90 ppm can be attributed to the two H8 protons of the dinucleotide while the resonance at 7.80 ppm is assigned to the H8 resonance of the mononucleotide. The sample was too impure to make definitive assignments of the sugar protons. The attempted purification of the dinucleotide, which involved numerous manipulations, only served to make the sample more impure. The spectrum depicted in Figure 9 supports the conclusion that impurities were introduced into the sample.

The ^{1}H NMR spectrum of the products obtained from the reaction between **(11)** and the impure dinucleotide suggests that there are competing reactions (Figure 10). The most notable feature of the NMR spectrum is a

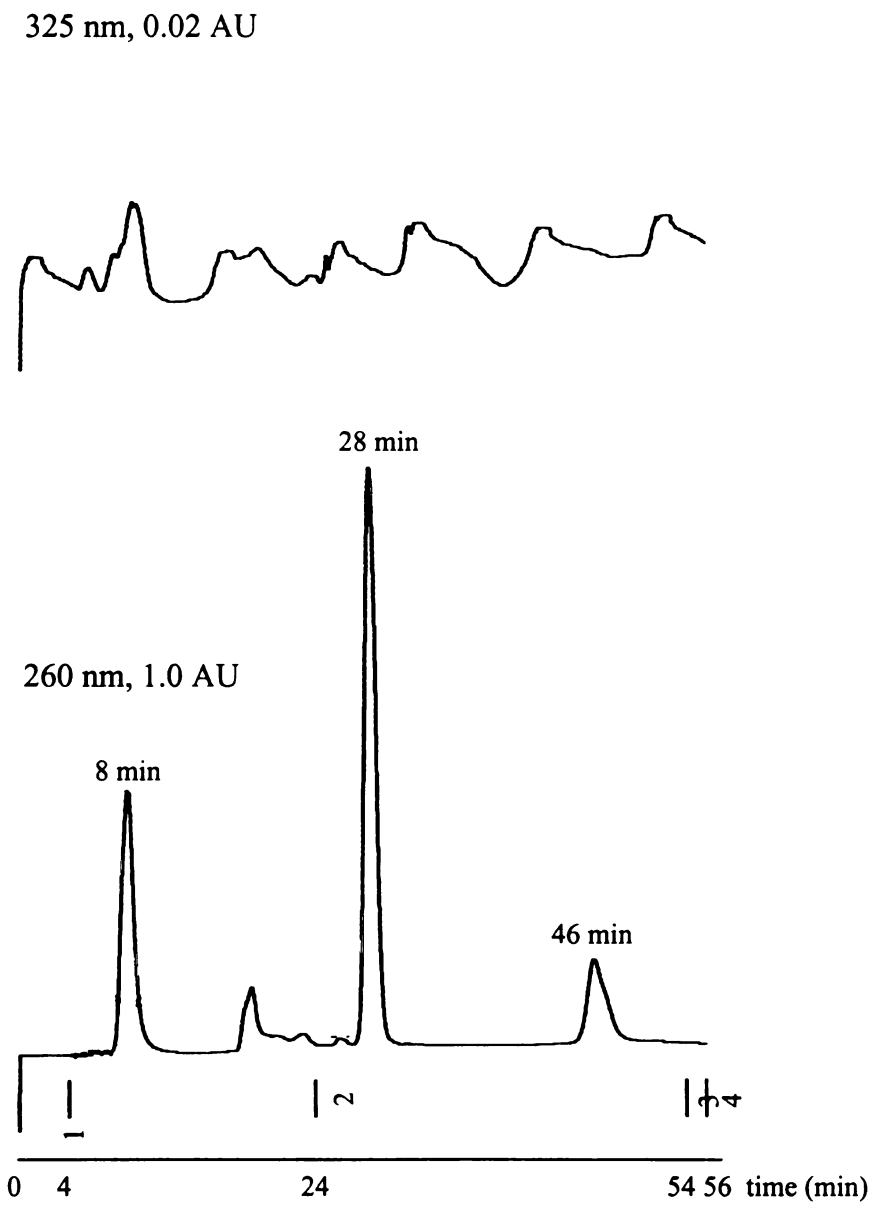


Figure 7. HPLC chromatogram of 5'-pGpG-3'.

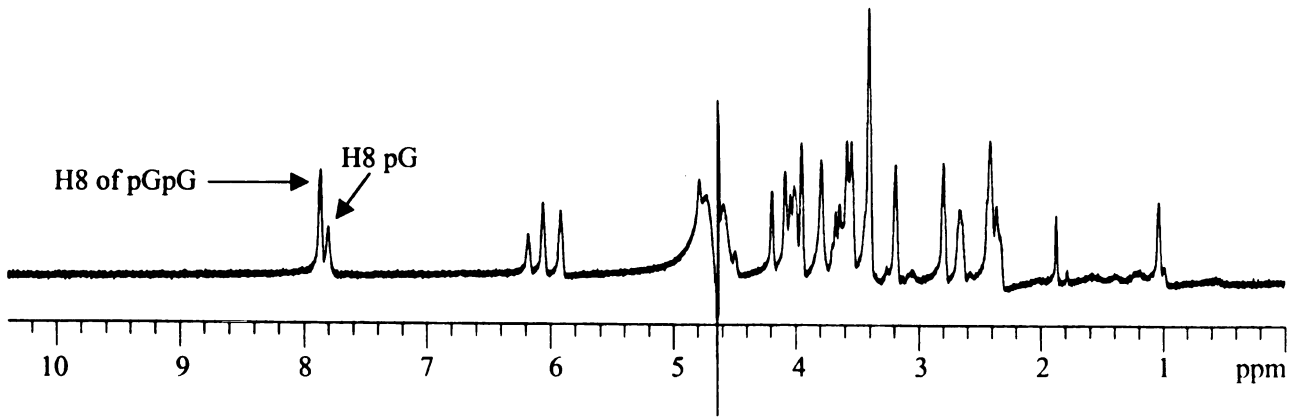


Figure 8. ^{1}H NMR spectrum of 5'-pGpG-3' in D_2O.

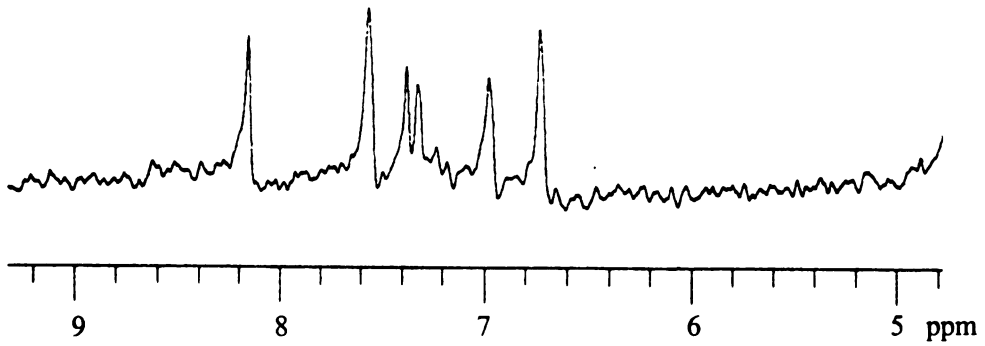


Figure 9. ^1H NMR spectrum in D_2O depicting the H8 region of 5'-pGpG-3' after HPLC purification.

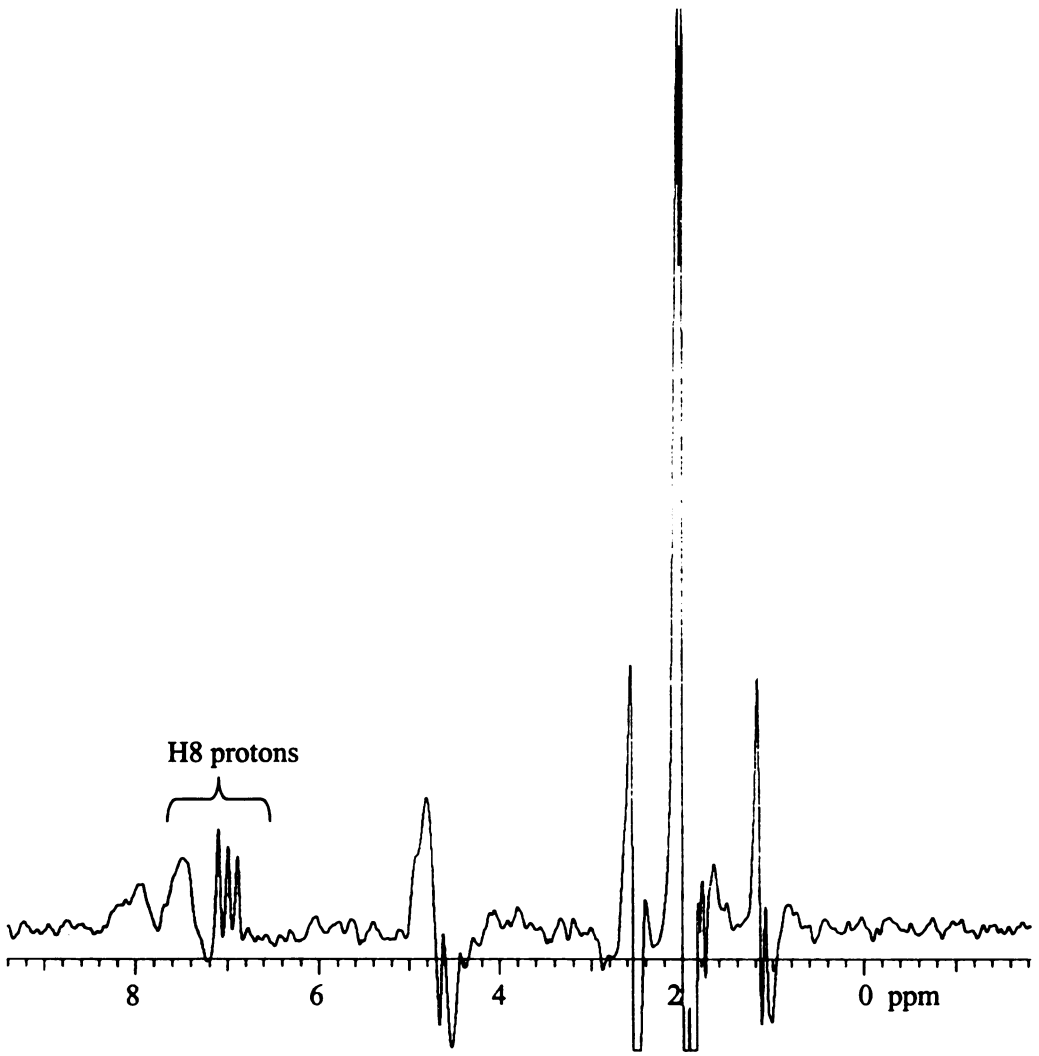


Figure 10. ^{1}H NMR spectrum of the products from the reaction of **(11)** with impure 5'-pGpG-3'. Spectrum obtained in D_2O using the binomial water suppression technique at 10 °C

resonance attributable to an acetate proton. Whether or not this resonance can be assigned as a coordinated acetate ligand was not determined. The H8 region exhibited three singlets at ~7.0 ppm. These resonances are shifted ~1 ppm upfield from the H8 resonances in the unreacted sample. Previous reactions with the modified guanine base, 9-ethylguanine, indicate that a downfield shift of the H8 proton is expected in the ^{1}H NMR spectrum.

B. Reaction of $[Rh_2(O_2CCH_3)_2(CH_3CN)_6][BF_4]_2$ (12) with 5'-pGpG-3' Dinucleotide (13)

(1) Synthesis. The strategy of solvating the *cis*-$PtCl_2(NH_3)_2$ by removing the chloride atoms is often used in cisplatin DNA chemistry to render the compound more reactive. In this vein, by starting with the solvated cation **(12),** one eliminates the need to displace two of the acetate ligands *in situ* to give the the product, $[Rh_2(O_2CCH_3)_2(5'\text{-pGpG-}3')(H_2O)_2$ **(13)** (Figure 11). It is expected that the reaction between compound **(12)** and the impure dinucleotide will form the same products as the reaction with compound **(11).**

(2) HPLC Chromatography. An aliquot (5 μL) from the reaction was diluted to 100 mL and chromatographed by anion exchange HPLC chromatography. The chromatogram depicted in Figure 12 suggests that 80% - 90% of the dirhodium compound is associated with the dinucleotide.

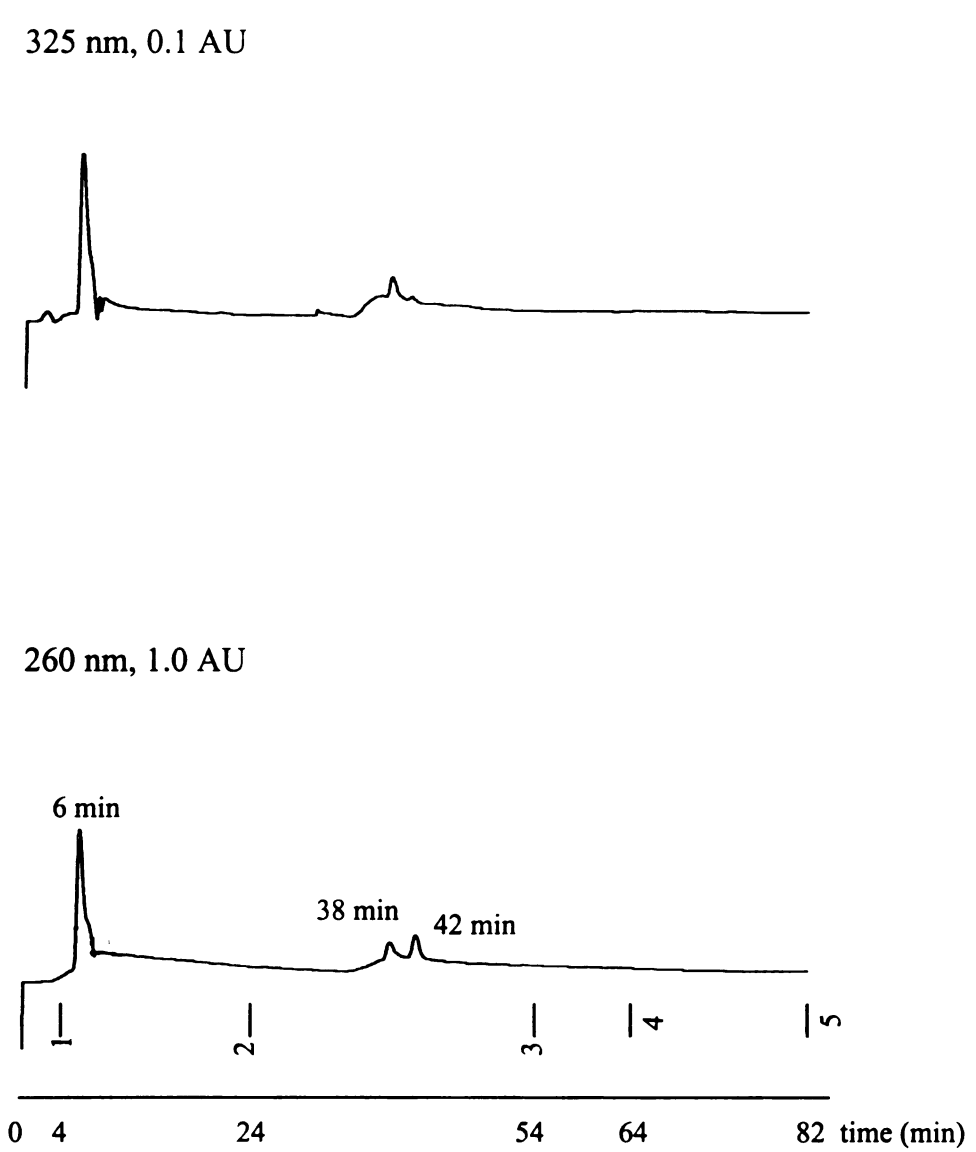


Figure 12. HPLC chromatogram $Rh_2(O_2CCH_3)_2(5'\text{-pGpG-}3')(H_2O)_2$ **(13)**.

The first peak elutes at 6.0 minutes, and is probably a mixture of different isomers. Since the charge on each isomers is the same, separation by anion exchange is not possible. We were able to determine that the dirhodium cation is associated with the small segment of DNA from the chromatogram by measuring the absorbance in the range of 325 ± 15 nm (Figure 12). The dication, $[Rh_2(O_2CCH_3)_2(CH_3CN)_6]^{2+}$ **(12)**, exhibits a very weak electronic transition at 364 nm in water. During the HPLC purification, the absorption at 364 nm was scanned simultaneously with the DNA absorption at 260 nm. We can rule out that the peak that elutes of the column at 6.0 minutes is unreacted compound **(12)** since dications would not bind to the anionic-exchange resin of the column.

C. Reaction of $Rh_2(DTolF)_2(O_2CCF_3)_2(H_2O)_2$ (3) with 5'-pGpG-3' Dinucleotide to form $[Rh_2(DTolF)_2(5'\text{-}pGpG\text{-}3')(H_2O)_2$ (14)

(1) Synthesis. This reaction was first attempted with a 1:1 ratio of compound **(3)** and the dinucleotide in 600 μL of D_2O. Although compound **(3)** is a bis-water adduct, it is insoluble in water even with heating. The reaction was also attempted in CD_3CN and D_2O/CH_3CN, but the results were the same. This led us to investigate the methods employed by Piraino and coworkers for biological reactions of the same compound.[10] Piraino reported that the *in vivo* and *in vitro* reactions were performed in a

water/DMSO mixture. Unfortunately, our attempts to perform the reaction in this solvent mixture were also unsuccessful as the dinucleotide precipitated from solution.

D. Reaction of $Rh_2(O_2CCH_3)_4(H_2O)_2$ (11) with GG-12mer

(1) Synthesis. An immediate reaction between $Rh_2(O_2CCH_3)_4(H_2O)_2$ **(11)** and the GG-12mer takes place upon mixing solutions of each reactant (Figure 13) as evidenced by an instantaneous color change from blue-green to pink. Similar observations were described for other DNA reactions with compound **(11)** performed by Farrell and independently by Bear and coworkers.[11] In the case of the adenine containing reactions, this initial reaction is thought to be a reversible axial interaction between the N7 atom of adenine and compound **(11)**. In our case, however, there are no adenine bases present. The initial color change in our reaction can best be described as an axial interaction between the dirhodium carboxylate and one of the guanine bases in the GG-12mer. It is important to recall that the literature mentions that dirhodium compounds do not have an affinity for G, C and T nucleobases even if the DNA is single-stranded. Since the axial interaction was said to be reversible, it was thought to be impossible to attempt to purify this adduct by HPLC chromatography.

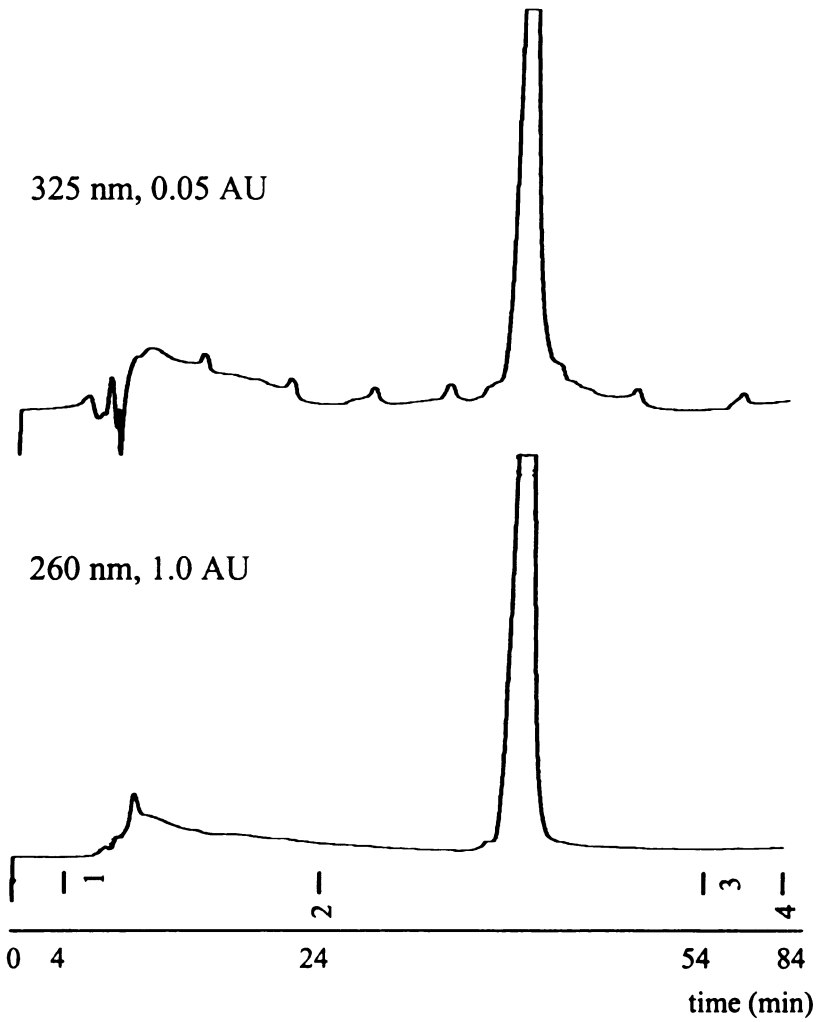


Figure 14. HPLC chromatogram of $Rh_2(O_2CCH_3)_x$(GG-12mer)

In order to decrease the reaction time, the mixture was heated to 70 °C, a method also used by those working with cisplatin. During this time the pink color changed to green. This suggests that the pink color is a kinetic product and the green compound is a thermodynamic one, and further hints that the DNA interaction with $Rh_2(O_2CCH_3)_4(H_2O)_2$ **(11)** does not involve only an axial coordination. The single-strand product was purified by HPLC chromatography, which will be described later in this chapter. The double-stranded product was formed by the addition of an equimolar amount of the CC-12mer to the adduct, ss[$Rh_2(O_2CCH_3)_2$(GG-12mer)] **(15)**.

Following the collection of the fractions containing the ss[$Rh_2(O_2CCH_3)_2$(GG-12mer)] **(15)**, the compound was treated with Chelex-100 resin to exchange any dications in solution with Na^+. Paramagnetic impurities are randomly associated with DNA. These impurities can cause a broadening of the ^1H NMR resonances, and thus must be removed.[12] Chelex-100 resin treatment involves soaking the DNA (in our case metallated DNA) in a suspension of Chelex-100 resin for no less than 2 h followed by filtration, and washing with a 50 mM NaCl solution. The metallated DNA was desalted on a G-10 Sephadex column to remove the excess NaCl and the salts introduced during the HPLC purification. The complimentary strand, CC-12mer, was also treated with Chelex-100 resin

and Sephadex after purification by anion exchange HPLC chromatography. Equimolar quantities of the two strands were mixed, and the solution was treated with a Centricon-3, which separates the DNA by size exclusion, thereby separating any single-strand impurities from the double-strand DNA.

(2) HPLC Chromatography. The single-strand product, ss[$Rh_2(O_2CCH_3)_2$(GG-12mer)] **(15)**, was purified by anion exchange HPLC chromatography by the method described earlier. A representative chromatogram from the purification is depicted in Figure 14. It can be seen that no compounds elute off of the column until the high salt concentration is reached. It appears that only one product is formed from the reaction, and this is supported by the results of ^{1}H NMR spectroscopy.

(3) ^{1}H NMR Spectroscopy. The ^{1}H NMR spectrum of ds[$Rh_2(O_2CCH_3)_2$(GG-12mer)] **(7)** was obtained at 10 °C in D_2O, and is depicted in Figure 15. From this spectrum it is obvious that the resonances are not well resolved. The resonances at 2.8 and 3.1 ppm can be assigned to the methyl protons of bound acetate ligands. The resonance at 2.0 ppm exceeds the vertical scale, and can be assigned to free acetate ion. This resonance exceeds the dynamic range of the NMR receiver. When the dynamic range of signal intensity exceeds the range of the digitizer, the weakest signal in the NMR spectrum becomes comparable to noise. Thus,

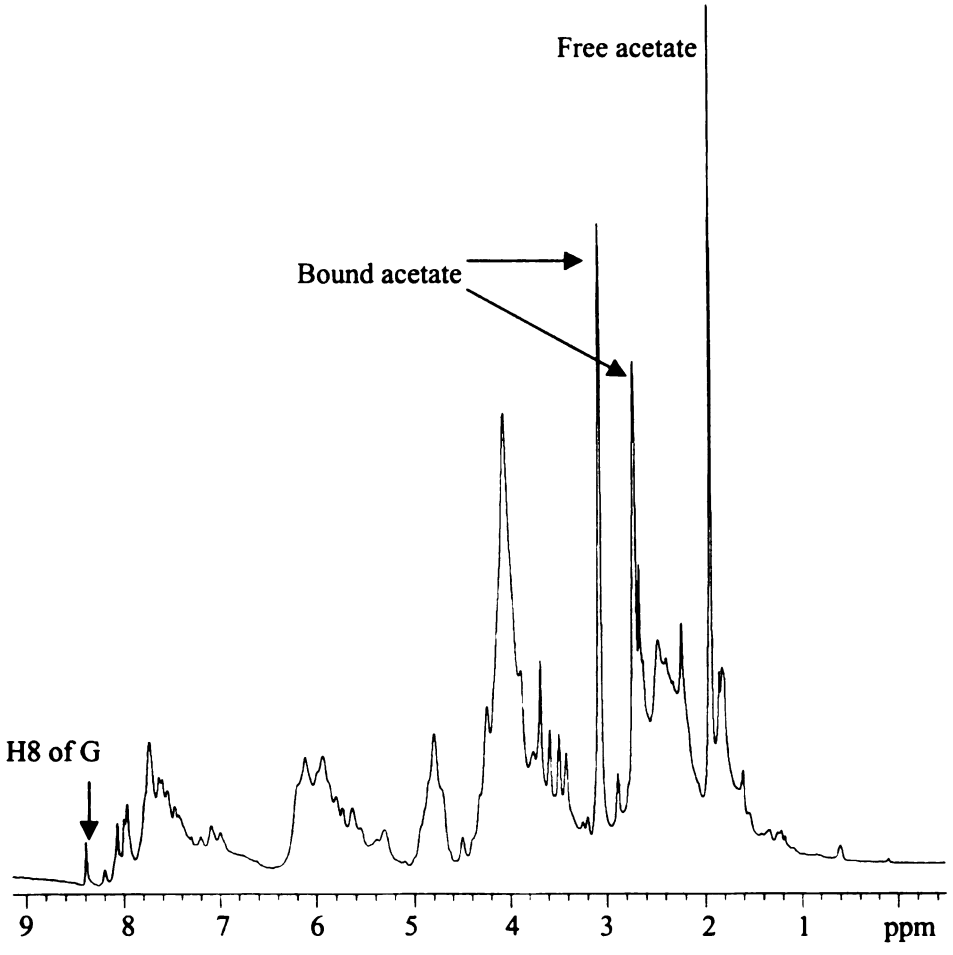


Figure 15. ^{1}H NMR spectrum of ds[$Rh_2(O_2CCH_3)_x$(GG12mer)] at 10 °C in D_2O.

the smaller resonances due to the DNA sugar protons and the nucleobase protons are broadened and not resolved.

In order to determine whether or not the DNA was double-stranded we measured the ^{1}H NMR spectrum in 10% D_2O. The presence of H_2O is necessary to observe the resonances of the imino protons which resonate downfield, > 10 ppm (Figure 16). These protons are the exchangeable protons of DNA, and thus if the spectrum was performed in D_2O one would lose these signals due to H-D exchange. The ^{1}H NMR spectra in the imino region at various temperatures are depicted in Figure 17. These spectra suggest that the double-stranded DNA is destabilized by the coordination of the $[Rh_2(O_2CCH_3)_2]^{2+}$ core at 60 °C (The DNA itself melts above 70 °C). The ^{1}H NMR spectrum in Figure 18 shows the differences in the imino region between the metallated and unmetallated DNA. The differences between spectra of the metallated and the unmetallated DNA supports the conclusion that the dirhodium center is coordinated. Although we cannot comment on the mode of binding at this time, the structure of ds[$Rh_2(O_2CCH_3)_2$(GG-12mer)] does not preclude the formation of the double-stranded structure.

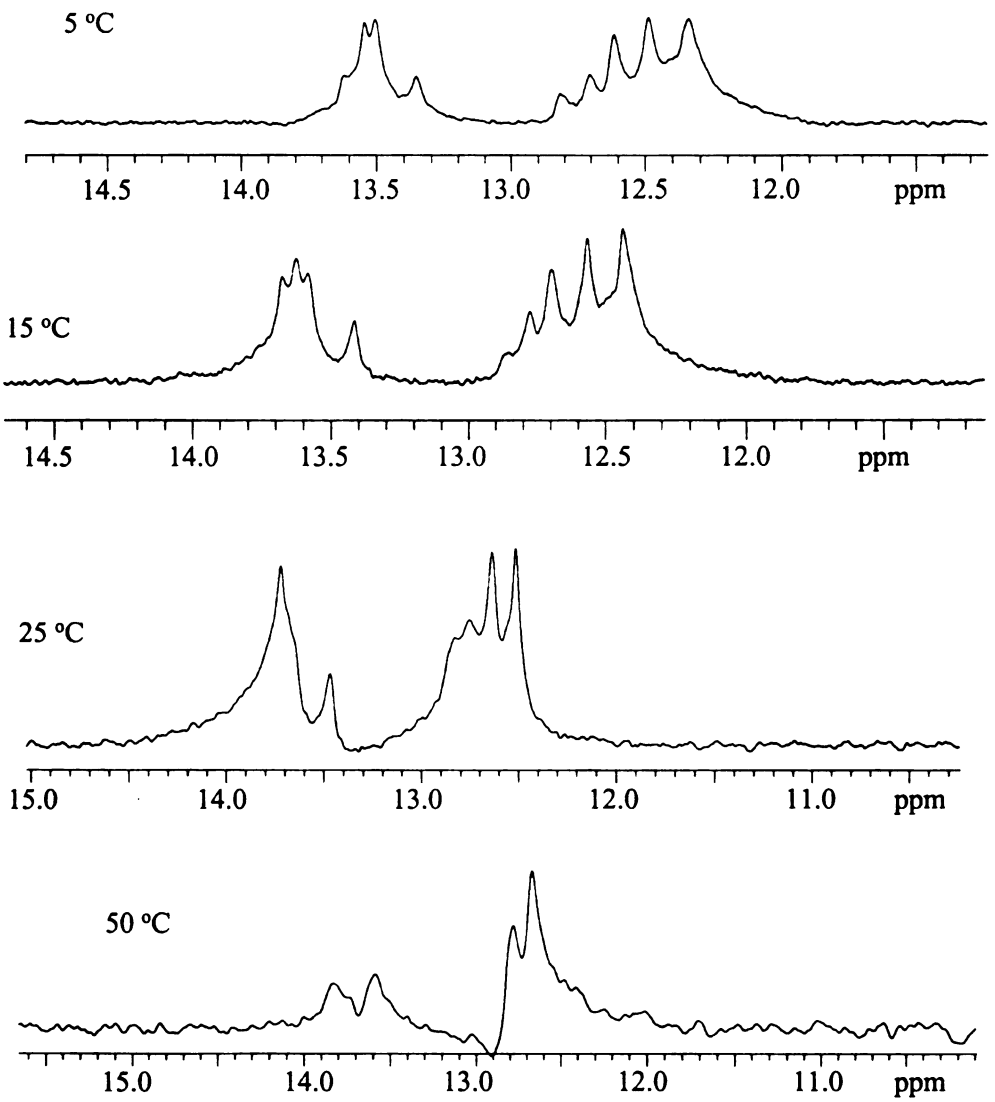


Figure 17. ^{1}H NMR spectra depicting the imino region of ds[$Rh_2(O_2CCH_3)_x$(GG-12mer)] in 10% D_2O at various temperatures.

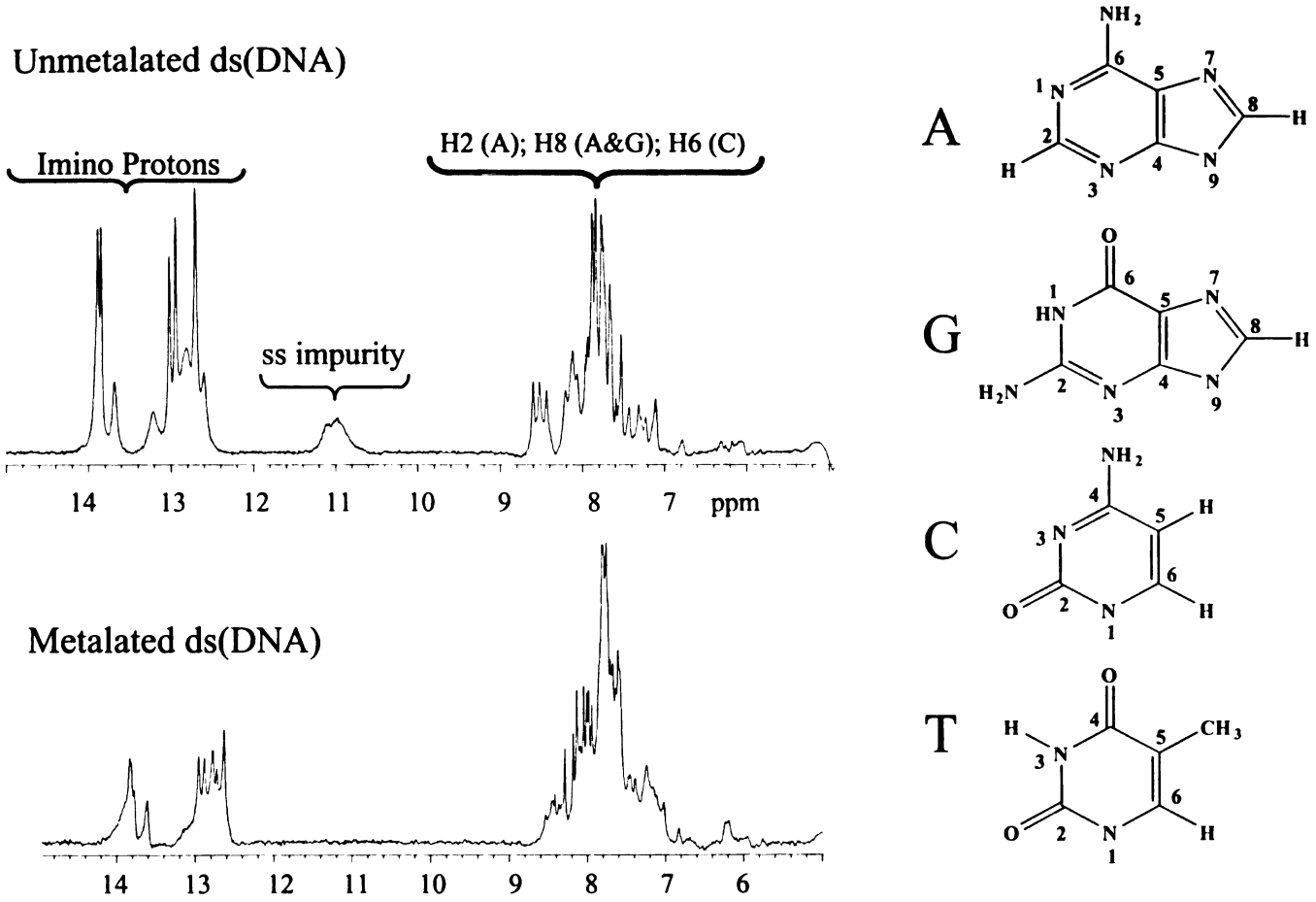


Figure 18. ^{1}H NMR Spectra of ds(GG-12mer) and ds[$Rh_2(OAc)_x$(GG-12mer) at 20 °C, 90% H_2O

E. Reaction of $[Rh_2(O_2CCH_3)_2(CH_3CN)_6][BF_4]_2$ (12) with the GG-12mer

(1) Synthesis. In an attempt to enhance the signals of the DNA protons by preventing the the signal overflow caused by the displaced acetate resonance, we reacted the GG-12mer with an equimolar amount of the partially solvated compound $[Rh_2(O_2CCH_3)_2(CH_3CN)_6][BF_4]_2$ **(12)**. Analogous to the reaction with $Rh_2(O_2CCH_3)_4(H_2O)_2$ **(1)**, an immediate color change from purple to orange takes place upon mixing the two solutions (Figure 19). After gradually heating the mixture at 70 °C for 50 h, the reaction mixture changed color to green. The procedure for purification and preparing the double-stranded complex was the same as described in the previous section D.

(2) HPLC Chromatography. The chromatogram of ss$[Rh_2(O_2CCH_3)_2$(GG-12mer)] (6), depicted in Figure 20, is identical to the chromatogram of the reaction product obtained from the analogous tetra-acetate reaction portrayed in Figure 14. The metallated DNA adheres to the column, and is eluted only at high KCl concentrations, (> 80%).

(3) ^{1}H NMR Spectroscopy. The ^{1}H NMR spectrum of the imino region of ds$[Rh_2(O_2CCH_3)_2$(GG-12mer)] **(7),** which was obtained from the

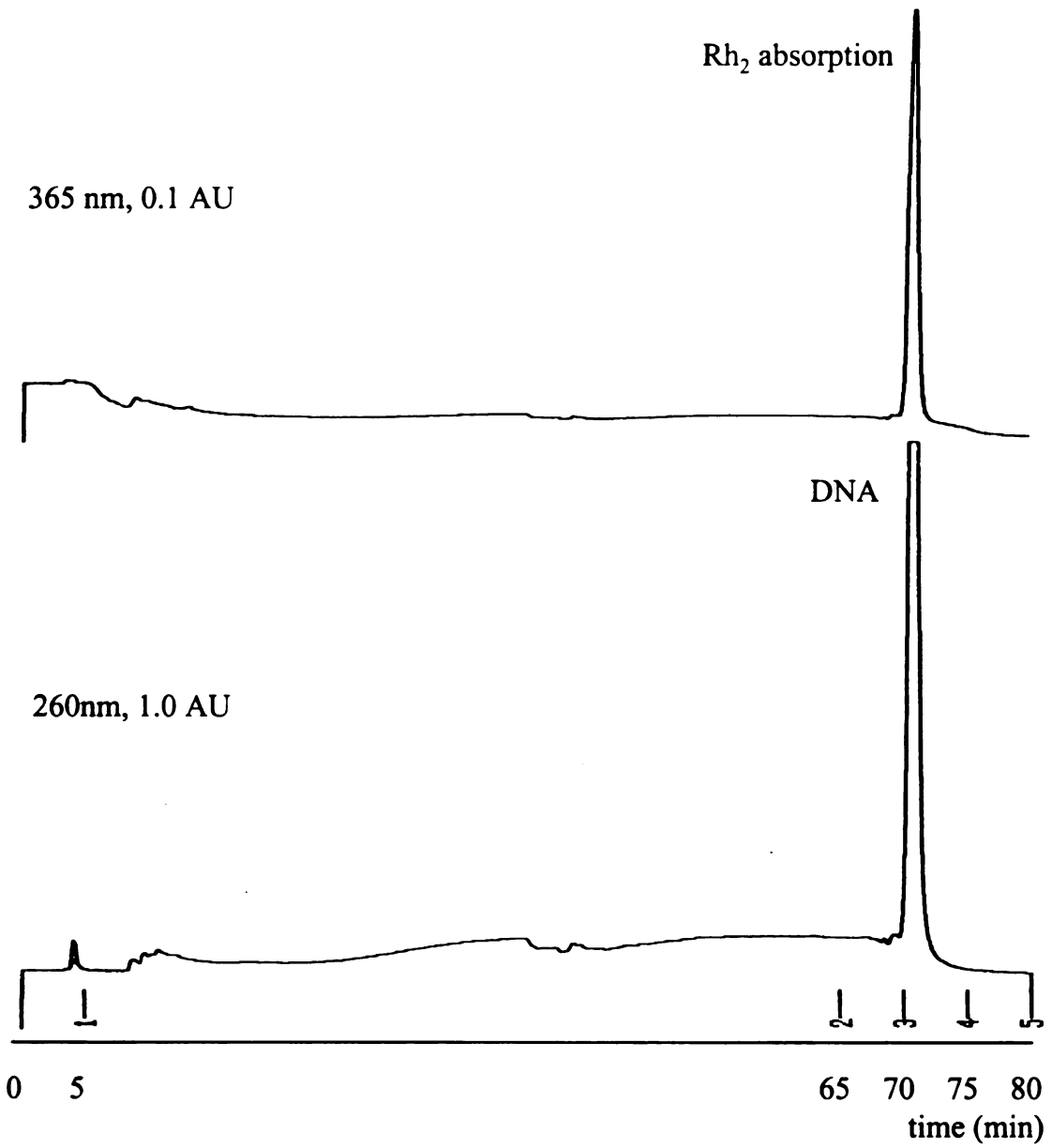


Figure 20. HPLC chromatogram of ss[$Rh_2(O_2CCH_3)_2$(GG-12mer)] adduct.

reaction with compound **(12),** is much more resolved than the spectrum from the tetra-acetate reaction (Figure 21). After 45 °C, however, the stability of the double helix is compromised, and the DNA becomes single-stranded. Once again we can conclude that the dirhodium centers are coordinated to the DNA, but we cannot comment with certainty on the mode of binding. Whether the binding occurs at the guanine bases and is bridging or chelating remains to be determined. One way to discern binding sites is to digest the metallated DNA with snake venom phosphoesterase to obtain the nucleotide fragments, and then separate them by HPLC chromatography. By the elution times, one could determine which nucleotides were bound and how many were involved. ^{1}H NMR spectroscopy could also be used to determine to which bases the dirhodium core is coordinated. A similar experiment was performed on some other DNA sequences by a previous worker in our laboratories.[13] The solution structure of the metallated DNA compound should be possible to determine from NMR spectroscopy, but only at much higher concentrations than what we have employed. The concentrations used by Reedijk and coworkers were 13 times greater than the concentrations used in our experiments. Efforts to solve the solution structure by NMR spectroscopy as well as in the solid-state by X-ray crystallography are in progress.

3. Summary

Recent developments outlined in this chapter support the formation of dirhodium-DNA adducts. Whether the adducts formed are due to the interaction of the central guanine bases coordinating to the Rh atoms in a bridging eq mode or not cannot be discerned from the current data. It is clear, however, that whatever the interaction, it is fairly stable and not interrupted during the course of purification. Annealing of the complimentary strand of DNA in the GG-12mer reactions was not prevented by the coordination of the dirhodium unit. In addition, the binding of dirhodium compounds destabilizes the DNA helix as determined by the low melting point of the metallated dsDNA. Structural information of the ds(Rh_2-DNA) adduct obtained by two-dimensional NMR studies and X-ray crystallography are in progress.

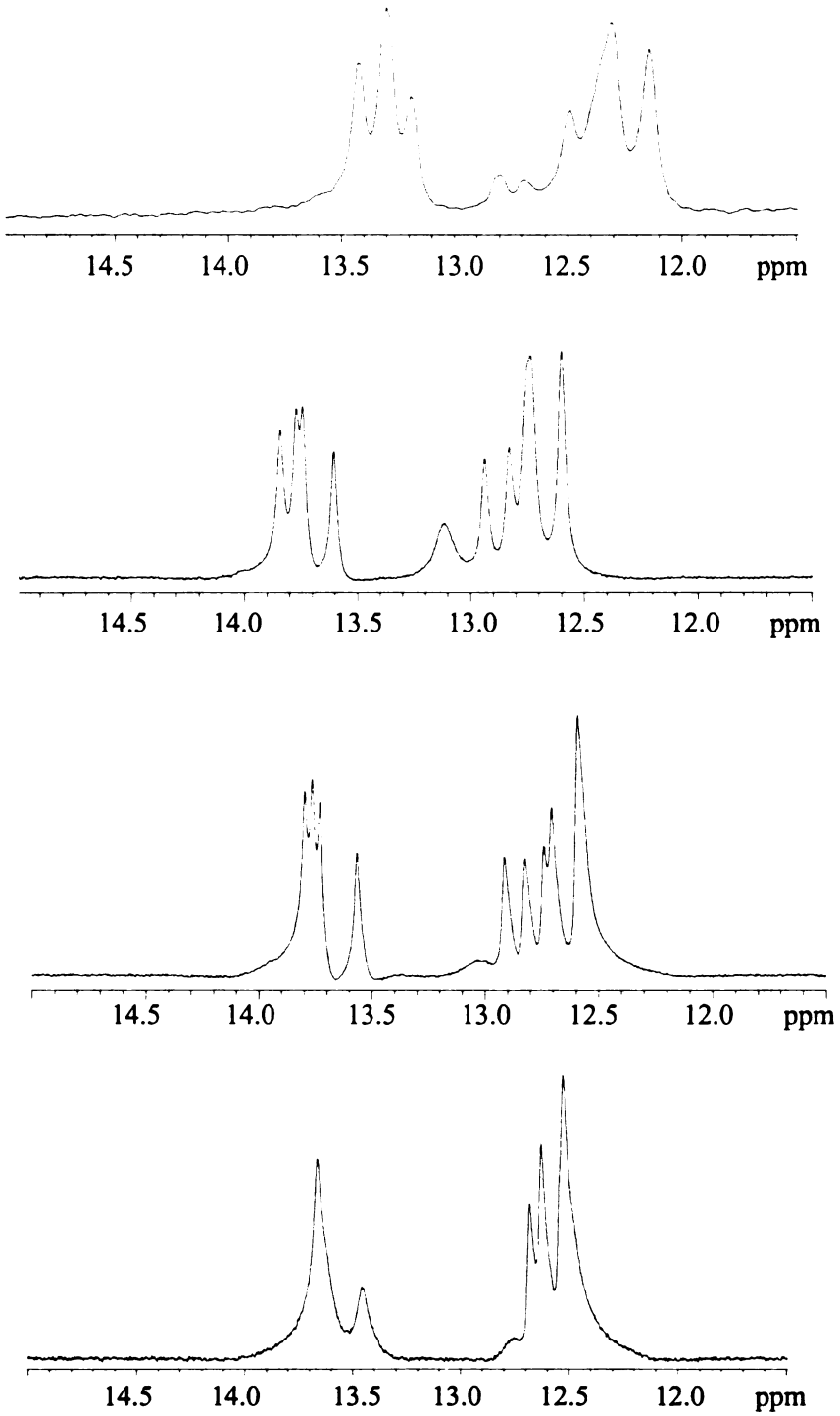


Figure 21. ^{1}H NMR spectra depicting the imino region of ds[$Rh_2(O_2CCH_3)_2$(GG-12mer)] in 10% D_2O.

List of References

1. (a) Rosenberg, B.; VanCamp, L. *Nature*, **1969**, *222*, 385. (b) Rosenberg, B. in *Metal Ions in Biology*, Spiro, T. G., Ed.; Wiley, New York, **1980**, *1*, 1. (c) Umapathy, P. *Coord. Chem. Rev.* **1989**, *95*, 129. (d) Lippert, B. Chapter 1 in *Prog. Inorg. Chem.* Lippard, S. J., Ed.; Wiley, New York, **1989**, *37*, 1. (e) Sherman, S. E.; Lippard, S. J. *J. Chem. Rev.* **1987**, *87*, 1153. (f) Sundquist, W. I.; Lippard, S. J. *J. Coord. Chem. Rev.* **1990**, *100*, 293. (g) Reedijk, J. *Pure Appl. Chem.* **1987**, *59*, 181. (h) Eastman, A. *Pharmac. Ther.* **1987**, *34*, 155. (i) Pasini, A.; Zunino, F. *Angew. Chem. Int. Ed. Engl.* **1987**, *26*, 615. (j) Frey, U.; Ranford, J. D.; Sadler, P. J. *Inorg. Chem.* **1993**, *32*, 1333. (k) *Platinum and Other Metal Complexes in Cancer Chemotherapy*, Howell, S. B., Ed.; Plenum Press, New York, **1991**. (l) *Platinum Coordination Complexes in Cancer Chemotherapy*, Hacker, M. P.; Double, E. B.; Krakoff, I. H., Eds.; Martinus Nijhoff, Boston, **1984**.
2. Baker, S. A-.B.; Perez-Soler, R.; Khokhar, A. R. J. *Coord. Chem.* **1993**, *29*, 1.
3. (a) Sherman, S. E.; Gibson, D.; Wang, A.H.-J.; Lippard, S. J. *Science,* **1985**, *230,* 412. (b) Sherman, S. E.; Gibson, D.; Wang, A.H.-J.; Lippard, S. J. *J. Am. Chem. Soc.* **1988**, *110,* 7368. (c) Coll, M.; Sherman, S. E.; Gibson, D.; Lippard, S. J.;Wang, A. H.-J. J. *Biomol. Struct. Dyn.* **1990**, *8*, 315. (d) Chottard, J. C.; Girault, J. P.; Chottard, G.; Lallemand, J. Y.; Mansuy, D. *J. Am. Chem. Soc.* **1980**, *102*, 5565. (e) Dijt, F. J.; Canters, G. W.; den Hartog, J. H. J.; Marcelis, A.T.M. and Reedijk, J. *J. Am. Chem. Soc.* **1984**, *106,* 3644. (f) den Hartog, J. H. J.; Altona, C.; van Boom, J. H.; van derMarel, G. A.; Haasnoot, C. A. G.; Reedijk, J. J. *Biomol. Struct. Dyn.* **1985**, *2(6)*, 1137. (g) den Hartog, J. H. J.; Altona, C.; van Boom, J. H.; van der Marel, G. A.; Haasnoot, C. A. G.; Reedijk, J. *J. Am. Chem. Soc.* **1984**, *106,* 1528. (h) Herman, F.; Kozelka, J.; Guittet, E.; Girault, J.-P.; Huyni-Dinh, T.; Igolen, J.; Lallemand, J.-Y.; Chottard, J. C. *Eur. J. Biochem.* **1990**, *194,* 119. (i) Kozelka, J.; Fouchet, M.-H.; Chottard, J. C. *Eur. J. Biochem.* **1992**, *205,* 895. (j) Iwamoto, M.; Mukundan, S. Jr.; Marzilli, L. G. *J. Am. Chem. Soc.* **1994**, *116,* 6238. (k) Kozelka, J.; Petsko, G. A.; Lippard, S. J. *J. Am. Chem. Soc.* **1985**, *107,* 4079. (l) Kozelka, J.; Petsko, G. A.; Quigley, J. D.; Lippard, S. J. *J. Am. Chem. Soc.* **1986**, *25,* 1075. (m) Kozelka, J.; Archer, S.; Petsko, G. A.; Lippard, S. J.; Quigley, J. *Biopolymers,* **1987**, *26*, 1245. (n) Kozelka, J.; Chottard, J.- C. *Biophys. Chem.* **1990**, *35,* 165. (o) Yao, S.; Plastaras, J. P. and Marzilli, L. G. *Inorg. Chem.* **1994**, *33*, 6061.

4. (a) Sherman, S. E.; Gibson, D.; Wang, A. H. –J.; Lippard, S. J. *Science*, **1985**, *230*, 412. (b) *J. Am. Chem. Soc.* **1988**, *110*, 7368. (c) den Hartog, J. H. J.; Altona, C.; Girault, J. P.; Lallemand, J. Y.; Marcelis, A.T.M.; Reedijk, J. *Nucleic Acids Res.* **1982**, *10*, 4715. (d) Girault, J. P.; Chottard, G.; Lallemand, J. Y.; Chottard, J. C. *Biochemistry*, **1982**, *21*, 1352.
5. Huang, H.; Zhu, L.; Reid, B. R.; Drobny, G. P.; Hopkins, P. B. *Science*, **1995**, *270*, 1842.
6. Chifotides, H. T.; Dunbar, K. R.; Young, D. C. unpublished results.
7. Den Hartog, J. H. J.; Altona, C.; van Boom, J. H.; van der Marel, G. A.; Haasnoot, C. A. G.; Reedijk, J. *J. of Biomolec. Struct. Dyn.* **1985**, *2*, 1137.
8. (a) Baker, T. A.; Kornberg, A. *DNA Replication*, Freeman and Co. 2nd Edition, **1992**. (b) Stryer, L. *Biochemistry*, Freeman and Co. 4th Edition, **1995**. (c) Lewin, B. *Genes V*, Oxford University Press, **1994**.
9. Gibson, D.; Lippard, S. J. *Inorg. Chem.* **1987**, *26*, 2275.
10. Fimiani, V.; Ainis, T.; Cavallaro, A.; Piraino, P. J. *Chemother.* **1990**, *2*, 319.
11. (a) Farrell, N. *J. Inorg. Biochem.* **1981**, *14*, 261. (b) Bear, J. L.; Gray, Jr. H. B.; Rainen, L.; Chang, I. M.; Howard, R.; Serio, G.; Kimball, A. P. *Cancer Chemother. Reports Part 1*, **1975**, *59*, 611.
12. Sletten, E; Froystein, N. Å. in *Metal Ions in Biological Systems: Interactions of Metals with Nucleotides, Nucleic Acids, and Their Constituents 32*, Sigel, A.; Sigel, H., Ed. Marcel Dekker, Inc. New York, **1996**, Ch. 11.
13. Dunbar, K. R.; Chifotides, H. T.; Patel, D. unpublished results.

Chapter V

Inhibition of DNA Replication

1. Introduction

A. Inhibition of DNA Replication by Cisplatin.

While the mechanism of cisplatin is not fully understood, evidence supports the conclusion that DNA interactions are responsible for its anticancer activity. It is not known, however, whether platination of DNA is the sole cellular event that leads to the tumor cell death. Experiments measuring the rates of DNA, RNA, and protein syntheses in cisplatin-treated cells reveal that DNA synthesis is preferentially inhibited, while RNA and protein syntheses are only slightly affected.[1] It is currently believed that platination of DNA inhibits the activity of DNA polymerases, thereby preventing cancer cells from replicating. Whether this inhibition is the result of Pt-enzyme or Pt-DNA interactions has also been explored.[3-5]

Before discussing inhibition of DNA replication by cisplatin, it is important to briefly describe, in general, the replication process exhibited in prokaryotic and eukaryotic systems. Three DNA polymerases are responsible for replication in prokaryotic systems: DNA polymerase I (pol I), DNA polymerase II (pol II) and DNA polymerase III (pol III).[2] The discussion will be limited to the polymerase activity of pol I, as the general DNA replication processes of pol II and pol III are similar although more complicated. Pol I contains a template binding site, a primer binding site, a

primer terminus site, and a site for the incoming four deoxyribonucleoside 5'-triphosphates, dNTPs, (dNTP = dATP, dGTP, dCTP, dTTP). Pol I requires a template strand of DNA, Mg^{2+} cations, and primer in order to synthesize DNA (Figure 1). The template-binding site of pol I binds only to single-stranded DNA at a ratio of 1 enzyme per 300 bases. Binding to double-stranded DNA has been observed unless the DNA is in a denatured state. DNA synthesis occurs by nucleophilic attack of the 3'-OH end of the primer on the α P atom of the incoming dNTP. A phosphodiester bond is formed, and pyrophosphate (PP_i) is released. The reaction is driven by the

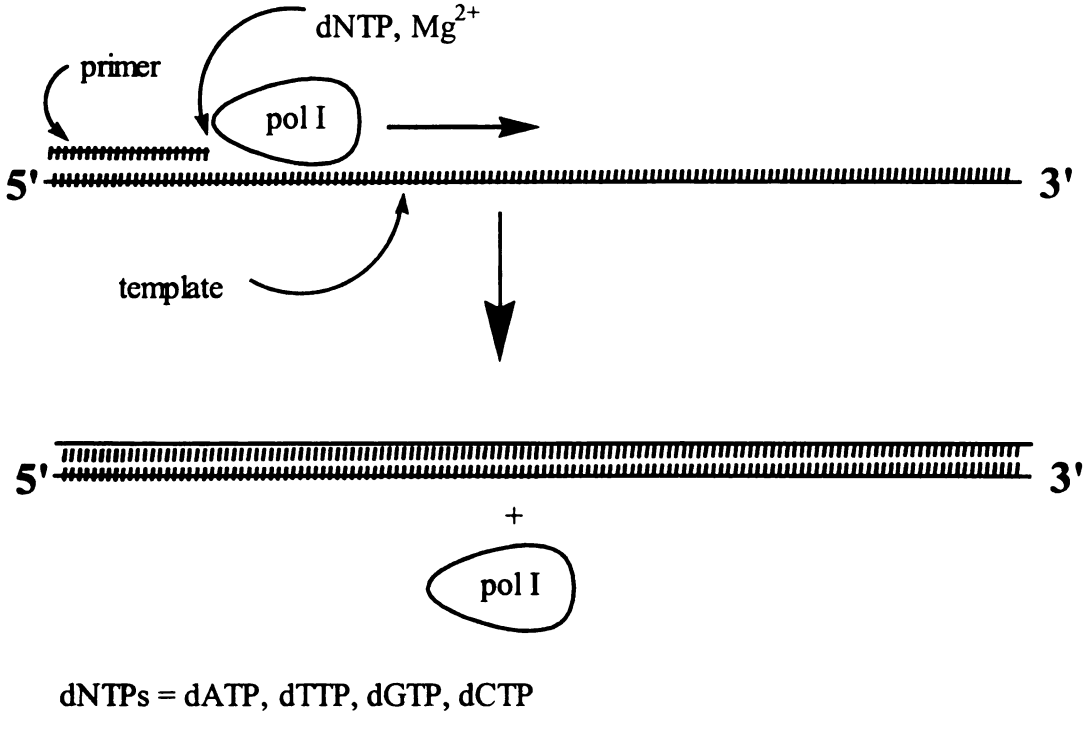


Figure 1. Schematic repsentation of DNA replication by DNA pol I.

subsequent hydrolysis of PP_i by inorganic pyrophosphatase. Extension of the primer DNA strand occurs in the 5'→ 3' direction of the template strand. pol I is moderately processive, in that it catalyzes the formation of ~20 phosphodiester bonds before dissociating from the template. It is also important to mention that Pol I contains a 3'→ 5' exonuclease (proofreading) activity as well as a 5'→ 3' exonuclease (repair) activity. Similarly, pol II has the same properties as pol I, however pol III, which is the major replicative polymerase of prokaryotes, does not possess the 3'→ 5' exonuclease activity.

Eukaryotic cells contain five types of DNA polymerases. The polymerases α, β, γ, δ, and ε all have slightly different functions within the cell. DNA polymerases α (pol α) and δ (pol δ) play major roles in chromosomal replication. The other enzymes are responsible for repair mechanisms with the exception of pol γ, which is the DNA replication enzyme of mitochondria. These enzymes, like the prokaryotic polymerases, require dNTPs to carry out template-directed elongation of the primer in the 5'→ 3' direction. Similar to the prokaryotic polymerases, pol δ, pol ε, and pol γ possess 3'→ 5' exonuclease (proofreading) activity. Like prokaryotic DNA replication, eukaryotic DNA replication requires a template and primer.[2]

E. coli pol I was used in an experiment designed by Bernges and Holler to investigate the inhibition of DNA synthesis by both cisplatin and transplatin DNA adducts. Both isomers inhibit the replicative process of pol I at high and low concentrations *in vitro*.[3] The authors suggest that DNA synthesis is uninhibited until the polymerase reaches the platinated DNA sight. At this junction, the polymerase simply dissociates from the template strand (Figure 2). The proofreading ability of pol I was also terminated on the 5' side of each platinated nucleotide in the primer strand.[3] A similar study by Villani and coworkers involving pol I led to comparable results.[4] In the same study, however, the researchers performed *in vitro* experiments with eukaryotic polymerase pol α . The results of these studies showed that DNA replication by this enzyme was terminated at the sites where Pt was coordinated. *In vivo* studies with the DNA tumor virus SV40 carried out by Lippard and coworkers also support the termination of DNA polymerases by Pt bound to the template strand.[5]

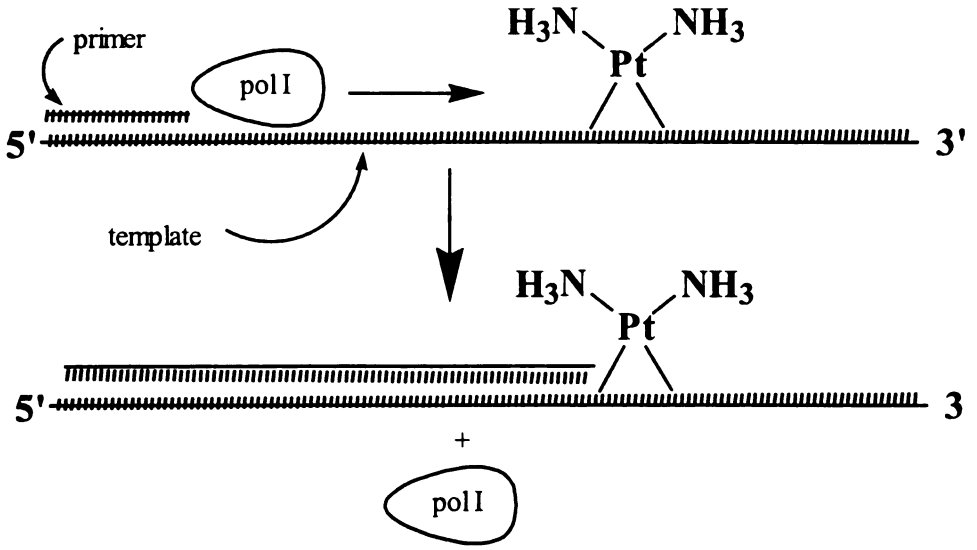


Figure 2. Schematic representation of the DNA replication process of DNA polymerase I (pol I).

Supporting evidence that DNA adducts of cisplatin rather than cisplatin bound to enzyme is responsible for the inhibition of the DNA replication process was reported by Harder and coworkers.[6] In this study, the researchers incubated Pt/DNA adducts of cisplatin and transplatin with pol α, pol β, and Rauscher murine leukemia virus reverse transcriptase (RMLVRT). They observed behavior similar to the inhibition exhibited with the prokaryotic polymerase pol I. In order to determine the significance of Pt-enzyme interaction, pol α was incubated with various concentrations of both Pt compounds in distilled water at 37 °C for three days. A time course study was performed where at several intervals up to 110 minutes

after incubation, aliquots of the Pt-enzyme mixtures were removed and added to an assay mixture containing activate enzyme. It was observed that pol α was inactivated at a concentration of 500 μM cisplatin after 30 minutes. This is 100 times the concentration of cisplatin required to inhibit DNA replication *in vivo*. Transplatin, on the other hand, inactivated pol α 7 to 10 times more effectively than cisplatin. The results of this study allowed the researchers to conclude that inactivation of pol α by cisplatin and transplatin were biologically insignificant compared to the effects of the reactions of the platinum compounds with the template. In other words, DNA replication is inhibited by the interaction of Pt with the DNA template, which renders the DNA unsuitable or unrecognizable for use by pol α. Thus the Pt-enzyme interactions are of negligible importance. Furthermore, the above studies found that the 5'→ 3' exonuclease activity of pol α was inhibited by platination of the template.

B. Inhibition of DNA Replication by Dirhodium Tetracarboxylates.

Dirhodium tetracarboxylates, $Rh_2(O_2CR)_4(H_2O)_2$ (R = Me, Et, Pr) have also been reported to inhibit DNA replication. Studies by Bear and coworkers probed the mechanism by which inhibition of replication takes place.[7] Like cisplatin researchers, these investigators also questioned the significance of metal-DNA interactions as well as the inactivation of the

polymerase by metal-enzyme interactions. Unlike the studies with cisplatin and related Pt compounds where reaction times between the metal compound and DNA range from 24 h to two weeks, the dirhodium compounds were incubated with DNA for no more than 1 h before the addition of pol I and the measurements made. This could account for the observation that the inhibition of replication increased with time since more of the $Rh_2(O_2CR)_4(H_2O)_2$ reacted with the DNA. The same difference in incubation time is noticed for the enzyme inactivation study, *viz.* 0.5 h incubation of $Rh_2(O_2CR)_4(H_2O)_2$ with the enzyme before any measurements were made, *versus* 3 days for cisplatin and transplatin.[6,7] Even at these short incubation times, Bear and coworkers observed inhibition of the replicative properties of pol I. They could not explain however, what was responsible for these effects. Three possible explanations were proposed for their observations: (a) inhibition due to Rh_2-enzyme interaction either at the active site or on the surface of the enzyme; (b) inhibition due to binding of the substrate pool, particularly those molecules containing adenine; and (c) inhibition due to binding of the drug to single-stranded regions of the template. The investigators attempted to differentiate between these possibilities by exploring one system in which $Rh_2(O_2CR)_4(H_2O)_2$ was allowed to react with poly-dA, poly-dT, dATP and dTTP and another system

containing poly-dC, poly-dG, dCTP, and dGTP. Their reasoning for the two different systems is that the assay containing poly-dG would not exhibit any binding of the $Rh_2(OCR)_4(H_2O)_2$ to the template since previous results obtained by the researchers suggest that $Rh_2(OCCH_3)_4(H_2O)_2$ **(11)** does not bind to guanine bases.[7] If DNA binding is not allowed, then the Rh_2 compound can only bind to the enzyme. When R = Me the Rh_2 compound inhibited replication of the poly-dA system by 83.9% and the poly-G system by 55.7%. In the cases where the carboxylate was propionate or butyrate, the poly-dG replication was inhibited by 71.3% and by 49.3%, respectively, whereas the replication of the poly-dA system was inhibited by 33.1% for propionate and by 20.0% for butyrate. The conclusion offered by Bear is that the inhibition of the poly-dG replication was due to binding of the dirhodium compound to the enzyme, and in the case for the poly-dA system the inhibition was due to the binding of the dATP substrate pool. Unfortunately, the study failed to provide satisfactory methods of characterization for the dirhodium compounds produced in these studies. The only methods that were used to follow the reactions involved the measurement of ^{3}H-dTTP and ^{3}H-dCTP incorporation into the newly synthesized DNA.[7] An equally acceptable interpretation of Bear's results would be that metal-DNA binding and not metal-pol I or metal-substrate

pool interactions is the cause of inhibition. Furthermore, previous research in our labs, discussed in chapter 2 of this dissertation, has demonstrated that dirhodium compounds actually bind guanine bases quite readily, counter to the earlier claims. The aim of the research described in this chapter is to repeat these early studies of $Rh_2(O_2CCH_3)_4(H_2O)_2$ **(11)** performed by Bear, and to also investigate whether analogous inhibition of DNA replication by $[Re_2(O_2CCH_2CH_3)_4][SO_4]$ also occurs. Evidence that $Rh_2(O_2CCH_3)_4(H_2O)_2$ **(11)** does in fact react with double-stranded DNA is also presented.

2. Experimental

A. Synthesis

The compounds $Rh_2(O_2CCH_3)_4(H_2O)_2$ **(11)** and $[Re_2(O_2CCH_2CH_3)_4][SO_4]$ **(13)** were prepared by literature procedures.[9] Since PCR (Polymerase Chain Reaction) requires a specialized knowledge of biochemical lab techniques, this work was carried out in collaboration with Dr. Karl Bishop and Lee Bickerstaff. A brief description of the biochemical experiment follows.

Varying concentrations of the dinuclear transition metal carboxylate were added to solutions with constant concentrations of plasmid PBR322 at r.t. for 12 h. The appropriate buffers containing the substrates (dNTPs), the ^{32}P labeled 5'-primer, unlabeled 3'-primer and the Taq polymerase were

added, and the PCR process started. The PCR products were analyzed by denaturing polyacrlimide gel electrophoresis (% acrylimide, 7mM urea) followed by autoradiography.

3. Results

A. Autoradiograph of the PCR Inhibition by $Rh_2(O_2CCH_3)_4(H_2O_2)$ (11)

PCR is a sensitive process; minute quantities of contaminant DNA or proteins can have devastating results.[2] PCR requires two fragments, typically 20 base pairs (bp) long, that are used as a primer for the polymerase. These primers are complementary images to each end of the DNA sequence of interest, in this case a 315-bp section of the PBR322 plasmid. The primers plus the dNTPs are added to a solution of the template along with a heat-stable polymerase called Taq polymerase. Unlike most DNA polymerases such as pol I or pol α, Taq resists denaturation at 95 °C. Taq is isolated from the bacterium known as *Thermus aquaticus* which is found in the hot springs of Yellowstone National Park.

The DNA mixture is heated to 95 °C to melt the double-stranded DNA into two single strands. The reaction mixture is cooled to 55 °C which allows the primers to bind to their complementary sites (Figure 3). The entire sample of DNA is now single-stranded except for the two small regions where the 15-base primers are bound. The temperature is increased

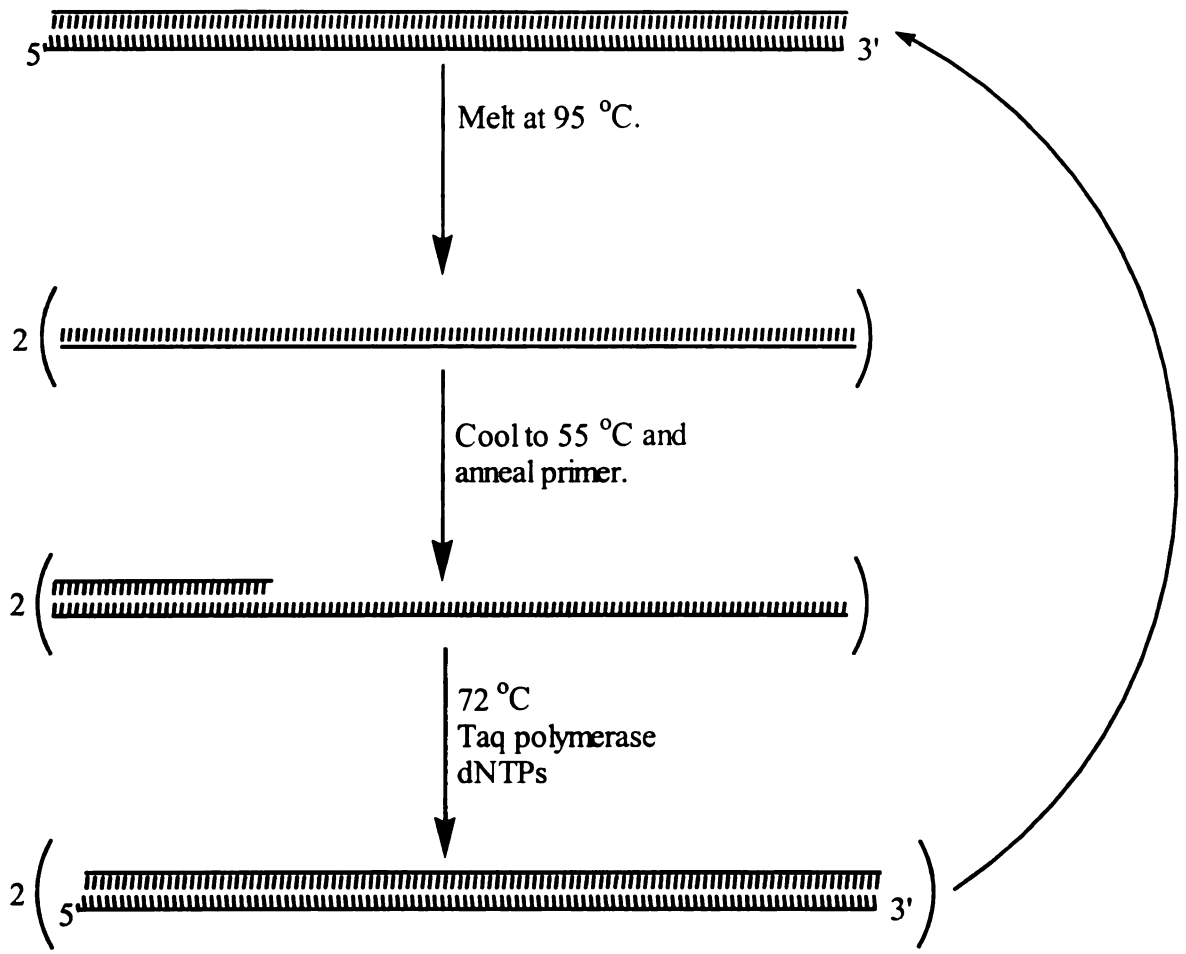


Figure 3. Schematic representation of the steps of the Polymerase Chain Reaction (PCR).

to 72 °C and the replication process begins from the 3'-OH end of the primer. The proficiency at which Taq synthesizes DNA is at a rate of 20 nucleotides/sec. After a short period of time, the temperature is raised to 95 °C which causes the DNA template to become single-stranded. At the end of the first cycle, there are two strands of the original template. The temperature is again lowered to 55 °C to begin the process of annealing the

primers again. The process is repeated, thereby amplifying the amount of 315-bp template. In our experiment, Taq would theoretically synthesize DNA until it reached a metallated site of the DNA, and then dissociate from the template (Figure 4). The products of the PCR reaction are then verified by gel electrophoresis.

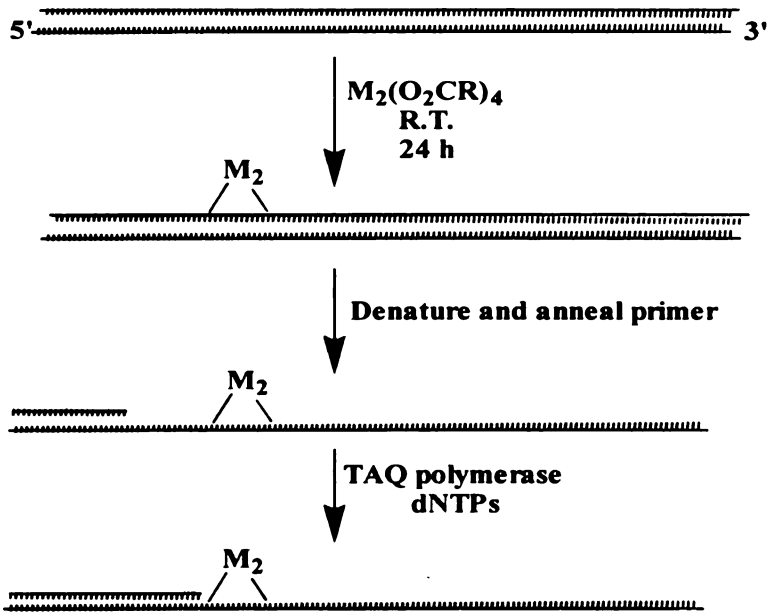


Figure 4. Schematic of the inhibition of PCR by dinuclear transition metal compounds.

The autoradiograph presented in Figure 5 depicts 9 lanes labeled 1 - 9. The band at the top of lane 1 represents the PCR control reaction where no $Rh_2(O_2CCH_3)_4(H_2O)_2$/plasmid incubation was performed. Lanes 2 - 8 represent the PCR products with varying concentrations of $Rh_2(O_2CCH_3)_4(H_2O)_2$ incubated with the template. Lane 9 contains a 100-bp

Table 1. Summary of the $Rh_2^{II,II}$ concentrations used to inhibit DNA replication by Bear and coworkers.[7]

	calf thymus	poly-A/poly-T	poly-G/poly-C
$Rh_2(O_2CCH_3)_4$ (μM)	10 - 40	40	40
$Rh_2(O_2CEt)_4$ (μM)	10 - 40	4	4
$Rh_2(O_2CPr)_4$ (μM)	10 - 40	4	4
dNTPs (μM)	10	5	5
Template (μg)	5	10	10
Polymerase (units)	2.32	4.64	4.64

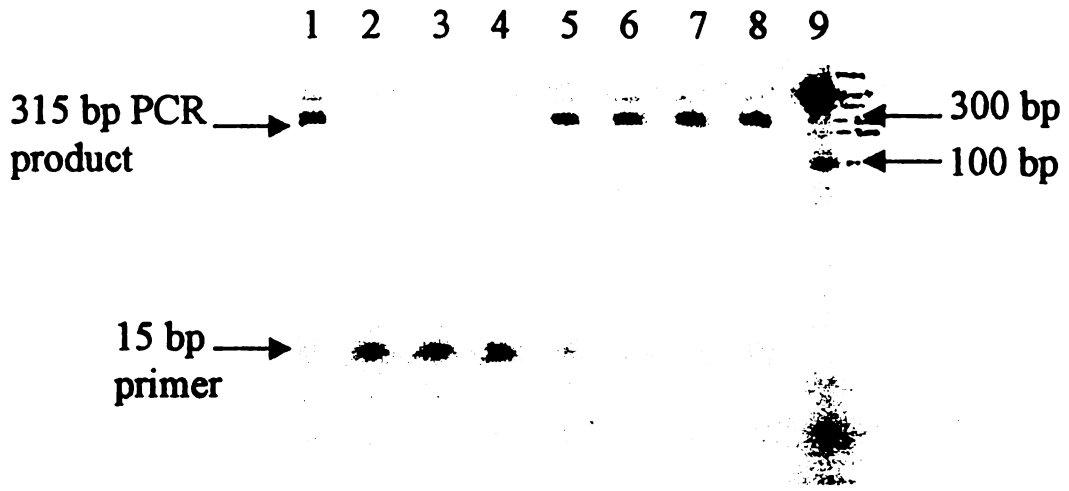
DNA molecular ladder (i.e. 100-bp, 200-bp, 300-bp, ... 1500-bp) used to compare with the molecular weight of the amplified DNA.

In lane 1 only one band is observed at about 300-bp. This is the 315-bp PCR product with no inhibition of the DNA synthesis. Lanes 2 – 3 exhibit no bands that can be assigned as the 315-bp product. A single band in each of these lanes is observed much lower than the 100-bp molecular weight marker. These lower bands are assigned to the 15-bp primer and the short pieces of DNA synthesized that are about the same length as the primer. It can be observed that these bands become more faint from lanes 3 - 8 as the band for the 315-bp product becomes more intense. This indicates that DNA replication was inhibited at the concentrations ranging from 1.5 μM to 15 nM. The DNA replication was not significantly affected at concentrations at or below 1.5 nM.

The question arises as to whether the inhibition is due to the interaction of $Rh_2(O_2CCH_3)_4(H_2O)_2$ with the template, the substrate pool, or the Taq. Interactions with the substrate pool can be eliminated as a cause of inhibition since at the highest concentration of $Rh_2(O_2CCH_3)_4(H_2O)_2$ (1.5 μM) the concentration of the dNTPs in the PCR process is at least an order of magnitude greater. Thus, if all of the $Rh_2(O_2CCH_3)_4(H_2O)_2$ were reacting with the dNTPs such as dATP and dGTP, enough substrate is present to

allow the DNA replication process to occur. Unfortunately, it is impossible to have a definitive control experiment where $Rh_2(O_2CCH_3)_4(H_2O)_2$ is first incubated with Taq before the PCR process due to the findings that $Rh_2(O_2CCH_3)_4(H_2O)_2$ reacts with single-stranded DNA almost instantaneously (as presented in Chapter IV), and the PCR process requires the presence of single-stranded DNA in order for the primer to bind. It can be argued however, that $Rh_2(O_2CCH_3)_4(H_2O)_2$ is in excess compared to the polymerase at each concentration in the PCR experiment. Therefore, one would expect the inactivation of the enzyme at the lowest concentration of 1.5 pM if the reaction between $Rh_2(O_2CCH_3)_4(H_2O)_2$ and Taq took place more efficiently than the reactions between the dirhodium compound and the overwhelming concentrations of dATP and dGTP which we also know to occur at rapid rates.[8] The concentration used by Bear in the early studies of $Rh_2(O_2CR)_4(H_2O)_2$ were equimolar or in excess to the concentrations of dNTPs (Table 24).

An additional study was performed to determine if binding to the double-stranded plasmid was actually occurring. Solutions of $Rh_2(O_2CCH_3)_4(H_2O)_2$ at the same concentrations used in the PCR experiment were incubated with the 315-bp PBR322 for 24 h at r.t. The Rh_2-DNA adducts were then intercalated with ethidium bromide and gel



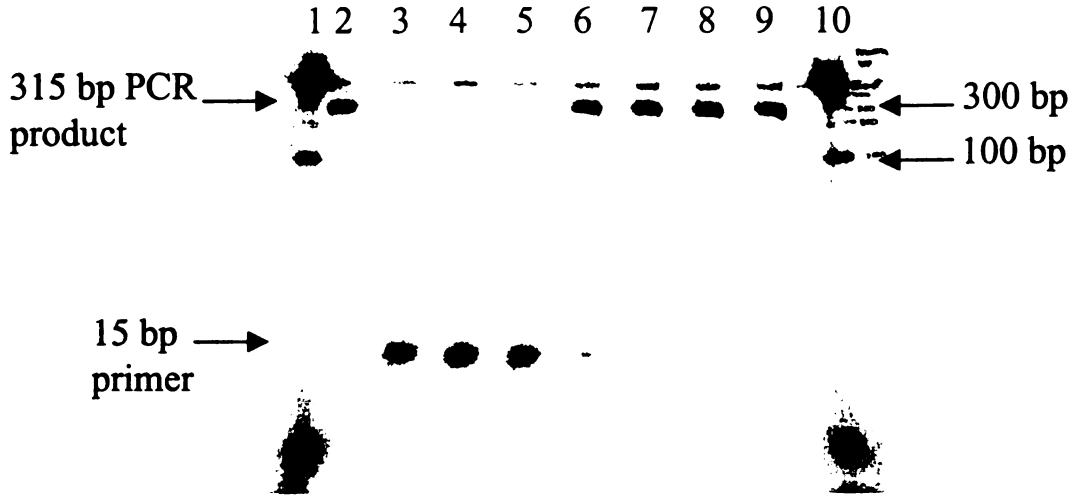
Lanes 1 - 9:
1) control
2) 1.5 μM **(11)**
3) 150 nM **(11)**
4) 15 nM **(11)**
5) 1.5 nM **(11)**
6)150 pM **(11)**
7) 15 pM **(11)**
8) 1.5 pM **(11)**
9) molecular weight marker

Figure 5. Autoradiograph of the inhibition of PCR by $Rh_2(O_2CCH_3)_4(H_2O)_2$ **(11)**.

electrophoresed on a non-denaturing gel. The results of this study proved that not only was $Rh_2(O_2CCH_3)_4(H_2O)_2$ binding to double-stranded DNA, but that it altered the structure of the plasmid at different concentrations.[8]

B. Autoradiograph of the PCR Inhibition by $[Re_2(O_2CCH_2CH_3)_4][SO_4]$

Under the same PCR conditions as the dirhodium tetracarboxylate, $[Re_2(O_2CCH_2CH_3)_4][SO_4]$ was incubated with the 315-bp plasmid, and the adduct subjected to PCR. The autoradiograph presented in Figure 6 exhibits bands comparable to the bands in Figure 5. The autoradiograph has 10 lanes with lanes 1 and 10 representing the 100-bp molecular weight ladders. $[Re_2(O_2CCH_2CH_3)_4][SO_4]$ inhibits the PCR reaction at the same concentrations as $Rh_2(O_2CCH_3)_4(H_2O)_2$ (1.5 μM, 150 nM, and 15 nM), as only bands for short strands of DNA are observed and the bands for the 315-bp PCR product are absent in lanes 2 – 4. Lanes 5 – 8 contain the PCR product as the concentration of the dirhenium compound is decreased. This is an important result, as no other DNA inhibition studies have ever been performed on a dirhenium compound. It is known that the dirhenium tetracarboxylates $Re_2(O_2CR)_4X_y$ and the dirhenium biscarboxylates *cis*-$Re_2(O_2CR)_2X_4L_2$ (R = Me, Et, Pr; X = Cl^-, Br^-, SO_4^{2-}, BF_4^-; L = H_2O, CH_3OH) react with 9-EtGH and 9-EtAH.[9] *In vivo* studies with test animals infected with various cancers show signs of marked improvement when



Lanes 1 - 9:
1) molecular weight marker
2) control
3) 1.5 μM **(11)**
4) 150 nM **(11)**
5) 15 nM **(11)**
6) 1.5 nM **(11)**
7)150 pM **(11)**
8) 15 pM **(11)**
9) 1.5 pM **(11)**
10) molecular weight marker

Figure 6. Autoradiograph of the inhibition of PCR by $[Re_2(O_2CCH_2CH_3)_4(H_2O)_2][SO_4]$.

treated with these compounds.[9] To our knowledge, no other investigations between the antitumor active dirhenium compounds and enzymes or with DNA have been reported.

4. Conclusions

Recent results involving the reactions of dinuclear rhodium and dinuclear rhenium tetracarboxylate compounds with double-stranded DNA under mild conditions reveal that both $Rh_2(O_2CCH_3)_4(H_2O)_2$ and $[Re_2(O_2CCH_2CH_3)_4][SO_4]$ inhibit the DNA synthesis by PCR. It was reported in previous literature that while dinuclear rhodium(II) compounds have a high affinity for single-stranded DNA, they do not bind to double-stranded DNA.[7] Contradicting evidence that supports the binding of the dinuclear rhodium and rhenium compounds to double-stranded DNA has been presented. In addition, previous researchers concluded that dirhodium tetracarboxylate compounds inactivate enzymes containing SH groups, but that they do not definitively inactivate DNA or RNA polymerases.[7] Evidence presented in this chapter supports that inhibition of PCR can be attributed to the binding of the dinuclear transition complexes to DNA. The actual mode of binding to the DNA has not been established, and is the subject of further study.

List of References

1. (a) Harder, H. C.; Rosenberg, B. *Int. J. Cancer.* **1970**, *6*, 207. (b) Howle, J. A.; Gale, G. R. *Biochem. Pharmocol.* **1970**, *19*, 2757. (c) Sherman, S. E. Lippard, S. J. *Chem. Rev.* **1987**, *87*, 1153.
2. (a) Baker, T. A.; Kornberg, A. *DNA Replication*, Freeman and Co. 2nd Edition, **1992**. (b) Stryer, L. *Biochemistry*, Freeman and Co. 4th Edition, **1995**. (c) Lewin, B. *Genes V*, Oxford University Press, **1994**.
3. Bernges, F.; Holler, E. *Biochemistry.* **1988**, *27*, 6398.
4. Hoffman, J.-S.; Johnson, N. P.; Villani, G. *J. Biol. Chem.* **1989**, *264*, 15130.
5. Ciccarelli, R. B.; Solomon, M. J.; Varshavsky, A.; Lippard, S. J. *Biochemistry.* **1985**, *24*, 7533.
6. Harder, H. C.; Smith, R. G.; Leroy, A. F. *Cancer Res.* **1976**, *36*, 3821.
7. (a) Howard, R. A.; Spring, T. G.; Bear, J. L. *Cancer Research* **1976**, *36*,4402. (b) Bear, J. L.; Gray, Jr., H. B.; Rainen, L.; Chang, I. M.; Howard, R.; Serio, G.; Kimball, A. P. *Cancer Chemother. Reports* Part 1, **1975**, *59*, 611.
8. Bishop, K.; Bickerstaff, L.; Catalan, K. V.; Lozada, E. U.; Dunbar, K. R. unpublished results.
9. (a) Dmitrov, N. V.; Eastwood, G. W. *Current Chemother. Proc. Int. Cong. Chemother. 10th 1977.* **1978**, *2*, 1319. (b) Eastland, G. W.; Yang, G.; Thompson, T. *Meth. and Find. Exptl. Clin. Biochem.* **1989**, *10*, 41.

Appendix

TABLES OF ATOMIC POSITIONAL PARAMTERS AND EQUIVALENT ISOTROPIC DISPLACEMENT PARAMETERS FOR X-RAY CRYSTALLOGRAPHIC STRUCTURES

Table A1. Crystal data and structure refinement for $Rh_2(DTolF)_2(O_2CCF_3)_2(CH_3CN)_2$ (1).

Identification code	$Rh_2(DTolF)_2(O_2CCF_3)_2(CH_3CN)$
Empirical formula	C38 H36 F6 N6 O4 Rh2
Formula weight	960.55 g/mol
Temperature	293(2) K
Wavelength	0.71073 Å
Crystal system	Monoclinic
Space group	$P2_1/n$
Unit cell dimensions	a = 10.8495(3) Å
	b = 21.4349(6) Å
	c = 18.6766(3) Å
	$\alpha = 90^\circ$
	$\beta = 92.0590(10)^\circ$
	$\gamma = 90^\circ$
Volume	4340.6(2) $Å^3$
Z	4
ρ_{calc}	1.470 g/cm^3
μ	0.829 cm^{-3}
F(000)	1928

Table A1 continued.

Crystal size	0.31 x 0.11 x 0.10 mm^3
Theta range for data collection	1.90 to 28.39°.
Index ranges	-14<=h<=14, -28<=k<=27, -15<=l<=23
Reflections collected	25160
Independent reflections	10101 [R(int) = 0.1177]
Refinement method	Full-matrix least-squares on F^2
Data / restraints / parameters	10101 / 31 / 506
Goodness-of-fit on F^2	0.717
Final R indices [$I>2\sigma(I)$]	R1 = 0.0451, wR2 = 0.0904
R indices (all data)	R1 = 0.1390, wR2 = 0.1116
Largest diff. peak and hole	0.780 and -1.134 $e^-/Å^3$

Table A1 continued.

Atomic coordinates (x 10^4) and equivalent isotropic displacement parameters ($Å^2$ x 10^3).

	x	y	z	U(eq)	Occ.
Rh(1)	265(1)	1968(1)	3162(1)	47(1)	1
Rh(2)	562(1)	1972(1)	4482(1)	46(1)	1
O(1)	-201(3)	2871(1)	4465(2)	57(1)	1
O(2)	1986(3)	2412(2)	3115(2)	57(1)	1
O(3)	-649(3)	2821(1)	3278(2)	56(1)	1
O(4)	2330(3)	2332(2)	4321(2)	58(1)	1
N(1)	-1359(4)	1542(2)	3295(2)	49(1)	1
N(2)	-1155(4)	1628(2)	4544(2)	50(1)	1
N(3)	-8(5)	2169(2)	1976(3)	64(1)	1
N(4)	1059(4)	2055(2)	5667(2)	58(1)	1
N(5)	1157(4)	1144(2)	3142(2)	52(1)	1
N(6)	1280(4)	1111(2)	4400(2)	54(1)	1
C(1)	-4612(7)	1016(4)	867(4)	122(3)	1
C(2)	1900(9)	-165(4)	482(4)	164(4)	1
C(4)	3873(6)	-17(3)	6800(3)	109(3)	1
C(5)	-2581(7)	933(3)	1543(3)	82(2)	1
C(6)	-4127(6)	1505(3)	2076(4)	82(2)	1
C(7)	-3750(7)	1154(3)	1509(4)	78(2)	1
C(8)	-1795(6)	1055(3)	2132(3)	72(2)	1
C(9)	1440(6)	1976(3)	6235(3)	66(2)	1
C(10)	1924(7)	282(2)	6129(3)	67(2)	1
C(11)	1704(7)	176(4)	1196(4)	97(2)	1
C(12)	1934(7)	1853(3)	6954(3)	104(3)	1
C(13)	1226(6)	-116(3)	1784(4)	88(2)	1
C(15)	2040(6)	792(3)	1282(3)	94(2)	1
C(16)	-155(6)	2323(3)	1405(4)	87(2)	1

Table A1 continued.

C(17)	1891(5)	1100(3)	1917(3)	70(2)	1
C(18)	-373(8)	2517(5)	645(4)	177(4)	1
C(19)	-2805(5)	850(2)	6024(3)	57(2)	1
C(20)	3175(6)	802(2)	5031(3)	67(2)	1
C(21)	-2866(5)	1318(2)	6540(3)	53(1)	1
C(22)	3796(6)	524(3)	5603(4)	81(2)	1
C(23)	1049(6)	188(3)	2433(3)	72(2)	1
C(24)	1293(5)	553(2)	5559(3)	61(2)	1
C(25)	-3516(6)	1209(2)	7230(3)	76(2)	1
C(27)	-3374(6)	1638(2)	2665(3)	64(2)	1
C(28)	-663(5)	3061(2)	3884(3)	57(2)	1
C(29)	3183(7)	274(3)	6166(3)	68(2)	1
C(30)	-1798(5)	1990(2)	5724(3)	53(1)	1
C(31)	2589(5)	2466(2)	3686(3)	56(2)	1
C(32)	1376(5)	802(3)	2499(3)	56(2)	1
C(33)	-2184(6)	1414(2)	2699(3)	54(1)	1
C(34)	1928(6)	820(2)	4992(3)	52(1)	1
C(35)	-2239(5)	942(2)	5372(3)	50(1)	1
C(36)	-2350(5)	1887(2)	6368(3)	57(2)	1
C(37)	-1738(5)	1516(2)	5211(3)	47(1)	1
C(39)	1492(5)	884(2)	3756(3)	56(2)	1
C(40)	-1773(5)	1469(2)	3954(3)	54(1)	1
F(4)	-596(9)	4117(3)	4028(6)	289(6)	1
F(1)	4726(4)	2370(2)	3926(2)	126(2)1	1
F(2)	4232(4)	2828(2)	2978(2)	137(2)	1
F(3)	4026(4)	3259(2)	3976(3)	149(2)	1
C(41)	3894(7)	2729(4)	3626(4)	81(2)	1
C(3)	-1393(13)	3650(4)	3900(5)	148(5)	1
F(5)	-1890(9)	3758(4)	4468(4)	254(5)	1
F(6)	-1891(7)	3843(3)	3389(3)	240(4)	1

U(eq) is defined as one third of the trace of the orthogonalized Uij tensor.

Table A1 continued.

Bond lengths [Å] and angles [°].

Rh(1)-N(1)	2.007(4)
Rh(1)-N(5)	2.015(4)
Rh(1)-O(3)	2.094(3)
Rh(1)-O(2)	2.101(3)
Rh(1)-N(3)	2.267(5)
Rh(1)-Rh(2)	2.4743(5)
Rh(2)-N(6)	2.011(4)
Rh(2)-N(2)	2.011(4)
Rh(2)-O(1)	2.098(3)
Rh(2)-O(4)	2.100(3)
Rh(2)-N(4)	2.265(5)
O(1)-C(28)	1.248(6)
O(2)-C(31)	1.238(6)
O(3)-C(28)	1.245(6)
O(4)-C(31)	1.262(6)
N(1)-C(40)	1.335(6)
N(1)-C(33)	1.429(6)
N(2)-C(40)	1.313(6)
N(2)-C(37)	1.438(5)
N(3)-C(16)	1.122(7)
N(4)-C(9)	1.137(7)
N(5)-C(39)	1.313(6)
N(5)-C(32)	1.313(6)
N(6)-C(39)	1.326(6)
N(6)-C(34)	1.431(6)
C(1)-C(7)	1.524(8)
C(2)-C(11)	1.543(8)
C(4)-C(29)	1.512(7)
C(5)-C(7)	1.354(8)
C(5)-C(8)	1.392(8)

Table A1 continued.

C(6)-C(7)	1.372(8)
C(6)-C(27)	1.377(8)
C(8)-C(33)	1.388(7)
C(9)-C(12)	1.452(8)
C(10)-C(29)	1.365(8)
C(10)-C(24)	1.373(7)
C(11)-C(15)	1.379(8)
C(11)-C(13)	1.380(8)
C(13)-C(23)	1.396(7)
C(15)-C(17)	1.372(7)
C(16)-C(18)	1.489(9)
C(17)-C(32)	1.395(6)
C(19)-C(21)	1.394(6)
C(19)-C(35)	1.398(6)
C(20)-C(34)	1.354(7)
C(20)-C(22)	1.378(7)
C(21)-C(36)	1.386(6)
C(21)-C(25)	1.509(6)
C(22)-C(29)	1.374(7)
C(23)-C(32)	1.366(7)
C(24)-C(34)	1.405(6)
C(27)-C(33)	1.377(7)
C(28)-C(3)	1.492(8)
C(30)-C(36)	1.380(6)
C(30)-C(37)	1.399(6)
C(31)-C(41)	1.531(8)
C(35)-C(37)	1.381(6)
F(4)-C(3)	1.339(12)
F(1)-C(41)	1.297(7)
F(2)-C(41)	1.294(6)
F(3)-C(41)	1.317(7)
C(3)-F(6)	1.157(8)
C(3)-F(5)	1.229(8)
N(1)-Rh(1)-N(5)	91.6(2)
N(1)-Rh(1)-O(3)	87.93(14)
N(5)-Rh(1)-O(3)	175.2(2)
N(1)-Rh(1)-O(2)	175.4(2)
N(5)-Rh(1)-O(2)	88.2(2)

Table A1 continued.

O(3)-Rh(1)-O(2)	91.92(14)
N(1)-Rh(1)-N(3)	97.0(2)
N(5)-Rh(1)-N(3)	101.2(2)
O(3)-Rh(1)-N(3)	83.64(14)
O(2)-Rh(1)-N(3)	87.6(2)
N(1)-Rh(1)-Rh(2)	87.85(12)
N(5)-Rh(1)-Rh(2)	88.61(12)
O(3)-Rh(1)-Rh(2)	86.56(9)
O(2)-Rh(1)-Rh(2)	87.51(10)
N(3)-Rh(1)-Rh(2)	168.88(11)
N(6)-Rh(2)-N(2)	91.7(2)
N(6)-Rh(2)-O(1)	174.8(2)
N(2)-Rh(2)-O(1)	88.4(2)
N(6)-Rh(2)-O(4)	88.2(2)
N(2)-Rh(2)-O(4)	175.0(2)
O(1)-Rh(2)-O(4)	91.22(14)
N(6)-Rh(2)-N(4)	93.9(2)
N(2)-Rh(2)-N(4)	99.3(2)
O(1)-Rh(2)-N(4)	91.27(14)
O(4)-Rh(2)-N(4)	85.7(2)
N(6)-Rh(2)-Rh(1)	87.60(13)
N(2)-Rh(2)-Rh(1)	88.15(12)
O(1)-Rh(2)-Rh(1)	87.19(9)
O(4)-Rh(2)-Rh(1)	86.90(10)
N(4)-Rh(2)-Rh(1)	172.37(11)
C(28)-O(1)-Rh(2)	117.3(3)
C(31)-O(2)-Rh(1)	116.7(3)
C(28)-O(3)-Rh(1)	118.4(3)
C(31)-O(4)-Rh(2)	117.0(4)
C(40)-N(1)-C(33)	118.2(5)
C(40)-N(1)-Rh(1)	119.5(4)
C(33)-N(1)-Rh(1)	121.3(3)
C(40)-N(2)-C(37)	117.1(4)
C(40)-N(2)-Rh(2)	119.5(4)
C(37)-N(2)-Rh(2)	123.2(4)
C(16)-N(3)-Rh(1)	173.7(5)
C(9)-N(4)-Rh(2)	164.8(5)
C(39)-N(5)-C(32)	117.7(4)

Table A1 continued.

C(39)-N(5)-Rh(1)	118.3(3)
C(32)-N(5)-Rh(1)	123.9(3)
C(39)-N(6)-C(34)	116.4(4)
C(39)-N(6)-Rh(2)	119.0(4)
C(34)-N(6)-Rh(2)	121.5(3)
C(7)-C(5)-C(8)	121.2(6)
C(7)-C(6)-C(27)	123.0(6)
C(5)-C(7)-C(6)	117.4(6)
C(5)-C(7)-C(1)	121.1(7)
C(6)-C(7)-C(1)	121.5(7)
C(33)-C(8)-C(5)	120.9(6)
N(4)-C(9)-C(12)	178.1(6)
C(29)-C(10)-C(24)	121.0(6)
C(15)-C(11)-C(13)	116.5(6)
C(15)-C(11)-C(2)	120.7(7)
C(13)-C(11)-C(2)	122.8(7)
C(11)-C(13)-C(23)	123.2(6)
C(11)-C(15)-C(17)	121.5(6)
N(3)-C(16)-C(18)	178.7(9)
C(15)-C(17)-C(32)	121.0(6)
C(21)-C(19)-C(35)	122.2(5)
C(34)-C(20)-C(22)	120.9(6)
C(36)-C(21)-C(19)	116.4(4)
C(36)-C(21)-C(25)	122.6(5)
C(19)-C(21)-C(25)	121.0(5)
C(20)-C(22)-C(29)	121.7(6)
C(32)-C(23)-C(13)	118.9(6)
C(10)-C(24)-C(34)	120.8(6)
C(33)-C(27)-C(6)	119.6(6)
O(3)-C(28)-O(1)	129.7(5)
O(3)-C(28)-C(3)	113.1(6)
O(1)-C(28)-C(3)	117.1(5)
C(10)-C(29)-C(22)	117.8(6)
C(10)-C(29)-C(4)	120.8(6)
C(22)-C(29)-C(4)	121.4(7)
C(36)-C(30)-C(37)	120.9(5)
O(2)-C(31)-O(4)	131.4(5)
O(2)-C(31)-C(41)	115.6(5)

Table A1 continued.

O(4)-C(31)-C(41)	113.0(6)
C(23)-C(32)-C(17)	118.8(5)
C(23)-C(32)-N(5)	121.1(5)
C(17)-C(32)-N(5)	120.1(5)
C(27)-C(33)-C(8)	117.9(6)
C(27)-C(33)-N(1)	122.0(5)
C(8)-C(33)-N(1)	120.1(6)
C(20)-C(34)-C(24)	117.6(5)
C(20)-C(34)-N(6)	121.1(5)
C(24)-C(34)-N(6)	121.3(5)
C(37)-C(35)-C(19)	120.3(4)
C(30)-C(36)-C(21)	122.2(5)
C(35)-C(37)-C(30)	117.9(4)
C(35)-C(37)-N(2)	121.7(4)
C(30)-C(37)-N(2)	120.3(4)
N(5)-C(39)-N(6)	125.8(5)
N(2)-C(40)-N(1)	124.4(5)
F(2)-C(41)-F(1)	106.6(6)
F(2)-C(41)-F(3)	107.0(6)
F(1)-C(41)-F(3)	103.6(7)
F(2)-C(41)-C(31)	115.1(6)
F(1)-C(41)-C(31)	112.4(6)
F(3)-C(41)-C(31)	111.4(6)
F(6)-C(3)-F(5)	116.1(10)
F(6)-C(3)-F(4)	99.2(10)
F(5)-C(3)-F(4)	90.4(7)
F(6)-C(3)-C(28)	121.2(7)
F(5)-C(3)-C(28)	115.2(8)
F(4)-C(3)-C(28)	107.2(10)

Table A1 continued.

Anisotropic displacement parameters ($Å^2 \times 10^3$).

	U11	U22	U33	U23	U13	U12
Rh(1)	58(1)	50(1)	32(1)	-2(1)	2(1)	4(1)
Rh(2)	55(1)	48(1)	34(1)	-2(1)	1(1)	3(1)
O(1)	85(3)	47(2)	38(2)	-3(2)	-3(2)	12(2)
O(2)	58(3)	70(3)	42(2)	5(2)	-1(2)	-5(2)
O(3)	73(3)	53(2)	40(2)	-3(2)	-6(2)	16(2)
O(4)	52(3)	72(2)	51(2)	2(2)	2(2)	-2(2)
N(1)	49(3)	57(3)	41(3)	-9(2)	-4(2)	0(2)
N(2)	58(3)	52(3)	40(3)	-8(2)	5(2)	-1(2)
N(3)	76(4)	73(3)	43(3)	-4(3)	-5(3)	5(3)
N(4)	70(4)	59(3)	47(3)	-8(3)	10(3)	-3(2)
N(5)	67(3)	52(3)	38(3)	-1(2)	5(2)	11(2)
N(6)	69(3)	51(3)	41(3)	-2(2)	1(2)	13(2)
C(1)	108(7)	175(7)	80(5)	-4(5)	-57(5)	-1(5)
C(2)	238(11)	167(8)	91(6)	-67(6)	49(7)	14(7)
C(4)	136(7)	88(5)	98(6)	36(4)	-62(5)	-34(5)
C(5)	89(6)	107(5)	49(4)	-31(4)	0(4)	-10(4)
C(6)	70(5)	98(5)	75(5)	-1(4)	-23(4)	13(4)
C(7)	76(5)	98(5)	58(5)	2(4)	-19(4)	-10(4)
C(8)	67(5)	93(5)	54(4)	-20(4)	-3(4)	-6(4)
C(9)	88(5)	71(4)	40(4)	-11(4)	1(4)	6(4)
C(10)	100(6)	54(4)	46(4)	8(3)	-1(4)	-7(4)
C(11)	128(7)	102(6)	61(5)	-29(4)	18(5)	7(5)
C(12)	153(7)	109(5)	47(4)	-13(4)	-31(4)	38(5)
C(13)	117(6)	64(4)	84(5)	-26(4)	4(5)	4(4)
C(15)	109(6)	108(6)	68(5)	-15(4)	36(4)	3(5)
C(16)	93(6)	115(6)	52(5)	10(4)	2(4)	13(4)

Table A1 continued.

C(17)	68(5)	82(4)	60(4)	-9(4)	13(4)	9(3)
C(18)	194(11)	290(13)	47(5)	38(6)	-13(6)	21(9)
C(19)	62(4)	47(3)	63(4)	-1(3)	12(3)	1(3)
C(20)	64(5)	68(4)	70(4)	24(3)	5(4)	-1(3)
C(21)	53(4)	63(4)	43(3)	1(3)	6(3)	6(3)
C(22)	73(5)	79(4)	91(5)	22(4)	-19(4)	-10(4)
C(23)	100(5)	59(4)	58(4)	-17(3)	8(4)	10(3)
C(24)	63(4)	61(4)	59(4)	5(3)	12(3)	-1(3)
C(25)	108(6)	70(4)	51(4)	-2(3)	28(4)	-7(4)
C(27)	72(5)	65(4)	53(4)	-4(3)	-4(4)	7(3)
C(28)	72(4)	54(3)	45(4)	-2(3)	-1(3)	6(3)
C(29)	92(5)	53(4)	57(4)	7(3)	-30(4)	-15(4)
C(30)	55(4)	52(3)	52(3)	-8(3)	6(3)	-1(3)
C(31)	53(4)	61(4)	54(4)	-1(3)	12(3)	-1(3)
C(32)	60(4)	71(4)	36(3)	-10(3)	1(3)	15(3)
C(33)	64(4)	57(4)	39(3)	1(3)	1(3)	-7(3)
C(34)	64(4)	42(3)	49(4)	-2(3)	1(3)	8(3)
C(35)	59(4)	46(3)	46(3)	-8(3)	5(3)	3(3)
C(36)	64(4)	56(3)	53(4)	-20(3)	10(3)	-7(3)
C(37)	47(4)	54(3)	40(3)	-2(3)	2(3)	7(3)
C(39)	65(4)	47(3)	56(4)	4(3)	4(3)	12(3)
C(40)	58(4)	54(3)	49(4)	-7(3)	3(3)	-3(3)
F(4)	387(13)	87(4)	379(14)	-55(6)	-164(11)	78(6)
F(1)	64(3)	196(5)	117(4)	33(3)	9(3)	16(3)
F(2)	78(3)	270(5)	63(3)	39(3)	6(2)	-52(3)
F(3)	123(4)	122(3)	205(6)	-37(4)	46(4)	-55(3)
C(41)	83(6)	91(5)	68(5)	8(4)	11(4)	-7(5)
C(3)	278(14)	95(7)	67(6)	-46(5)	-38(8)	112(8)
F(5)	391(12)	244(8)	132(5)	39(5)	84(6)	249(8)
F(6)	399(10)	191(5)	118(4)	-81(4)	-140(5)	230(6)

The anisotropic displacement factor exponent takes the form:
-2 pi^2 [h^2 a*^2 U11 + ... + 2 h k a* b* U12]

Table A1 continued.
Hydrogen coordinates (x 10^4) and isotropic displacement parameters ($Å^2$ x 10^3).

	x	y	z	U(eq)	Occ.
H(1A)	-5399(7)	1208(4)	937(4)	184	1
H(1B)	-4717(7)	573(4)	819(4)	184	1
H(1C)	-4265(7)	1180(4)	441(4)	184	1
H(2A)	1616(9)	-588(4)	517(4)	246	1
H(2B)	2762(9)	-164(4)	381(4)	246	1
H(2C)	1445(9)	44(4)	102(4)	246	1
H(4A)	4744(6)	17(3)	6736(3)	163	1
H(4B)	3651(6)	-449(3)	6836(3)	163	1
H(4C)	3662(6)	196(3)	7231(3)	163	1
H(5)	-2297(7)	696(3)	1166(3)	98	1
H(6)	-4929(6)	1659(3)	2061(4)	98	1
H(8)	-999(6)	893(3)	2146(3)	86	1
H(10)	1487(7)	101(2)	6495(3)	80	1
H(12A)	2132(7)	2241(3)	7187(3)	156	1
H(12B)	2666(7)	1604(3)	6928(3)	156	1
H(12C)	1331(7)	1634(3)	7221(3)	156	1
H(13)	1012(6)	-535(3)	1746(4)	106	1
H(15)	2376(6)	1004(3)	901(3)	113	1
H(17)	2138(5)	1514(3)	1961(3)	84	1
H(18A)	223(8)	2320(5)	352(4)	266	1
H(18B)	-296(8)	2962(5)	609(4)	266	1
H(18C)	-1188(8)	2394(5)	485(4)	266	1
H(19)	-3153(5)	463(2)	6117(3)	69	1
H(20)	3620(6)	980(2)	4666(3)	80	1
H(22)	4653(6)	506(3)	5608(4)	98	1
H(23)	714(6)	-23(3)	2815(3)	87	1
H(24)	436(5)	561(2)	5549(3)	73	1
H(25A)	-3806(6)	786(2)	7245(3)	114	1
H(25B)	-4204(6)	1489(2)	7255(3)	114	1
H(25C)	-2953(6)	1282(2)	7629(3)	114	1
H(27)	-3667(6)	1878(2)	3037(3)	76	1
H(30)	-1461(5)	2379(2)	5630(3)	63	1
H(35)	-2199(5)	617(2)	5045(3)	60	1

Table A1 continued.

H(36)	-2377(5)	2212(2)	6698(3)	69	1
H(39)	1916(5)	508(2)	3736(3)	67	1
H(40)	-2552(5)	1295(2)	3999(3)	64	1

Table A1 continued.

Torsion angles [°].

N(1) Rh(1) Rh(2) N(6)	86.2(2)
N(5) Rh(1) Rh(2) N(6)	-5.4(2)
O(3) Rh(1) Rh(2) N(6)	174.3(2)
O(2) Rh(1) Rh(2) N(6)	-93.7(2)
N(3) Rh(1) Rh(2) N(6)	-157.4(6)
N(1) Rh(1) Rh(2) N(2)	-5.6(2)
N(5) Rh(1) Rh(2) N(2)	-97.2(2)
O(3) Rh(1) Rh(2) N(2)	82.4(2)
O(2) Rh(1) Rh(2) N(2)	174.52(14)
N(3) Rh(1) Rh(2) N(2)	110.7(6)
N(1) Rh(1) Rh(2) O(1)	-94.1(2)
N(5) Rh(1) Rh(2) O(1)	174.3(2)
O(3) Rh(1) Rh(2) O(1)	-6.03(14)
O(2) Rh(1) Rh(2) O(1)	86.05(14)
N(3) Rh(1) Rh(2) O(1)	22.3(6)
N(1) Rh(1) Rh(2) O(4)	174.54(14)
N(5) Rh(1) Rh(2) O(4)	82.9(2)
O(3) Rh(1) Rh(2) O(4)	-97.40(13)
O(2) Rh(1) Rh(2) O(4)	-5.32(13)
N(3) Rh(1) Rh(2) O(4)	-69.1(6)
N(1) Rh(1) Rh(2) N(4)	-172.5(8)
N(5) Rh(1) Rh(2) N(4)	95.8(8)
O(3) Rh(1) Rh(2) N(4)	-84.5(8)
O(2) Rh(1) Rh(2) N(4)	7.6(8)
N(3) Rh(1) Rh(2) N(4)	-56.2(11)
N(6) Rh(2) O(1) C(28)	12(2)
N(2) Rh(2) O(1) C(28)	-79.5(4)
O(4) Rh(2) O(1) C(28)	95.6(4)
N(4) Rh(2) O(1) C(28)	-178.7(4)
Rh(1) Rh(2) O(1) C(28)	8.7(4)
N(1) Rh(1) O(2) C(31)	5(2)

Table A1 continued.

N(5) Rh(1) O(2) C(31)	-81.8(4)
O(3) Rh(1) O(2) C(31)	93.4(4)
N(3) Rh(1) O(2) C(31)	176.9(4)
Rh(2) Rh(1) O(2) C(31)	6.9(4)
N(1) Rh(1) O(3) C(28)	93.6(4)
N(5) Rh(1) O(3) C(28)	9(2)
O(2) Rh(1) O(3) C(28)	-81.8(4)
N(3) Rh(1) O(3) C(28)	-169.1(4)
Rh(2) Rh(1) O(3) C(28)	5.6(4)
N(6) Rh(2) O(4) C(31)	93.3(4)
N(2) Rh(2) O(4) C(31)	4(2)
O(1) Rh(2) O(4) C(31)	-81.5(4)
N(4) Rh(2) O(4) C(31)	-172.7(4)
Rh(1) Rh(2) O(4) C(31)	5.6(4)
N(5) Rh(1) N(1) C(40)	95.3(4)
O(3) Rh(1) N(1) C(40)	-79.9(4)
O(2) Rh(1) N(1) C(40)	8(2)
N(3) Rh(1) N(1) C(40)	-163.3(4)
Rh(2) Rh(1) N(1) C(40)	6.7(4)
N(5) Rh(1) N(1) C(33)	-96.2(4)
O(3) Rh(1) N(1) C(33)	88.6(4)
O(2) Rh(1) N(1) C(33)	177(27)
N(3) Rh(1) N(1) C(33)	5.3(4)
Rh(2) Rh(1) N(1) C(33)	175.3(4)
N(6) Rh(2) N(2) C(40)	-81.4(4)
O(1) Rh(2) N(2) C(40)	93.3(4)
O(4) Rh(2) N(2) C(40)	8(2)
N(4) Rh(2) N(2) C(40)	-175.7(4)
Rh(1) Rh(2) N(2) C(40)	6.1(4)
N(6) Rh(2) N(2) C(37)	95.4(4)
O(1) Rh(2) N(2) C(37)	-89.8(4)
O(4) Rh(2) N(2) C(37)	-175(2)
N(4) Rh(2) N(2) C(37)	1.2(4)
Rh(1) Rh(2) N(2) C(37)	-177.0(3)
N(1) Rh(1) N(3) C(16)	108(5)
N(5) Rh(1) N(3) C(16)	-159(5)
O(3) Rh(1) N(3) C(16)	21(5)
O(2) Rh(1) N(3) C(16)	-71(5)
Rh(2) Rh(1) N(3) C(16)	-8(6)

Table A1 continued.

N(6) Rh(2) N(4) C(9)	7(2)
N(2) Rh(2) N(4) C(9)	100(2)
O(1) Rh(2) N(4) C(9)	-172(2)
O(4) Rh(2) N(4) C(9)	-81(2)
Rh(1) Rh(2) N(4) C(9)	-94(2)
N(1) Rh(1) N(5) C(39)	-83.7(4)
O(3) Rh(1) N(5) C(39)	0(2)
O(2) Rh(1) N(5) C(39)	91.7(4)
N(3) Rh(1) N(5) C(39)	178.8(4)
Rh(2) Rh(1) N(5) C(39)	4.1(4)
N(1) Rh(1) N(5) C(32)	91.9(4)
O(3) Rh(1) N(5) C(32)	176(2)
O(2) Rh(1) N(5) C(32)	-92.8(4)
N(3) Rh(1) N(5) C(32)	-5.6(4)
Rh(2) Rh(1) N(5) C(32)	179.7(4)
N(2) Rh(2) N(6) C(39)	96.2(4)
O(1) Rh(2) N(6) C(39)	5(2)
O(4) Rh(2) N(6) C(39)	-78.8(4)
N(4) Rh(2) N(6) C(39)	-164.4(4)
Rh(1) Rh(2) N(6) C(39)	8.1(4)
N(2) Rh(2) N(6) C(34)	-104.3(4)
O(1) Rh(2) N(6) C(34)	164(2)
O(4) Rh(2) N(6) C(34)	80.7(4)
N(4) Rh(2) N(6) C(34)	-4.9(4)
Rh(1) Rh(2) N(6) C(34)	167.6(4)
C(8) C(5) C(7) C(6)	0.3(10)
C(8) C(5) C(7) C(1)	-179.5(6)
C(27) C(6) C(7) C(5)	0.1(10)
C(27) C(6) C(7) C(1)	179.9(6)
C(7) C(5) C(8) C(33)	-0.9(10)
Rh(2) N(4) C(9) C(12)	-17(23)
C(15) C(11) C(13) C(23)	1.7(12)
C(2) C(11) C(13) C(23)	179.8(7)
C(13) C(11) C(15) C(17)	-0.8(11)
C(2) C(11) C(15) C(17)	-178.9(7)
Rh(1) N(3) C(16) C(18)	-128(29)
C(11) C(15) C(17) C(32)	-0.9(11)
C(35) C(19) C(21) C(36)	1.0(8)

Table A1 continued.

C(35) C(19) C(21) C(25)	178.2(5)
C(34) C(20) C(22) C(29)	-2.2(10)
C(11) C(13) C(23) C(32)	-0.9(11)
C(29) C(10) C(24) C(34)	1.2(8)
C(7) C(6) C(27) C(33)	0.0(9)
Rh(1) O(3) C(28) O(1)	0.0(8)
Rh(1) O(3) C(28) C(3)	-177.2(7)
Rh(2) O(1) C(28) O(3)	-7.4(8)
Rh(2) O(1) C(28) C(3)	169.7(7)
C(24) C(10) C(29) C(22)	-2.4(9)
C(24) C(10) C(29) C(4)	179.1(5)
C(20) C(22) C(29) C(10)	2.9(9)
C(20) C(22) C(29) C(4)	-178.6(6)
Rh(1) O(2) C(31) O(4)	-4.8(8)
Rh(1) O(2) C(31) C(41)	173.8(4)
Rh(2) O(4) C(31) O(2)	-1.7(8)
Rh(2) O(4) C(31) C(41)	179.7(4)
C(13) C(23) C(32) C(17)	-0.9(9)
C(13) C(23) C(32) N(5)	176.9(5)
C(15) C(17) C(32) C(23)	1.8(9)
C(15) C(17) C(32) N(5)	-176.1(6)
C(39) N(5) C(32) C(23)	48.0(8)
Rh(1) N(5) C(32) C(23)	-127.6(5)
C(39) N(5) C(32) C(17)	-134.2(6)
Rh(1) N(5) C(32) C(17)	50.2(7)
C(6) C(27) C(33) C(8)	-0.5(8)
C(6) C(27) C(33) N(1)	179.6(5)
C(5) C(8) C(33) C(27)	0.9(8)
C(5) C(8) C(33) N(1)	-179.1(5)
C(40) N(1) C(33) C(27)	46.5(7)
Rh(1) N(1) C(33) C(27)	-122.2(5)
C(40) N(1) C(33) C(8)	-133.4(5)
Rh(1) N(1) C(33) C(8)	57.9(6)
C(22) C(20) C(34) C(24)	0.9(8)
C(22) C(20) C(34) N(6)	179.7(5)
C(10) C(24) C(34) C(20)	-0.4(8)
C(10) C(24) C(34) N(6)	-179.2(5)
C(39) N(6) C(34) C(20)	58.8(7)

Table A1 continued.

Rh(2) N(6) C(34) C(20)	-101.2(5)
C(39) N(6) C(34) C(24)	-122.4(5)
Rh(2) N(6) C(34) C(24)	77.5(5)
C(21) C(19) C(35) C(37)	-1.5(8)
C(37) C(30) C(36) C(21)	0.1(9)
C(19) C(21) C(36) C(30)	-0.4(8)
C(25) C(21) C(36) C(30)	-177.5(5)
C(19) C(35) C(37) C(30)	1.2(8)
C(19) C(35) C(37) N(2)	-179.6(5)
C(36) C(30) C(37) C(35)	-0.5(8)
C(36) C(30) C(37) N(2)	-179.7(5)
C(40) N(2) C(37) C(35)	50.5(7)
Rh(2) N(2) C(37) C(35)	-126.5(5)
C(40) N(2) C(37) C(30)	-130.3(5)
Rh(2) N(2) C(37) C(30)	52.7(6)
C(32) N(5) C(39) N(6)	-174.7(5)
Rh(1) N(5) C(39) N(6)	1.1(8)
C(34) N(6) C(39) N(5)	-168.2(5)
Rh(2) N(6) C(39) N(5)	-7.7(8)
C(37) N(2) C(40) N(1)	-179.8(4)
Rh(2) N(2) C(40) N(1)	-2.7(7)
C(33) N(1) C(40) N(2)	-173.0(5)
Rh(1) N(1) C(40) N(2)	-4.1(7)
O(2) C(31) C(41) F(2)	-3.8(9)
O(4) C(31) C(41) F(2)	175.0(6)
O(2) C(31) C(41) F(1)	-126.1(6)
O(4) C(31) C(41) F(1)	52.8(8)
O(2) C(31) C(41) F(3)	118.2(6)
O(4) C(31) C(41) F(3)	-63.0(8)
O(3) C(28) C(3) F(6)	1(2)
O(1) C(28) C(3) F(6)	-176.9(12)
O(3) C(28) C(3) F(5)	149.3(11)
O(1) C(28) C(3) F(5)	-28(2)
O(3) C(28) C(3) F(4)	-111.9(9)
O(1) C(28) C(3) F(4)	70.5(12)

Table A2. Positional Parameters and Equivalent Isotropic Thermal Parameters for $[Rh_2(DTolF)_2(9\text{-}EtAH)_2(CH_3CN)][BF_4]_2$ (4).

Identification code	$[Rh_2(DTolF)_2(9\text{-}EtAH)_2(CH_3CN)][BF_4]_2$
Empirical formula	C46 H48 B2 F8 N15 Rh2
Formula weight	1190.40 g/mol
Temperature	293(2) K
Wavelength	0.71073 Å
Crystal system	Monoclinic
Space group	$P2_1/c$
Unit cell dimensions	a = 15.648(8) Å
	b = 16.515(5) Å
	c = 20.026(8) Å
	$\alpha = 90^\circ$
	$\beta = 105.17(4)^\circ$
	$\gamma = 90^\circ$
Volume	4994(6) $Å^3$
Z	4
ρ_{calc}	1.583 g/cm^3
μ	0.740 cm^{-3}

Table A2 continued.

Crystal size	0.31 x 0.23 x 0.18mm^3
Theta range for data collection	1.90 to 22.50°.
Index ranges	$15 < 2\theta < 21°$
Reflections collected	7151
Independent reflections	6841 [R(int) = 0.119]
Refinement method	Full-matrix least-squares on F
Goodness-of-fit on F	1.30
Final R indices [$I>3\sigma(I)$]	$R_1 = 0.063$, $R_w = 0.073$
Largest diff. peak and hole	0.780 and -1.134 $e^-/Å^3$

Table A2. Positional Parameters and Equivalent Isotropic Thermal Parameters for $[Rh_2(DTolF)_2(9\text{-}EtAH)_2(CH_3CN)][BF_4]_2$ **(4)**.

atom	x	y	z	B_{eq}	
Rh(1)	0.7682(1)		0.1470(1)	0.1467(1)	2.52(5)
Rh(2)	0.7122(1)		0.2177(1)	0.2378(1)	2.60(5)
N(1)	0.872(1)	0.122(1)	0.230(1)	3.2(6)	
N(2)	0.662(1)	0.173(1)	0.0662(10)	3.2(6)	
N(3)	0.696(1)	0.050(1)	0.1685(8)	2.1(S)	
N(4)	0.833(1)	0.245(1)	0.128(1)	3.1(6)	
N(S)	0.806(1)	0.078(1)	0.074(1)	2.9(6)	
N(6)	0.641(1)	0.302(1)	0.173(1)	3.2(6)	
N(7)	0.609(1)	0.142(1)	0.2107(9)	3.0(S)	
N(8)	0.815(1)	0.296(1)	0.2712(10)	3.1(5)	
N(9)	0.781(1)	0.132(1)	0.303(1)	3.2(5)	
N(10)	0.930(2)	0.388(1)	0.267(1)	6.2(8)	
N(11)	0.991(2)	0.412(2)	0.174(2)	8(1)	
N(12)	0.928(2)	0.320(1)	0.081(1)	5.6(8)	
N(13)	0.542(1)	0.242(1)	-0.009(1)	4.3(7)	
N(14)	0.475(2)	0.361(2)	0.023(2)	6.5(9)	
N(15)	0.543(2)	0.400(2)	0.139(2)	6.0(8)	
C(1)	0.856(2)	0.104(1)	0.291(1)	3.3(7)	
C(2)	0.617(2)	0.069(2)	0.183(1)	3.7(8)	
C(3)	0.965(2)	0.123(1)	0.233(1)	2.5(6)	
C(4)	1.028(2)	0.142(2)	0.296(1)	4.4(6)	
C(S)	1.117(2)	0.125(2)	0.300(1)	4.5(6)	
C(6)	1.147(2)	0.099(2)	0.245(1)	4.3(6)	
C(7)	1.089(2)	0.091(1)	0.183(1)	3.3(5)	
C(8)	0.998(2)	0.102(1)	0.176(1)	3.4(5)	
C(9)	1.244(2)	0.076(2)	0.257(2)	6.8(8)	
C(10)	0.761(1)	0.100(1)	0.362(1)	3.1(7)	
C(11)	0.728(1)	0.155(2)	0.405(1)	3.3(5)	
C(12)	0.711(2)	0.125(1)	0.463(1)	3.7(6)	
C(13)	0.728(2)	0.043(2)	0.487(1)	3.6(6)	
C(14)	0.762(2)	-0.010(2)	0.444(1)	5.0(7)	
C(15)	0.776(2)	0.022(2)	0.381(1)	3.8(6)	
C(16)	0.714(2)	0.016(2)	0.555(1)	6.0(7)	
C(17)	0.521(2)	0.166(1)	0.205(1)	2.8(S)	
C(18)	0.449(1)	0.146(1)	0.150(1)	3.0(5)	

Table A2 continued.

C(19)	0.352(2)	0.237(2)	0.192(1)	4.6(6)
C(20)	0.424(2)	0.258(1)	0.246(1)	3.5(5)
C(21)	0.507(2)	0.223(2)	0.253(1)	3.7(5)
C(22)	0.260(2)	0.280(2)	0.180(1)	6.4(7)
C(23)	0.703(1)	-0.029(1)	0.139(1)	2.3(5)
C(24)	0.778(2)	-0.073(1)	0.169(1)	3.4(5)
C(25)	0.793(2)	-0.146(2)	0.140(1)	4.3(6)
C(26)	0.736(2)	-0.175(1)	0.083(1)	3.6(S)
C(27)	0.660(2)	-0.130(2)	0.054(1)	4.8(6)
C(28)	0.645(2)	-0.056(1)	0.083(1)	3.2(5)
C(29)	0.754(2)	-0.253(2)	0.047(1)	6.1(7)
C(30)	0.814(2)	0.037(2)	0.030(2)	3.8(8)
C(31)	0.828(2)	-0.020(2)	-0.028(2)	6.4(7)
C(32)	0.872(2)	0.329(2)	0.240(1)	4.0(9)
C(33)	0.985(2)	0.425(2)	0.232(3)	9(1)
C(34)	0.935(2)	0.353(2)	0.147(2)	5.6(9)
C(35)	0.876(2)	0.306(2)	0.172(2)	3.4(7)
C(36)	0.867(2)	0.255(1)	0.075(1)	3.6(7)
C(37)	0.969(3)	0.363(3)	0.021(2)	10(1)
C(38)	1.049(3)	0.340(2)	0.045(2)	9.6(9)
C(39)	0.607(2)	0.231(2)	0.058(2)	3.5(8)
C(40)	0.485(2)	0.306(2)	-0.021(2)	6(1)
C(41)	0.536(2)	0.352(2)	0.084(2)	5.2(9)
C(42)	0.599(2)	0.293(2)	0.105(2)	2.9(7)
C(43)	0.607(2)	0.370(2)	0.192(1)	3.9(8)
C(44)	0.472(3)	0.466(3)	0.151(2)	11(1)
C(45)	0.509(3)	0.530(3)	0.143(2)	13(1)
C(46)	0.365(2)	0.184(1)	0.146(1)	4.1(6)
B(1)	0.975(2)	0.148(3)	-0.055(2)	5(1)
B(2*)	0.615(5)	0.410(2)	0.384(3)	10(2)
F(1)	0.979(1)	0.079(1)	-0.0904(9)	8.0(6)
F(2)	1.004(1)	0.141(1)	0.0129(8)	7.8(6)
F(3)	1.018(1)	0.210(1)	-0.0819(10)	8.2(6)
F(4)	0.885(1)	0.172(1)	-0.0722(8)	7.5(6)
F(5*)	0.676(2)	0.376(2)	0.366(1)	17(1)
F(6*)	0.569(2)	0.339(2)	0.388(1)	16(1)

Table A2 continued.

F(7*)	0.566(2)	0.444(1)	0.327(1)	14.5(10)
F(8*)	0.623(1)	0.448(1)	0.4400(8)	7.3(5)

$B_{eq} = (8/3)\pi^2 (U_{11}(aa^*)^2 + U_{22}(bb^*)^2 + U_{33}(cc^*)^2 +$
$2U_{12}aa^*bb^*\cos\gamma) + 2U_{13}aa^*cc^* \cos\alpha) +$
$2U_{23}bb^*cc^* \cos\alpha)$

Table A3. Crystal data and structure refinement for $[Rh_2(DTolF)_2(9\text{-}EtGH)_2(CH_3CN)][BF_4]_2$ (7).

Identification code	$[Rh_2(DTolF)_2(9\text{-}EtGH)_2(CH_3CN)][BF_4]_2$
Empirical formula	C46 H53 B2 F8 N15 O2 Rh2
Formula weight	1227.47 g/mol
Temperature	293(2) K
Wavelength	0.71073 Å
Crystal system	Monoclinic
Space group	$P2_1/n$
Unit cell dimensions	a = 11.3612(9) A
	b = 20.803(2) Å
	c = 22.617(2) Å
	$\alpha = 90^\circ$
	$\beta = 100.021(2)^\circ$
	$\gamma = 90^\circ$
Volume	5264.0(7) $Å^3$
Z	4
ρ_{calc}	1.549 g/cm^3
μ	0.709 cm^{-3}

Table A3 continued.

F(000)	2488
Crystal size	0.10 x 0.08 x 0.06 mm^3
Theta range for data collection	1.83 to 28.34°
Index ranges	-14<=h<=13, -27<=k<=24, -29<=l<=19
Reflections collected	31002
Independent reflections	12287 [R(int) = 0.1480]
Refinement method	Full-matrix least-squares on F^2
Data / restraints / parameters	12287 / 95 / 694
Goodness-of-fit on F^2	0.974
Final R indices [$I>2\sigma(I)$]	R1 = 0.0898, wR2 = 0.1484
R indices (all data)	R1 = 0.2472, wR2 = 0.1994
Largest diff. Peak and hole	1.427 and –0.732 $e^-/Å^3$

Table A3 continued.

Atomic Coordinates and equivalent isotropic displacement parameters ($Å^2$).

	x	y	z	U(eq)	Occ.
Rh1	0.02424(6)	0.76234(3)	0.08567(3)	0.0246(2)	1
Rh2	0.15992(6)	0.76375(3)	0.18613(3)	0.0239(2)	1
C1	0.1673(12)	1.0115(5)	0.2533(5)	0.069(4)	1
C3	0.0325(9)	0.8907(5)	-0.0277(5)	0.048(3)	1
C4	-0.3092(10)	0.5224(5)	0.0468(5)	0.069(4)	1
C5	0.1972(13)	1.0390(5)	0.3633(5)	0.085(5)	1
C6	0.1965(9)	0.9919(5)	0.3112(5)	0.043(3)	1
C7	-0.1014(7)	0.8469(4)	0.1723(4)	0.024(2)	1
C8	0.2277(9)	0.9278(5)	0.3222(5)	0.045(3)	1
C9	0.0390(10)	0.9108(5)	-0.0858(5)	0.055(3)	1
C10	0.7688(8)	0.7180(5)	0.2723(5)	0.060(3)	1
C11	0.1433(12)	0.9322(5)	-0.1717(5)	0.075(4)	1
C12	0.1400(11)	0.9074(4)	-0.1079(5)	0.043(3)	1
C13	0.1633(9)	0.9681(4)	0.2051(5)	0.044(3)	1
C14	-0.1759(9)	0.7537(5)	-0.1144(4)	0.052(3)	1
C15	0.1953(8)	0.9031(4)	0.2157(4)	0.030(2)	1
C16	0.2394(10)	0.8806(5)	-0.0717(5)	0.054(3)	1
C17	-0.0605(8)	0.5527(4)	0.2441(4)	0.030(2)	1
C18	-0.1902(8)	0.8927(4)	0.1694(4)	0.028(2)	1
C19	-0.0485(8)	0.6449(4)	0.1599(4)	0.025(2)	1
C20	0.6221(9)	0.7356(5)	0.1773(5)	0.049(3)	1
C21	-0.1569(8)	0.9099(4)	0.2676(4)	0.029(2)	1
C22	0.1728(8)	0.8763(4)	0.1128(4)	0.029(2)	1
C23	-0.1400(8)	0.6009(4)	0.1588(4)	0.029(2)	1
C24	-0.3434(9)	0.9402(5)	0.0827(5)	0.046(3)	1
C25	0.5446(9)	0.7228(4)	0.2666(5)	0.042(3)	1
C26	0.2314(9)	0.8573(4)	-0.0139(5)	0.040(3)	1
C27	-0.1242(8)	0.7570(4)	-0.0518(5)	0.035(2)	1
C28	-0.3340(8)	0.5781(5)	0.0862(5)	0.045(3)	1
C29	0.4096(8)	0.7344(4)	0.1727(4)	0.034(2)	1
C30	0.6433(9)	0.7267(5)	0.2379(5)	0.039(3)	1

Table A3 continued.

C31	0.2597(8)	0.7060(4)	0.0895(4)	0.025(2)	1
C32	0.5054(9)	0.7397(5)	0.1434(5)	0.042(3)	1
C33	-0.1783(8)	0.6663(4)	0.0808(4)	0.035(3)	1
C34	-0.0399(8)	0.8275(4)	0.2280(4)	0.029(2)	1
C35	0.2288(8)	0.8849(4)	0.2751(4)	0.030(2)	1
C36	0.0503(8)	0.6393(4)	0.2060(4)	0.024(2)	1
C37	0.1289(8)	0.8629(4)	0.0087(4)	0.029(2)	1
C38	-0.1815(8)	0.8573(4)	0.0792(4)	0.029(2)	1
C39	0.4304(9)	0.7267(4)	0.2342(4)	0.038(3)	1
C40	0.1298(9)	0.6721(4)	0.0028(5)	0.034(2)	1
C41	0.0454(9)	0.6245(5)	-0.0091(6)	0.054(3)	1
C42	0.0175(10)	0.5972(6)	-0.0662(6)	0.063(4)	1
C43	0.1853(10)	0.6913(5)	-0.0423(5)	0.049(3)	1
C44	-0.4588(9)	0.9068(5)	0.0755(6)	0.073(4)	1
C45	0.1574(11)	0.6660(6)	-0.0999(5)	0.065(4)	1
C46	0.0719(12)	0.6192(6)	-0.1130(6)	0.069(4)	1
C47	0.0310(11)	0.5941(7)	-0.1770(6)	0.111(6)	1
O1	0.1464(5)	0.6702(2)	0.2154(3)	0.0243(14)	1
O2	0.0375(5)	0.7843(3)	0.2409(2)	0.0249(14)	1
N15	0.1844(6)	0.8569(3)	0.1686(3)	0.0278(18)	1
N14	0.1221(6)	0.8399(3)	0.0675(3)	0.0250(18)	1
N13	0.0366(6)	0.5923(3)	0.2478(3)	0.0259(18)	1
N12	-0.0981(6)	0.8249(3)	0.1135(3)	0.0261(18)	1
N11	-0.2398(6)	0.8994(3)	0.1093(3)	0.0286(19)	1
N10	-0.2225(6)	0.6148(3)	0.1089(3)	0.032(2)	1
N9	-0.0725(6)	0.8621(3)	0.2746(3)	0.0292(19)	1
N8	-0.0732(7)	0.6854(3)	0.1103(3)	0.0310(19)	1
N7	-0.1510(6)	0.5555(3)	0.1994(3)	0.0294(19)	1
N6	-0.0806(6)	0.7602(3)	-0.0027(3)	0.0282(18)	1
N5	0.2895(6)	0.7353(3)	0.1420(3)	0.0257(17)	1
N4	-0.2213(6)	0.9248(3)	0.2162(3)	0.0302(19)	1
N3	0.1497(6)	0.7030(3)	0.0599(3)	0.0247(18)	1
N2	-0.0593(7)	0.5102(3)	0.2888(3)	0.039(2)	1
N1	-0.1705(7)	0.9421(4)	0.3178(4)	0.047(2)	1
F1	-0.4381(7)	0.9417(4)	-0.0970(3)	0.114(3)	1
F2	-0.2489(8)	0.9717(4)	-0.0621(4)	0.110(3)	1
F3	-0.2932(6)	0.9088(3)	-0.1460(3)	0.0647(19)	1
F4	-0.3033(6)	0.8726(3)	-0.0539(3)	0.081(2)	1

Table A3 continued.

B1	-0.3236(12)	0.9246(6)	-0.0913(6)	0.039(3)	1
B2	0.0415(6)	0.8453(3)	0.4388(3)	0.035(3)	1
F5	0.0062(6)	0.8073(3)	0.3878(3)	0.064(2)	1
F6	0.0043(5)	0.9088(3)	0.4253(3)	0.058(2)	1
F7	0.1663(5)	0.8466(3)	0.4544(3)	0.053(2)	1
F8	-0.0067(6)	0.8240(4)	0.4874(3)	0.071(3)	1
B2B	0.013(2)	0.8001(12)	0.4346(10)	0.035(3)	1
F5B	-0.050(3)	0.8511(13)	0.4041(14)	0.064(2)	1
F6B	0.013(3)	0.7480(13)	0.3953(15)	0.058(2)	1
F7B	0.130(2)	0.8194(15)	0.4561(16)	0.053(2)	1
F8B	-0.041(4)	0.781(2)	0.4826(15)	0.33(8)	1

Table A3 continued.

Bond lengths [Å] and angles [°].

Rh1-N14	2.042(7)
Rh1-N3	2.046(7)
Rh1-N8	2.076(7)
Rh1-N12	2.080(7)
Rh1-N6	2.142(8)
Rh1-Rh2	2.5140(10)
Rh2-N5	2.006(7)
Rh2-N15	2.007(7)
Rh2-O2	2.062(6)
Rh2-O1	2.070(5)
C1-C6	1.356(14)
C1-C13	1.410(13)
C3-C37	1.378(12)
C3-C9	1.394(13)
C4-C28	1.518(14)
C5-C6	1.532(14)
C6-C8	1.390(13)
C7-C18	1.381(11)
C7-C34	1.389(12)
C7-N12	1.412(11)
C8-C35	1.392(12)
C9-C12	1.331(13)
C10-C30	1.512(12)
C11-C12	1.539(13)
C12-C16	1.391(14)
C13-C15	1.410(11)
C14-C27	1.438(13)
C15-C35	1.383(12)
C15-N15	1.424(11)
C16-C26	1.413(13)
C17-N7	1.312(11)
C17-N2	1.341(10)
C17-N13	1.366(10)
C18-N4	1.349(10)

Table A3 continued.

C18-N11	1.386(10)
C19-C23	1.382(11)
C19-N8	1.392(11)
C19-C36	1.398(12)
C20-C30	1.361(13)
C20-C32	1.415(13)
C21-N4	1.299(11)
C21-N1	1.349(11)
C21-N9	1.372(10)
C22-N15	1.309(11)
C22-N14	1.323(10)
C23-N7	1.339(10)
C23-N10	1.366(10)
C24-C44	1.468(13)
C24-N11	1.491(10)
C25-C39	1.377(12)
C25-C30	1.393(12)
C26-C37	1.355(12)
C27-N6	1.135(11)
C28-N10	1.492(10)
C29-C32	1.373(12)
C29-C39	1.379(12)
C29-N5	1.419(11)
C31-N3	1.312(10)
C31-N5	1.326(10)
C33-N8	1.324(10)
C33-N10	1.383(10)
C34-O2	1.256(10)
C34-N9	1.378(10)
C36-O1	1.252(9)
C36-N13	1.388(10)
C37-N14	1.428(11)
C38-N12	1.303(10)
C38-N11	1.351(10)
C40-C43	1.351(13)
C40-C41	1.372(13)
C40-N3	1.425(11)
C41-C42	1.397(15)

Table A3 continued.

C42-C46	1.393(17)
C43-C45	1.388(14)
C45-C46	1.372(16)
C46-C47	1.533(15)
B1-F1	1.333(13)
B1-F2	1.385(13)
B1-F3	1.380(13)
B1-F4	1.369(13)
B2-F8	1.383(7)
B2-F5	1.398(7)
B2-F7	1.400(7)
B2-F6	1.404(7)
B2B-F7B	1.395(8)
B2B-F5B	1.395(7)
B2B-F8B	1.396(8)
B2B-F6B	1.402(8)
N14-Rh1-N3	89.3(3)
N14-Rh1-N8	176.1(3)
N3-Rh1-N8	92.4(3)
N14-Rh1-N12	89.0(3)
N3-Rh1-N12	177.8(3)
N8-Rh1-N12	89.2(3)
N14-Rh1-N6	93.5(3)
N3-Rh1-N6	91.3(3)
N8-Rh1-N6	89.9(3)
N12-Rh1-N6	90.2(3)
N14-Rh1-Rh2	84.4(2)
N3-Rh1-Rh2	85.2(2)
N8-Rh1-Rh2	92.2(2)
N12-Rh1-Rh2	93.2(2)
N6-Rh1-Rh2	176.0(2)
N5-Rh2-N15	92.8(3)
N5-Rh2-O2	171.9(2)
N15-Rh2-O2	92.8(3)
N5-Rh2-O1	89.0(3)
N15-Rh2-O1	172.6(3)
O2-Rh2-O1	84.7(2)
N5-Rh2-Rh1	86.3(2)

Table A3 continued.

N15-Rh2-Rh1	85.2(2)
O2-Rh2-Rh1	100.00(16)
O1-Rh2-Rh1	102.10(16)
C6-C1-C13	121.6(10)
C37-C3-C9	121.5(10)
C1-C6-C8	118.2(10)
C1-C6-C5	121.2(10)
C8-C6-C5	120.5(10)
C18-C7-C34	119.4(9)
C18-C7-N12	108.6(8)
C34-C7-N12	131.9(8)
C6-C8-C35	120.9(10)
C12-C9-C3	121.9(11)
C9-C12-C16	117.8(10)
C9-C12-C11	119.8(11)
C16-C12-C11	122.4(11)
C1-C13-C15	120.6(10)
C35-C15-C13	116.6(9)
C35-C15-N15	121.0(8)
C13-C15-N15	122.2(8)
C12-C16-C26	120.3(11)
N7-C17-N2	120.9(8)
N7-C17-N13	122.5(8)
N2-C17-N13	116.7(8)
N4-C18-C7	126.4(8)
N4-C18-N11	127.1(8)
C7-C18-N11	106.5(8)
C23-C19-N8	109.9(8)
C23-C19-C36	117.6(8)
N8-C19-C36	132.4(8)
C30-C20-C32	122.5(9)
N4-C21-N1	120.4(8)
N4-C21-N9	123.3(8)
N1-C21-N9	116.3(8)
N15-C22-N14	121.8(8)
N7-C23-N10	125.7(8)
N7-C23-C19	127.9(8)
N10-C23-C19	106.3(8)

Table A3 continued.

C44-C24-N11	113.6(8)
C39-C25-C30	120.6(10)
C37-C26-C16	121.2(10)
N6-C27-C14	178.1(11)
N10-C28-C4	111.1(8)
C32-C29-C39	119.0(9)
C32-C29-N5	122.6(9)
C39-C29-N5	118.4(8)
C20-C30-C25	117.5(10)
C20-C30-C10	121.3(9)
C25-C30-C10	121.1(10)
N3-C31-N5	123.5(8)
C29-C32-C20	118.7(10)
N8-C33-N10	111.7(8)
O2-C34-N9	117.7(8)
O2-C34-C7	129.8(8)
N9-C34-C7	112.5(8)
C15-C35-C8	122.0(9)
O1-C36-N13	116.4(8)
O1-C36-C19	130.3(8)
N13-C36-C19	113.3(8)
C26-C37-C3	117.2(9)
C26-C37-N14	120.7(9)
C3-C37-N14	122.0(9)
N12-C38-N11	113.9(8)
C25-C39-C29	121.6(9)
C43-C40-C41	117.9(10)
C43-C40-N3	122.0(9)
C41-C40-N3	119.9(10)
C40-C41-C42	120.9(12)
C46-C42-C41	120.7(12)
C40-C43-C45	122.4(11)
C46-C45-C43	120.7(13)
C45-C46-C42	117.4(12)
C45-C46-C47	122.2(14)
C42-C46-C47	120.3(13)
C36-O1-Rh2	122.6(5)
C34-O2-Rh2	121.8(6)

Table A3 continued.

C22-N15-C15	119.6(7)
C22-N15-Rh2	119.6(6)
C15-N15-Rh2	120.0(6)
C22-N14-C37	116.3(7)
C22-N14-Rh1	118.3(6)
C37-N14-Rh1	124.9(6)
C17-N13-C36	124.6(8)
C38-N12-C7	104.9(7)
C38-N12-Rh1	126.7(6)
C7-N12-Rh1	128.1(6)
C38-N11-C18	106.1(7)
C38-N11-C24	126.0(8)
C18-N11-C24	127.7(8)
C23-N10-C33	106.9(8)
C23-N10-C28	126.5(8)
C33-N10-C28	126.4(8)
C21-N9-C34	124.5(8)
C33-N8-C19	105.1(7)
C33-N8-Rh1	125.0(6)
C19-N8-Rh1	129.8(6)
C17-N7-C23	113.9(7)
C27-N6-Rh1	172.0(8)
C31-N5-C29	120.4(8)
C31-N5-Rh2	119.1(6)
C29-N5-Rh2	119.1(6)
C21-N4-C18	113.6(7)
C31-N3-C40	118.1(8)
C31-N3-Rh1	118.3(6)
C40-N3-Rh1	121.5(6)
F1-B1-F4	109.1(11)
F1-B1-F3	111.6(10)
F4-B1-F3	108.9(9)
F1-B1-F2	111.4(10)
F4-B1-F2	103.9(9)
F3-B1-F2	111.5(11)
F8-B2-F5	112.2(5)
F8-B2-F7	109.2(5)
F5-B2-F7	110.6(5)

Table A3 continued.

F8-B2-F6	109.1(5)
F5-B2-F6	108.7(5)
F7-B2-F6	106.9(5)
F7B-B2B-F5B	109.6(6)
F7B-B2B-F8B	109.4(6)
F5B-B2B-F8B	109.5(6)
F7B-B2B-F6B	109.7(6)
F5B-B2B-F6B	109.4(6)
F8B-B2B-F6B	109.2(6)

Table A3 continued.

Anisotropic displacement parameters ($Å^2$).

Rh1	0.0304(4)	0.0215(4)	0.0217(4)	0.0010(4)	0.0041(3)	0.0019(4)
Rh2	0.0267(4)	0.0211(4)	0.0235(4)	0.0011(4)	0.0033(3)	0.0006(4)
C1	0.141(13)	0.020(6)	0.049(8)	-0.004(6)	0.021(8)	-0.003(7)
C3	0.045(7)	0.066(8)	0.037(7)	0.024(6)	0.016(6)	0.000(6)
C4	0.086(10)	0.048(7)	0.067(9)	-0.010(7)	-0.004(8)	-0.033(7)
C5	0.155(14)	0.048(8)	0.056(9)	-0.025(7)	0.027(9)	-0.018(8)
C6	0.055(7)	0.036(6)	0.037(7)	-0.005(5)	0.006(6)	-0.014(5)
C7	0.024(5)	0.020(5)	0.028(6)	0.002(4)	0.005(4)	0.010(4)
C8	0.063(8)	0.042(7)	0.029(6)	0.000(5)	0.006(6)	-0.003(6)
C9	0.042(7)	0.083(9)	0.044(8)	0.036(7)	0.015(6)	0.003(6)
C10	0.019(6)	0.092(9)	0.064(8)	-0.009(7)	-0.008(6)	0.000(5)
C11	0.126(12)	0.058(8)	0.044(8)	0.010(7)	0.023(8)	-0.019(8)
C12	0.070(9)	0.029(6)	0.028(6)	0.000(5)	0.004(6)	-0.016(6)
C13	0.069(8)	0.027(6)	0.034(7)	0.001(5)	0.005(6)	0.002(5)
C14	0.066(8)	0.059(8)	0.029(6)	-0.010(5)	0.000(6)	0.004(6)
C15	0.036(6)	0.019(5)	0.032(6)	0.004(5)	0.003(5)	0.000(4)
C16	0.055(8)	0.065(8)	0.042(7)	0.003(6)	0.013(6)	0.000(6)
C17	0.032(6)	0.020(5)	0.038(6)	0.000(5)	0.005(5)	0.000(4)
C18	0.041(6)	0.023(5)	0.018(5)	-0.004(4)	-0.001(5)	-0.001(4)
C19	0.022(5)	0.027(5)	0.026(6)	-0.004(4)	0.003(4)	0.000(4)
C20	0.042(7)	0.051(6)	0.060(8)	-0.007(7)	0.027(6)	-0.011(6)
C21	0.026(6)	0.036(6)	0.026(6)	-0.005(5)	0.003(5)	0.009(4)
C22	0.036(6)	0.021(5)	0.034(6)	0.000(5)	0.014(5)	-0.002(4)
C23	0.023(5)	0.032(6)	0.026(6)	0.000(5)	-0.012(5)	-0.001(4)
C24	0.063(8)	0.036(6)	0.036(7)	0.003(5)	0.001(6)	0.018(6)
C25	0.046(7)	0.038(7)	0.044(7)	0.008(5)	0.012(6)	0.008(5)
C26	0.042(7)	0.040(6)	0.036(7)	0.008(5)	-0.001(6)	-0.005(5)
C27	0.036(6)	0.031(6)	0.039(6)	-0.003(6)	0.005(5)	0.008(5)
C28	0.025(6)	0.062(8)	0.041(7)	0.017(6)	-0.014(5)	-0.022(5)
C29	0.029(6)	0.027(5)	0.048(7)	0.001(6)	0.012(5)	0.003(5)
C30	0.036(6)	0.041(7)	0.041(7)	0.000(6)	0.011(5)	-0.005(5)
C31	0.025(5)	0.020(5)	0.032(6)	0.002(5)	0.005(5)	0.004(4)
C32	0.041(6)	0.047(6)	0.040(6)	0.001(6)	0.011(5)	-0.013(5)
C33	0.037(7)	0.033(6)	0.032(6)	0.012(5)	-0.001(5)	0.004(5)
C34	0.038(6)	0.033(6)	0.018(5)	-0.006(5)	0.008(5)	-0.008(5)
C35	0.036(6)	0.029(5)	0.021(5)	-0.007(5)	-0.003(5)	-0.004(4)

Table A3 continued.

C36	0.020(5)	0.024(5)	0.026(6)	0.001(4)	0.001(4)	-0.005(4)
C37	0.027(6)	0.032(6)	0.030(6)	0.005(5)	0.008(5)	-0.008(4)
C38	0.033(6)	0.038(6)	0.012(5)	0.000(5)	-0.004(5)	0.011(5)
C39	0.036(6)	0.051(7)	0.031(6)	0.001(6)	0.015(5)	0.005(5)
C40	0.040(7)	0.028(6)	0.035(7)	-0.010(5)	0.009(5)	0.010(5)
C41	0.036(7)	0.063(8)	0.061(9)	-0.014(7)	0.000(6)	0.013(6)
C42	0.040(8)	0.072(9)	0.075(10)	-0.032(8)	0.004(7)	0.000(6)
C43	0.072(8)	0.044(7)	0.035(7)	-0.016(6)	0.021(6)	0.001(6)
C44	0.033(7)	0.062(8)	0.109(12)	-0.005(8)	-0.026(7)	0.005(6)
C45	0.088(10)	0.065(9)	0.040(8)	-0.012(7)	0.007(7)	0.026(8)
C46	0.059(9)	0.076(10)	0.065(10)	-0.042(8)	-0.004(8)	0.022(7)
C47	0.066(10)	0.185(16)	0.072(10)	-0.083(11)	-0.016(8)	0.047(10)
O1	0.023(3)	0.021(3)	0.028(4)	0.008(3)	0.002(3)	0.001(3)
O2	0.029(4)	0.028(3)	0.017(3)	0.004(3)	0.003(3)	0.006(3)
N15	0.035(5)	0.027(4)	0.023(5)	0.003(4)	0.007(4)	0.004(3)
N14	0.026(4)	0.029(4)	0.020(4)	0.002(4)	0.005(4)	0.002(3)
N13	0.037(5)	0.025(4)	0.014(4)	0.006(3)	0.000(4)	-0.010(4)
N12	0.026(4)	0.033(5)	0.017(4)	-0.004(4)	-0.002(4)	0.003(3)
N11	0.030(5)	0.030(5)	0.023(5)	0.001(4)	-0.004(4)	0.006(4)
N10	0.030(5)	0.033(5)	0.030(5)	0.012(4)	-0.001(4)	-0.006(4)
N9	0.028(5)	0.038(5)	0.018(4)	-0.001(4)	-0.006(4)	0.008(4)
N8	0.032(5)	0.028(4)	0.031(5)	0.006(4)	0.000(4)	-0.002(4)
N7	0.025(5)	0.030(5)	0.030(5)	0.009(4)	-0.006(4)	-0.017(3)
N6	0.037(5)	0.022(4)	0.026(4)	0.001(4)	0.006(4)	0.004(4)
N5	0.029(4)	0.023(4)	0.026(4)	0.011(4)	0.008(3)	0.004(4)
N4	0.028(5)	0.032(4)	0.027(5)	0.003(4)	-0.004(4)	0.015(4)
N3	0.030(5)	0.016(4)	0.028(5)	0.000(4)	0.003(4)	0.000(3)
N2	0.046(5)	0.039(5)	0.028(5)	0.013(4)	-0.003(4)	-0.017(4)
N1	0.057(6)	0.049(5)	0.033(5)	-0.001(5)	0.001(5)	0.031(5)
F1	0.079(6)	0.201(9)	0.059(5)	0.008(6)	0.003(4)	0.068(6)
F2	0.147(8)	0.099(6)	0.082(6)	-0.026(5)	0.017(6)	-0.034(6)
F3	0.073(5)	0.090(5)	0.027(4)	0.001(4)	-0.005(3)	-0.001(4)
F4	0.103(6)	0.084(5)	0.051(5)	0.014(4)	-0.002(4)	0.030(4)
B1	0.050(9)	0.031(7)	0.031(8)	-0.009(6)	-0.008(7)	0.011(6)
F5	0.091(6)	0.061(6)	0.031(4)	0.001(4)	-0.019(4)	0.016(4)
F6	0.052(5)	0.063(5)	0.050(5)	-0.020(4)	-0.014(4)	0.018(4)
F7	0.045(5)	0.060(6)	0.047(4)	-0.007(4)	-0.013(4)	-0.009(4)
F8	0.063(6)	0.099(7)	0.047(5)	-0.005(5)	-0.001(5)	-0.033(5)

Table A3 continued.

F5B	0.091(6)	0.061(6)	0.031(4)	0.001(4)	-0.019(4)	0.016(4)
F6B	0.052(5)	0.063(5)	0.050(5)	-0.020(4)	-0.014(4)	0.018(4)
F7B	0.045(5)	0.060(6)	0.047(4)	-0.007(4)	-0.013(4)	-0.009(4)
F8B	0.06(4)	0.55(16)	0.40(13)	0.42(13)	0.08(6)	0.02(7)

Table A3 continued.

Hydrogen coordinates and isotropic displacement parameters ($Å^2$).

	x	y	z	U(eq)	Occ.
H1A	0.1495	1.0545	0.2452	0.083	1
H3A	-0.0386	0.8961	-0.0131	0.058	1
H4A	-0.3821	0.4995	0.0329	0.103	1
H4B	-0.2520	0.4939	0.0695	0.103	1
H4C	-0.2779	0.5387	0.0129	0.103	1
H5A	0.1745	1.0809	0.3477	0.128	1
H5B	0.2759	1.0408	0.3870	0.128	1
H5C	0.1415	1.0247	0.3879	0.128	1
H8A	0.2481	0.9135	0.3616	0.054	1
H9A	-0.0292	0.9272	-0.1098	0.066	1
H10A	0.8250	0.7223	0.2454	0.091	1
H10B	0.7763	0.6760	0.2903	0.091	1
H10C	0.7848	0.7501	0.3032	0.091	1
H11A	0.0663	0.9489	-0.1889	0.113	1
H11B	0.1637	0.8975	-0.1960	0.113	1
H11C	0.2021	0.9656	-0.1699	0.113	1
H13A	0.1393	0.9824	0.1659	0.053	1
H14A	-0.1330	0.7818	-0.1368	0.079	1
H14B	-0.2581	0.7668	-0.1198	0.079	1
H14C	-0.1712	0.7104	-0.1284	0.079	1
H16A	0.3116	0.8780	-0.0857	0.064	1
H20A	0.6870	0.7392	0.1575	0.058	1
H22A	0.2011	0.9168	0.1048	0.035	1
H24A	-0.3463	0.9776	0.1081	0.055	1
H24B	-0.3309	0.9554	0.0437	0.055	1
H25A	0.5559	0.7176	0.3081	0.051	1
H26A	0.2975	0.8378	0.0091	0.048	1
H28A	-0.3926	0.6066	0.0634	0.054	1
H28B	-0.3672	0.5617	0.1200	0.054	1
H31A	0.3199	0.6865	0.0728	0.030	1

Table A3 continued.

H32A	0.4937	0.7458	0.1021	0.051	1
H33A	-0.2176	0.6851	0.0456	0.042	1
H35A	0.2528	0.8427	0.2838	0.035	1
H38A	-0.1994	0.8518	0.0378	0.035	1
H39A	0.3657	0.7240	0.2543	0.046	1
H41A	0.0062	0.6103	0.0213	0.065	1
H42A	-0.0380	0.5639	-0.0730	0.076	1
H43A	0.2444	0.7226	-0.0346	0.058	1
H44A	-0.5213	0.9355	0.0579	0.109	1
H44B	-0.4733	0.8929	0.1141	0.109	1
H44C	-0.4572	0.8701	0.0499	0.109	1
H45A	0.1971	0.6810	-0.1298	0.078	1
H47A	0.0775	0.6141	-0.2036	0.167	1
H47B	-0.0520	0.6041	-0.1900	0.167	1
H47C	0.0419	0.5483	-0.1777	0.167	1
H13B	0.0931	0.5877	0.2781	0.031	1
H9B	-0.0375	0.8530	0.3104	0.035	1
H7A	-0.2118	0.5304	0.1964	0.035	1
H4D	-0.2784	0.9524	0.2123	0.036	1
H2A	-0.1184	0.4843	0.2883	0.047	1
H2B	0.0005	0.5089	0.3178	0.047	1
H1B	-0.2221	0.9726	0.3158	0.057	1
H1C	-0.1276	0.9321	0.3517	0.057	1

Table A3 continued.

N14	Rh1	Rh2	N5	-69.6(3)
N3	Rh1	Rh2	N5	20.2(3)
N8	Rh1	Rh2	N5	112.4(3)
N12	Rh1	Rh2	N5	-158.3(3)
N6	Rh1	Rh2	N5	-10(3)
N14	Rh1	Rh2	N15	23.5(3)
N3	Rh1	Rh2	N15	113.2(3)
N8	Rh1	Rh2	N15	-154.5(3)
N12	Rh1	Rh2	N15	-65.2(3)
N6	Rh1	Rh2	N15	83(3)
N14	Rh1	Rh2	O2	115.5(2)
N3	Rh1	Rh2	O2	-154.7(2)
N8	Rh1	Rh2	O2	-62.5(3)
N12	Rh1	Rh2	O2	26.8(2)
N6	Rh1	Rh2	O2	175(3)
N14	Rh1	Rh2	O1	-157.8(3)
N3	Rh1	Rh2	O1	-68.0(2)
N8	Rh1	Rh2	O1	24.2(3)
N12	Rh1	Rh2	O1	113.5(3)
N6	Rh1	Rh2	O1	-98(3)
C13	C1	C6	C8	2.7(19)
C13	C1	C6	C5	-178.2(11)
C1	C6	C8	C35	-0.1(16)
C5	C6	C8	C35	-179.2(10)
C37	C3	C9	C12	-3.6(18)
C3	C9	C12	C16	2.2(17)
C3	C9	C12	C11	-178.1(10)
C6	C1	C13	C15	-3.1(19)
C1	C13	C15	C35	0.7(15)
C1	C13	C15	N15	175.5(10)
C9	C12	C16	C26	0.9(16)
C11	C12	C16	C26	-178.7(9)
C34	C7	C18	N4	3.9(14)
N12	C7	C18	N4	179.6(8)
C34	C7	C18	N11	-176.4(8)
N12	C7	C18	N11	-0.8(10)
N8	C19	C23	N7	-177.8(9)
C36	C19	C23	N7	5.4(14)

Table A3 continued.

N8	C19	C23	N10	-0.9(10)
C36	C19	C23	N10	-177.7(8)
C12	C16	C26	C37	-2.9(16)
C32	C20	C30	C25	-1.4(16)
C32	C20	C30	C10	175.8(9)
C39	C25	C30	C20	1.4(15)
C39	C25	C30	C10	-175.8(9)
C39	C29	C32	C20	1.3(15)
N5	C29	C32	C20	-177.3(8)
C30	C20	C32	C29	0.0(16)
C18	C7	C34	O2	174.9(9)
N12	C7	C34	O2	0.4(17)
C18	C7	C34	N9	-4.5(12)
N12	C7	C34	N9	-179.0(9)
C13	C15	C35	C8	1.9(14)
N15	C15	C35	C8	-173.0(9)
C6	C8	C35	C15	-2.3(15)
C23	C19	C36	O1	175.7(9)
N8	C19	C36	O1	-0.2(17)
C23	C19	C36	N13	-5.1(12)
N8	C19	C36	N13	179.0(8)
C16	C26	C37	C3	1.6(15)
C16	C26	C37	N14	-179.2(9)
C9	C3	C37	C26	1.5(15)
C9	C3	C37	N14	-177.7(9)
C30	C25	C39	C29	0.0(15)
C32	C29	C39	C25	-1.3(15)
N5	C29	C39	C25	177.4(8)
C43	C40	C41	C42	-0.3(15)
N3	C40	C41	C42	174.8(9)
C40	C41	C42	C46	-2.2(17)
C41	C40	C43	C45	1.9(16)
N3	C40	C43	C45	-173.1(9)
C40	C43	C45	C46	-0.8(18)
C43	C45	C46	C42	-1.7(18)
C43	C45	C46	C47	174.7(11)
C41	C42	C46	C45	3.2(18)
C41	C42	C46	C47	-173.3(11)

Table A3 continued.

N13	C36	O1	Rh2	-151.7(6)
C19	C36	O1	Rh2	27.5(13)
N5	Rh2	O1	C36	-123.8(7)
N15	Rh2	O1	C36	132.4(19)
O2	Rh2	O1	C36	61.3(7)
Rh1	Rh2	O1	C36	-37.8(7)
N9	C34	O2	Rh2	-145.7(6)
C7	C34	O2	Rh2	34.9(13)
N5	Rh2	O2	C34	174.0(17)
N15	Rh2	O2	C34	40.3(7)
O1	Rh2	O2	C34	-146.8(6)
Rh1	Rh2	O2	C34	-45.4(6)
N14	C22	N15	C15	-156.0(8)
N14	C22	N15	Rh2	14.1(12)
C35	C15	N15	C22	-168.3(9)
C13	C15	N15	C22	17.1(13)
C35	C15	N15	Rh2	21.6(11)
C13	C15	N15	Rh2	-153.0(7)
N5	Rh2	N15	C22	58.6(7)
O2	Rh2	N15	C22	-127.3(7)
O1	Rh2	N15	C22	162.2(17)
Rh1	Rh2	N15	C22	-27.4(7)
N5	Rh2	N15	C15	-131.3(7)
O2	Rh2	N15	C15	42.9(6)
O1	Rh2	N15	C15	-28(2)
Rh1	Rh2	N15	C15	142.7(6)
N15	C22	N14	C37	-172.1(8)
N15	C22	N14	Rh1	15.2(11)
C26	C37	N14	C22	77.1(11)
C3	C37	N14	C22	-103.7(10)
C26	C37	N14	Rh1	-110.7(9)
C3	C37	N14	Rh1	68.5(11)
N3	Rh1	N14	C22	-112.8(7)
N8	Rh1	N14	C22	3(4)
N12	Rh1	N14	C22	65.8(6)
N6	Rh1	N14	C22	155.9(6)
Rh2	Rh1	N14	C22	-27.5(6)
N3	Rh1	N14	C37	75.2(7)

Table A3 continued.

N8	Rh1	N14	C37	-169(4)
N12	Rh1	N14	C37	-106.3(7)
N6	Rh1	N14	C37	-16.1(7)
Rh2	Rh1	N14	C37	160.4(7)
N7	C17	N13	C36	0.6(14)
N2	C17	N13	C36	-179.5(8)
O1	C36	N13	C17	-178.1(8)
C19	C36	N13	C17	2.6(12)
N11	C38	N12	C7	0.6(10)
N11	C38	N12	Rh1	-173.4(6)
C18	C7	N12	C38	0.1(10)
C34	C7	N12	C38	175.1(9)
C18	C7	N12	Rh1	174.0(6)
C34	C7	N12	Rh1	-11.1(14)
N14	Rh1	N12	C38	79.0(8)
N3	Rh1	N12	C38	120(7)
N8	Rh1	N12	C38	-104.4(8)
N6	Rh1	N12	C38	-14.5(8)
Rh2	Rh1	N12	C38	163.4(7)
N14	Rh1	N12	C7	-93.6(7)
N3	Rh1	N12	C7	-53(8)
N8	Rh1	N12	C7	82.9(7)
N6	Rh1	N12	C7	172.9(7)
Rh2	Rh1	N12	C7	-9.2(7)
N12	C38	N11	C18	-1.1(11)
N12	C38	N11	C24	-176.5(8)
N4	C18	N11	C38	-179.3(9)
C7	C18	N11	C38	1.1(10)
N4	C18	N11	C24	-4.0(15)
C7	C18	N11	C24	176.4(8)
C44	C24	N11	C38	82.8(12)
C44	C24	N11	C18	-91.5(12)
N7	C23	N10	C33	177.6(9)
C19	C23	N10	C33	0.6(10)
N7	C23	N10	C28	-7.0(15)
C19	C23	N10	C28	176.0(9)
N8	C33	N10	C23	-0.1(11)
N8	C33	N10	C28	-175.5(9)

Table A3 continued.

C4	C28	N10	C23	-85.4(12)
C4	C28	N10	C33	89.1(11)
N4	C21	N9	C34	5.0(14)
N1	C21	N9	C34	-174.9(8)
O2	C34	N9	C21	-178.9(8)
C7	C34	N9	C21	0.6(13)
N10	C33	N8	C19	-0.5(10)
N10	C33	N8	Rh1	-178.5(6)
C23	C19	N8	C33	0.8(10)
C36	C19	N8	C33	177.0(9)
C23	C19	N8	Rh1	178.7(6)
C36	C19	N8	Rh1	-5.1(15)
N14	Rh1	N8	C33	135(4)
N3	Rh1	N8	C33	-108.8(8)
N12	Rh1	N8	C33	72.7(8)
N6	Rh1	N8	C33	-17.5(8)
Rh2	Rh1	N8	C33	165.9(7)
N14	Rh1	N8	C19	-42(4)
N3	Rh1	N8	C19	73.7(8)
N12	Rh1	N8	C19	-104.7(8)
N6	Rh1	N8	C19	165.0(8)
Rh2	Rh1	N8	C19	-11.6(7)
N2	C17	N7	C23	179.0(8)
N13	C17	N7	C23	-1.1(13)
N10	C23	N7	C17	-178.4(9)
C19	C23	N7	C17	-2.0(14)
C14	C27	N6	Rh1	-36(39)
N14	Rh1	N6	C27	68(6)
N3	Rh1	N6	C27	-21(6)
N8	Rh1	N6	C27	-114(6)
N12	Rh1	N6	C27	157(6)
Rh2	Rh1	N6	C27	8(8)
N3	C31	N5	C29	177.5(7)
N3	C31	N5	Rh2	10.9(11)
C32	C29	N5	C31	38.6(13)
C39	C29	N5	C31	-140.0(9)
C32	C29	N5	Rh2	-154.8(7)
C39	C29	N5	Rh2	26.6(11)

Table A3 continued.

N15	Rh2	N5	C31	-107.7(6)
O2	Rh2	N5	C31	118.5(18)
O1	Rh2	N5	C31	79.5(6)
Rh1	Rh2	N5	C31	-22.7(6)
N15	Rh2	N5	C29	85.5(6)
O2	Rh2	N5	C29	-48(2)
O1	Rh2	N5	C29	-87.3(6)
Rh1	Rh2	N5	C29	170.5(6)
N1	C21	N4	C18	174.2(8)
N9	C21	N4	C18	-5.6(13)
C7	C18	N4	C21	1.4(14)
N11	C18	N4	C21	-178.2(9)
N5	C31	N3	C40	177.8(8)
N5	C31	N3	Rh1	14.0(11)
C43	C40	N3	C31	-57.2(12)
C41	C40	N3	C31	127.9(9)
C43	C40	N3	Rh1	106.1(10)
C41	C40	N3	Rh1	-68.8(10)
N14	Rh1	N3	C31	60.6(6)
N8	Rh1	N3	C31	-115.9(7)
N12	Rh1	N3	C31	20(8)
N6	Rh1	N3	C31	154.1(7)
Rh2	Rh1	N3	C31	-23.9(6)
N14	Rh1	N3	C40	-102.6(7)
N8	Rh1	N3	C40	80.9(7)
N12	Rh1	N3	C40	-143(7)
N6	Rh1	N3	C40	-9.1(7)
Rh2	Rh1	N3	C40	172.9(7)

Table A5. Crystal data and structure refinement for $[Rh_2(DTolF)_2(bpy)(CH_3CN)_3][BF_4]_2 \cdot OC(CH_3)_2 \cdot H_2O$ (7a).

Identification code	$[Rh_2(DTolF)_2(bpy)_2(CH_3CN)_3][BF_4]_2 \cdot OC(CH_3)_2 \cdot H_2O$
Empirical formula	C49 H53 B2 F8 N10 Rh2
Formula weight	1179.44 g/mol
Temperature	293(2) K
Wavelength	0.71073 Å
Crystal system	monoclinic
Space group	$P2_1/n$
Unit cell dimensions	a = 13.5856(2) Å
	b = 18.0420(2) Å
	c = 21.4791(3) Å
	$\alpha = 90^\circ$
	$\beta = 101.0440(10)^\circ$
	$\gamma = 90^\circ$
Volume	5167.27(12) $Å^3$
Z	4
ρ_{calc}	1.516 g/cm^3

Table A5 continued.

μ	0.716 cm^{-3}
F(000)	2392
Crystal size	0.31 x 0.26 x 0.21 mm^3
Theta range for data collection	1.49 to 27.66°
Index ranges	-16<=h<=17, -15<=k<=23, -26<=l<=26
Reflections collected	27163
Independent reflections	10679 [R(int) = 0.0595]
Refinement method	Full-matrix least-squares on F^2
Data / restraints / parameters	10674 / 42 / 654
Goodness-of-fit on F^2	1.014
Final R indices [$I>2\sigma(I)$]	R1 = 0.0539, wR2 = 0.1012
R indices (all data)	R1 = 0.1065, wR2 = 0.1186
Largest diff. peak and hole	0.855 and -0.497 $e^-/Å^{-3}$

Table A5 continued.

Atomic coordinates (x 10^4) and equivalent isotropic displacement parameters ($Å^2$ x 10^3).

	x	y	z	U(eq)	Occ.
B1	0.7445(5)	0.3456(3)	-0.0023(3)	0.047(2)	1
B2	0.9991(8)	0.9632(5)	-0.2334(4)	0.080(3)	1
C1	1.0277(4)	0.7394(3)	-0.1485(3)	0.056(2)	1
C10	0.8070(5)	0.4688(3)	0.1815(3)	0.062(2)	1
C11	0.4944(4)	0.5808(3)	-0.0485(3)	0.0452(14)	1
C12	0.6902(4)	0.6731(3)	0.1882(2)	0.0399(13)	1
C13	0.9375(4)	0.5168(3)	-0.1050(2)	0.0400(13)	1
C14	0.7627(4)	0.7936(3)	0.1861(2)	0.0416(13)	1
C15	0.6050(4)	0.9098(3)	-0.0726(2)	0.0413(13)	1
C16	0.4809(4)	0.8584(3)	-0.0206(2)	0.0414(13)	1
C17	0.7839(4)	0.7948(3)	0.2512(3)	0.0470(15)	1
C18	0.8020(4)	0.5284(3)	0.1352(2)	0.0361(12)	1
C19	1.0866(4)	0.6942(3)	0.1282(2)	0.0319(12)	1
C2	0.7624(5)	0.7358(4)	0.2866(2)	0.056(2)	1
C20	1.0390(4)	0.6340(3)	0.2367(2)	0.0363(12)	1
C21	0.9432(4)	0.7437(3)	-0.1162(2)	0.0358(12)	1
C22	0.4400(4)	0.9635(3)	-0.0906(2)	0.0385(13)	1
C23	0.8364(4)	0.5158(3)	-0.1058(2)	0.0364(12)	1
C24	0.5782(4)	0.8575(2)	-0.0318(2)	0.0306(12)	1
C25	0.9869(4)	0.6921(2)	0.1344(2)	0.0280(11)	1
C26	1.1395(4)	0.6364(3)	0.2311(2)	0.0355(12)	1
C27	0.6167(4)	0.7042(3)	-0.1634(2)	0.0365(12)	1
C28	0.6168(4)	0.5222(3)	-0.0975(2)	0.0375(13)	1
C29	0.6899(4)	0.5630(2)	-0.0595(2)	0.0302(11)	1
C3	0.3642(4)	1.0196(3)	-0.1240(3)	0.052(2)	1
C30	0.9993(4)	0.5606(3)	-0.0618(2)	0.0335(12)	1
C31	0.5708(4)	0.6201(3)	-0.0108(2)	0.0387(13)	1

Table A5 continued.

C32	1.1617(4)	0.6664(3)	0.1762(2)	0.0332(12)	1
C33	0.9571(4)	0.6026(2)	-0.0203(2)	0.0293(11)	1
C34	0.9641(4)	0.6620(2)	0.1896(2)	0.0300(11)	1
C35	0.7938(6)	0.7351(4)	0.3588(2)	0.090(3)	1
C36	1.2217(4)	0.6062(3)	0.2821(2)	0.058(2)	1
C37	0.8624(4)	1.0267(3)	0.0515(3)	0.0452(14)	1
C38	0.8735(4)	0.9309(3)	-0.0467(2)	0.0371(12)	1
C39	0.8635(4)	1.0556(3)	-0.0083(3)	0.0451(14)	1
C4	0.5177(4)	0.5320(3)	-0.0926(3)	0.0482(15)	1
C40	0.6508(4)	0.7856(3)	0.0567(2)	0.0328(12)	1
C41	0.8648(4)	0.9514(3)	0.0625(2)	0.0358(12)	1
C42	0.8703(4)	1.0069(3)	-0.0571(3)	0.0402(13)	1
C43	0.8598(5)	1.1390(3)	-0.0193(3)	0.067(2)	1
C44	0.9199(4)	0.7917(2)	0.0704(2)	0.0275(11)	1
C45	0.7969(4)	0.5595(2)	-0.0626(2)	0.0280(11)	1
C46	0.8685(3)	0.9025(2)	0.0130(2)	0.0293(11)	1
C47	1.1007(8)	0.3619(7)	0.2931(5)	0.122(4)	1
C48	1.2030(8)	0.3637(6)	0.2808(6)	0.187(6)	1
C49	1.0793(13)	0.3129(12)	0.3390(7)	0.368(16)	1
C5	0.4148(4)	0.9117(3)	-0.0488(2)	0.0446(14)	1
C6	0.7134(4)	0.6760(3)	0.2545(3)	0.051(2)	1
C7	0.5359(4)	0.9610(3)	-0.1024(2)	0.0443(14)	1
C8	0.5547(5)	0.6752(3)	-0.2219(3)	0.062(2)	1
C9	0.7183(4)	0.7324(3)	0.1537(2)	0.0310(11)	1
F1	0.9333(15)	1.0129(10)	-0.2230(12)	0.207(15)	0.50
F1'	0.9194(11)	1.0084(8)	-0.2370(11)	0.094(6)	0.50
F2	0.9677(5)	0.9194(3)	-0.2870(2)	0.148(2)	1
F3	1.0826(4)	0.9972(3)	-0.2399(3)	0.147(2)	1
F4	1.0127(4)	0.9139(2)	-0.1848(2)	0.108(2)	1
F5	0.6649(3)	0.2997(2)	-0.0030(2)	0.0775(11)	1
F6	0.7433(3)	0.4004(2)	0.0421(2)	0.0879(13)	1
F7	0.8343(3)	0.3069(2)	0.0135(2)	0.0652(10)	1
F8	0.7377(3)	0.3766(2)	-0.0609(2)	0.107(2)	1
N1	0.8782(3)	0.7478(2)	-0.0903(2)	0.0303(10)	1
N2	0.6513(3)	0.8049(2)	-0.0024(2)	0.0303(9)	1
N3	0.6659(3)	0.7264(2)	-0.1183(2)	0.0300(9)	1
N4	0.7020(3)	0.7299(2)	0.0857(2)	0.0310(9)	1
N5	0.9104(3)	0.7214(2)	0.0850(2)	0.0269(9)	1

Table A5 continued.

N6	0.7998(3)	0.5769(2)	0.1013(2)	0.0309(9)	1
N7	0.8585(3)	0.6020(2)	-0.0199(2)	0.0253(9)	1
N8	0.8630(3)	0.8242(2)	0.0211(2)	0.0288(9)	1
N9	0.6671(3)	0.6115(2)	-0.0158(2)	0.0286(9)	1
O1	1.0381(5)	0.4003(4)	0.2628(3)	0.127(2)	1
O2	1.0435(27)	0.2015(20)	0.3799(17)	0.789(23)	1
Rh1	0.78623(3)	0.66547(2)	0.03670(2)	0.02496(11)	1
Rh2	0.76382(3)	0.77165(2)	-0.04512(2)	0.02611(11)	1

U(eq) is defined as one third of the trace of the orthogonalized Uij tensor.

Table A5 continued.

Bond lengths [Å] and angles [°].

Rh1	N9	2.034(4)
Rh1	N7	2.053(4)
Rh1	N4	2.057(4)
Rh1	N5	2.066(4)
Rh1	N6	2.101(4)
Rh1	Rh2	2.5780(5)
Rh2	N8	2.001(4)
Rh2	N2	2.020(4)
Rh2	N3	2.026(4)
Rh2	N1	2.030(4)
N1	C21	1.134(6)
N2	C40	1.317(5)
N2	C24	1.430(6)
N3	C27	1.139(6)
N4	C40	1.311(6)
N4	C9	1.435(5)
N5	C44	1.320(5)
N5	C25	1.436(6)
N6	C18	1.136(6)
N7	C33	1.340(6)
N7	C45	1.354(5)
N8	C44	1.323(5)
N8	C46	1.427(5)
N9	C31	1.342(6)
N9	C29	1.363(5)
B1	F5	1.359(7)
B1	F8	1.364(7)
B1	F6	1.376(7)
B1	F7	1.389(7)
B2	F1	1.31(2)
B2	F3	1.321(9)
B2	F1'	1.35(2)
B2	F4	1.357(8)
B2	F2	1.395(9)
C1	C21	1.452(7)

Table A5 continued.

C2	C17	1.372(8)
C2	C6	1.382(8)
C2	C35	1.527(7)
C3	C22	1.521(7)
C4	C11	1.374(7)
C4	C28	1.382(7)
C5	C16	1.374(7)
C5	C22	1.385(7)
C6	C12	1.399(7)
C7	C22	1.375(7)
C7	C15	1.385(7)
C8	C27	1.468(7)
C9	C14	1.382(7)
C9	C12	1.396(6)
C10	C18	1.457(7)
C11	C31	1.383(7)
C13	C23	1.370(7)
C13	C30	1.375(7)
C14	C17	1.372(7)
C15	C24	1.383(6)
C16	C24	1.389(7)
C19	C25	1.387(6)
C19	C32	1.398(6)
C20	C34	1.386(6)
C20	C26	1.393(7)
C23	C45	1.399(6)
C25	C34	1.392(6)
C26	C32	1.382(6)
C26	C36	1.509(7)
C28	C29	1.371(7)
C29	C45	1.470(7)
C30	C33	1.377(6)
C37	C41	1.380(6)
C37	C39	1.389(7)
C38	C42	1.387(6)
C38	C46	1.396(6)
C39	C42	1.383(7)
C39	C43	1.522(7)

Table A5 continued.

C41	C46	1.388(6)	
C47	O1	1.190(9)	
C47	C49	1.40(2)	
C47	C48	1.464(13)	
N9	Rh1	N7	79.9(2)
N9	Rh1	N4	95.3(2)
N7	Rh1	N4	174.19(15)
N9	Rh1	N5	176.57(14)
N7	Rh1	N5	97.63(14)
N4	Rh1	N5	87.01(15)
N9	Rh1	N6	87.80(15)
N7	Rh1	N6	88.62(14)
N4	Rh1	N6	94.50(14)
N5	Rh1	N6	94.57(14)
N9	Rh1	Rh2	90.03(10)
N7	Rh1	Rh2	91.03(9)
N4	Rh1	Rh2	85.66(10)
N5	Rh1	Rh2	87.61(10)
N6	Rh1	Rh2	177.83(10)
N8	Rh2	N2	90.1(2)
N8	Rh2	N3	174.28(15)
N2	Rh2	N3	91.7(2)
N8	Rh2	N1	88.1(2)
N2	Rh2	N1	174.86(15)
N3	Rh2	N1	89.6(2)
N8	Rh2	Rh1	83.79(10)
N2	Rh2	Rh1	84.94(11)
N3	Rh2	Rh1	101.78(10)
N1	Rh2	Rh1	99.64(10)
C21	N1	Rh2	171.6(4)
C40	N2	C24	118.0(4)
C40	N2	Rh2	120.2(3)
C24	N2	Rh2	121.2(3)
C27	N3	Rh2	172.9(4)
C40	N4	C9	115.0(4)
C40	N4	Rh1	119.2(3)
C9	N4	Rh1	123.1(3)
C44	N5	C25	116.0(4)

Table A5 continued.

C44	N5	Rh1	117.3(3)
C25	N5	Rh1	126.7(3)
C18	N6	Rh1	176.5(4)
C33	N7	C45	119.3(4)
C33	N7	Rh1	126.2(3)
C45	N7	Rh1	114.4(3)
C44	N8	C46	120.0(4)
C44	N8	Rh2	124.8(3)
C46	N8	Rh2	115.2(3)
C31	N9	C29	118.8(4)
C31	N9	Rh1	125.8(3)
C29	N9	Rh1	115.3(3)
F5	B1	F8	109.0(6)
F5	B1	F6	109.3(5)
F8	B1	F6	109.7(5)
F5	B1	F7	110.9(5)
F8	B1	F7	109.5(5)
F6	B1	F7	108.5(5)
F1	B2	F3	109.1(11)
F1	B2	F1'	14.3(17)
F3	B2	F1'	114.2(10)
F1	B2	F4	108.3(12)
F3	B2	F4	113.1(8)
F1'	B2	F4	115.5(12)
F1	B2	F2	114.6(13)
F3	B2	F2	108.0(7)
F1'	B2	F2	100.4(11)
F4	B2	F2	103.8(6)
C17	C2	C6	117.6(5)
C17	C2	C35	121.4(7)
C6	C2	C35	120.9(6)
C11	C4	C28	119.4(5)
C16	C5	C22	122.4(5)
C2	C6	C12	122.0(5)
C22	C7	C15	121.3(5)
C14	C9	C12	118.8(5)
C14	C9	N4	120.4(4)
C12	C9	N4	120.8(5)

Table A5 continued.

C4	C11	C31	119.1(5)
C9	C12	C6	118.8(5)
C23	C13	C30	119.8(5)
C17	C14	C9	120.8(5)
C24	C15	C7	120.8(5)
C5	C16	C24	119.8(5)
C2	C17	C14	121.8(6)
N6	C18	C10	176.9(5)
C25	C19	C32	120.5(4)
C34	C20	C26	121.3(5)
N1	C21	C1	178.8(5)
C7	C22	C5	117.3(5)
C7	C22	C3	121.0(5)
C5	C22	C3	121.7(5)
C13	C23	C45	119.7(5)
C15	C24	C16	118.4(4)
C15	C24	N2	119.2(4)
C16	C24	N2	122.4(4)
C19	C25	C34	118.2(4)
C19	C25	N5	120.1(4)
C34	C25	N5	121.7(4)
C32	C26	C20	117.7(5)
C32	C26	C36	120.5(5)
C20	C26	C36	121.8(5)
N3	C27	C8	179.1(6)
C29	C28	C4	119.5(5)
N9	C29	C28	121.4(5)
N9	C29	C45	114.6(4)
C28	C29	C45	124.1(4)
C13	C30	C33	118.5(5)
N9	C31	C11	121.9(5)
C26	C32	C19	121.5(5)
N7	C33	C30	122.6(4)
C20	C34	C25	120.9(5)
C41	C37	C39	121.6(5)
C42	C38	C46	120.4(5)
C42	C39	C37	118.4(5)
C42	C39	C43	121.1(5)

Table A5 continued.

C37	C39	C43	120.5(5)
N4	C40	N2	124.1(4)
C37	C41	C46	119.9(5)
C39	C42	C38	120.7(5)
N5	C44	N8	123.2(4)
N7	C45	C23	120.1(5)
N7	C45	C29	115.7(4)
C23	C45	C29	124.2(4)
C41	C46	C38	119.0(4)
C41	C46	N8	121.7(4)
C38	C46	N8	119.3(4)
O1	C47	C49	122.1(12)
O1	C47	C48	119.5(12)
C49	C47	C48	118.4(11)

Symmetry transformations used to generate equivalent atoms:
#1 -x-1,-y+1,-z+1

Table A5 continued.

Anisotropic displacement parameters ($Å^2$ x 10^3).

	U11	U22	U33	U23	U13	U12
Rh1	0.0297(2)	0.0210(2)	0.0250(2)	0.0012(2)	0.0072(2)	0.0031(2)
Rh2	0.0307(2)	0.0227(2)	0.0249(2)	0.0008(2)	0.0051(2)	0.0029(2)
N1	0.037(3)	0.025(2)	0.029(2)	0.005(2)	0.008(2)	0.003(2)
N2	0.034(3)	0.027(2)	0.031(2)	0.002(2)	0.008(2)	0.008(2)
N3	0.034(3)	0.025(2)	0.030(2)	0.001(2)	0.004(2)	0.003(2)
N4	0.043(3)	0.025(2)	0.026(2)	0.003(2)	0.010(2)	0.008(2)
N5	0.031(2)	0.026(2)	0.024(2)	0.001(2)	0.006(2)	0.004(2)
N6	0.035(3)	0.029(2)	0.029(2)	-0.002(2)	0.006(2)	0.002(2)
N7	0.032(2)	0.020(2)	0.024(2)	0.004(2)	0.005(2)	0.004(2)
N8	0.034(2)	0.024(2)	0.028(2)	0.003(2)	0.005(2)	0.000(2)
N9	0.031(2)	0.024(2)	0.032(2)	0.003(2)	0.009(2)	0.002(2)
B1	0.058(5)	0.037(4)	0.056(4)	0.004(3)	0.037(4)	0.000(3)
B2	0.101(9)	0.072(7)	0.068(6)	0.008(5)	0.017(6)	0.012(6)
C1	0.050(4)	0.059(4)	0.067(4)	0.002(3)	0.028(3)	0.004(3)
C2	0.054(4)	0.089(5)	0.026(3)	0.002(3)	0.014(3)	0.034(4)
C3	0.047(4)	0.049(4)	0.061(4)	0.011(3)	0.011(3)	0.023(3)
C4	0.043(4)	0.044(3)	0.054(4)	0.001(3)	-0.002(3)	-0.007(3)
C5	0.038(3)	0.044(3)	0.053(3)	0.002(3)	0.012(3)	0.005(3)
C6	0.054(4)	0.066(4)	0.040(3)	0.023(3)	0.025(3)	0.023(3)
C7	0.051(4)	0.046(3)	0.040(3)	0.012(3)	0.017(3)	0.010(3)
C8	0.062(4)	0.059(4)	0.051(4)	-0.004(3)	-0.021(3)	-0.010(3)
C9	0.032(3)	0.036(3)	0.029(3)	0.006(2)	0.015(2)	0.015(2)
C10	0.096(5)	0.042(4)	0.049(4)	0.019(3)	0.017(4)	0.001(3)
C11	0.029(3)	0.052(4)	0.057(4)	-0.002(3)	0.013(3)	-0.002(3)
C12	0.041(3)	0.043(3)	0.040(3)	0.004(3)	0.018(3)	0.009(3)
C13	0.048(4)	0.036(3)	0.042(3)	-0.009(3)	0.024(3)	0.004(3)
C14	0.050(4)	0.038(3)	0.040(3)	-0.008(3)	0.015(3)	0.009(3)
C15	0.037(3)	0.047(3)	0.043(3)	0.008(3)	0.014(3)	0.010(3)
C16	0.039(3)	0.036(3)	0.050(3)	0.012(3)	0.010(3)	0.002(2)
C17	0.045(4)	0.058(4)	0.038(3)	-0.016(3)	0.009(3)	0.013(3)

Table A5 continued.

C18	0.043(3)	0.032(3)	0.035(3)	-0.003(2)	0.009(3)	-0.001(2)
C19	0.040(3)	0.027(3)	0.029(3)	-0.002(2)	0.006(2)	0.004(2)
C20	0.045(4)	0.037(3)	0.025(3)	0.003(2)	0.004(2)	0.004(3)
C21	0.044(3)	0.027(3)	0.037(3)	0.001(2)	0.009(3)	0.004(2)
C22	0.044(4)	0.032(3)	0.038(3)	-0.001(2)	0.004(3)	0.012(2)
C23	0.044(3)	0.029(3)	0.037(3)	-0.011(2)	0.010(3)	-0.001(2)
C24	0.040(3)	0.021(3)	0.031(3)	-0.001(2)	0.007(2)	0.009(2)
C25	0.035(3)	0.022(2)	0.025(3)	-0.003(2)	0.003(2)	0.004(2)
C26	0.048(4)	0.028(3)	0.027(3)	-0.005(2)	0.000(2)	0.004(2)
C27	0.042(3)	0.028(3)	0.039(3)	0.005(2)	0.008(3)	0.005(2)
C28	0.042(4)	0.028(3)	0.042(3)	0.000(2)	0.005(3)	-0.002(2)
C29	0.034(3)	0.022(3)	0.035(3)	0.004(2)	0.009(2)	0.003(2)
C30	0.034(3)	0.029(3)	0.039(3)	-0.001(2)	0.011(2)	0.006(2)
C31	0.034(3)	0.037(3)	0.048(3)	0.002(3)	0.015(3)	0.001(2)
C32	0.029(3)	0.034(3)	0.036(3)	-0.009(2)	0.005(2)	0.003(2)
C33	0.029(3)	0.021(3)	0.036(3)	0.001(2)	0.004(2)	0.003(2)
C34	0.034(3)	0.030(3)	0.026(3)	-0.005(2)	0.006(2)	0.003(2)
C35	0.088(6)	0.158(8)	0.025(3)	0.004(4)	0.010(3)	0.046(5)
C36	0.054(4)	0.074(4)	0.039(3)	0.001(3)	-0.005(3)	0.022(3)
C37	0.044(4)	0.033(3)	0.058(4)	-0.007(3)	0.009(3)	-0.001(2)
C38	0.040(3)	0.030(3)	0.038(3)	0.004(2)	0.000(2)	-0.004(2)
C39	0.035(3)	0.024(3)	0.074(4)	0.008(3)	0.004(3)	0.000(2)
C40	0.043(3)	0.029(3)	0.030(3)	-0.005(2)	0.015(2)	0.005(2)
C41	0.039(3)	0.029(3)	0.038(3)	0.003(2)	0.006(2)	-0.001(2)
C42	0.033(3)	0.028(3)	0.057(4)	0.015(3)	0.004(3)	-0.003(2)
C43	0.059(4)	0.024(3)	0.120(6)	0.009(3)	0.023(4)	-0.003(3)
C44	0.033(3)	0.025(3)	0.025(2)	-0.003(2)	0.005(2)	-0.003(2)
C45	0.038(3)	0.017(2)	0.027(3)	0.003(2)	0.004(2)	0.001(2)
C46	0.027(3)	0.020(3)	0.037(3)	0.005(2)	-0.001(2)	0.003(2)
C47	0.103(9)	0.171(10)	0.089(7)	-0.030(7)	0.009(6)	0.077(8)
C48	0.103(10)	0.177(12)	0.271(16)	0.064(11)	0.011(10)	0.019(8)
C49	0.319(23)	0.587(35)	0.260(18)	0.310(22)	0.215(17)	0.265(23)
F1	0.234(25)	0.116(17)	0.322(33)	0.138(18)	0.186(23)	0.112(15)
F1'	0.065(9)	0.056(10)	0.165(13)	0.031(9)	0.037(9)	0.003(7)
F2	0.213(6)	0.141(5)	0.074(3)	0.012(3)	-0.014(4)	0.039(4)
F3	0.081(4)	0.139(5)	0.223(6)	0.057(5)	0.034(4)	-0.005(3)
F4	0.175(5)	0.082(3)	0.058(2)	0.021(2)	-0.002(3)	0.022(3)
F5	0.083(3)	0.076(3)	0.075(2)	-0.009(2)	0.017(2)	-0.032(2)
F6	0.058(3)	0.083(3)	0.130(3)	-0.061(3)	0.035(2)	-0.011(2)
F7	0.073(3)	0.053(2)	0.072(2)	0.000(2)	0.019(2)	0.018(2)
F8	0.136(4)	0.101(3)	0.103(3)	0.063(3)	0.071(3)	0.053(3)

Table A5 continued.

O1	0.106(5)	0.141(6)	0.126(5)	-0.028(4)	-0.001(4)	0.049(4)

The anisotropic displacement factor exponent takes the form:
$-2\pi^2 [h^2 a^{*2} U11 + ... + 2 h k a^* b^* U12]$

Table A5 continued.

Hydrogen coordinates (x 10^4) and isotropic displacement parameters ($Å^2$ x 10^3).

	x	y	z	U(eq)	Occ.
H10A	0.8732(5)	0.4478(3)	0.1895(3)	0.093	1
H10B	0.7591(5)	0.4311(3)	0.1651(3)	0.093	1
H10C	0.7921(5)	0.4882(3)	0.2202(3)	0.093	1
H11A	0.4282(4)	0.5873(3)	-0.0441(3)	0.054	1
H12A	0.6567(4)	0.6325(3)	0.1675(2)	0.048	1
H13A	0.9642(4)	0.4879(3)	-0.1335(2)	0.048	1
H14A	0.7785(4)	0.8346(3)	0.1636(2)	0.050	1
H15A	0.6702(4)	0.9105(3)	-0.0801(2)	0.050	1
H16A	0.4605(4)	0.8231(3)	0.0058(2)	0.050	1
H17A	0.8137(4)	0.8368(3)	0.2719(3)	0.056	1
H19A	1.1036(4)	0.7143(3)	0.0918(2)	0.038	1
H1A	1.0248(4)	0.7802(3)	-0.1776(3)	0.084	1
H1B	1.0249(4)	0.6936(3)	-0.1715(3)	0.084	1
H1C	1.0892(4)	0.7418(3)	-0.1179(3)	0.084	1
H20A	1.0219(4)	0.6131(3)	0.2728(2)	0.044	1
H23A	0.7942(4)	0.4863(3)	-0.1348(2)	0.044	1
H28A	0.6338(4)	0.4882(3)	-0.1262(2)	0.045	1
H30A	1.0680(4)	0.5618(3)	-0.0607(2)	0.040	1
H31A	0.5549(4)	0.6534(3)	0.0188(2)	0.046	1
H32A	1.2281(4)	0.6681(3)	0.1711(2)	0.040	1
H33A	0.9986(4)	0.6326(2)	0.0087(2)	0.035	1
H34A	0.8978(4)	0.6607(2)	0.1949(2)	0.036	1
H35A	0.7723(6)	0.6896(4)	0.3751(2)	0.136	1
H35B	0.7634(6)	0.7762(4)	0.3763(2)	0.136	1
H35C	0.8655(6)	0.7390(4)	0.3703(2)	0.136	1
H36A	1.1932(4)	0.5877(3)	0.3166(2)	0.087	1
H36B	1.2686(4)	0.6450(3)	0.2972(2)	0.087	1
H36C	1.2558(4)	0.5668(3)	0.2650(2)	0.087	1

Table A5 continued.

H37A	0.8600(4)	1.0590(3)	0.0849(3)	0.054	1
H38A	0.8789(4)	0.8988(3)	-0.0797(2)	0.045	1
H3A	0.3017(4)	1.0132(3)	-0.1101(3)	0.078	1
H3B	0.3541(4)	1.0119(3)	-0.1690(3)	0.078	1
H3C	0.3890(4)	1.0688(3)	-0.1141(3)	0.078	1
H40A	0.6116(4)	0.8133(3)	0.0793(2)	0.039	1
H41A	0.8640(4)	0.9333(3)	0.1029(2)	0.043	1
H42A	0.8729(4)	1.0252(3)	-0.0972(3)	0.048	1
H43A	0.8551(5)	1.1638(3)	0.0195(3)	0.101	1
H43B	0.8023(5)	1.1511(3)	-0.0512(3)	0.101	1
H43C	0.9196(5)	1.1546(3)	-0.0331(3)	0.101	1
H44A	0.9691(4)	0.8198(2)	0.0960(2)	0.033	1
H48A	1.2070(8)	0.3997(6)	0.2484(6)	0.281	1
H48B	1.2203(8)	0.3157(6)	0.2668(6)	0.281	1
H48C	1.2488(8)	0.3769(6)	0.3190(6)	0.281	1
H49A	1.0100(13)	0.3175(12)	0.3421(7)	0.551	1
H49B	1.1208(13)	0.3244(12)	0.3793(7)	0.551	1
H49C	1.0924(13)	0.2630(12)	0.3272(7)	0.551	1
H4A	0.4672(4)	0.5059(3)	-0.1190(3)	0.058	1
H5A	0.3508(4)	0.9130(3)	-0.0393(2)	0.054	1
H6A	0.6954(4)	0.6364(3)	0.2777(3)	0.061	1
H7A	0.5547(4)	0.9944(3)	-0.1310(2)	0.053	1
H8A	0.5293(5)	0.7156(3)	-0.2493(3)	0.092	1
H8B	0.4997(5)	0.6474(3)	-0.2116(3)	0.092	1
H8C	0.5946(5)	0.6434(3)	-0.2430(3)	0.092	1

Symmetry transformations used to generate equivalent atoms:
#1 -x-1,-y+1,-z+1

Table A5 continued.

Torsion angles [°].

N9	Rh1	Rh2	N8	169.2(2)
N7	Rh1	Rh2	N8	-110.9(2)
N4	Rh1	Rh2	N8	73.9(2)
N5	Rh1	Rh2	N8	-13.28(14)
N6	Rh1	Rh2	N8	168.4(28)
N9	Rh1	Rh2	N2	78.6(2)
N7	Rh1	Rh2	N2	158.5(2)
N4	Rh1	Rh2	N2	-16.7(2)
N5	Rh1	Rh2	N2	-103.90(15)
N6	Rh1	Rh2	N2	77.8(28)
N9	Rh1	Rh2	N3	-12.1(2)
N7	Rh1	Rh2	N3	67.8(2)
N4	Rh1	Rh2	N3	-107.4(2)
N5	Rh1	Rh2	N3	165.37(15)
N6	Rh1	Rh2	N3	-13.0(28)
N9	Rh1	Rh2	N1	-103.7(2)
N7	Rh1	Rh2	N1	-23.8(2)
N4	Rh1	Rh2	N1	160.9(2)
N5	Rh1	Rh2	N1	73.76(15)
N6	Rh1	Rh2	N1	-104.6(28)
N8	Rh2	N1	C21	-61.6(28)
N2	Rh2	N1	C21	8.0(40)
N3	Rh2	N1	C21	113.1(28)
Rh1	Rh2	N1	C21	-145.0(28)
N8	Rh2	N2	C40	-59.9(4)
N3	Rh2	N2	C40	125.5(4)
N1	Rh2	N2	C40	-129.4(16)
Rh1	Rh2	N2	C40	23.9(4)
N8	Rh2	N2	C24	111.6(4)
N3	Rh2	N2	C24	-63.0(4)
N1	Rh2	N2	C24	42.1(19)
Rh1	Rh2	N2	C24	-164.6(3)
N8	Rh2	N3	C27	28.6(42)
N2	Rh2	N3	C27	137.0(33)
N1	Rh2	N3	C27	-38.0(33)
Rh1	Rh2	N3	C27	-137.8(32)

Table A5 continued.

N9	Rh1	N4	C40	-74.4(4)
N7	Rh1	N4	C40	-40.1(16)
N5	Rh1	N4	C40	103.1(4)
N6	Rh1	N4	C40	-162.6(4)
Rh2	Rh1	N4	C40	15.3(4)
N9	Rh1	N4	C9	125.1(4)
N7	Rh1	N4	C9	159.4(13)
N5	Rh1	N4	C9	-57.4(4)
N6	Rh1	N4	C9	36.9(4)
Rh2	Rh1	N4	C9	-145.3(4)
N9	Rh1	N5	C44	62.6(25)
N7	Rh1	N5	C44	106.8(3)
N4	Rh1	N5	C44	-69.7(3)
N6	Rh1	N5	C44	-164.0(3)
Rh2	Rh1	N5	C44	16.1(3)
N9	Rh1	N5	C25	-119.0(23)
N7	Rh1	N5	C25	-74.8(4)
N4	Rh1	N5	C25	108.7(4)
N6	Rh1	N5	C25	14.4(4)
Rh2	Rh1	N5	C25	-165.5(3)
N9	Rh1	N6	C18	-25.4(60)
N7	Rh1	N6	C18	-105.3(60)
N4	Rh1	N6	C18	69.8(60)
N5	Rh1	N6	C18	157.1(60)
Rh2	Rh1	N6	C18	-24.6(82)
N9	Rh1	N7	C33	177.5(4)
N4	Rh1	N7	C33	142.9(13)
N5	Rh1	N7	C33	0.0(4)
N6	Rh1	N7	C33	-94.5(4)
Rh2	Rh1	N7	C33	87.7(3)
N9	Rh1	N7	C45	1.4(3)
N4	Rh1	N7	C45	-33.3(16)
N5	Rh1	N7	C45	-176.1(3)
N6	Rh1	N7	C45	89.4(3)
Rh2	Rh1	N7	C45	-88.4(3)
N2	Rh2	N8	C44	100.1(4)
N3	Rh2	N8	C44	-151.4(14)
N1	Rh2	N8	C44	-84.7(4)

Table A5 continued.

Rh1	Rh2	N8	C44	15.2(4)
N2	Rh2	N8	C46	-78.7(3)
N3	Rh2	N8	C46	29.8(17)
N1	Rh2	N8	C46	96.5(3)
Rh1	Rh2	N8	C46	-163.6(3)
N7	Rh1	N9	C31	-179.5(4)
N4	Rh1	N9	C31	-2.8(4)
N5	Rh1	N9	C31	-134.9(23)
N6	Rh1	N9	C31	91.5(4)
Rh2	Rh1	N9	C31	-88.5(4)
N7	Rh1	N9	C29	0.2(3)
N4	Rh1	N9	C29	176.9(3)
N5	Rh1	N9	C29	44.8(25)
N6	Rh1	N9	C29	-88.8(3)
Rh2	Rh1	N9	C29	91.2(3)
C17	C2	C6	C12	2.9(8)
C35	C2	C6	C12	-175.4(5)
C40	N4	C9	C14	-55.1(6)
Rh1	N4	C9	C14	106.2(5)
C40	N4	C9	C12	125.3(5)
Rh1	N4	C9	C12	-73.4(5)
C28	C4	C11	C31	1.3(8)
C14	C9	C12	C6	-3.7(7)
N4	C9	C12	C6	175.9(4)
C2	C6	C12	C9	0.6(8)
C12	C9	C14	C17	3.4(7)
N4	C9	C14	C17	-176.2(4)
C22	C7	C15	C24	2.6(8)
C22	C5	C16	C24	2.9(8)
C6	C2	C17	C14	-3.3(8)
C35	C2	C17	C14	175.0(5)
C9	C14	C17	C2	0.2(8)
Rh1	N6	C18	C10	-124.1(94)
Rh2	N1	C21	C1	48.7(318)
C15	C7	C22	C5	-1.4(8)
C15	C7	C22	C3	-179.5(5)
C16	C5	C22	C7	-1.4(8)
C16	C5	C22	C3	176.7(5)

Table A5 continued.

C30	C13	C23	C45	0.0(7)
C7	C15	C24	C16	-1.0(7)
C7	C15	C24	N2	179.3(4)
C5	C16	C24	C15	-1.6(8)
C5	C16	C24	N2	178.1(5)
C40	N2	C24	C15	142.6(5)
Rh2	N2	C24	C15	-29.1(6)
C40	N2	C24	C16	-37.0(7)
Rh2	N2	C24	C16	151.3(4)
C32	C19	C25	C34	0.4(7)
C32	C19	C25	N5	179.5(4)
C44	N5	C25	C19	-58.0(6)
Rh1	N5	C25	C19	123.7(4)
C44	N5	C25	C34	121.1(5)
Rh1	N5	C25	C34	-57.3(5)
C34	C20	C26	C32	-1.3(7)
C34	C20	C26	C36	179.9(5)
Rh2	N3	C27	C8	47.9(344)
C11	C4	C28	C29	-2.0(8)
C31	N9	C29	C28	-1.1(6)
Rh1	N9	C29	C28	179.1(4)
C31	N9	C29	C45	178.1(4)
Rh1	N9	C29	C45	-1.7(5)
C4	C28	C29	N9	1.9(7)
C4	C28	C29	C45	-177.2(4)
C23	C13	C30	C33	0.0(7)
C29	N9	C31	C11	0.4(7)
Rh1	N9	C31	C11	-179.9(4)
C4	C11	C31	N9	-0.5(8)
C20	C26	C32	C19	0.7(7)
C36	C26	C32	C19	179.6(5)
C25	C19	C32	C26	-0.3(7)
C45	N7	C33	C30	-1.1(6)
Rh1	N7	C33	C30	-177.0(3)
C13	C30	C33	N7	0.6(7)
C26	C20	C34	C25	1.4(7)
C19	C25	C34	C20	-0.9(7)
N5	C25	C34	C20	-180.0(4)

Table A5 continued.

C41	C37	C39	C42	-2.1(8)
C41	C37	C39	C43	179.5(5)
C9	N4	C40	N2	160.3(5)
Rh1	N4	C40	N2	-1.8(7)
C24	N2	C40	N4	168.5(4)
Rh2	N2	C40	N4	-19.7(7)
C39	C37	C41	C46	0.0(8)
C37	C39	C42	C38	1.6(8)
C43	C39	C42	C38	-179.9(5)
C46	C38	C42	C39	0.8(8)
C25	N5	C44	N8	171.4(4)
Rh1	N5	C44	N8	-10.0(6)
C46	N8	C44	N5	171.7(4)
Rh2	N8	C44	N5	-7.1(6)
C33	N7	C45	C23	1.1(6)
Rh1	N7	C45	C23	177.5(3)
C33	N7	C45	C29	-179.1(4)
Rh1	N7	C45	C29	-2.7(5)
C13	C23	C45	N7	-0.6(7)
C13	C23	C45	C29	179.7(4)
N9	C29	C45	N7	2.9(6)
C28	C29	C45	N7	-177.9(4)
N9	C29	C45	C23	-177.3(4)
C28	C29	C45	C23	1.9(7)
C37	C41	C46	C38	2.4(7)
C37	C41	C46	N8	-174.9(5)
C42	C38	C46	C41	-2.8(7)
C42	C38	C46	N8	174.6(4)
C44	N8	C46	C41	-48.1(6)
Rh2	N8	C46	C41	130.8(4)
C44	N8	C46	C38	134.6(5)
Rh2	N8	C46	C38	-46.5(5)

Table A6. Crystal data and structure refinement for $[Rh_2(DTolF)_2(bpy)(CH_3CN)_4][BF_4]_2$ (7b).

Identification code	$[Rh_2(DTolF)_2(bpy)(CH_3CN)_4][BF_4]_2$
Empirical formula	C48 H50 B2 F8 N10 Rh2
Formula weight	1146.42 g/mol
Temperature	293(2) K
Wavelength	0.71073 Å
Crystal system	monoclinic
Space group	$P2_1/n$
Unit cell dimensions	a = 10.9339(2) Å
	b = 24.48580(10) Å
	c = 19.4874(3) Å
	$\alpha = 90^\circ$
	$\beta = 94.3290(10)^\circ$
	$\gamma = 90^\circ$
Volume	5202.38(13) $Å^3$
Z	4
ρ_{calc}	1.464 g/cm^3

Table A6 continued.

μ	0.706 cm^{-3}
F(000)	2320
Crystal size	0.39 x 0.39 x 0.31 mm^3
Theta range for data collection	1.66 to 27.52°
Index ranges	-13<=h<=13, -30<=k<=26, -17<=l<=23
Reflections collected	5450
Independent reflections	4269 [R(int) = 0.0341]
Refinement method	Full-matrix least-squares on F^2
Data / restraints / parameters	5450 / 140 / 720
Goodness-of-fit on F^2	0.944
Final R indices [$I>2\sigma(I)$]	R1 = 0.0462, wR2 = 0.1134
R indices (all data)	R1 = 0.0670, wR2 = 0.1249
Largest diff. peak and hole	1.113 and -0.363 $e^-/Å^{-3}$

Table A6 continued.

Atomic coordinates (x 10^4) and equivalent isotropic displacement parameters ($Å^2$ x 10^3).

	x	y	z	U(eq)	Occ.
B1	0.4673(11)	0.0122(4)	-0.1775(6)	0.060(3)	1.054(13)
B2	0.9563(8)	0.0079(4)	-0.0539(6)	0.065(6)	0.545(8)
B2A	0.1073(17)	0.0844(8)	0.3307(10)	0.061(8)	0.455(8)
C1	0.4690(7)	0.1616(4)	0.1707(5)	0.025(2)	1
C10	0.4389(7)	0.0886(3)	-0.0030(4)	0.028(2)	1
C11	0.6402(8)	0.2482(26)	-0.2527(4)	0.041(3)	1
C12	0.3725(7)	0.3208(3)	0.0095(4)	0.025(2)	1
C13	0.2573(7)	0.3125(3)	-0.0246(4)	0.029(2)	1
C14	0.1647(7)	0.3511(4)	-0.0215(4)	0.037(2)	1
C15	0.1820(8)	0.3986(4)	0.0175(5)	0.040(2)	1
C16	0.2976(8)	0.4058(3)	0.0525(4)	0.039(2)	1
C17	0.4443(8)	0.3245(4)	0.2052(5)	0.035(2)	1
C18	0.2366(7)	0.1517(3)	0.1048(4)	0.035(2)	1
C19	0.2689(8)	0.1194(4)	0.1612(5)	0.043(2)	1
C2	0.4907(8)	0.2654(3)	-0.0576(4)	0.024(2)	1
C20	0.3919(8)	0.3685(3)	0.0478(4)	0.032(2)	1
C21	0.3212(7)	0.1878(3)	0.0829(4)	0.029(2)	1
C22	0.7768(7)	0.2170(3)	0.1923(4)	0.030(2)	1
C23	0.8296(8)	0.1910(4)	0.2502(5)	0.039(2)	1
C24	0.7632(9)	0.1541(4)	0.2853(5)	0.042(2)	1
C25	0.9315(7)	0.2517(11)	-0.0955(4)	0.035(2)	1
C26	0.9005(6)	0.2145(3)	-0.0431(4)	0.026(2)	1
C27	0.9683(7)	0.1674(3)	-0.0292(4)	0.032(2)	1
C28	0.7021(8)	0.3913(4)	0.0282(5)	0.037(2)	1
C29	0.7323(8)	0.3693(4)	0.1481(4)	0.037(2)	1
C3	0.7950(13)	0.2775(6)	0.0243(5)	0.024(2)	1
C30	0.7330(11)	0.4235(4)	0.1640(5)	0.050(3)	1
C31	0.3518(8)	0.0439(4)	-0.0039(5)	0.043(2)	1

Table A6 continued.

C32	0.7860(7)	0.0960(3)	0.1071(4)	0.034(2)	1
C33	0.7009(9)	0.4459(4)	0.0444(5)	0.045(2)	1
C34	0.7152(10)	0.4632(4)	0.1127(5)	0.049(2)	1
C35	1.0685(7)	0.1560(4)	-0.0665(4)	0.034(2)	1
C36	1.1025(7)	0.1903(4)	-0.1186(4)	0.036(2)	1
C37	1.0342(7)	0.2370(4)	-0.1323(4)	0.039(3)	1
C38	0.3852(7)	0.1248(4)	0.1947(5)	0.039(2)	1
C39	0.0766(14)	0.4374(5)	0.0263(8)	0.063(4)	1
C4	0.5782(6)	0.2178(3)	-0.1453(4)	0.0239(15)	1
C40	0.3829(9)	0.3583(5)	0.2540(6)	0.060(3)	1
C41	0.5381(8)	0.1667(4)	-0.2504(4)	0.038(2)	1
C42	0.5923(8)	0.2075(4)	-0.2881(4)	0.037(2)	1
C43	0.5962(9)	0.2030(5)	-0.3649(4)	0.055(3)	1
C44	0.8459(10)	0.0555(4)	0.1538(6)	0.060(3)	1
C45	1.2132(8)	0.1767(4)	-0.1575(5)	0.049(2)	1
C46	0.7159(14)	0.5236(4)	0.1301(7)	0.079(4)	1
C47b	0.7672(39)	0.0809(12)	-0.1057(23)	0.328(23)	1.07(2)
C48A	0.8263(60)	0.0459(25)	-0.1541(30)	0.582(50)	1.07(2)
C5	0.6333(7)	0.2580(16)	-0.1815(4)	0.034(7)	1
C6	0.5324(7)	0.1719(3)	-0.1797(4)	0.032(2)	1
C7	0.5927(7)	0.1703(3)	0.2016(4)	0.028(2)	1
C8	0.6437(8)	0.1426(3)	0.2603(4)	0.038(2)	1
C9	0.7174(12)	0.3513(4)	0.0796(7)	0.028(2)	1
F1	0.3738(6)	0.0491(3)	-0.1731(3)	0.080(2)	1.054(13)
F2	0.4420(8)	-0.0338(3)	-0.1424(6)	0.135(4)	1.054(13)
F3	0.5706(13)	0.0324(6)	-0.1471(10)	0.184(9)	1.054(13)
F4	0.4905(12)	0.0002(5)	-0.2404(4)	0.181(7)	1.054(13)
F5	1.0703(9)	0.0174(6)	-0.0278(8)	0.098(5)	0.545(8)
F5A	0.2176(12)	0.1079(8)	0.3337(8)	0.099(6)	0.455(8)
F6	0.8735(10)	0.0319(5)	-0.0173(6)	0.076(4)	0.545(8)
F6A	0.1124(24)	0.0341(6)	0.3603(11)	0.090(8)	0.455(8)
F7	0.9446(15)	0.0299(7)	-0.1165(6)	0.129(7)	0.545(8)
F7b	0.0286(13)	0.1135(7)	0.3665(10)	0.109(7)	0.455(8)
F8	0.9394(15)	-0.0458(4)	-0.0513(11)	0.098(7)	0.545(8)
F8A	0.0596(16)	0.0804(12)	0.2670(7)	0.159(13)	0.455(8)
N1	0.7246(5)	0.1180(3)	-0.0812(3)	0.032(2)	1.07(2)
N10	0.5072(5)	0.1236(3)	-0.0018(3)	0.0252(13)	1
N2	0.4933(6)	0.2994(3)	0.1660(4)	0.0336(15)	1

Table A6 continued.

N3	0.4684(5)	0.2808(2)	0.0053(3)	0.0247(13)	1
N4	0.7116(5)	0.2949(3)	0.0630(3)	0.0259(13)	1
N5	0.7987(10)	0.2275(4)	-0.0027(4)	0.019(2)	1
N6	0.5629(6)	0.2250(3)	-0.0726(3)	0.0243(13)	1
N7	0.4363(5)	0.1932(2)	0.1140(3)	0.0230(12)	1
N8	0.6611(5)	0.2071(2)	0.1687(3)	0.0242(13)	1
N9	0.7381(9)	0.1270(4)	0.0705(5)	0.025(2)	1
Rh1	0.65161(5)	0.17687(2)	-0.00081(3)	0.0203(2)	1
Rh2	0.56873(4)	0.2469(15)	0.08715(3)	0.023(2)	1

U(eq) is defined as one third of the trace of the orthogonalized Uij tensor.

Table A6 continued.

Bond lengths [Å] and angles [°].

Rh1	N6	2.020(6)
Rh1	N9	2.030(10)
Rh1	N5	2.033(11)
Rh1	N10	2.047(6)
Rh1	N1	2.315(6)
Rh1	Rh2	2.63(2)
Rh2	N4	2.04(2)
Rh2	N3	2.04(2)
Rh2	N7	2.05(2)
Rh2	N8	2.06(2)
Rh2	N2	2.21(2)
C1	N7	1.373(10)
C1	C38	1.391(12)
C1	C7	1.454(11)
C2	N6	1.314(9)
C2	N3	1.323(10)
C3	N4	1.298(14)
C3	N5	1.335(9)
C4	C5	1.38(3)
C4	C6	1.384(11)
C4	N6	1.450(9)
C5	C11	1.42(2)
C6	C41	1.388(11)
C7	N8	1.361(10)
C7	C8	1.409(11)
C8	C24	1.388(12)
C9	C28	1.400(12)
C9	C29	1.40(2)
C9	N4	1.418(12)
C10	N10	1.137(9)
C10	C31	1.450(11)
C11	C42	1.30(5)
C12	C20	1.393(11)
C12	C13	1.395(11)
C12	N3	1.442(9)

Table A6 continued.

C13	C14	1.389(11)
C14	C15	1.394(12)
C15	C16	1.402(12)
C15	C39	1.513(14)
C16	C20	1.387(11)
C17	N2	1.144(11)
C17	C40	1.464(13)
C18	C21	1.371(11)
C18	C19	1.377(12)
C19	C38	1.391(12)
C21	N7	1.361(9)
C22	N8	1.336(9)
C22	C23	1.384(11)
C23	C24	1.373(13)
C25	C37	1.424(15)
C25	C26	1.43(2)
C26	C27	1.388(11)
C26	N5	1.447(12)
C27	C35	1.387(11)
C28	C33	1.375(12)
C29	C30	1.362(13)
C30	C34	1.397(14)
C32	N9	1.141(13)
C32	C44	1.467(12)
C33	C34	1.394(13)
C34	C46	1.518(13)
C35	C36	1.391(12)
C36	C37	1.381(12)
C36	C45	1.513(11)
C41	C42	1.398(13)
C42	C43	1.505(11)
C47b	N1	1.141(11)
C47b	C48A	1.461(11)
B2A	F8A	1.31(2)
B2A	F5A	1.33(2)
B2A	F7b	1.35(2)
B2A	F6A	1.36(2)
B2	F5	1.3305(11)
B2	F6	1.3305(11)

Table A6 continued.

B2	F7	1.3303(11)	
B2	F8	1.3305(11)	
B1	F4	1.303(12)	
B1	F3	1.330(15)	
B1	F2	1.358(12)	
B1	F1	1.372(12)	
N6	Rh1	N9	178.6(3)
N6	Rh1	N5	88.4(3)
N9	Rh1	N5	92.9(4)
N6	Rh1	N10	92.0(2)
N9	Rh1	N10	86.7(3)
N5	Rh1	N10	177.4(3)
N6	Rh1	N1	93.8(2)
N9	Rh1	N1	85.5(3)
N5	Rh1	N1	93.1(3)
N10	Rh1	N1	84.3(2)
N6	Rh1	Rh2	84.3(4)
N9	Rh1	Rh2	96.4(5)
N5	Rh1	Rh2	85.8(5)
N10	Rh1	Rh2	96.8(5)
N1	Rh1	Rh2	177.8(6)
N4	Rh2	N3	87.8(10)
N4	Rh2	N7	174.8(14)
N3	Rh2	N7	96.4(4)
N4	Rh2	N8	96.4(3)
N3	Rh2	N8	175.3(16)
N7	Rh2	N8	79.3(9)
N4	Rh2	N2	99.1(13)
N3	Rh2	N2	95.8(11)
N7	Rh2	N2	83.6(2)
N8	Rh2	N2	85.7(3)
N4	Rh2	Rh1	85.3(3)
N3	Rh2	Rh1	87.0(4)
N7	Rh2	Rh1	91.8(12)
N8	Rh2	Rh1	91.2(10)
N2	Rh2	Rh1	174.9(13)
N7	C1	C38	119.8(7)
N7	C1	C7	115.4(7)
C38	C1	C7	124.9(8)

Table A6 continued.

N6	C2	N3	125.2(6)
N4	C3	N5	125.0(14)
C5	C4	C6	119.3(11)
C5	C4	N6	120.1(11)
C6	C4	N6	120.5(7)
C4	C5	C11	116.0(33)
C4	C6	C41	120.8(8)
N8	C7	C8	120.2(7)
N8	C7	C1	115.4(7)
C8	C7	C1	124.4(7)
C24	C8	C7	119.5(8)
C28	C9	C29	117.3(9)
C28	C9	N4	121.1(10)
C29	C9	N4	121.5(9)
N10	C10	C31	179.6(8)
C42	C11	C5	127.0(36)
C20	C12	C13	118.3(7)
C20	C12	N3	121.2(7)
C13	C12	N3	120.5(7)
C14	C13	C12	120.9(8)
C13	C14	C15	121.5(8)
C14	C15	C16	116.8(7)
C14	C15	C39	120.8(9)
C16	C15	C39	122.2(9)
C20	C16	C15	122.2(8)
N2	C17	C40	178.0(12)
C21	C18	C19	118.7(8)
C18	C19	C38	119.4(8)
C16	C20	C12	120.2(8)
N7	C21	C18	123.1(7)
N8	C22	C23	121.6(7)
C24	C23	C22	120.3(8)
C23	C24	C8	118.6(8)
C37	C25	C26	115.9(17)
C27	C26	C25	121.2(10)
C27	C26	N5	119.9(7)
C25	C26	N5	118.9(10)
C35	C27	C26	119.8(7)
C33	C28	C9	121.2(9)

Table A6 continued.

C30	C29	C9	121.4(9)
C29	C30	C34	121.1(8)
N9	C32	C44	179.0(10)
C28	C33	C34	120.8(9)
C33	C34	C30	118.1(8)
C33	C34	C46	120.5(9)
C30	C34	C46	121.4(9)
C27	C35	C36	121.7(8)
C37	C36	C35	118.2(7)
C37	C36	C45	121.7(8)
C35	C36	C45	120.1(8)
C36	C37	C25	123.2(11)
C19	C38	C1	120.4(8)
C6	C41	C42	120.7(8)
C11	C42	C41	115.9(14)
C11	C42	C43	122.9(15)
C41	C42	C43	121.1(9)
N1	C47b	C48A	162.0(58)
C47b	N1	Rh1	161.9(26)
C17	N2	Rh2	173.9(8)
C2	N3	C12	115.6(6)
C2	N3	Rh2	118.9(7)
C12	N3	Rh2	125.5(7)
C3	N4	C9	115.5(9)
C3	N4	Rh2	121.9(10)
C9	N4	Rh2	122.1(10)
C3	N5	C26	117.6(11)
C3	N5	Rh1	120.3(12)
C26	N5	Rh1	121.2(7)
C2	N6	C4	115.1(6)
C2	N6	Rh1	123.4(5)
C4	N6	Rh1	121.4(5)
C21	N7	C1	118.6(7)
C21	N7	Rh2	126.5(6)
C1	N7	Rh2	114.8(6)
C22	N8	C7	119.9(6)
C22	N8	Rh2	125.1(7)
C7	N8	Rh2	114.9(7)
C32	N9	Rh1	175.0(9)

Table A6 continued.

C10	N10	Rh1	170.5(6)
F8A	B2A	F5A	111.5(16)
F8A	B2A	F7b	107.7(16)
F5A	B2A	F7b	111.1(15)
F8A	B2A	F6A	109.5(17)
F5A	B2A	F6A	111.4(16)
F7b	B2A	F6A	105.4(15)
F5	B2	F6	111.9(10)
F5	B2	F7	107.6(10)
F6	B2	F7	106.9(10)
F5	B2	F8	106.7(10)
F6	B2	F8	108.2(10)
F7	B2	F8	115.6(12)
F4	B1	F3	106.5(13)
F4	B1	F2	110.3(10)
F3	B1	F2	106.4(11)
F4	B1	F1	114.1(9)
F3	B1	F1	109.8(10)
F2	B1	F1	109.4(9)

Symmetry transformations used to generate equivalent atoms:
#1 -x-1,-y+1,-z+1

Table A6 continued.

Anisotropic displacement parameters ($Å^2 \times 10^3$).

	U11	U22	U33	U23	U13	U12
Rh1	0.0180(3)	0.0202(3)	0.0227(3)	0.0007(2)	0.0010(2)	0.0007(2)
Rh2	0.0210(2)	0.027(6)	0.0203(2)	0.0025(14)	-0.00009(15)	0.0018(11)
C1	0.019(4)	0.031(5)	0.026(5)	0.000(4)	0.006(3)	0.003(3)
C2	0.028(4)	0.026(6)	0.019(4)	0.004(2)	-0.003(3)	0.005(3)
C3	0.026(5)	0.029(5)	0.016(6)	0.005(5)	-0.001(5)	-0.004(4)
C4	0.018(3)	0.030(4)	0.023(4)	0.004(3)	0.000(3)	0.000(3)
C5	0.030(3)	0.041(22)	0.029(3)	0.010(6)	0.001(3)	-0.001(5)
C6	0.029(4)	0.042(5)	0.027(4)	0.002(3)	0.005(3)	0.000(3)
C7	0.033(4)	0.026(4)	0.025(4)	-0.001(3)	-0.003(3)	0.002(3)
C8	0.040(5)	0.033(5)	0.041(5)	0.009(4)	0.000(4)	-0.002(4)
C9	0.038(6)	0.016(6)	0.031(5)	0.001(5)	-0.002(4)	0.000(5)
C10	0.023(4)	0.030(4)	0.032(4)	-0.005(3)	0.004(3)	-0.002(3)
C11	0.043(5)	0.048(9)	0.031(3)	0.001(17)	0.009(3)	0.020(17)
C12	0.027(4)	0.025(4)	0.025(4)	0.005(3)	0.004(3)	0.006(3)
C13	0.030(4)	0.029(4)	0.028(4)	0.003(3)	0.006(3)	0.004(3)
C14	0.028(4)	0.043(5)	0.039(5)	0.007(4)	-0.002(3)	0.010(4)
C15	0.038(5)	0.034(5)	0.049(5)	0.010(4)	0.010(4)	0.013(4)
C16	0.052(5)	0.027(4)	0.039(5)	-0.005(3)	0.004(4)	0.010(4)
C17	0.030(5)	0.037(5)	0.039(5)	-0.003(4)	-0.001(4)	0.002(4)
C18	0.028(4)	0.038(5)	0.040(5)	-0.007(4)	0.002(3)	-0.002(4)
C19	0.030(4)	0.039(5)	0.060(6)	0.007(4)	0.010(4)	-0.008(4)
C20	0.036(4)	0.024(4)	0.036(4)	0.001(3)	-0.001(3)	0.004(3)
C21	0.021(4)	0.037(4)	0.028(4)	-0.005(3)	-0.001(3)	-0.002(3)
C22	0.029(4)	0.029(4)	0.030(4)	0.004(3)	-0.007(3)	-0.002(3)
C23	0.035(5)	0.034(5)	0.046(5)	0.002(4)	-0.016(4)	0.003(4)
C24	0.050(5)	0.038(5)	0.036(5)	0.013(4)	-0.014(4)	0.008(4)
C25	0.032(4)	0.034(5)	0.038(4)	0.011(10)	-0.001(3)	-0.029(9)
C26	0.019(3)	0.028(4)	0.031(4)	-0.001(3)	0.002(3)	-0.004(3)
C27	0.022(4)	0.037(5)	0.037(4)	0.009(4)	0.001(3)	-0.002(3)
C28	0.050(5)	0.032(5)	0.029(4)	0.003(4)	0.002(4)	0.002(4)

Table A6 continued.

C29	0.047(5)	0.031(5)	0.030(4)	0.000(3)	-0.005(4)	-0.009(4)
C30	0.082(7)	0.042(5)	0.026(4)	-0.010(4)	0.000(5)	-0.016(5)
C31	0.035(5)	0.036(5)	0.058(6)	-0.008(4)	0.008(4)	-0.016(4)
C32	0.029(4)	0.032(4)	0.040(5)	0.000(4)	0.004(3)	0.003(3)
C33	0.069(6)	0.028(4)	0.040(5)	0.002(4)	0.007(4)	-0.002(4)
C34	0.066(6)	0.030(5)	0.050(6)	-0.009(4)	0.011(5)	-0.009(4)
C35	0.022(4)	0.036(5)	0.044(5)	-0.003(4)	0.004(3)	0.007(3)
C36	0.023(4)	0.043(5)	0.041(5)	-0.006(4)	0.006(3)	-0.006(4)
C37	0.033(4)	0.051(10)	0.033(4)	0.001(3)	0.011(3)	-0.011(4)
C38	0.034(4)	0.041(5)	0.041(5)	0.015(4)	0.007(4)	-0.005(4)
C39	0.060(7)	0.019(6)	0.108(11)	-0.007(6)	-0.009(7)	0.023(6)
C40	0.050(6)	0.069(7)	0.059(7)	-0.029(6)	-0.004(5)	0.025(5)
C41	0.031(4)	0.042(5)	0.040(5)	-0.012(4)	0.004(4)	0.003(4)
C42	0.031(4)	0.055(6)	0.024(4)	-0.005(4)	0.005(3)	0.008(4)
C43	0.058(6)	0.083(8)	0.023(4)	-0.003(5)	0.006(4)	-0.002(6)
C44	0.066(7)	0.051(6)	0.062(7)	0.017(5)	-0.010(5)	0.019(5)
C45	0.037(5)	0.059(6)	0.053(6)	-0.006(5)	0.015(4)	0.001(4)
C46	0.124(11)	0.034(6)	0.083(9)	-0.020(6)	0.027(8)	-0.018(7)
N1	0.023(3)	0.032(4)	0.041(4)	-0.012(3)	0.004(3)	0.001(3)
N2	0.030(4)	0.034(5)	0.037(4)	0.004(3)	0.000(3)	0.003(3)
N3	0.027(3)	0.025(3)	0.021(3)	0.001(2)	0.000(2)	0.003(3)
N4	0.030(3)	0.026(3)	0.021(3)	-0.001(2)	0.003(3)	-0.003(3)
N5	0.017(3)	0.024(3)	0.018(5)	0.000(4)	0.004(4)	-0.003(2)
N6	0.019(3)	0.032(3)	0.022(3)	0.003(2)	0.006(3)	0.005(3)
N7	0.023(3)	0.024(3)	0.022(3)	-0.001(2)	0.001(2)	0.000(2)
N8	0.027(3)	0.023(3)	0.022(3)	-0.002(2)	-0.001(2)	0.002(2)
N9	0.025(4)	0.015(5)	0.035(5)	0.001(5)	0.001(3)	-0.002(4)
N10	0.022(3)	0.029(3)	0.025(3)	-0.002(2)	0.002(2)	0.005(3)
B2A	0.042(15)	0.089(23)	0.052(16)	-0.012(15)	-0.002(12)	-0.016(15)
F5A	0.059(10)	0.147(18)	0.088(12)	0.005(11)	-0.010(8)	0.016(11)
F6A	0.147(23)	0.033(9)	0.090(14)	0.017(9)	0.003(14)	-0.007(11)
F7b	0.053(9)	0.085(13)	0.188(21)	0.001(13)	0.004(11)	0.015(9)
F8A	0.087(14)	0.327(42)	0.059(11)	0.013(17)	-0.025(10)	-0.036(19)
B2	0.057(9)	0.068(10)	0.070(10)	-0.008(8)	0.010(8)	-0.007(8)
F5	0.055(8)	0.096(11)	0.141(14)	0.017(10)	-0.005(8)	-0.026(7)
F6	0.065(8)	0.064(8)	0.101(10)	-0.016(7)	0.028(7)	-0.002(6)
F7	0.113(14)	0.167(19)	0.105(13)	-0.031(13)	-0.010(10)	0.005(13)
F8	0.072(10)	0.010(7)	0.214(21)	0.022(9)	0.013(11)	-0.001(6)
B1	0.084(9)	0.038(6)	0.056(7)	-0.008(5)	-0.002(6)	0.004(6)
F1	0.089(5)	0.065(4)	0.086(5)	-0.003(3)	-0.003(4)	0.031(4)
F2	0.117(7)	0.069(5)	0.227(11)	0.048(6)	0.068(7)	0.030(5)

Table A6 continued.

F3	0.108(9)	0.140(13)	0.287(21)	-0.053(12)	-0.093(10)	0.009(8)
F4	0.261(15)	0.216(13)	0.065(6)	0.005(6)	0.013(7)	0.157(12)

The anisotropic displacement factor exponent takes the form:
$-2\pi^2 [h^2 a^{*2} U11 + ... + 2 h k a^* b^* U12]$

Table A6 continued.

Hydrogen coordinates (x 10^4) and isotropic displacement parameters ($Å^2$ x 10^3).

	x	y	z	U(eq)	Occ.
H11	0.6784(94)	0.2816(39)	-0.2712(51)	0.049	1
H13	0.2403(73)	0.2815(33)	-0.0534(42)	0.035	1
H14	0.0896(7)	0.3452(4)	-0.0460(4)	0.044	1
H16A	0.3115(8)	0.4367(3)	0.0798(4)	0.047	1
H18	0.1589(7)	0.1490(3)	0.0821(4)	0.043	1
H19A	0.2135(8)	0.0943(4)	0.1767(5)	0.051	1
H2	0.4694(82)	0.2818(38)	-0.0799(45)	0.029	1
H20	0.4659(82)	0.3781(36)	0.0605(45)	0.039	1
H21	0.3092(73)	0.2095(34)	0.0414(44)	0.034	1
H22	0.8268(54)	0.2466(93)	0.1664(30)	0.036	1
H23	0.9067(85)	0.1998(39)	0.2659(47)	0.047	1
H24	0.7882(88)	0.1330(42)	0.3201(50)	0.051	1
H25	0.8925(82)	0.2801(36)	-0.1125(47)	0.042	1
H27	0.9541(75)	0.1412(35)	0.0121(43)	0.039	1
H28A	0.6924(8)	0.3806(4)	-0.0177(5)	0.044	1
H29	0.7503(83)	0.3440(41)	0.1782(47)	0.044	1
H3	0.8606(71)	0.3037(34)	0.0170(40)	0.029	1
H30	0.7248(97)	0.4305(43)	0.2040(56)	0.060	1
H31A	0.3635(8)	0.0205(4)	-0.0424(5)	0.064	1
H31B	0.2698(8)	0.0582(4)	-0.0079(5)	0.064	1
H31C	0.3643(8)	0.0233(4)	0.0380(5)	0.064	1
H33	0.6905(9)	0.4717(4)	0.0094(5)	0.055	1
H35	1.1123(83)	0.1268(39)	-0.0599(46)	0.041	1
H37	1.0564(7)	0.2600(4)	-0.1673(4)	0.046	1
H38A	0.4070(7)	0.1037(4)	0.2333(5)	0.046	1
H39A	0.1049(14)	0.4676(5)	0.0545(8)	0.095	1
H39B	0.0128(14)	0.4185(5)	0.0479(8)	0.095	1
H39C	0.0452(14)	0.4505(5)	-0.0180(8)	0.095	1

Table A6 continued.

H40A	0.4379(9)	0.3650(5)	0.2939(6)	0.090	1
H40B	0.3113(9)	0.3397(5)	0.2676(6)	0.090	1
H40C	0.3592(9)	0.3925(5)	0.2327(6)	0.090	1
H41	0.5130(82)	0.1326(40)	-0.2711(47)	0.045	1
H43A	0.5558(9)	0.1700(5)	-0.3807(4)	0.082	1
H43B	0.6801(9)	0.2022(5)	-0.3765(4)	0.082	1
H43C	0.5554(9)	0.2339(5)	-0.3866(4)	0.082	1
H44A	0.7988(10)	0.0508(4)	0.1930(6)	0.090	1
H44B	0.9269(10)	0.0678(4)	0.1687(6)	0.090	1
H44C	0.8511(10)	0.0213(4)	0.1301(6)	0.090	1
H45A	1.2483(8)	0.1429(4)	-0.1407(5)	0.073	1
H45B	1.2729(8)	0.2053(4)	-0.1508(5)	0.073	1
H45C	1.1886(8)	0.1734(4)	-0.2056(5)	0.073	1
H46A	0.7265(14)	0.5281(4)	0.1791(7)	0.119	1
H46B	0.6396(14)	0.5397(4)	0.1130(7)	0.119	1
H46C	0.7822(14)	0.5412(4)	0.1091(7)	0.119	1
H48A	0.8272(60)	0.0089(25)	-0.1378(30)	0.873	0.535(10)
H48B	0.9089(60)	0.0581(25)	-0.1580(30)	0.873	0.535(10)
H48C	0.7815(60)	0.0477(25)	-0.1984(30)	0.873	0.535(10)
H48D	0.8512(60)	0.0676(25)	-0.1917(30)	0.873	0.535(10)
H48E	0.7695(60)	0.0184(25)	-0.1715(30)	0.873	0.535(10)
H48F	0.8969(60)	0.0287(25)	-0.1311(30)	0.873	0.535(10)
H5	0.6699(81)	0.2906(38)	-0.1591(45)	0.040	1
H6	0.4973(7)	0.1441(3)	-0.1552(4)	0.039	1
H8	0.5976(79)	0.1131(38)	0.2908(45)	0.045	1

Symmetry transformations used to generate equivalent atoms:
#1 -x-1,-y+1,-z+1

Table A6 continued.

Torsion angles [°].

N6	Rh1	Rh2	N4	-80.3(5)
N9	Rh1	Rh2	N4	101.0(5)
N5	Rh1	Rh2	N4	8.5(5)
N10	Rh1	Rh2	N4	-171.6(4)
N1	Rh1	Rh2	N4	-50.7(55)
N6	Rh1	Rh2	N3	7.8(6)
N9	Rh1	Rh2	N3	-171.0(6)
N5	Rh1	Rh2	N3	96.6(7)
N10	Rh1	Rh2	N3	-83.5(7)
N1	Rh1	Rh2	N3	37.4(62)
N6	Rh1	Rh2	N7	104.1(4)
N9	Rh1	Rh2	N7	-74.7(5)
N5	Rh1	Rh2	N7	-167.1(5)
N10	Rh1	Rh2	N7	12.8(5)
N1	Rh1	Rh2	N7	133.7(60)
N6	Rh1	Rh2	N8	-176.6(7)
N9	Rh1	Rh2	N8	4.7(7)
N5	Rh1	Rh2	N8	-87.8(6)
N10	Rh1	Rh2	N8	92.1(6)
N1	Rh1	Rh2	N8	-147.0(53)
N6	Rh1	Rh2	N2	130.1(21)
N9	Rh1	Rh2	N2	-48.7(21)
N5	Rh1	Rh2	N2	-141.2(21)
N10	Rh1	Rh2	N2	38.7(21)
N1	Rh1	Rh2	N2	159.7(66)
C6	C4	C5	C11	-1.0(21)
N6	C4	C5	C11	-177.8(14)
C5	C4	C6	C41	-1.9(14)
N6	C4	C6	C41	174.9(7)
N7	C1	C7	N8	-2.2(11)
C38	C1	C7	N8	178.0(8)
N7	C1	C7	C8	179.4(8)
C38	C1	C7	C8	-0.5(14)
N8	C7	C8	C24	1.4(12)
C1	C7	C8	C24	179.9(8)
C4	C5	C11	C42	5.5(36)

Table A6 continued.

C20	C12	C13	C14	1.1(11)
N3	C12	C13	C14	-179.2(7)
C12	C13	C14	C15	-2.2(12)
C13	C14	C15	C16	0.9(12)
C13	C14	C15	C39	-173.7(10)
C14	C15	C16	C20	1.4(13)
C39	C15	C16	C20	175.9(10)
C21	C18	C19	C38	0.8(13)
C15	C16	C20	C12	-2.5(13)
C13	C12	C20	C16	1.2(11)
N3	C12	C20	C16	-178.5(7)
C19	C18	C21	N7	0.5(12)
N8	C22	C23	C24	-0.3(13)
C22	C23	C24	C8	1.6(14)
C7	C8	C24	C23	-2.2(14)
C37	C25	C26	C27	0.6(14)
C37	C25	C26	N5	178.7(9)
C25	C26	C27	C35	0.4(13)
N5	C26	C27	C35	-177.8(8)
C29	C9	C28	C33	-0.4(16)
N4	C9	C28	C33	176.4(10)
C28	C9	C29	C30	-0.6(16)
N4	C9	C29	C30	-177.3(10)
C9	C29	C30	C34	1.9(17)
C9	C28	C33	C34	0.0(16)
C28	C33	C34	C30	1.2(15)
C28	C33	C34	C46	179.0(11)
C29	C30	C34	C33	-2.2(17)
C29	C30	C34	C46	-179.9(11)
C26	C27	C35	C36	-1.0(13)
C27	C35	C36	C37	0.7(12)
C27	C35	C36	C45	179.4(8)
C35	C36	C37	C25	0.3(13)
C45	C36	C37	C25	-178.4(10)
C26	C25	C37	C36	-0.9(15)
C18	C19	C38	C1	-1.3(14)
N7	C1	C38	C19	0.5(14)
C7	C1	C38	C19	-179.7(8)

Table A6 continued.

C4	C6	C41	C42	1.1(12)
C5	C11	C42	C41	-6.2(34)
C5	C11	C42	C43	175.0(21)
C6	C41	C42	C11	2.8(17)
C6	C41	C42	C43	-178.5(8)
C48A	C47b	N1	Rh1	-160.3(130)
N6	Rh1	N1	C47b	-167.0(78)
N9	Rh1	N1	C47b	11.7(79)
N5	Rh1	N1	C47b	104.4(79)
N10	Rh1	N1	C47b	-75.4(78)
Rh2	Rh1	N1	C47b	163.5(87)
C40	C17	N2	Rh2	-118.6(262)
N4	Rh2	N2	C17	151.9(96)
N3	Rh2	N2	C17	63.2(105)
N7	Rh2	N2	C17	-32.6(102)
N8	Rh2	N2	C17	-112.3(96)
Rh1	Rh2	N2	C17	-58.7(111)
N6	C2	N3	C12	-171.2(7)
N6	C2	N3	Rh2	8.6(14)
C20	C12	N3	C2	-128.5(8)
C13	C12	N3	C2	51.9(9)
C20	C12	N3	Rh2	51.7(13)
C13	C12	N3	Rh2	-127.9(11)
N4	Rh2	N3	C2	74.8(13)
N7	Rh2	N3	C2	-102.1(7)
N8	Rh2	N3	C2	-77.9(88)
N2	Rh2	N3	C2	173.7(6)
Rh1	Rh2	N3	C2	-10.6(10)
N4	Rh2	N3	C12	-105.4(6)
N7	Rh2	N3	C12	77.7(14)
N8	Rh2	N3	C12	101.9(96)
N2	Rh2	N3	C12	-6.5(14)
Rh1	Rh2	N3	C12	169.2(6)
N5	C3	N4	C9	-173.0(11)
N5	C3	N4	Rh2	-1.1(17)
C28	C9	N4	C3	62.5(14)
C29	C9	N4	C3	-120.9(11)
C28	C9	N4	Rh2	-109.3(11)

Table A6 continued.

C29	C9	N4	Rh2	67.2(13)
N3	Rh2	N4	C3	-94.0(12)
N7	Rh2	N4	C3	49.8(77)
N8	Rh2	N4	C3	83.8(10)
N2	Rh2	N4	C3	170.5(8)
Rh1	Rh2	N4	C3	-6.9(9)
N3	Rh2	N4	C9	77.4(9)
N7	Rh2	N4	C9	-138.8(79)
N8	Rh2	N4	C9	-104.8(12)
N2	Rh2	N4	C9	-18.1(10)
Rh1	Rh2	N4	C9	164.5(7)
N4	C3	N5	C26	-178.3(9)
N4	C3	N5	Rh1	12.2(16)
C27	C26	N5	C3	129.4(9)
C25	C26	N5	C3	-48.8(14)
C27	C26	N5	Rh1	-61.2(10)
C25	C26	N5	Rh1	120.6(9)
N6	Rh1	N5	C3	71.4(8)
N9	Rh1	N5	C3	-109.2(8)
N10	Rh1	N5	C3	169.7(66)
N1	Rh1	N5	C3	165.2(8)
Rh2	Rh1	N5	C3	-12.9(8)
N6	Rh1	N5	C26	-97.7(7)
N9	Rh1	N5	C26	81.7(7)
N10	Rh1	N5	C26	0.6(75)
N1	Rh1	N5	C26	-4.0(7)
Rh2	Rh1	N5	C26	177.9(8)
N3	C2	N6	C4	-176.8(7)
N3	C2	N6	Rh1	1.5(11)
C5	C4	N6	C2	63.9(12)
C6	C4	N6	C2	-112.9(8)
C5	C4	N6	Rh1	-114.4(10)
C6	C4	N6	Rh1	68.8(8)
N9	Rh1	N6	C2	112.4(136)
N5	Rh1	N6	C2	-93.4(6)
N10	Rh1	N6	C2	89.1(6)
N1	Rh1	N6	C2	173.6(6)
Rh2	Rh1	N6	C2	-7.5(7)

Table A6 continued.

N9	Rh1	N6	C4	-69.4(137)
N5	Rh1	N6	C4	84.7(6)
N10	Rh1	N6	C4	-92.7(5)
N1	Rh1	N6	C4	-8.3(5)
Rh2	Rh1	N6	C4	170.6(7)
C18	C21	N7	C1	-1.3(11)
C18	C21	N7	Rh2	-178.4(10)
C38	C1	N7	C21	0.8(12)
C7	C1	N7	C21	-179.1(7)
C38	C1	N7	Rh2	178.3(10)
C7	C1	N7	Rh2	-1.6(12)
N4	Rh2	N7	C21	-145.2(73)
N3	Rh2	N7	C21	-1.6(14)
N8	Rh2	N7	C21	-179.6(6)
N2	Rh2	N7	C21	93.5(6)
Rh1	Rh2	N7	C21	-88.7(10)
N4	Rh2	N7	C1	37.6(82)
N3	Rh2	N7	C1	-178.8(7)
N8	Rh2	N7	C1	3.1(10)
N2	Rh2	N7	C1	-83.7(8)
Rh1	Rh2	N7	C1	94.0(5)
C23	C22	N8	C7	-0.5(12)
C23	C22	N8	Rh2	175.7(10)
C8	C7	N8	C22	-0.1(11)
C1	C7	N8	C22	-178.6(7)
C8	C7	N8	Rh2	-176.6(10)
C1	C7	N8	Rh2	4.8(12)
N4	Rh2	N8	C22	2.3(14)
N3	Rh2	N8	C22	154.8(86)
N7	Rh2	N8	C22	179.3(6)
N2	Rh2	N8	C22	-96.4(6)
Rh1	Rh2	N8	C22	87.7(11)
N4	Rh2	N8	C7	178.6(7)
N3	Rh2	N8	C7	-28.9(95)
N7	Rh2	N8	C7	-4.3(10)
N2	Rh2	N8	C7	79.9(10)
Rh1	Rh2	N8	C7	-96.0(5)
C44	C32	N9	Rh1	-41.3(588)

Table A6 continued.

N6	Rh1	N9	C32	36.7(207)
N5	Rh1	N9	C32	-117.4(95)
N10	Rh1	N9	C32	60.0(95)
N1	Rh1	N9	C32	-24.5(95)
Rh2	Rh1	N9	C32	156.5(95)
C31	C10	N10	Rh1	101.2(1000)
N6	Rh1	N10	C10	132.7(36)
N9	Rh1	N10	C10	-46.7(36)
N5	Rh1	N10	C10	34.5(89)
N1	Rh1	N10	C10	39.1(36)
Rh2	Rh1	N10	C10	-142.8(36)

Table A6 continued.

N9	Rh1	N6	C4	-69.4(137)
N5	Rh1	N6	C4	84.7(6)
N10	Rh1	N6	C4	-92.7(5)
N1	Rh1	N6	C4	-8.3(5)
Rh2	Rh1	N6	C4	170.6(7)
C18	C21	N7	C1	-1.3(11)
C18	C21	N7	Rh2	-178.4(10)
C38	C1	N7	C21	0.8(12)
C7	C1	N7	C21	-179.1(7)
C38	C1	N7	Rh2	178.3(10)
C7	C1	N7	Rh2	-1.6(12)
N4	Rh2	N7	C21	-145.2(73)
N3	Rh2	N7	C21	-1.6(14)
N8	Rh2	N7	C21	-179.6(6)
N2	Rh2	N7	C21	93.5(6)
Rh1	Rh2	N7	C21	-88.7(10)
N4	Rh2	N7	C1	37.6(82)
N3	Rh2	N7	C1	-178.8(7)
N8	Rh2	N7	C1	3.1(10)
N2	Rh2	N7	C1	-83.7(8)
Rh1	Rh2	N7	C1	94.0(5)
C23	C22	N8	C7	-0.5(12)
C23	C22	N8	Rh2	175.7(10)
C8	C7	N8	C22	-0.1(11)
C1	C7	N8	C22	-178.6(7)
C8	C7	N8	Rh2	-176.6(10)
C1	C7	N8	Rh2	4.8(12)
N4	Rh2	N8	C22	2.3(14)
N3	Rh2	N8	C22	154.8(86)
N7	Rh2	N8	C22	179.3(6)
N2	Rh2	N8	C22	-96.4(6)
Rh1	Rh2	N8	C22	87.7(11)
N4	Rh2	N8	C7	178.6(7)
N3	Rh2	N8	C7	-28.9(95)
N7	Rh2	N8	C7	-4.3(10)
N2	Rh2	N8	C7	79.9(10)
Rh1	Rh2	N8	C7	-96.0(5)
C44	C32	N9	Rh1	-41.3(588)

Table A7. Crystal data and structure refinement for $[Rh_2(DTolF)_2(bpy)_2(CH_3CN)][BF_4]_2$ (8a).

Identification code	$[Rh_2(DTolF)_2(bpy)_2(CH_3CN)][BF_4]_2$
Empirical formula	C52 H49 B2 F8 N9 Rh2
Formula weight	1179.44 g/mol
Temperature	293(2) K
Wavelength	0.71073 Å
Crystal system	monoclinic
Space group	$P2_1/c$
Unit cell dimensions	a = 19.4534(4) Å
	b = 13.8298(3) Å
	c = 19.8218(5) Å
	$\alpha = 90^\circ$
	$\beta = 109.189(1)^\circ$
	$\gamma = 90^\circ$
Volume	5036.5(2) $Å^3$
Z	4
ρ_{calc}	1.555 g/cm^3

Table A7 continued.

μ	0.731 cm^{-3}
F(000)	2384
Crystal size	0.13 x 0.13 x 0.10 mm^3
Theta range for data collection	1.83 to 28.29°
Index ranges	-22<=h<=25, -18<=k<=17, -26<=l<=25
Reflections collected	36549
Independent reflections	11838 [R(int) = 0.0767]
Refinement method	Full-matrix least-squares on F^2
Data / restraints / parameters	11838 / 0 / 668
Goodness-of-fit on F^2	1.024
Final R indices [$I>2\sigma(I)$]	R1 = 0.0600, wR2 = 0.0891
R indices (all data)	R1 = 0.1268, wR2 = 0.1052
Largest diff. peak and hole	0.492 and -0.520 $e^-/Å^{-3}$

Table A7 continued.

Atomic coordinates (x 10^4) and equivalent isotropic displacement parameters ($Å^2$ x 10^3).

	x	y	z	U(eq)	Occ.
B1	0.4593(4)	0.6097(6)	0.1589(3)	0.051(2)	1
B2	0.1422(4)	0.4291(5)	0.1622(4)	0.051(2)	1
C1	0.3253(3)	0.2353(4)	0.4747(3)	0.0454(14)	1
C10	0.1561(3)	-0.1807(4)	0.2757(3)	0.0419(14)	1
C11	0.1276(3)	-0.2643(4)	0.2943(3)	0.0445(14)	1
C12	0.3949(3)	0.1577(3)	0.0429(3)	0.0413(13)	1
C13	0.4780(3)	-0.2893(4)	0.3959(3)	0.0379(13)	1
C14	0.4673(3)	-0.1759(4)	0.4822(3)	0.0403(13)	1
C15	0.1693(3)	-0.3271(3)	0.3445(3)	0.0336(12)	1
C16	0.2915(2)	0.1688(3)	0.3561(2)	0.0261(11)	1
C17	0.1466(3)	0.1347(3)	0.1754(3)	0.0355(12)	1
C18	0.0776(3)	0.1578(4)	0.1308(3)	0.0393(13)	1
C19	0.2532(3)	-0.0826(3)	0.0617(2)	0.0296(11)	1
C2	0.2414(3)	-0.3036(4)	0.3767(3)	0.058(2)	1
C20	0.2998(3)	0.3253(4)	0.4484(3)	0.0426(14)	1
C21	0.3313(3)	-0.0843(3)	0.0742(2)	0.0334(12)	1
C22	0.3092(3)	-0.3085(4)	0.2208(3)	0.0373(12)	1
C23	0.4367(2)	-0.1274(3)	0.3592(2)	0.0281(11)	1
C24	0.2007(3)	-0.0812(3)	-0.0067(3)	0.0425(14)	1
C25	0.3019(3)	-0.4116(4)	0.2318(3)	0.064(2)	1
C26	0.4600(2)	0.1904(3)	0.2882(2)	0.0283(11)	1
C27	0.5356(3)	0.1887(4)	0.3121(2)	0.0345(12)	1
C28	0.4554(2)	-0.2193(3)	0.3429(2)	0.0313(11)	1
C29	0.5745(3)	0.2740(4)	0.3260(3)	0.0395(13)	1
C3	0.2706(3)	-0.2202(4)	0.3578(3)	0.053(2)	1
C30	0.2677(2)	0.2601(3)	0.3291(2)	0.0300(11)	1
C31	0.1953(3)	0.1537(3)	0.0842(2)	0.0299(11)	1

Table A7 continued.

C32	0.4461(3)	-0.0796(3)	0.1617(3)	0.0411(13)	1
C33	0.4420(2)	0.0282(3)	0.3159(2)	0.0296(11)	1
C34	0.2629(3)	0.1530(3)	0.0658(2)	0.0287(11)	1
C35	0.2283(2)	-0.1581(3)	0.3061(2)	0.0256(10)	1
C36	0.2717(3)	0.3375(4)	0.3748(3)	0.0379(13)	1
C37	0.3218(3)	0.1574(4)	0.4295(2)	0.0380(13)	1
C38	0.1623(3)	-0.0793(3)	0.1128(2)	0.0326(11)	1
C39	0.4659(3)	0.3644(3)	0.2845(3)	0.0352(12)	1
C4	0.3633(3)	-0.0910(3)	0.0218(3)	0.0454(15)	1
C40	0.4261(3)	0.2798(3)	0.2730(2)	0.0339(12)	1
C41	0.4445(2)	-0.1059(4)	0.4299(2)	0.0334(12)	1
C42	0.3896(3)	0.1439(3)	0.1101(3)	0.0345(12)	1
C43	0.2626(2)	0.0057(3)	0.3237(2)	0.0253(11)	1
C44	0.3035(4)	0.4094(4)	0.4990(3)	0.075(2)	1
C45	0.5059(3)	-0.3470(4)	0.5232(3)	0.062(2)	1
C46	0.4378(4)	-0.0917(4)	0.0401(3)	0.056(2)	1
C47	0.4805(3)	-0.0862(4)	0.1103(3)	0.052(2)	1
C48	0.5838(3)	0.4558(4)	0.3311(3)	0.051(2)	1
C49	0.1280(3)	0.1756(3)	0.0366(3)	0.0373(13)	1
C5	0.1281(3)	-0.0779(3)	-0.0127(3)	0.0450(14)	1
C50	0.2654(3)	0.1666(3)	-0.0030(3)	0.0392(13)	1
C51	0.4835(3)	-0.2691(4)	0.4661(3)	0.0394(13)	1
C52	0.5408(3)	0.3633(4)	0.3131(3)	0.0337(12)	1
C6	0.1083(3)	-0.0781(4)	0.0475(3)	0.0412(13)	1
C7	0.0688(3)	0.1788(3)	0.0604(3)	0.0384(13)	1
C8	0.1372(3)	-0.4184(4)	0.3643(3)	0.0489(14)	1
C9	0.3314(3)	0.1681(3)	-0.0148(3)	0.0458(15)	1
F1	0.3879(2)	0.5886(3)	0.1236(2)	0.0929(14)	1
F2	0.5020(2)	0.5379(3)	0.1484(2)	0.0846(12)	1
F3	0.4711(2)	0.6218(3)	0.2306(2)	0.0759(11)	1
F4	0.4620(11)	0.6962(9)	0.1366(10)	0.181(12)	0.530(7)
F4A	0.4887(7)	0.6826(12)	0.1239(9)	0.114(7)	0.530(7)
F5	0.1549(2)	0.4468(3)	0.2331(2)	0.0805(11)	1
F6	0.1967(2)	0.3677(2)	0.1552(2)	0.0748(11)	1
F7	0.0743(2)	0.3878(2)	0.1308(2)	0.0757(11)	1
F8	0.1454(2)	0.5150(2)	0.1270(2)	0.0608(9)	1
N1	0.3259(2)	0.1400(2)	0.1224(2)	0.0262(9)	1
N2	0.4165(2)	0.1055(3)	0.2773(2)	0.0272(9)	1

Table A7 continued.

N3	0.2848(2)	0.0902(2)	0.3079(2)	0.0245(9)	1
N4	0.2050(2)	0.1320(3)	0.1545(2)	0.0255(9)	1
N5	0.3160(2)	-0.2275(3)	0.2150(2)	0.0312(9)	1
N6	0.3740(2)	-0.0781(3)	0.1452(2)	0.0311(9)	1
N7	0.4100(2)	-0.0567(3)	0.3040(2)	0.0274(9)	1
N8	0.2583(2)	-0.0729(3)	0.2847(2)	0.0287(9)	1
N9	0.2333(2)	-0.0807(2)	0.1206(2)	0.0264(9)	1
Rh1	0.30997(2)	0.11177(3)	0.21729(2)	0.02391(10)	1
Rh2	0.31749(2)	-0.07455(3)	0.21531(2)	0.02421(10)	1

U(eq) is defined as one third of the trace of the orthogonalized Uij tensor.

Table A7 continued.

Bond lengths [Å] and angles [°].

Rh1	N2	2.023(4)
Rh1	N3	2.032(3)
Rh1	N4	2.032(4)
Rh1	N1	2.042(3)
Rh1	Rh2	2.5820(5)
Rh2	N6	2.037(4)
Rh2	N9	2.047(3)
Rh2	N8	2.064(3)
Rh2	N7	2.076(4)
Rh2	N5	2.115(4)
N1	C42	1.341(5)
N1	C34	1.374(5)
N2	C33	1.314(5)
N2	C26	1.422(5)
N3	C43	1.319(5)
N3	C16	1.426(5)
N4	C17	1.331(5)
N4	C31	1.376(5)
N5	C22	1.139(6)
N6	C32	1.331(6)
N6	C21	1.382(6)
N7	C33	1.315(5)
N7	C23	1.430(5)
N8	C43	1.319(5)
N8	C35	1.439(5)
N9	C38	1.339(5)
N9	C19	1.345(5)
F1	B1	1.366(7)
F2	B1	1.353(7)
F3	B1	1.374(7)
F4	F4A	0.67(4)
F4	B1	1.283(15)
F4A	B1	1.44(2)
F5	B2	1.366(7)
F6	B2	1.400(7)

Table A7 continued.

F7	B2	1.384(8)
F8	B2	1.389(7)
C1	C20	1.378(7)
C1	C37	1.388(6)
C2	C15	1.376(7)
C2	C3	1.389(7)
C3	C35	1.382(6)
C4	C46	1.373(7)
C4	C21	1.378(6)
C5	C6	1.368(7)
C5	C24	1.378(7)
C6	C38	1.373(6)
C7	C18	1.379(7)
C7	C49	1.382(7)
C8	C15	1.517(6)
C9	C50	1.379(7)
C9	C12	1.389(7)
C10	C35	1.371(6)
C10	C11	1.384(7)
C11	C15	1.368(7)
C12	C42	1.381(6)
C13	C51	1.389(7)
C13	C28	1.389(6)
C14	C41	1.381(6)
C14	C51	1.388(7)
C16	C37	1.388(6)
C16	C30	1.389(6)
C17	C18	1.382(6)
C19	C24	1.403(6)
C19	C21	1.457(6)
C20	C36	1.388(6)
C20	C44	1.523(6)
C22	C25	1.457(7)
C23	C28	1.389(6)
C23	C41	1.393(6)
C26	C40	1.387(6)
C26	C27	1.390(6)
C27	C29	1.379(6)

Table A7 continued.

C29	C52	1.383(6)	
C30	C36	1.388(6)	
C31	C49	1.373(6)	
C31	C34	1.477(6)	
C32	C47	1.393(7)	
C34	C50	1.392(6)	
C39	C52	1.379(6)	
C39	C40	1.380(6)	
C45	C51	1.519(7)	
C46	C47	1.367(8)	
C48	C52	1.507(6)	
N2	Rh1	N3	88.36(14)
N2	Rh1	N4	174.20(14)
N3	Rh1	N4	94.36(14)
N2	Rh1	N1	96.55(15)
N3	Rh1	N1	174.53(14)
N4	Rh1	N1	80.53(14)
N2	Rh1	Rh2	85.08(10)
N3	Rh1	Rh2	84.15(10)
N4	Rh1	Rh2	100.28(10)
N1	Rh1	Rh2	98.63(10)
N6	Rh2	N9	79.73(15)
N6	Rh2	N8	178.65(15)
N9	Rh2	N8	99.12(14)
N6	Rh2	N7	93.97(15)
N9	Rh2	N7	172.25(14)
N8	Rh2	N7	87.24(14)
N6	Rh2	N5	89.03(14)
N9	Rh2	N5	87.11(14)
N8	Rh2	N5	90.21(15)
N7	Rh2	N5	97.37(15)
N6	Rh2	Rh1	94.62(10)
N9	Rh2	Rh1	91.34(10)
N8	Rh2	Rh1	86.09(10)
N7	Rh2	Rh1	84.63(10)
N5	Rh2	Rh1	175.72(11)
C42	N1	C34	118.3(4)
C42	N1	Rh1	127.2(3)

Table A7 continued.

C34	N1	Rh1	114.4(3)
C33	N2	C26	119.4(4)
C33	N2	Rh1	119.7(3)
C26	N2	Rh1	119.9(3)
C43	N3	C16	118.8(4)
C43	N3	Rh1	122.2(3)
C16	N3	Rh1	119.0(3)
C17	N4	C31	117.6(4)
C17	N4	Rh1	127.0(3)
C31	N4	Rh1	115.2(3)
C22	N5	Rh2	170.2(4)
C32	N6	C21	118.8(4)
C32	N6	Rh2	126.4(3)
C21	N6	Rh2	114.7(3)
C33	N7	C23	116.2(4)
C33	N7	Rh2	119.1(3)
C23	N7	Rh2	124.2(3)
C43	N8	C35	117.1(4)
C43	N8	Rh2	117.2(3)
C35	N8	Rh2	123.8(3)
C38	N9	C19	118.6(4)
C38	N9	Rh2	126.2(3)
C19	N9	Rh2	115.2(3)
F4A	F4	B1	89.6(23)
F4	F4A	B1	62.7(21)
F4	B1	F2	122.3(13)
F4	B1	F1	99.9(10)
F2	B1	F1	109.7(5)
F4	B1	F3	103.4(10)
F2	B1	F3	110.3(5)
F1	B1	F3	110.6(6)
F4	B1	F4A	27.8(15)
F2	B1	F4A	94.5(9)
F1	B1	F4A	113.5(7)
F3	B1	F4A	117.0(9)
F5	B2	F7	111.0(6)
F5	B2	F8	109.9(5)
F7	B2	F8	108.7(5)

Table A7 continued.

F5	B2	F6	108.9(5)
F7	B2	F6	110.3(5)
F8	B2	F6	108.0(5)
C20	C1	C37	121.4(5)
C15	C2	C3	121.0(5)
C35	C3	C2	121.3(5)
C46	C4	C21	120.0(5)
C6	C5	C24	119.9(5)
C5	C6	C38	118.3(5)
C18	C7	C49	120.0(5)
C50	C9	C12	119.0(5)
C35	C10	C11	121.1(5)
C15	C11	C10	122.0(5)
C42	C12	C9	118.7(5)
C51	C13	C28	121.2(5)
C41	C14	C51	121.4(5)
C11	C15	C2	117.2(4)
C11	C15	C8	121.4(5)
C2	C15	C8	121.4(5)
C37	C16	C30	118.7(4)
C37	C16	N3	122.0(4)
C30	C16	N3	119.3(4)
N4	C17	C18	123.8(5)
C7	C18	C17	117.9(5)
N9	C19	C24	120.9(5)
N9	C19	C21	115.7(4)
C24	C19	C21	123.4(4)
C1	C20	C36	118.5(4)
C1	C20	C44	120.5(5)
C36	C20	C44	121.1(5)
C4	C21	N6	120.1(5)
C4	C21	C19	125.3(5)
N6	C21	C19	114.6(4)
N5	C22	C25	177.4(6)
C28	C23	C41	118.7(4)
C28	C23	N7	120.3(4)
C41	C23	N7	121.0(4)
C5	C24	C19	118.9(5)

Table A7 continued.

C40	C26	C27	117.6(4)
C40	C26	N2	119.1(4)
C27	C26	N2	123.3(4)
C29	C27	C26	120.2(5)
C23	C28	C13	120.3(4)
C27	C29	C52	122.0(5)
C36	C30	C16	120.6(4)
C49	C31	N4	121.8(4)
C49	C31	C34	123.8(4)
N4	C31	C34	114.4(4)
N6	C32	C47	122.8(5)
N2	C33	N7	123.8(4)
N1	C34	C50	120.7(4)
N1	C34	C31	115.2(4)
C50	C34	C31	124.1(4)
C10	C35	C3	117.2(4)
C10	C35	N8	120.9(4)
C3	C35	N8	121.8(4)
C30	C36	C20	120.7(5)
C1	C37	C16	120.1(5)
N9	C38	C6	123.4(4)
C52	C39	C40	121.2(5)
C39	C40	C26	121.2(4)
C14	C41	C23	120.4(5)
N1	C42	C12	123.2(5)
N8	C43	N3	123.6(4)
C4	C46	C47	120.2(5)
C46	C47	C32	118.0(5)
C31	C49	C7	119.0(5)
C9	C50	C34	120.1(5)
C13	C51	C14	118.0(5)

Table A7 continued.

C13	C51	C45	120.8(5)
C14	C51	C45	121.2(5)
C39	C52	C29	117.4(4)
C39	C52	C48	121.1(5)
C29	C52	C48	121.5(5)

Symmetry transformations used to generate equivalent atoms:
#1 -x-1,-y+1,-z+1

Table A7 continued.

Anisotropic displacement parameters ($Å^2 \times 10^3$).

	U11	U22	U33	U23	U13	U12
Rh1	0.0227(2)	0.0222(2)	0.0253(2)	-0.0019(2)	0.00580(15)	-0.0012(2)
Rh2	0.0245(2)	0.0221(2)	0.0251(2)	-0.0030(2)	0.00676(15)	-0.0029(2)
N1	0.027(2)	0.019(2)	0.034(2)	-0.001(2)	0.012(2)	-0.004(2)
N2	0.023(2)	0.019(2)	0.037(2)	-0.001(2)	0.006(2)	-0.003(2)
N3	0.026(2)	0.021(2)	0.024(2)	-0.002(2)	0.004(2)	0.000(2)
N4	0.024(2)	0.025(2)	0.026(2)	-0.002(2)	0.006(2)	-0.004(2)
N5	0.030(2)	0.032(2)	0.028(2)	-0.002(2)	0.005(2)	-0.001(2)
N6	0.033(2)	0.019(2)	0.043(2)	-0.002(2)	0.016(2)	0.000(2)
N7	0.022(2)	0.022(2)	0.033(2)	0.000(2)	0.002(2)	0.000(2)
N8	0.031(2)	0.028(2)	0.029(2)	0.000(2)	0.011(2)	-0.003(2)
N9	0.032(2)	0.019(2)	0.025(2)	-0.002(2)	0.006(2)	-0.005(2)
F1	0.047(2)	0.158(4)	0.062(2)	-0.040(2)	0.002(2)	0.005(2)
F2	0.078(3)	0.097(3)	0.080(3)	-0.028(2)	0.028(2)	0.022(2)
F3	0.069(2)	0.101(3)	0.043(2)	-0.029(2)	-0.002(2)	0.022(2)
F4	0.391(30)	0.016(5)	0.085(9)	0.031(5)	0.011(14)	0.001(10)
F4A	0.066(6)	0.136(14)	0.105(11)	0.005(8)	-0.018(6)	-0.051(7)
F5	0.113(3)	0.081(3)	0.045(2)	-0.005(2)	0.022(2)	-0.005(2)
F6	0.083(3)	0.064(2)	0.069(2)	-0.002(2)	0.014(2)	0.022(2)
F7	0.073(3)	0.047(2)	0.091(3)	-0.004(2)	0.005(2)	-0.012(2)
F8	0.067(2)	0.047(2)	0.068(2)	0.013(2)	0.022(2)	0.002(2)
B1	0.048(4)	0.050(5)	0.040(4)	-0.011(3)	-0.005(3)	0.003(4)
B2	0.066(5)	0.040(4)	0.044(4)	-0.007(3)	0.016(4)	-0.001(4)
C1	0.067(4)	0.042(3)	0.023(3)	-0.009(2)	0.010(3)	0.001(3)
C2	0.033(3)	0.058(4)	0.077(4)	0.040(3)	0.012(3)	0.006(3)
C3	0.028(3)	0.068(4)	0.052(4)	0.025(3)	0.000(3)	-0.010(3)
C4	0.073(4)	0.029(3)	0.049(3)	-0.006(2)	0.040(3)	0.001(3)
C5	0.055(4)	0.027(3)	0.036(3)	0.003(2)	-0.007(3)	-0.006(3)
C6	0.033(3)	0.037(3)	0.044(3)	0.001(2)	0.000(2)	-0.003(3)

Table A7 continued.

C7	0.029(3)	0.031(3)	0.045(3)	-0.004(2)	-0.001(2)	0.002(2)
C8	0.049(4)	0.034(3)	0.072(4)	-0.001(3)	0.031(3)	-0.009(3)
C9	0.077(5)	0.028(3)	0.041(3)	0.001(2)	0.031(3)	0.000(3)
C10	0.023(3)	0.044(4)	0.050(3)	0.012(3)	0.001(2)	-0.003(3)
C11	0.022(3)	0.057(4)	0.047(3)	0.008(3)	0.001(2)	-0.013(3)
C12	0.053(4)	0.025(3)	0.058(4)	0.000(3)	0.035(3)	-0.002(3)
C13	0.034(3)	0.028(3)	0.049(3)	-0.001(2)	0.009(3)	0.002(2)
C14	0.038(3)	0.051(4)	0.029(3)	-0.001(2)	0.007(2)	0.002(3)
C15	0.034(3)	0.024(3)	0.050(3)	-0.004(2)	0.024(3)	-0.004(2)
C16	0.025(3)	0.027(3)	0.027(3)	-0.005(2)	0.008(2)	-0.004(2)
C17	0.024(3)	0.038(3)	0.044(3)	-0.001(2)	0.011(2)	-0.004(2)
C18	0.029(3)	0.038(3)	0.051(3)	-0.003(3)	0.013(3)	-0.002(2)
C19	0.046(3)	0.017(3)	0.028(3)	-0.005(2)	0.015(2)	-0.007(2)
C20	0.053(4)	0.036(3)	0.036(3)	-0.014(2)	0.011(3)	0.005(3)
C21	0.056(4)	0.017(3)	0.037(3)	-0.002(2)	0.028(3)	-0.002(2)
C22	0.032(3)	0.035(3)	0.040(3)	-0.008(3)	0.005(2)	0.000(3)
C23	0.021(3)	0.028(3)	0.031(3)	0.000(2)	0.002(2)	-0.003(2)
C24	0.071(4)	0.024(3)	0.029(3)	-0.002(2)	0.014(3)	-0.008(3)
C25	0.080(5)	0.028(4)	0.080(5)	0.002(3)	0.021(4)	-0.007(3)
C26	0.025(3)	0.026(3)	0.034(3)	-0.005(2)	0.008(2)	-0.002(2)
C27	0.028(3)	0.029(3)	0.044(3)	0.000(2)	0.009(2)	0.004(2)
C28	0.027(3)	0.031(3)	0.032(3)	-0.004(2)	0.003(2)	-0.001(2)
C29	0.019(3)	0.043(3)	0.056(4)	-0.003(3)	0.012(2)	-0.008(2)
C30	0.029(3)	0.031(3)	0.028(3)	0.004(2)	0.006(2)	0.000(2)
C31	0.032(3)	0.025(3)	0.031(3)	-0.004(2)	0.008(2)	0.002(2)
C32	0.041(3)	0.028(3)	0.059(3)	-0.003(3)	0.022(3)	-0.002(3)
C33	0.024(3)	0.027(3)	0.037(3)	-0.006(2)	0.008(2)	0.000(2)
C34	0.033(3)	0.017(2)	0.035(3)	0.000(2)	0.009(2)	-0.001(2)
C35	0.026(3)	0.028(3)	0.024(2)	-0.001(2)	0.010(2)	-0.003(2)
C36	0.043(3)	0.032(3)	0.038(3)	-0.008(2)	0.011(3)	0.002(2)
C37	0.047(3)	0.031(3)	0.029(3)	0.001(2)	0.003(2)	0.007(3)
C38	0.034(3)	0.029(3)	0.031(3)	-0.006(2)	0.005(2)	-0.006(2)
C39	0.037(3)	0.024(3)	0.045(3)	-0.001(2)	0.014(3)	-0.001(2)
C40	0.018(3)	0.035(3)	0.044(3)	-0.002(2)	0.004(2)	-0.002(2)
C41	0.028(3)	0.034(3)	0.036(3)	-0.004(2)	0.006(2)	-0.001(2)
C42	0.039(3)	0.024(3)	0.042(3)	0.000(2)	0.016(2)	-0.001(2)
C43	0.020(2)	0.031(3)	0.023(2)	0.001(2)	0.003(2)	0.004(2)
C44	0.108(6)	0.051(4)	0.055(4)	-0.027(3)	0.012(4)	0.016(4)

Table A7 continued.

C45	0.071(5)	0.057(4)	0.053(4)	0.017(3)	0.017(3)	0.007(3)
C46	0.078(5)	0.035(4)	0.080(5)	0.002(3)	0.061(4)	0.008(3)
C47	0.050(4)	0.038(4)	0.084(5)	-0.003(3)	0.045(4)	0.002(3)
C48	0.042(3)	0.036(3)	0.077(4)	-0.010(3)	0.019(3)	-0.015(3)
C49	0.044(3)	0.026(3)	0.033(3)	-0.003(2)	0.001(3)	0.002(2)
C50	0.056(4)	0.031(3)	0.032(3)	0.001(2)	0.017(3)	-0.005(3)
C51	0.037(3)	0.044(3)	0.035(3)	0.010(2)	0.009(2)	0.002(3)
C52	0.029(3)	0.032(3)	0.040(3)	-0.004(2)	0.012(2)	-0.012(2)

The anisotropic displacement factor exponent takes the form:
$-2\pi^2 [h^2 a^{*2} U11 + ... + 2 h k a^* b^* U12]$

Table A7 continued.

Hydrogen coordinates (x 10^4) and isotropic displacement parameters ($Å^2$ x 10^3).

	x	y	z	U(eq)	Occ.
H1	0.3452(3)	0.2265(4)	0.5238(3)	0.054	1
H10	0.1258(3)	-0.1393(4)	0.2419(3)	0.050	1
H11	0.0785(3)	-0.2782(4)	0.2721(3)	0.053	1
H12	0.4401(3)	0.1599(3)	0.0365(3)	0.050	1
H13	0.4897(3)	-0.3508(4)	0.3841(3)	0.045	1
H14	0.4720(3)	-0.1604(4)	0.5291(3)	0.048	1
H17	0.1527(3)	0.1202(3)	0.2229(3)	0.043	1
H18	0.0382(3)	0.1591(4)	0.1476(3)	0.047	1
H2	0.2712(3)	-0.3441(4)	0.4116(3)	0.069	1
H24	0.2147(3)	-0.0824(3)	-0.0472(3)	0.051	1
H25A	0.3489(3)	-0.4417(4)	0.2449(3)	0.096	1
H25B	0.2705(3)	-0.4402(4)	0.1884(3)	0.096	1
H25C	0.2814(3)	-0.4210(4)	0.2692(3)	0.096	1
H27	0.5601(3)	0.1298(4)	0.3188(2)	0.041	1
H28	0.4528(2)	-0.2340(3)	0.2964(2)	0.038	1
H29	0.6251(3)	0.2713(4)	0.3445(3)	0.047	1
H3	0.3195(3)	-0.2059(4)	0.3804(3)	0.063	1
H30	0.2489(2)	0.2694(3)	0.2800(2)	0.036	1
H32	0.4747(3)	-0.0761(3)	0.2095(3)	0.049	1
H33	0.4853(2)	0.0339(3)	0.3539(2)	0.036	1
H36	0.2555(3)	0.3982(4)	0.3560(3)	0.045	1
H37	0.3398(3)	0.0974(4)	0.4485(2)	0.046	1
H38	0.1488(3)	-0.0791(3)	0.1536(2)	0.039	1
H39	0.4418(3)	0.4233(3)	0.2727(3)	0.042	1
H4	0.3344(3)	-0.0950(3)	-0.0259(3)	0.055	1
H40	0.3755(3)	0.2828(3)	0.2548(2)	0.041	1

H41	0.4342(2)	-0.0438(4)	0.4421(2)	0.040	1
H42	0.4323(3)	0.1371(3)	0.1486(3)	0.041	1

Table A7 continued.

H43	0.2493(2)	0.0012(3)	0.3645(2)	0.030	1
H44A	0.2836(4)	0.4663(4)	0.4718(3)	0.112	1
H44B	0.3533(4)	0.4211(4)	0.5273(3)	0.112	1
H44C	0.2759(4)	0.3939(4)	0.5298(3)	0.112	1
H45A	0.5069(3)	-0.3203(4)	0.5682(3)	0.092	1
H45B	0.5535(3)	-0.3706(4)	0.5270(3)	0.092	1
H45C	0.4716(3)	-0.3993(4)	0.5105(3)	0.092	1
H46	0.4593(4)	-0.0959(4)	0.0047(3)	0.067	1
H47	0.5309(3)	-0.0869(4)	0.1233(3)	0.062	1
H48A	0.6347(3)	0.4410(4)	0.3504(3)	0.077	1
H48B	0.5692(3)	0.4915(4)	0.3657(3)	0.077	1
H48C	0.5748(3)	0.4940(4)	0.2886(3)	0.077	1
H49	0.1224(3)	0.1881(3)	-0.0111(3)	0.045	1
H5	0.0927(3)	-0.0756(3)	-0.0576(3)	0.054	1
H50	0.2224(3)	0.1746(3)	-0.0411(3)	0.047	1
H6	0.0595(3)	-0.0775(4)	0.0442(3)	0.049	1
H7	0.0231(3)	0.1950(3)	0.0290(3)	0.046	1
H8A	0.1744(3)	-0.4531(4)	0.4001(3)	0.073	1
H8B	0.1181(3)	-0.4584(4)	0.3227(3)	0.073	1
H8C	0.0988(3)	-0.4016(4)	0.3826(3)	0.073	1
H9	0.3333(3)	0.1760(3)	-0.0608(3)	0.055	1

Symmetry transformations used to generate equivalent atoms:
#1 -x-1,-y+1,-z+1

Table A7 continued.

Torsion angles [°].

N2	Rh1	Rh2	N6	-74.2(2)
N3	Rh1	Rh2	N6	-163.03(15)
N4	Rh1	Rh2	N6	103.57(15)
N1	Rh1	Rh2	N6	21.7(2)
N2	Rh1	Rh2	N9	-153.98(14)
N3	Rh1	Rh2	N9	117.17(14)
N4	Rh1	Rh2	N9	23.78(14)
N1	Rh1	Rh2	N9	-58.09(14)
N2	Rh1	Rh2	N8	106.97(14)
N3	Rh1	Rh2	N8	18.12(14)
N4	Rh1	Rh2	N8	-75.27(14)
N1	Rh1	Rh2	N8	-157.13(15)
N2	Rh1	Rh2	N7	19.39(14)
N3	Rh1	Rh2	N7	-69.47(14)
N4	Rh1	Rh2	N7	-162.86(14)
N1	Rh1	Rh2	N7	115.28(15)
N2	Rh1	Rh2	N5	137.3(14)
N3	Rh1	Rh2	N5	48.5(14)
N4	Rh1	Rh2	N5	-44.9(14)
N1	Rh1	Rh2	N5	-126.8(14)
N2	Rh1	N1	C42	4.2(4)
N3	Rh1	N1	C42	158.0(13)
N4	Rh1	N1	C42	179.2(4)
Rh2	Rh1	N1	C42	-81.8(4)
N2	Rh1	N1	C34	-177.8(3)
N3	Rh1	N1	C34	-24.1(16)
N4	Rh1	N1	C34	-2.9(3)
Rh2	Rh1	N1	C34	96.2(3)
N3	Rh1	N2	C33	57.6(3)
N4	Rh1	N2	C33	175.7(13)
N1	Rh1	N2	C33	-124.8(3)
Rh2	Rh1	N2	C33	-26.7(3)
N3	Rh1	N2	C26	-110.6(3)
N4	Rh1	N2	C26	7.5(16)
N1	Rh1	N2	C26	66.9(3)
Rh2	Rh1	N2	C26	165.1(3)

Table A7 continued.

N2	Rh1	N3	C43	-103.0(3)
N4	Rh1	N3	C43	82.2(3)
N1	Rh1	N3	C43	103.1(15)
Rh2	Rh1	N3	C43	-17.7(3)
N2	Rh1	N3	C16	76.9(3)
N4	Rh1	N3	C16	-97.9(3)
N1	Rh1	N3	C16	-77.0(15)
Rh2	Rh1	N3	C16	162.1(3)
N2	Rh1	N4	C17	-113.9(14)
N3	Rh1	N4	C17	4.0(4)
N1	Rh1	N4	C17	-174.0(4)
Rh2	Rh1	N4	C17	88.8(4)
N2	Rh1	N4	C31	59.8(15)
N3	Rh1	N4	C31	177.7(3)
N1	Rh1	N4	C31	-0.4(3)
Rh2	Rh1	N4	C31	-97.5(3)
N6	Rh2	N5	C22	-175.6(25)
N9	Rh2	N5	C22	-95.8(25)
N8	Rh2	N5	C22	3.3(25)
N7	Rh2	N5	C22	90.5(25)
Rh1	Rh2	N5	C22	-27.0(36)
N9	Rh2	N6	C32	-177.8(4)
N8	Rh2	N6	C32	-146.6(63)
N7	Rh2	N6	C32	6.8(4)
N5	Rh2	N6	C32	-90.5(4)
Rh1	Rh2	N6	C32	91.7(4)
N9	Rh2	N6	C21	-1.1(3)
N8	Rh2	N6	C21	30.0(65)
N7	Rh2	N6	C21	-176.5(3)
N5	Rh2	N6	C21	86.2(3)
Rh1	Rh2	N6	C21	-91.6(3)
N6	Rh2	N7	C33	75.4(3)
N9	Rh2	N7	C33	40.0(12)
N8	Rh2	N7	C33	-105.2(3)
N5	Rh2	N7	C33	164.9(3)
Rh1	Rh2	N7	C33	-18.9(3)
N6	Rh2	N7	C23	-113.1(3)
N9	Rh2	N7	C23	-148.5(9)

Table A7 continued.

N8	Rh2	N7	C23	66.3(3)
N5	Rh2	N7	C23	-23.6(4)
Rh1	Rh2	N7	C23	152.6(3)
N6	Rh2	N8	C43	-146.4(63)
N9	Rh2	N8	C43	-115.4(3)
N7	Rh2	N8	C43	60.1(3)
N5	Rh2	N8	C43	157.5(3)
Rh1	Rh2	N8	C43	-24.7(3)
N6	Rh2	N8	C35	49.8(65)
N9	Rh2	N8	C35	80.8(3)
N7	Rh2	N8	C35	-103.7(3)
N5	Rh2	N8	C35	-6.4(3)
Rh1	Rh2	N8	C35	171.5(3)
N6	Rh2	N9	C38	-178.2(4)
N8	Rh2	N9	C38	2.5(4)
N7	Rh2	N9	C38	-142.2(10)
N5	Rh2	N9	C38	92.3(4)
Rh1	Rh2	N9	C38	-83.7(4)
N6	Rh2	N9	C19	-0.9(3)
N8	Rh2	N9	C19	179.8(3)
N7	Rh2	N9	C19	35.1(12)
N5	Rh2	N9	C19	-90.4(3)
Rh1	Rh2	N9	C19	93.6(3)
B1	F4	F4A	B1	0.000(2)
F4A	F4	B1	F2	-1.5(31)
F4A	F4	B1	F1	-122.5(25)
F4A	F4	B1	F3	123.4(26)
F4A	F4	B1	F4A	0.000(3)
F4	F4A	B1	F4	0.000(4)
F4	F4A	B1	F2	178.7(26)
F4	F4A	B1	F1	64.9(29)
F4	F4A	B1	F3	-65.8(27)
C15	C2	C3	C35	-0.1(9)
C24	C5	C6	C38	1.5(8)
C35	C10	C11	C15	1.1(8)
C50	C9	C12	C42	1.4(7)
C10	C11	C15	C2	0.6(8)
C10	C11	C15	C8	-179.9(5)

Table A7 continued.

C3	C2	C15	C11	-1.1(9)
C3	C2	C15	C8	179.4(5)
C43	N3	C16	C37	42.7(6)
Rh1	N3	C16	C37	-137.1(4)
C43	N3	C16	C30	-137.9(4)
Rh1	N3	C16	C30	42.3(5)
C31	N4	C17	C18	0.1(7)
Rh1	N4	C17	C18	173.7(4)
C49	C7	C18	C17	0.4(7)
N4	C17	C18	C7	0.3(7)
C38	N9	C19	C24	1.2(6)
Rh2	N9	C19	C24	-176.3(3)
C38	N9	C19	C21	-179.9(4)
Rh2	N9	C19	C21	2.6(5)
C37	C1	C20	C36	-1.4(8)
C37	C1	C20	C44	179.4(5)
C46	C4	C21	N6	0.1(7)
C46	C4	C21	C19	179.9(4)
C32	N6	C21	C4	-0.6(7)
Rh2	N6	C21	C4	-177.5(3)
C32	N6	C21	C19	179.7(4)
Rh2	N6	C21	C19	2.7(5)
N9	C19	C21	C4	176.7(4)
C24	C19	C21	C4	-4.4(7)
N9	C19	C21	N6	-3.5(6)
C24	C19	C21	N6	175.3(4)
Rh2	N5	C22	C25	-56.8(141)
C33	N7	C23	C28	-129.3(5)
Rh2	N7	C23	C28	58.9(5)
C33	N7	C23	C41	50.6(6)
Rh2	N7	C23	C41	-121.1(4)
C6	C5	C24	C19	-1.3(7)
N9	C19	C24	C5	-0.1(7)
C21	C19	C24	C5	-178.9(4)
C33	N2	C26	C40	-152.5(4)
Rh1	N2	C26	C40	15.8(5)
C33	N2	C26	C27	28.9(7)
Rh1	N2	C26	C27	-162.8(4)

Table A7 continued.

C40	C26	C27	C29	5.6(7)
N2	C26	C27	C29	-175.8(4)
C41	C23	C28	C13	3.1(7)
N7	C23	C28	C13	-176.9(4)
C51	C13	C28	C23	-1.0(7)
C26	C27	C29	C52	-3.6(7)
C37	C16	C30	C36	-2.3(7)
N3	C16	C30	C36	178.3(4)
C17	N4	C31	C49	-1.3(7)
Rh1	N4	C31	C49	-175.6(3)
C17	N4	C31	C34	177.6(4)
Rh1	N4	C31	C34	3.4(5)
C21	N6	C32	C47	0.6(7)
Rh2	N6	C32	C47	177.2(4)
C26	N2	C33	N7	-171.4(4)
Rh1	N2	C33	N7	20.3(6)
C23	N7	C33	N2	-167.6(4)
Rh2	N7	C33	N2	4.5(6)
C42	N1	C34	C50	2.3(6)
Rh1	N1	C34	C50	-175.8(3)
C42	N1	C34	C31	-176.4(4)
Rh1	N1	C34	C31	5.5(5)
C49	C31	C34	N1	173.1(4)
N4	C31	C34	N1	-5.9(6)
C49	C31	C34	C50	-5.5(7)
N4	C31	C34	C50	175.5(4)
C11	C10	C35	C3	-2.2(8)
C11	C10	C35	N8	177.8(5)
C2	C3	C35	C10	1.7(8)
C2	C3	C35	N8	-178.3(5)
C43	N8	C35	C10	95.4(5)
Rh2	N8	C35	C10	-100.7(5)
C43	N8	C35	C3	-84.7(6)
Rh2	N8	C35	C3	79.2(5)
C16	C30	C36	C20	0.2(7)
C1	C20	C36	C30	1.7(8)
C44	C20	C36	C30	-179.1(5)
C20	C1	C37	C16	-0.7(8)

Table A7 continued.

C30	C16	C37	C1	2.6(7)
N3	C16	C37	C1	-178.0(4)
C19	N9	C38	C6	-1.0(7)
Rh2	N9	C38	C6	176.2(3)
C5	C6	C38	N9	-0.3(8)
C52	C39	C40	C26	-1.6(7)
C27	C26	C40	C39	-3.1(7)
N2	C26	C40	C39	178.3(4)
C51	C14	C41	C23	0.4(8)
C28	C23	C41	C14	-2.8(7)
N7	C23	C41	C14	177.2(4)
C34	N1	C42	C12	-2.0(7)
Rh1	N1	C42	C12	175.9(3)
C9	C12	C42	N1	0.1(7)
C35	N8	C43	N3	-175.8(4)
Rh2	N8	C43	N3	19.3(6)
C16	N3	C43	N8	-176.3(4)
Rh1	N3	C43	N8	3.6(6)
C21	C4	C46	C47	0.3(8)
C4	C46	C47	C32	-0.2(8)
N6	C32	C47	C46	-0.2(8)
N4	C31	C49	C7	2.0(7)
C34	C31	C49	C7	-176.8(4)
C18	C7	C49	C31	-1.6(7)
C12	C9	C50	C34	-1.1(7)
N1	C34	C50	C9	-0.8(7)
C31	C34	C50	C9	177.7(4)
C28	C13	C51	C14	-1.5(8)
C28	C13	C51	C45	178.0(5)
C41	C14	C51	C13	1.8(8)
C41	C14	C51	C45	-177.7(5)
C40	C39	C52	C29	3.7(7)
C40	C39	C52	C48	-175.1(5)
C27	C29	C52	C39	-1.1(7)
C27	C29	C52	C48	177.7(5)

Table A8. Crystal data and structure refinement for $[Rh_2(DTolF)_2(bpy)_2(H_2O)][BF_4][BPh_4]\cdot OC(CH_3)_2\cdot 3CH_3CH_2O_2CH_2CH_3$ (8b).

Identification code	$[Rh_2(DTolF)_2(bpy)_2(H_2O)][BF_4][BPh_4]$ $\cdot OC(CH_3)_2\cdot 3CH_3CH_2O_2CH_2CH_3$
Empirical formula	C89 H96 B2 F8 N8 O8 Rh2
Formula weight	1709.18 g/mol
Temperature	293(2) K
Wavelength	0.71073 Å
Crystal system	monoclinic
Space group	$P2_1/n$
Unit cell dimensions	a = 23.4894(11) Å
	b = 13.5583(6) Å
	c = 28.4811(13) Å
	$\alpha = 90^\circ$
	$\beta = 114.1180(10)^\circ$
	$\gamma = 90^\circ$
Volume	8278.7(7) $Å^3$
Z	4

ρ_{calc}	1.371 g/cm^3

Table A8 continued.

μ	0.469 cm^{-3}
F(000)	3544
Crystal size	0.46 x 0.36 x 0.18 mm^3
Theta range for data collection	1.46 to 27.44°
Index ranges	-30<=h<=24, -17<=k<=9, -35<=l<=36
Reflections collected	43882
Independent reflections	17926 [R(int) = 0.1489]
Refinement method	Full-matrix least-squares on F^2
Data / restraints / parameters	17921 / 28 / 1013
Goodness-of-fit on F^2	0.972
Final R indices [$I>2\sigma(I)$]	R1 = 0.1196, wR2 = 0.2267
R indices (all data)	R1 = 0.2585, wR2 = 0.2906
Largest diff. peak and hole	1.047 and -0.958 e$^-$/Å^{-3}

Table A8 continued.

Atomic coordinates (x 10^4) and equivalent isotropic displacement parameters ($Å^2$ x 10^3).

	x	y	z	U(eq)	Occ.
B1	0.0756(6)	0.2444(8)	0.1072(4)	0.036(3)	1
B2	0.8269(7)	0.2456(10)	0.1526(6)	0.070(5)	1
C1	0.9606(7)	0.8263(10)	0.4874(5)	0.070(4)	1
C10	0.7265(6)	0.9852(7)	0.1614(4)	0.044(3)	1
C11	0.2133(6)	0.3065(11)	0.0619(5)	0.066(4)	1
C12	0.6233(5)	0.5594(7)	0.1216(4)	0.042(3)	1
C13	0.5575(6)	1.0520(8)	0.0714(5)	0.060(3)	1
C14	1.0698(6)	0.3410(10)	0.4013(5)	0.075(4)	1
C15	0.1776(6)	0.4574(10)	0.0845(5)	0.063(4)	1
C16	1.0184(5)	0.9477(7)	0.1856(4)	0.042(3)	1
C17	0.1366(6)	0.0833(8)	0.1570(4)	0.052(3)	1
C18	0.7246(5)	0.8827(7)	0.1573(3)	0.030(2)	1
C19	0.1389(6)	0.3473(8)	0.2503(4)	0.056(3)	1
C2	0.1562(7)	-0.0162(9)	0.1601(5)	0.065(4)	1
C20	0.8827(5)	0.4672(7)	0.0969(4)	0.044(3)	1
C21	0.6163(5)	0.8906(8)	0.1012(4)	0.045(3)	1
C22	0.6716(6)	1.0385(8)	0.1334(4)	0.052(3)	1
C23	0.0650(5)	0.0585(8)	0.0703(5)	0.052(3)	1
C24	1.0372(5)	0.5092(9)	0.3587(4)	0.051(3)	1
C25	0.0859(7)	0.3548(9)	0.2601(5)	0.060(4)	1
C26	0.6156(5)	0.9923(8)	0.1021(4)	0.042(3)	1
C27	1.0238(6)	0.4082(8)	0.3604(4)	0.048(3)	1
C28	-0.1053(5)	0.2220(8)	0.0171(4)	0.052(3)	1
C29	1.0655(5)	0.6439(8)	0.1619(4)	0.044(3)	1
C30	0.7040(5)	0.6372(7)	0.2151(4)	0.042(3)	1
C31	0.1366(6)	0.4053(8)	0.0985(5)	0.054(3)	1
C32	0.8692(6)	0.8092(7)	0.3979(4)	0.043(3)	1

Table A8 continued.

C33	0.9682(5)	0.3758(7)	0.3238(4)	0.043(3)	1
C34	0.0259(5)	0.2969(6)	0.1744(4)	0.038(2)	1
C35	0.8701(5)	0.9827(8)	0.0837(4)	0.041(3)	1
C36	-0.0630(6)	0.3390(8)	-0.0216(4)	0.050(3)	1
C37	0.0298(6)	0.3287(7)	0.2225(4)	0.045(3)	1
C38	0.9732(5)	0.8210(8)	0.4024(4)	0.049(3)	1
C39	0.9086(5)	0.5070(8)	0.0652(4)	0.050(3)	1
C40	0.9038(5)	0.8356(8)	0.0545(3)	0.039(3)	1
C41	0.9253(5)	0.4347(7)	0.2869(4)	0.034(2)	1
C42	0.6871(5)	0.5638(7)	0.1336(4)	0.040(3)	1
C43	0.5991(5)	0.5914(7)	0.1554(4)	0.042(3)	1
C44	0.8995(5)	0.9372(8)	0.0563(4)	0.045(3)	1
C45	0.6692(5)	0.8360(7)	0.1275(4)	0.038(2)	1
C46	0.6392(5)	0.6285(7)	0.2019(4)	0.040(3)	1
C47	0.1302(5)	0.3022(8)	0.0936(4)	0.045(3)	1
C48	0.9605(5)	1.0478(7)	0.2200(4)	0.039(2)	1
C49	0.9074(5)	0.6099(8)	0.0590(4)	0.047(3)	1
C5	0.1293(6)	-0.0771(9)	0.1168(5)	0.060(3)	1
C50	1.0014(5)	1.0408(7)	0.1969(4)	0.041(3)	1
C51	0.1691(5)	0.2555(9)	0.0752(4)	0.046(3)	1
C52	0.0782(5)	0.2870(7)	0.1626(4)	0.035(2)	1
C53	0.8589(4)	0.5304(7)	0.1227(4)	0.037(2)	1
C54	0.9382(5)	0.5368(7)	0.2878(4)	0.034(2)	1
C55	0.0919(5)	0.1239(7)	0.1121(4)	0.038(2)	1
C56	0.9946(5)	0.5720(7)	0.3223(4)	0.042(3)	1
C57	-0.1145(6)	0.2856(8)	-0.0233(4)	0.052(3)	1
C58	-0.0461(5)	0.2102(7)	0.0568(4)	0.045(3)	1
C59	1.0393(5)	0.5689(7)	0.1796(4)	0.037(2)	1
C6	0.0842(7)	-0.0406(9)	0.0732(6)	0.067(4)	1
C60	-0.0042(5)	0.3272(8)	0.0185(4)	0.044(3)	1
C61	1.0096(4)	0.7628(7)	0.1893(4)	0.034(2)	1
C62	0.1347(5)	0.3157(8)	0.2026(4)	0.048(3)	1
C63	0.8346(5)	0.5794(7)	0.2318(4)	0.033(2)	1
C64	0.9336(6)	0.8197(7)	0.4279(4)	0.048(3)	1
C65	0.9364(5)	0.9618(6)	0.2305(4)	0.034(2)	1
C66	0.8450(5)	0.8032(7)	0.3447(4)	0.038(2)	1
C67	0.9498(5)	0.8160(7)	0.3490(4)	0.038(2)	1
C68	0.8085(5)	0.8394(6)	0.2349(4)	0.030(2)	1

Table A8 continued.

C69	0.8855(5)	0.8079(6)	0.3197(4)	0.034(2)	1
C70	0.8823(5)	0.6699(7)	0.0869(4)	0.033(2)	1
C71	0.0074(5)	0.2620(7)	0.0601(4)	0.038(2)	1
C72	1.0509(5)	0.7413(7)	0.1667(4)	0.041(3)	1
C73	0.7275(5)	0.6062(6)	0.1795(4)	0.032(2)	1
C74	0.8802(5)	0.7792(7)	0.0831(3)	0.035(2)	1
C75	0.8468(5)	0.9221(7)	0.1116(4)	0.033(2)	1
C76	0.9942(4)	0.8654(6)	0.1984(4)	0.029(2)	1
C77	0.9988(5)	0.5960(7)	0.2016(4)	0.035(2)	1
C78	1.1377(8)	0.7749(14)	0.3125(6)	0.112(7)	1
C79	1.1537(9)	0.6739(14)	0.3230(8)	0.147(9)	1
C8	0.2174(6)	0.4074(10)	0.0677(5)	0.062(4)	1
C80	1.1736(8)	0.8368(12)	0.2940(6)	0.109(6)	1
C81	0.2451(12)	-0.3658(17)	0.1864(9)	0.121(7)	1
C82	0.2245(11)	-0.4268(22)	0.2259(11)	0.220(14)	1
C83	0.3273(20)	-0.3631(24)	0.1533(13)	0.314(33)	1
C84	0.3754(14)	-0.4045(24)	0.1501(20)	0.353(34)	1
C85	0.3760(10)	0.4411(22)	0.0416(11)	0.236(17)	1
C86	0.3214(10)	0.4984(23)	0.0085(8)	0.132(9)	1
C87	0.2643(8)	0.6458(13)	-0.0116(8)	0.105(6)	1
C88	0.2781(12)	0.7537(19)	0.0026(11)	0.227(16)	1
C9	0.5297(5)	0.5864(8)	0.1419(5)	0.054(3)	1
C91	1.2011(13)	0.5722(24)	0.4852(10)	0.230(20)	1
C92	1.1615(31)	0.5391(69)	0.5074(23)	1.052(133)	1
C93	1.2489(11)	0.5002(25)	0.4459(15)	0.267(28)	1
C94	1.2247(10)	0.4453(17)	0.3924(10)	0.174(11)	1
F1	0.8826(6)	0.2666(10)	0.1932(6)	0.214(8)	1
F2	0.7954(5)	0.3283(8)	0.1435(5)	0.165(5)	1
F3	0.8453(7)	0.2215(8)	0.1166(4)	0.173(6)	1
F4	0.8040(6)	0.1773(9)	0.1705(5)	0.199(7)	1
N1	0.9512(4)	0.8710(5)	0.2200(3)	0.028(2)	1
N2	0.9825(4)	0.6894(5)	0.2056(3)	0.029(2)	1
N3	0.8942(4)	0.6008(5)	0.2510(3)	0.034(2)	1
N4	0.8527(4)	0.8224(6)	0.1124(3)	0.030(2)	1
N5	0.8585(4)	0.6286(6)	0.1180(3)	0.032(2)	1
N6	0.7824(4)	0.8295(6)	0.1845(3)	0.033(2)	1
N7	0.7934(4)	0.6211(5)	0.1913(3)	0.032(2)	1
N8	0.8643(4)	0.8020(5)	0.2648(3)	0.029(2)	1

Table A8 continued.

O1	1.0913(7)	0.8130(12)	0.3222(6)	0.157(6)	1
O2	0.2730(6)	0.4580(9)	-0.0294(5)	0.111(4)	1
O3	0.2096(8)	-0.3011(12)	0.1562(7)	0.184(7)	1
O4	0.3208(7)	0.5870(11)	0.0239(7)	0.149(7)	1
O5	0.2994(8)	-0.3977(12)	0.1854(7)	0.181(7)	1
O6	1.2293(6)	0.6392(9)	0.5067(6)	0.137(5)	1
O7	1.2018(15)	0.5104(27)	0.4585(10)	0.324(23)	1
O8	0.7356(3)	0.7172(5)	0.0779(3)	0.042(2)	1
Rh1	0.81990(4)	0.72614(5)	0.15142(3)	0.0283(2)	1
Rh2	0.92039(4)	0.73823(5)	0.23468(3)	0.0286(2)	1

U(eq) is defined as one third of the trace of the orthogonalized Uij tensor.

Table A8 continued.

Bond lengths [Å] and angles [°].

B1	C71	1.63(2)
B1	C52	1.657(14)
B1	C55	1.672(14)
B1	C47	1.676(15)
B2	F4	1.277(13)
B2	F3	1.306(14)
B2	F2	1.310(14)
B2	F1	1.38(2)
Rh1	N4	2.058(7)
Rh1	N5	2.045(7)
Rh1	N6	2.076(8)
Rh1	N7	2.070(7)
Rh1	O8	2.221(7)
Rh1	Rh2	2.5782(11)
Rh2	N8	2.036(7)
Rh2	N1	2.046(7)
Rh2	N2	2.061(7)
Rh2	N3	2.074(7)
N1	C65	1.345(11)
N1	C76	1.383(11)
N2	C77	1.341(11)
N2	C61	1.360(11)
N3	C63	1.310(12)
N3	C54	1.426(12)
N4	C75	1.358(11)
N4	C74	1.375(11)
N5	C53	1.337(11)
N5	C70	1.349(11)
N6	C68	1.317(11)
N6	C18	1.451(12)
N7	C63	1.294(12)
N7	C73	1.456(12)
N8	C68	1.336(11)
N8	C69	1.436(11)
C1	C64	1.55(2)

Table A8 continued.

C2	C17	1.42(2)
C2	C5	1.40(2)
C5	C6	1.35(2)
C6	C23	1.410(15)
C8	C11	1.38(2)
C8	C15	1.39(2)
C9	C43	1.515(14)
C10	C18	1.393(12)
C10	C22	1.407(15)
C11	C51	1.42(2)
C12	C43	1.374(14)
C12	C42	1.395(14)
C13	C26	1.519(15)
C14	C27	1.526(14)
C15	C31	1.38(2)
C16	C76	1.369(12)
C16	C50	1.400(13)
C17	C55	1.393(14)
C18	C45	1.382(13)
C19	C62	1.389(14)
C19	C25	1.39(2)
C20	C39	1.387(15)
C20	C53	1.386(13)
C21	C26	1.379(14)
C21	C45	1.375(14)
C22	C26	1.40(2)
C23	C55	1.411(14)
C24	C27	1.410(15)
C24	C56	1.398(14)
C25	C37	1.36(2)
C27	C33	1.37(2)
C28	C57	1.38(2)
C28	C58	1.399(15)
C29	C72	1.385(13)
C29	C59	1.387(14)
C30	C73	1.403(13)
C30	C46	1.416(14)
C31	C47	1.407(14)

Table A8 continued.

C32	C66	1.384(13)
C32	C64	1.41(2)
C33	C41	1.376(14)
C34	C37	1.403(13)
C34	C52	1.406(13)
C35	C44	1.380(14)
C35	C75	1.400(13)
C36	C57	1.39(2)
C36	C60	1.395(15)
C38	C67	1.392(14)
C38	C64	1.39(2)
C39	C49	1.405(14)
C40	C74	1.389(12)
C40	C44	1.384(14)
C41	C54	1.416(13)
C42	C73	1.387(13)
C43	C46	1.370(14)
C47	C51	1.380(14)
C48	C50	1.371(14)
C48	C65	1.382(13)
C49	C70	1.422(13)
C52	C62	1.405(14)
C54	C56	1.373(14)
C58	C71	1.409(14)
C59	C77	1.386(13)
C60	C71	1.412(14)
C61	C72	1.397(13)
C61	C76	1.486(13)
C66	C69	1.404(13)
C67	C69	1.399(14)
C70	C74	1.485(13)
C78	O1	1.33(2)
C78	C79	1.42(2)
C78	C80	1.43(2)
C81	O3	1.27(2)
C81	O5	1.36(2)
C81	C82	1.62(3)
C83	C84	1.30(4)

Table A8 continued.

C83	O5		1.41(3)
C85	C86		1.47(3)
C86	O4		1.28(3)
C86	O2		1.32(2)
C87	C88		1.52(3)
C87	O4		1.52(2)
C91	O6		1.14(2)
C91	O7		1.14(3)
C91	C92		1.40(4)
C93	O7		1.30(3)
C93	C94		1.58(3)
C71	B1	C52	111.9(8)
C71	B1	C55	109.0(8)
C52	B1	C55	110.1(8)
C71	B1	C47	109.2(8)
C52	B1	C47	108.8(8)
C55	B1	C47	107.8(8)
F4	B2	F3	117.4(14)
F4	B2	F2	113.8(13)
F3	B2	F2	113.5(12)
F4	B2	F1	103.1(12)
F3	B2	F1	101.9(12)
F2	B2	F1	104.8(13)
N4	Rh1	N5	79.8(3)
N4	Rh1	N6	98.0(3)
N5	Rh1	N6	177.8(3)
N4	Rh1	N7	174.9(3)
N5	Rh1	N7	95.7(3)
N6	Rh1	N7	86.4(3)
N4	Rh1	O8	84.9(3)
N5	Rh1	O8	85.4(3)
N6	Rh1	O8	94.9(3)
N7	Rh1	O8	97.4(3)
N4	Rh1	Rh2	93.0(2)
N5	Rh1	Rh2	93.2(2)
N6	Rh1	Rh2	86.4(2)
N7	Rh1	Rh2	84.7(2)
O8	Rh1	Rh2	177.6(2)

Table A8 continued.

N8	Rh2	N1	93.2(3)
N8	Rh2	N2	173.3(3)
N1	Rh2	N2	80.4(3)
N8	Rh2	N3	89.1(3)
N1	Rh2	N3	176.8(3)
N2	Rh2	N3	97.2(3)
N8	Rh2	Rh1	84.7(2)
N1	Rh2	Rh1	97.8(2)
N2	Rh2	Rh1	98.2(2)
N3	Rh2	Rh1	84.5(2)
C65	N1	C76	116.8(8)
C65	N1	Rh2	128.0(6)
C76	N1	Rh2	115.2(6)
C77	N2	C61	118.4(8)
C77	N2	Rh2	127.6(6)
C61	N2	Rh2	114.1(6)
C63	N3	C54	120.2(8)
C63	N3	Rh2	118.0(6)
C54	N3	Rh2	121.2(6)
C75	N4	C74	119.0(8)
C75	N4	Rh1	125.5(6)
C74	N4	Rh1	115.4(6)
C53	N5	C70	119.4(8)
C53	N5	Rh1	125.7(6)
C70	N5	Rh1	114.8(6)
C68	N6	C18	116.7(8)
C68	N6	Rh1	117.9(6)
C18	N6	Rh1	124.8(6)
C63	N7	C73	118.9(8)
C63	N7	Rh1	120.4(7)
C73	N7	Rh1	119.8(6)
C68	N8	C69	119.1(8)
C68	N8	Rh2	121.8(6)
C69	N8	Rh2	119.1(6)
C17	C2	C5	119.2(12)
C6	C5	C2	119.7(12)
C5	C6	C23	120.9(13)
C11	C8	C15	120.2(11)

Table A8 continued.

C18	C10	C22	118.4(10)
C8	C11	C51	118.3(12)
C43	C12	C42	121.7(10)
C31	C15	C8	119.9(12)
C76	C16	C50	119.0(10)
C55	C17	C2	122.5(11)
C45	C18	C10	119.8(9)
C45	C18	N6	122.8(8)
C10	C18	N6	117.4(9)
C62	C19	C25	120.5(11)
C39	C20	C53	118.9(10)
C26	C21	C45	122.9(11)
C26	C22	C10	122.4(10)
C55	C23	C6	121.8(12)
C27	C24	C56	121.0(11)
C37	C25	C19	118.8(10)
C21	C26	C22	116.3(10)
C21	C26	C13	122.5(10)
C22	C26	C13	121.2(10)
C33	C27	C24	116.3(10)
C33	C27	C14	123.2(11)
C24	C27	C14	120.6(11)
C57	C28	C58	120.7(11)
C72	C29	C59	119.9(10)
C73	C30	C46	118.8(10)
C15	C31	C47	122.7(12)
C66	C32	C64	121.9(10)
C27	C33	C41	124.6(10)
C37	C34	C52	123.2(10)
C44	C35	C75	117.4(10)
C57	C36	C60	121.6(11)
C25	C37	C34	120.3(10)
C67	C38	C64	121.2(11)
C20	C39	C49	118.5(10)
C74	C40	C44	118.2(9)
C33	C41	C54	118.0(10)
C73	C42	C12	120.2(10)
C46	C43	C12	118.4(10)

Table A8 continued.

C46	C43	C9	120.4(10)
C12	C43	C9	121.2(10)
C35	C44	C40	121.9(9)
C21	C45	C18	120.1(10)
C43	C46	C30	121.7(10)
C51	C47	C31	115.6(10)
C51	C47	B1	124.2(9)
C31	C47	B1	120.2(10)
C50	C48	C65	118.4(9)
C39	C49	C70	119.3(10)
C48	C50	C16	119.6(9)
C47	C51	C11	123.3(12)
C62	C52	C34	114.0(9)
C62	C52	B1	121.5(9)
C34	C52	B1	124.4(9)
N5	C53	C20	123.4(9)
C56	C54	C41	119.3(9)
C56	C54	N3	120.9(9)
C41	C54	N3	119.7(9)
C17	C55	C23	115.9(10)
C17	C55	B1	121.6(9)
C23	C55	B1	122.3(10)
C54	C56	C24	120.5(10)
C28	C57	C36	117.2(11)
C28	C58	C71	124.2(10)
C29	C59	C77	117.4(9)
C36	C60	C71	123.1(10)
N2	C61	C72	120.8(9)
N2	C61	C76	116.4(8)
C72	C61	C76	122.7(8)
C19	C62	C52	123.0(11)
N7	C63	N3	123.9(9)
C38	C64	C32	117.7(10)
C38	C64	C1	120.4(12)
C32	C64	C1	121.8(11)
N1	C65	C48	124.0(9)
C32	C66	C69	119.4(10)
C38	C67	C69	120.2(10)

Table A8 continued.

N6	C68	N8	123.7(9)
C67	C69	C66	119.4(9)
C67	C69	N8	117.6(9)
C66	C69	N8	123.0(9)
N5	C70	C49	120.5(9)
N5	C70	C74	116.8(8)
C49	C70	C74	122.7(9)
C60	C71	C58	113.3(10)
C60	C71	B1	124.7(9)
C58	C71	B1	122.0(9)
C29	C72	C61	119.5(9)
C42	C73	C30	119.0(10)
C42	C73	N7	122.0(9)
C30	C73	N7	119.0(9)
N4	C74	C40	121.3(9)
N4	C74	C70	113.1(8)
C40	C74	C70	125.6(9)
N4	C75	C35	122.1(9)
C16	C76	N1	122.2(9)
C16	C76	C61	124.0(9)
N1	C76	C61	113.8(7)
N2	C77	C59	124.0(9)
O1	C78	C79	120.0(14)
O1	C78	C80	120.1(15)
C79	C78	C80	119.8(14)
O3	C81	O5	124.7(23)
O3	C81	C82	121.4(24)
O5	C81	C82	113.6(23)
C84	C83	O5	123.5(43)
O4	C86	O2	122.8(23)
O4	C86	C85	113.9(22)
O2	C86	C85	122.6(27)
C88	C87	O4	107.1(16)
O6	C91	O7	141.4(33)
O6	C91	C92	111.1(36)
O7	C91	C92	105.1(35)
O7	C93	C94	107.8(21)
C86	O4	C87	113.1(17)

Table A8 continued.

C81	O5	C83	126.7(28)
C91	O7	C93	120.6(27)

Symmetry transformations used to generate equivalent atoms:
#1 -x-1,-y+1,-z+1

Table A8 continued.

Anisotropic displacement parameters ($Å^2$ x 10^3).

	U11	U22	U33	U23	U13	U12
B1	0.051(7)	0.029(6)	0.038(6)	0.004(5)	0.030(6)	0.003(5)
B2	0.070(11)	0.060(11)	0.087(12)	0.031(10)	0.039(10)	0.016(9)
Rh1	0.0363(4)	0.0218(4)	0.0336(4)	-0.0020(3)	0.0212(3)	-0.0020(3)
Rh2	0.0356(4)	0.0223(4)	0.0345(4)	0.0013(3)	0.0211(3)	-0.0001(3)
N1	0.033(5)	0.023(4)	0.028(4)	-0.001(3)	0.014(4)	0.000(3)
N2	0.037(5)	0.022(4)	0.031(4)	-0.004(3)	0.017(4)	-0.001(3)
N3	0.045(6)	0.023(4)	0.041(5)	0.000(4)	0.024(4)	-0.004(4)
N4	0.031(5)	0.037(5)	0.023(4)	-0.004(3)	0.014(4)	-0.004(3)
N5	0.036(5)	0.027(4)	0.036(5)	-0.010(4)	0.019(4)	-0.009(4)
N6	0.036(5)	0.034(5)	0.031(5)	0.005(4)	0.015(4)	-0.002(4)
N7	0.039(5)	0.027(4)	0.038(5)	0.000(4)	0.024(4)	-0.002(4)
N8	0.035(5)	0.027(4)	0.032(5)	0.001(3)	0.021(4)	0.008(3)
C1	0.090(11)	0.071(9)	0.047(8)	-0.005(7)	0.025(8)	0.003(8)
C2	0.090(11)	0.045(8)	0.069(9)	0.023(7)	0.042(8)	0.024(7)
C5	0.073(10)	0.038(7)	0.088(10)	0.011(7)	0.053(9)	0.003(6)
C6	0.089(11)	0.035(7)	0.104(12)	-0.014(7)	0.066(10)	0.001(7)
C8	0.035(7)	0.075(10)	0.069(9)	0.022(7)	0.012(6)	-0.016(6)
C9	0.041(7)	0.045(7)	0.079(9)	0.002(6)	0.026(7)	0.000(5)
C10	0.064(8)	0.020(5)	0.046(7)	-0.006(5)	0.022(6)	0.001(5)
C11	0.041(8)	0.101(12)	0.066(9)	0.020(8)	0.030(7)	0.003(7)
C12	0.038(7)	0.028(6)	0.056(7)	-0.011(5)	0.013(6)	-0.013(4)
C13	0.065(9)	0.044(7)	0.060(8)	0.001(6)	0.014(7)	0.007(6)
C14	0.059(9)	0.069(9)	0.087(11)	0.038(8)	0.020(8)	0.016(7)
C15	0.062(9)	0.058(8)	0.069(9)	0.012(7)	0.026(8)	-0.007(7)
C16	0.062(8)	0.027(6)	0.042(6)	0.002(5)	0.028(6)	-0.009(5)
C17	0.066(9)	0.048(7)	0.045(7)	0.000(5)	0.026(6)	0.008(6)
C18	0.038(6)	0.030(5)	0.023(5)	-0.003(4)	0.014(4)	0.001(4)
C19	0.075(9)	0.052(7)	0.025(6)	-0.007(5)	0.005(6)	0.004(6)
C20	0.037(6)	0.027(6)	0.075(8)	-0.015(5)	0.029(6)	-0.004(4)
C21	0.036(7)	0.049(7)	0.049(7)	0.001(5)	0.015(5)	0.003(5)

Table A8 continued.

C22	0.073(9)	0.029(6)	0.042(7)	0.000(5)	0.010(6)	0.007(6)
C23	0.049(7)	0.038(7)	0.078(9)	-0.012(6)	0.035(7)	0.002(5)
C24	0.046(7)	0.058(8)	0.041(7)	0.008(6)	0.011(6)	-0.001(6)
C25	0.095(11)	0.051(8)	0.038(7)	-0.005(6)	0.033(7)	0.013(7)
C26	0.051(7)	0.044(7)	0.032(6)	0.000(5)	0.017(5)	0.014(5)
C27	0.056(8)	0.046(7)	0.046(7)	0.020(5)	0.024(6)	0.013(6)
C28	0.050(7)	0.050(7)	0.054(7)	-0.012(6)	0.018(6)	-0.010(6)
C29	0.052(7)	0.046(7)	0.046(7)	-0.014(5)	0.031(6)	-0.003(5)
C30	0.051(7)	0.037(6)	0.036(6)	0.000(5)	0.017(5)	-0.004(5)
C31	0.062(8)	0.042(7)	0.065(8)	0.003(6)	0.035(7)	-0.007(6)
C32	0.062(8)	0.042(6)	0.029(6)	0.006(5)	0.024(6)	0.003(5)
C33	0.056(8)	0.025(5)	0.058(7)	0.006(5)	0.035(6)	0.001(5)
C34	0.053(7)	0.017(5)	0.050(7)	0.001(4)	0.028(6)	0.002(4)
C35	0.055(7)	0.039(6)	0.033(6)	-0.001(5)	0.021(5)	-0.008(5)
C36	0.058(8)	0.052(7)	0.045(7)	0.008(5)	0.026(6)	0.018(6)
C37	0.062(8)	0.032(6)	0.056(8)	-0.003(5)	0.042(7)	0.006(5)
C38	0.045(7)	0.045(7)	0.048(7)	-0.004(5)	0.009(6)	-0.006(5)
C39	0.056(8)	0.035(6)	0.064(8)	-0.030(6)	0.029(6)	-0.013(5)
C40	0.057(7)	0.049(7)	0.020(5)	0.001(4)	0.025(5)	-0.015(5)
C41	0.036(6)	0.033(6)	0.042(6)	0.004(5)	0.024(5)	0.000(4)
C42	0.061(8)	0.021(5)	0.047(7)	-0.006(5)	0.032(6)	-0.005(5)
C43	0.041(7)	0.024(5)	0.058(7)	0.013(5)	0.019(6)	0.004(4)
C44	0.065(8)	0.036(6)	0.038(6)	0.010(5)	0.026(6)	-0.016(5)
C45	0.039(6)	0.037(6)	0.042(6)	0.004(5)	0.022(5)	0.005(5)
C46	0.039(6)	0.033(6)	0.060(7)	0.016(5)	0.033(6)	0.001(5)
C47	0.053(7)	0.033(6)	0.047(7)	0.010(5)	0.019(6)	0.002(5)
C48	0.051(7)	0.030(6)	0.037(6)	-0.003(4)	0.020(5)	-0.004(5)
C49	0.051(8)	0.056(8)	0.045(7)	-0.017(5)	0.031(6)	-0.013(5)
C50	0.058(7)	0.021(5)	0.041(6)	-0.002(4)	0.018(6)	-0.007(5)
C51	0.044(6)	0.057(7)	0.040(6)	0.004(5)	0.020(5)	0.003(5)
C52	0.040(6)	0.027(5)	0.040(6)	0.005(4)	0.019(5)	0.007(4)
C53	0.033(6)	0.035(6)	0.050(7)	-0.010(5)	0.025(5)	-0.007(4)
C54	0.038(6)	0.034(6)	0.039(6)	0.005(4)	0.027(5)	0.007(5)
C55	0.041(6)	0.032(6)	0.047(7)	-0.004(5)	0.025(5)	-0.006(5)
C56	0.046(7)	0.030(6)	0.054(7)	0.017(5)	0.024(6)	0.003(5)
C57	0.057(8)	0.046(7)	0.043(7)	-0.017(5)	0.011(6)	0.004(6)
C58	0.059(8)	0.036(6)	0.042(6)	-0.001(5)	0.024(6)	-0.001(5)
C59	0.045(7)	0.030(6)	0.037(6)	0.003(4)	0.019(5)	-0.001(5)
C60	0.041(7)	0.050(7)	0.054(7)	-0.006(5)	0.033(6)	-0.001(5)
C61	0.037(6)	0.033(5)	0.034(5)	0.002(4)	0.017(4)	-0.007(4)
C62	0.045(7)	0.056(7)	0.052(7)	0.002(6)	0.031(6)	0.000(5)

Table A8 continued.

C63	0.040(6)	0.023(5)	0.048(6)	0.004(4)	0.031(5)	-0.001(4)
C64	0.078(9)	0.030(6)	0.040(7)	-0.002(5)	0.029(7)	0.005(6)
C65	0.047(6)	0.024(5)	0.040(6)	-0.007(4)	0.027(5)	0.001(4)
C66	0.051(7)	0.028(5)	0.041(6)	0.009(4)	0.024(5)	0.004(5)
C67	0.036(6)	0.034(6)	0.046(7)	-0.012(5)	0.019(5)	-0.007(4)
C68	0.042(6)	0.027(5)	0.031(6)	0.009(4)	0.023(5)	0.000(4)
C69	0.053(7)	0.016(5)	0.033(6)	0.000(4)	0.017(5)	-0.003(4)
C70	0.045(6)	0.030(5)	0.025(5)	-0.004(4)	0.015(5)	-0.001(4)
C71	0.054(7)	0.027(5)	0.041(6)	0.005(4)	0.028(5)	0.004(5)
C72	0.048(6)	0.037(6)	0.051(6)	0.005(5)	0.034(5)	-0.003(5)
C73	0.048(7)	0.017(5)	0.037(6)	0.007(4)	0.025(5)	-0.002(4)
C74	0.041(6)	0.047(6)	0.022(5)	-0.006(4)	0.018(4)	-0.006(5)
C75	0.044(6)	0.023(5)	0.035(6)	0.001(4)	0.018(5)	-0.006(4)
C76	0.022(5)	0.024(5)	0.039(6)	0.004(4)	0.010(4)	-0.003(4)
C77	0.049(7)	0.023(5)	0.039(6)	0.004(4)	0.024(5)	0.002(4)
C78	0.091(15)	0.164(21)	0.059(10)	0.002(12)	0.010(10)	-0.043(15)
C79	0.149(21)	0.159(22)	0.116(17)	0.023(15)	0.036(15)	-0.062(17)
C80	0.101(14)	0.106(14)	0.108(14)	0.006(11)	0.031(12)	-0.043(11)
C82	0.127(23)	0.266(35)	0.257(35)	0.054(28)	0.069(24)	-0.052(22)
C83	0.510(70)	0.271(40)	0.349(46)	-0.194(36)	0.366(54)	-0.327(49)
C84	0.209(35)	0.212(34)	0.800(103)	0.126(47)	0.373(54)	0.058(26)
C85	0.065(16)	0.265(34)	0.275(35)	-0.044(27)	-0.034(19)	0.058(18)
C86	0.084(16)	0.223(30)	0.094(15)	-0.025(17)	0.042(13)	-0.036(17)
C87	0.075(13)	0.095(14)	0.134(16)	-0.023(12)	0.031(12)	0.001(10)
C88	0.166(26)	0.171(27)	0.236(32)	-0.082(23)	-0.027(22)	0.017(20)
C91	0.221(32)	0.315(41)	0.172(27)	-0.154(27)	0.099(23)	-0.232(32)
C92	0.979(150)	1.859(287)	0.825(125)	-1.000(171)	0.885(133)	-1.000(184)
C93	0.073(17)	0.258(37)	0.362(51)	-0.266(39)	-0.022(21)	0.004(19)
C94	0.138(20)	0.164(22)	0.299(33)	-0.079(21)	0.168(24)	-0.027(16)
F1	0.119(11)	0.183(14)	0.291(20)	-0.070(13)	0.034(13)	-0.020(10)
F2	0.140(11)	0.130(10)	0.254(15)	0.067(10)	0.112(11)	0.043(8)
F3	0.302(18)	0.135(10)	0.141(10)	0.020(8)	0.151(12)	0.073(10)

Table A8 continued.

F4	0.225(15)	0.187(13)	0.200(14)	0.052(10)	0.101(12)	-0.097(11)
O1	0.107(12)	0.215(17)	0.167(15)	-0.011(12)	0.074(11)	-0.025(11)
O2	0.110(11)	0.118(10)	0.102(9)	-0.011(7)	0.040(8)	0.002(8)
O3	0.153(14)	0.149(14)	0.207(17)	0.065(13)	0.029(13)	0.047(11)
O4	0.132(13)	0.105(11)	0.232(18)	-0.101(12)	0.097(13)	-0.052(10)
O5	0.105(12)	0.145(14)	0.238(19)	-0.056(13)	0.014(12)	0.011(10)
O6	0.121(11)	0.081(9)	0.163(13)	-0.014(8)	0.013(10)	0.008(8)
O7	0.372(41)	0.429(46)	0.206(23)	-0.185(28)	0.154(29)	-0.327(39)
O8	0.039(4)	0.047(4)	0.055(5)	-0.007(3)	0.032(4)	-0.008(3)

The anisotropic displacement factor exponent takes the form:
$-2\pi^2 [h^2 a^{*2} U11 + ... + 2 h k a^* b^* U12]$

Table A8 continued.

Hydrogen coordinates (x 10^4) and isotropic displacement parameters ($Å^2$ x 10^3).

	x	y	z	U(eq)	Occ.
H10	0.7639(6)	1.0182(7)	0.1825(4)	0.052	1
H11	0.2394(6)	0.2718(11)	0.0494(5)	0.080	1
H12	0.5959(5)	0.5337(7)	0.0892(4)	0.051	1
H13A	0.5670(6)	1.1225(8)	0.0771(5)	0.090	1
H13B	0.5244(6)	1.0351(8)	0.0826(5)	0.090	1
H13C	0.5435(6)	1.0369(8)	0.0347(5)	0.090	1
H14A	1.1062(6)	0.3795(10)	0.4235(5)	0.113	1
H14B	1.0832(6)	0.2882(10)	0.3846(5)	0.113	1
H14C	1.0496(6)	0.3121(10)	0.4221(5)	0.113	1
H15	0.1787(6)	0.5274(10)	0.0864(5)	0.076	1
H16	1.0463(5)	0.9418(7)	0.1692(4)	0.050	1
H17	0.1547(6)	0.1239(8)	0.1866(4)	0.062	1
H19	0.1784(6)	0.3640(8)	0.2764(4)	0.067	1
H1A	0.9265(7)	0.8235(10)	0.4987(5)	0.106	1
H1B	0.9833(7)	0.8886(10)	0.4987(5)	0.106	1
H1C	0.9892(7)	0.7709(10)	0.5023(5)	0.106	1
H2	0.1872(7)	-0.0414(9)	0.1911(5)	0.078	1
H20	0.8813(5)	0.3978(7)	0.1009(4)	0.053	1
H21	0.5786(5)	0.8568(8)	0.0815(4)	0.054	1
H22	0.6726(6)	1.1084(8)	0.1358(4)	0.063	1
H23	0.0330(5)	0.0820(8)	0.0393(5)	0.063	1
H24	1.0757(5)	0.5350(9)	0.3827(4)	0.061	1
H25	0.0886(7)	0.3777(9)	0.2924(5)	0.072	1
H28	-0.1396(5)	0.1859(8)	0.0178(4)	0.063	1
H29	1.0934(5)	0.6285(8)	0.1464(4)	0.053	1
H30	0.7311(5)	0.6636(7)	0.2474(4)	0.050	1
H31	0.1116(6)	0.4404(8)	0.1119(5)	0.064	1

Table A8 continued.

H32	0.8416(6)	0.8062(7)	0.4146(4)	0.051	1
H33	0.9586(5)	0.3078(7)	0.3239(4)	0.052	1
H34	-0.0140(5)	0.2812(6)	0.1485(4)	0.046	1
H35	0.8657(5)	1.0524(8)	0.0836(4)	0.049	1
H36	-0.0680(6)	0.3845(8)	-0.0484(4)	0.060	1
H37	-0.0068(6)	0.3320(7)	0.2289(4)	0.053	1
H38	1.0170(5)	0.8253(8)	0.4218(4)	0.059	1
H39	0.9267(5)	0.4656(8)	0.0481(4)	0.060	1
H40	0.9225(5)	0.8052(8)	0.0342(3)	0.047	1
H41	0.8881(5)	0.4076(7)	0.2616(4)	0.041	1
H42	0.7029(5)	0.5376(7)	0.1104(4)	0.048	1
H44	0.9173(5)	0.9768(8)	0.0383(4)	0.054	1
H45	0.6677(5)	0.7661(7)	0.1252(4)	0.045	1
H46	0.6231(5)	0.6490(7)	0.2260(4)	0.048	1
H48	0.9491(5)	1.1103(7)	0.2285(4)	0.047	1
H49	0.9232(5)	0.6390(8)	0.0364(4)	0.056	1
H5	0.1425(6)	-0.1436(9)	0.1181(5)	0.072	1
H50	1.0181(5)	1.0988(7)	0.1886(4)	0.049	1
H51	0.1662(5)	0.1859(9)	0.0712(4)	0.055	1
H53	0.8419(4)	0.5026(7)	0.1448(4)	0.044	1
H56	1.0047(5)	0.6397(7)	0.3215(4)	0.051	1
H57	-0.1543(6)	0.2926(8)	-0.0511(4)	0.062	1
H58	-0.0416(5)	0.1642(7)	0.0833(4)	0.054	1
H59	1.0487(5)	0.5016(7)	0.1767(4)	0.044	1
H6	0.0654(7)	-0.0824(9)	0.0441(6)	0.081	1
H60	0.0296(5)	0.3649(8)	0.0178(4)	0.052	1
H62	0.1717(5)	0.3133(8)	0.1967(4)	0.057	1
H63	0.8208(5)	0.5302(7)	0.2485(4)	0.039	1
H65	0.9077(5)	0.9671(6)	0.2460(4)	0.040	1
H66	0.8014(5)	0.7960(7)	0.3254(4)	0.046	1
H67	0.9775(5)	0.8181(7)	0.3323(4)	0.045	1
H68	0.7865(5)	0.8751(6)	0.2509(4)	0.037	1
H72	1.0689(5)	0.7930(7)	0.1548(4)	0.049	1
H75	0.8263(5)	0.9516(7)	0.1307(4)	0.040	1
H77	0.9815(5)	0.5452(7)	0.2148(4)	0.042	1
H79A	1.1248(9)	0.6423(14)	0.3353(8)	0.221	1
H79B	1.1964(9)	0.6685(14)	0.3494(8)	0.221	1
H79C	1.1510(9)	0.6411(14)	0.2914(8)	0.221	1

Table A8 continued.

H8	0.2475(6)	0.4429(10)	0.0601(5)	0.075	1
H80A	1.1567(8)	0.9040(12)	0.2891(6)	0.163	1
H80B	1.1714(8)	0.8111(12)	0.2612(6)	0.163	1
H80C	1.2171(8)	0.8377(12)	0.3192(6)	0.163	1
H82A	0.2581(11)	-0.4717(22)	0.2464(11)	0.330	1
H82B	0.1867(11)	-0.4649(22)	0.2063(11)	0.330	1
H82C	0.2161(11)	-0.3806(22)	0.2487(11)	0.330	1
H83A	0.2941(20)	-0.3617(24)	0.1180(13)	0.377	1
H83B	0.3390(20)	-0.2935(24)	0.1632(13)	0.377	1
H84A	0.3867(14)	-0.3684(24)	0.1254(20)	0.529	1
H84B	0.3653(14)	-0.4729(24)	0.1386(20)	0.529	1
H84C	0.4106(14)	-0.4036(24)	0.1839(20)	0.529	1
H85A	0.3729(10)	0.3739(22)	0.0281(11)	0.354	1
H85B	0.3777(10)	0.4386(22)	0.0766(11)	0.354	1
H85C	0.4140(10)	0.4724(22)	0.0424(11)	0.354	1
H87A	0.2572(8)	0.6352(13)	-0.0480(8)	0.126	1
H87B	0.2266(8)	0.6248(13)	-0.0071(8)	0.126	1
H88A	0.2426(12)	0.7940(19)	-0.0194(11)	0.340	1
H88B	0.3155(12)	0.7737(19)	-0.0022(11)	0.340	1
H88C	0.2851(12)	0.7632(19)	0.0387(11)	0.340	1
H92A	1.1374(31)	0.4826(69)	0.4879(23)	1.578	1
H92B	1.1330(31)	0.5923(69)	0.5069(23)	1.578	1
H92C	1.1864(31)	0.5191(69)	0.5430(23)	1.578	1
H93A	1.2823(11)	0.4611(25)	0.4724(15)	0.320	1
H93B	1.2661(11)	0.5656(25)	0.4432(15)	0.320	1
H94A	1.2597(10)	0.4336(17)	0.3828(10)	0.262	1
H94B	1.1933(10)	0.4862(17)	0.3661(10)	0.262	1
H94C	1.2060(10)	0.3821(17)	0.3950(10)	0.262	1
H9A	0.5082(5)	0.5579(8)	0.1075(5)	0.082	1
H9B	0.5138(5)	0.6529(8)	0.1424(5)	0.082	1
H9C	0.5224(5)	0.5450(8)	0.1671(5)	0.082	1

Symmetry transformations used to generate equivalent atoms:
#1 -x-1,-y+1,-z+1

Table A8 continued.

Torsion angles [°].

N4	Rh1	Rh2	N8	114.6(3)
N5	Rh1	Rh2	N8	-165.4(3)
N6	Rh1	Rh2	N8	16.7(3)
N7	Rh1	Rh2	N8	-70.0(3)
O8	Rh1	Rh2	N8	141.5(43)
N4	Rh1	Rh2	N1	22.0(3)
N5	Rh1	Rh2	N1	102.0(3)
N6	Rh1	Rh2	N1	-75.9(3)
N7	Rh1	Rh2	N1	-162.5(3)
O8	Rh1	Rh2	N1	48.9(43)
N4	Rh1	Rh2	N2	-59.3(3)
N5	Rh1	Rh2	N2	20.7(3)
N6	Rh1	Rh2	N2	-157.2(3)
N7	Rh1	Rh2	N2	116.2(3)
O8	Rh1	Rh2	N2	-32.4(43)
N4	Rh1	Rh2	N3	-155.8(3)
N5	Rh1	Rh2	N3	-75.8(3)
N6	Rh1	Rh2	N3	106.3(3)
N7	Rh1	Rh2	N3	19.6(3)
O8	Rh1	Rh2	N3	-128.9(43)
N8	Rh2	N1	C65	1.7(8)
N2	Rh2	N1	C65	-176.2(8)
N3	Rh2	N1	C65	-135.9(51)
Rh1	Rh2	N1	C65	86.8(8)
N8	Rh2	N1	C76	179.2(6)
N2	Rh2	N1	C76	1.3(6)
N3	Rh2	N1	C76	41.7(56)
Rh1	Rh2	N1	C76	-95.7(6)
N8	Rh2	N2	C77	157.9(23)
N1	Rh2	N2	C77	176.2(8)
N3	Rh2	N2	C77	-1.7(8)
Rh1	Rh2	N2	C77	-87.2(8)
N8	Rh2	N2	C61	-21.5(29)
N1	Rh2	N2	C61	-3.2(6)
N3	Rh2	N2	C61	178.9(6)
Rh1	Rh2	N2	C61	93.4(6)

Table A8 continued.

N8	Rh2	N3	C63	56.5(7)
N1	Rh2	N3	C63	-165.9(50)
N2	Rh2	N3	C63	-125.9(7)
Rh1	Rh2	N3	C63	-28.3(7)
N8	Rh2	N3	C54	-114.7(7)
N1	Rh2	N3	C54	22.9(57)
N2	Rh2	N3	C54	63.0(7)
Rh1	Rh2	N3	C54	160.6(7)
N5	Rh1	N4	C75	179.4(8)
N6	Rh1	N4	C75	-1.1(8)
N7	Rh1	N4	C75	-150.4(32)
O8	Rh1	N4	C75	93.2(8)
Rh2	Rh1	N4	C75	-87.9(7)
N5	Rh1	N4	C74	2.5(6)
N6	Rh1	N4	C74	-177.9(7)
N7	Rh1	N4	C74	32.8(37)
O8	Rh1	N4	C74	-83.7(7)
Rh2	Rh1	N4	C74	95.2(6)
N4	Rh1	N5	C53	-179.4(8)
N6	Rh1	N5	C53	168.6(79)
N7	Rh1	N5	C53	3.1(8)
O8	Rh1	N5	C53	-93.8(8)
Rh2	Rh1	N5	C53	88.1(8)
N4	Rh1	N5	C70	-2.9(7)
N6	Rh1	N5	C70	-14.9(87)
N7	Rh1	N5	C70	179.7(7)
O8	Rh1	N5	C70	82.8(7)
Rh2	Rh1	N5	C70	-95.4(7)
N4	Rh1	N6	C68	-113.4(7)
N5	Rh1	N6	C68	-101.5(82)
N7	Rh1	N6	C68	63.9(7)
O8	Rh1	N6	C68	161.0(7)
Rh2	Rh1	N6	C68	-20.9(6)
N4	Rh1	N6	C18	75.2(7)
N5	Rh1	N6	C18	87.1(84)
N7	Rh1	N6	C18	-107.4(7)
O8	Rh1	N6	C18	-10.4(7)
Rh2	Rh1	N6	C18	167.7(7)

Table A8 continued.

N4	Rh1	N7	C63	44.5(37)
N5	Rh1	N7	C63	74.3(7)
N6	Rh1	N7	C63	-105.1(7)
O8	Rh1	N7	C63	160.4(7)
Rh2	Rh1	N7	C63	-18.4(7)
N4	Rh1	N7	C73	-146.3(32)
N5	Rh1	N7	C73	-116.4(7)
N6	Rh1	N7	C73	64.2(7)
O8	Rh1	N7	C73	-30.3(7)
Rh2	Rh1	N7	C73	150.9(6)
N1	Rh2	N8	C68	79.3(7)
N2	Rh2	N8	C68	97.4(26)
N3	Rh2	N8	C68	-102.8(7)
Rh1	Rh2	N8	C68	-18.2(7)
N1	Rh2	N8	C69	-100.0(7)
N2	Rh2	N8	C69	-81.9(27)
N3	Rh2	N8	C69	77.9(7)
Rh1	Rh2	N8	C69	162.5(6)
C17	C2	C5	C6	-1.3(19)
C2	C5	C6	C23	1.4(19)
C15	C8	C11	C51	-2.0(18)
C11	C8	C15	C31	4.0(19)
C5	C2	C17	C55	-0.8(19)
C22	C10	C18	C45	-1.8(15)
C22	C10	C18	N6	177.1(9)
C68	N6	C18	C45	-120.0(10)
Rh1	N6	C18	C45	51.5(12)
C68	N6	C18	C10	61.1(11)
Rh1	N6	C18	C10	-127.4(8)
C18	C10	C22	C26	0.3(17)
C5	C6	C23	C55	0.6(18)
C62	C19	C25	C37	1.3(17)
C45	C21	C26	C22	-2.6(16)
C45	C21	C26	C13	177.8(10)
C10	C22	C26	C21	1.8(17)
C10	C22	C26	C13	-178.5(10)
C56	C24	C27	C33	1.6(17)
C56	C24	C27	C14	-178.1(11)

Table A8 continued.

C8	C15	C31	C47	-3.9(19)
C24	C27	C33	C41	-0.8(17)
C14	C27	C33	C41	178.9(11)
C19	C25	C37	C34	-1.4(16)
C52	C34	C37	C25	2.1(15)
C53	C20	C39	C49	-2.4(16)
C27	C33	C41	C54	-2.5(16)
C43	C12	C42	C73	-3.7(15)
C42	C12	C43	C46	0.2(15)
C42	C12	C43	C9	180.0(9)
C75	C35	C44	C40	2.7(16)
C74	C40	C44	C35	-3.0(16)
C26	C21	C45	C18	1.2(16)
C10	C18	C45	C21	1.1(15)
N6	C18	C45	C21	-177.8(9)
C12	C43	C46	C30	1.9(14)
C9	C43	C46	C30	-177.9(9)
C73	C30	C46	C43	-0.5(14)
C15	C31	C47	C51	1.7(17)
C15	C31	C47	B1	-175.4(11)
C71	B1	C47	C51	-101.1(11)
C52	B1	C47	C51	136.6(10)
C55	B1	C47	C51	17.2(14)
C71	B1	C47	C31	75.8(12)
C52	B1	C47	C31	-46.6(13)
C55	B1	C47	C31	-165.9(10)
C20	C39	C49	C70	2.7(16)
C65	C48	C50	C16	-1.2(15)
C76	C16	C50	C48	-0.7(15)
C31	C47	C51	C11	0.3(16)
B1	C47	C51	C11	177.3(10)
C8	C11	C51	C47	-0.2(18)
C37	C34	C52	C62	-2.4(14)
C37	C34	C52	B1	176.8(9)
C71	B1	C52	C62	-154.7(9)
C55	B1	C52	C62	83.9(11)
C47	B1	C52	C62	-34.0(12)
C71	B1	C52	C34	26.1(12)

Table A8 continued.

C55	B1	C52	C34	-95.3(11)
C47	B1	C52	C34	146.8(9)
C70	N5	C53	C20	-0.1(15)
Rh1	N5	C53	C20	176.3(8)
C39	C20	C53	N5	1.1(16)
C33	C41	C54	C56	5.1(14)
C33	C41	C54	N3	-178.4(8)
C63	N3	C54	C56	-154.8(9)
Rh2	N3	C54	C56	16.2(12)
C63	N3	C54	C41	28.7(13)
Rh2	N3	C54	C41	-160.3(7)
C2	C17	C55	C23	2.7(17)
C2	C17	C55	B1	-172.7(10)
C6	C23	C55	C17	-2.6(16)
C6	C23	C55	B1	172.8(10)
C71	B1	C55	C17	-160.5(9)
C52	B1	C55	C17	-37.4(13)
C47	B1	C55	C17	81.1(12)
C71	B1	C55	C23	24.3(12)
C52	B1	C55	C23	147.4(10)
C47	B1	C55	C23	-94.0(11)
C41	C54	C56	C24	-4.4(15)
N3	C54	C56	C24	179.1(9)
C27	C24	C56	C54	1.0(17)
C58	C28	C57	C36	-2.1(16)
C60	C36	C57	C28	1.5(16)
C57	C28	C58	C71	1.9(16)
C72	C29	C59	C77	0.1(15)
C57	C36	C60	C71	-0.6(16)
C77	N2	C61	C72	3.0(13)
Rh2	N2	C61	C72	-177.5(7)
C77	N2	C61	C76	-175.0(8)
Rh2	N2	C61	C76	4.4(10)
C25	C19	C62	C52	-1.9(17)
C34	C52	C62	C19	2.4(15)
B1	C52	C62	C19	-176.9(10)
C73	N7	C63	N3	-167.8(8)
Rh1	N7	C63	N3	1.6(13)

Table A8 continued.

C54	N3	C63	N7	-165.3(9)
Rh2	N3	C63	N7	23.5(12)
C67	C38	C64	C32	2.5(16)
C67	C38	C64	C1	-179.4(10)
C66	C32	C64	C38	-1.9(15)
C66	C32	C64	C1	-179.9(10)
C76	N1	C65	C48	1.3(14)
Rh2	N1	C65	C48	178.8(7)
C50	C48	C65	N1	0.9(15)
C64	C32	C66	C69	-0.2(15)
C64	C38	C67	C69	-1.1(16)
C18	N6	C68	N8	-174.1(8)
Rh1	N6	C68	N8	13.8(12)
C69	N8	C68	N6	-173.4(8)
Rh2	N8	C68	N6	7.4(12)
C38	C67	C69	C66	-1.0(14)
C38	C67	C69	N8	-179.3(9)
C32	C66	C69	C67	1.6(14)
C32	C66	C69	N8	179.9(8)
C68	N8	C69	C67	-148.8(9)
Rh2	N8	C69	C67	30.5(10)
C68	N8	C69	C66	33.0(13)
Rh2	N8	C69	C66	-147.7(7)
C53	N5	C70	C49	0.3(14)
Rh1	N5	C70	C49	-176.5(8)
C53	N5	C70	C74	179.6(9)
Rh1	N5	C70	C74	2.8(11)
C39	C49	C70	N5	-1.7(16)
C39	C49	C70	C74	179.1(10)
C36	C60	C71	C58	0.2(14)
C36	C60	C71	B1	178.7(9)
C28	C58	C71	C60	-0.8(15)
C28	C58	C71	B1	-179.4(9)
C52	B1	C71	C60	112.1(10)
C55	B1	C71	C60	-125.9(10)
C47	B1	C71	C60	-8.4(13)
C52	B1	C71	C58	-69.5(12)
C55	B1	C71	C58	52.5(12)

Table A8 continued.

C47	B1	C71	C58	170.0(9)
C59	C29	C72	C61	-0.3(16)
N2	C61	C72	C29	-1.3(15)
C76	C61	C72	C29	176.7(9)
C12	C42	C73	C30	5.1(14)
C12	C42	C73	N7	-173.8(8)
C46	C30	C73	C42	-3.0(13)
C46	C30	C73	N7	175.9(8)
C63	N7	C73	C42	-120.5(10)
Rh1	N7	C73	C42	70.1(10)
C63	N7	C73	C30	60.7(12)
Rh1	N7	C73	C30	-108.8(8)
C75	N4	C74	C40	2.4(14)
Rh1	N4	C74	C40	179.5(7)
C75	N4	C74	C70	-178.9(8)
Rh1	N4	C74	C70	-1.8(10)
C44	C40	C74	N4	0.4(15)
C44	C40	C74	C70	-178.2(10)
N5	C70	C74	N4	-0.7(13)
C49	C70	C74	N4	178.6(9)
N5	C70	C74	C40	178.0(9)
C49	C70	C74	C40	-2.7(16)
C74	N4	C75	C35	-2.7(14)
Rh1	N4	C75	C35	-179.5(7)
C44	C35	C75	N4	0.2(15)
C50	C16	C76	N1	3.0(15)
C50	C16	C76	C61	-178.8(9)
C65	N1	C76	C16	-3.3(13)
Rh2	N1	C76	C16	178.9(8)
C65	N1	C76	C61	178.4(8)
Rh2	N1	C76	C61	0.6(10)
N2	C61	C76	C16	178.4(9)
C72	C61	C76	C16	0.4(15)
N2	C61	C76	N1	-3.3(12)
C72	C61	C76	N1	178.6(9)
C61	N2	C77	C59	-3.3(14)
Rh2	N2	C77	C59	177.3(7)
C29	C59	C77	N2	1.8(15)

Table A8 continued.

O2	C86	O4	C87	-10.3(28)
C85	C86	O4	C87	178.9(20)
C88	C87	O4	C86	-165.2(21)
O3	C81	O5	C83	3.1(37)
C82	C81	O5	C83	176.4(20)
C84	C83	O5	C81	-171.6(35)
O6	C91	O7	C93	3.7(89)
C92	C91	O7	C93	-155.5(61)
C94	C93	O7	C91	-154.6(34)

Table A9. Crystal data and structure refinement for $[Rh_2(DTolF)_2(phen)(H_2O)][BF_4][BPh_4]\cdot CH_3CH_2O_2CH_2CH_3\cdot 4H_2O$ (9).

Identification code	$[Rh_2(DTolF)_2(phen)(H_2O)][BF_4][BPh_4]$ $\cdot CH_3CH_2O_2CH_2CH_3\cdot 4H_2O$
Empirical formula	C52 H55 B2 F8 N9 O6 Rh2
Formula weight	1281.49 g/mol
Temperature	293(2) K
Wavelength	0.71073 Å
Crystal system	triclinic
Space group	P-1
Unit cell dimensions	a = 12.6346(2) Å
	b = 13.5872(2) Å
	c = 19.0597(3) Å
	α = 71.9480(10)°
	β = 73.6310(10)°
	γ = 71.3795(7)°
Volume	2886.70(8) $Å^3$
Z	2
ρ_{calc}	1.474 g/cm^3

Table A9 continued.

μ	0.652 cm^{-3}
F(000)	1300
Crystal size	0.31 x 0.23 x 0.13 mm^3
Theta range for data collection	1.63 to 28.24°
Index ranges	-8<=h<=16, -18<=k<=17, -25<=l<=24
Reflections collected	43882
Independent reflections	12465 [R(int) = 0.0167]
Refinement method	Full-matrix least-squares on F^2
Data / restraints / parameters	12465 / 129 / 708
Goodness-of-fit on F^2	1.039
Final R indices [$I>2\sigma(I)$]	R1 = 0.0449, wR2 = 0.125
R indices (all data)	R1 = 0.0620, wR2 = 0.1352
Largest diff. peak and hole	1.097 and –1.134 $e^-/Å^{-3}$

Table A9 continued.

Atomic coordinates (x 10^4) and equivalent isotropic displacement parameters ($Å^2$ x 10^3).

	x	y	z	U(eq)	Occ.
B1	0.1094(6)	0.7610(5)	0.3408(4)	0.0609(17)	1
B2	0.5005(5)	0.7168(5)	0.5594(3)	0.0573(15)	1
C1	-0.3204(4)	0.6773(4)	0.2983(3)	0.0459(11)	1
C10	-0.3260(4)	0.5747(4)	0.3011(3)	0.0468(11)	1
C11	0.3769(5)	-0.0992(4)	0.1712(3)	0.0558(13)	1
C12	0.1703(4)	0.3748(4)	0.5037(2)	0.0374(9)	1
C13	0.2890(4)	0.0846(3)	0.1760(2)	0.0339(9)	1
C14	-0.2054(4)	0.3329(4)	0.4453(2)	0.0379(9)	1
C15	0.1351(4)	-0.0485(3)	0.4401(2)	0.0396(10)	1
C16	0.1788(4)	0.0595(3)	0.5021(2)	0.0360(9)	1
C17	0.0911(3)	0.1654(3)	0.2092(2)	0.0304(8)	1
C18	-0.1053(3)	0.2368(3)	0.2299(2)	0.0305(8)	1
C19	0.1214(3)	0.4577(4)	0.4504(2)	0.0360(9)	1
C2	0.3912(4)	0.0979(4)	0.3449(2)	0.0375(9)	1
C20	-0.1145(4)	0.2711(4)	0.1543(2)	0.0397(10)	1
C21	0.1310(3)	0.1492(3)	0.4494(2)	0.0294(8)	1
C22	-0.2001(4)	0.2151(4)	0.2842(3)	0.0426(11)	1
C23	0.0881(4)	0.0449(3)	0.3903(2)	0.0334(9)	1
C24	0.3387(5)	0.4408(4)	-0.0614(3)	0.0505(12)	1
C25	0.1607(4)	0.4299(4)	0.0276(2)	0.0457(11)	1
C26	0.3156(4)	0.4400(3)	0.2838(2)	0.0355(9)	1
C27	-0.1194(3)	0.5162(3)	0.2668(2)	0.0323(8)	1
C28	0.1748(3)	0.2689(3)	0.5051(2)	0.0342(9)	1
C29	0.3883(4)	0.4231(4)	-0.0008(3)	0.0444(11)	1
C3	-0.3028(4)	0.3707(5)	0.5018(3)	0.0576(14)	1
C30	0.0485(3)	0.4549(3)	0.1836(2)	0.0297(8)	1
C31	0.3252(4)	0.4103(4)	0.0729(2)	0.0409(10)	1

Table A9 continued.

C32	0.2109(3)	0.4126(3)	0.0883(2)	0.0304(8)	1
C33	0.1288(3)	0.2551(3)	0.4508(2)	0.0289(8)	1
C34	0.0762(3)	0.4375(3)	0.3983(2)	0.0310(8)	1
C35	0.2857(4)	-0.0223(4)	0.1991(3)	0.0480(11)	1
C36	0.3845(4)	0.1114(4)	0.1254(3)	0.0493(12)	1
C37	0.4746(5)	0.0339(4)	0.0982(3)	0.0628(15)	1
C38	0.4718(5)	-0.0740(4)	0.1211(3)	0.0585(14)	1
C39	0.5709(6)	-0.1585(5)	0.0922(4)	0.085(2)	1
C4	0.2226(4)	0.1756(4)	0.5588(3)	0.0462(11)	1
C40	0.2237(5)	0.4445(5)	-0.0457(3)	0.0599(14)	1
C41	0.4101(6)	0.4553(6)	-0.1409(3)	0.0727(18)	1
C42	-0.4304(5)	0.7630(5)	0.3162(3)	0.0658(16)	1
C43	-0.2145(4)	0.6973(4)	0.2795(3)	0.0457(11)	1
C44	-0.2154(4)	0.2787(4)	0.1340(3)	0.0523(12)	1
C45	-0.3094(4)	0.2541(5)	0.1885(3)	0.0522(13)	1
C46	-0.4188(5)	0.2611(6)	0.1667(4)	0.083(2)	1
C5	-0.2264(4)	0.4962(4)	0.2844(3)	0.0404(10)	1
C51	0.4715(5)	0.0227(4)	0.3917(3)	0.0606(15)	1
C52	0.2244(4)	0.0764(4)	0.5571(2)	0.0452(11)	1
C53	0.7086(8)	-0.0205(8)	0.2653(5)	0.135(4)	1
C54	0.7888(11)	-0.0193(7)	0.2047(6)	0.242(12)	1
C56	0.878(3)	-0.026(6)	0.1301(18)	1.9(2)	1
C57	1.008(2)	-0.050(3)	0.111(2)	1.20(8)	1
C6	0.3616(5)	0.5099(4)	0.3057(3)	0.0509(12)	1
C7	0.1810(4)	-0.0413(4)	0.4954(3)	0.0433(10)	1
C8	-0.1147(4)	0.6185(3)	0.2649(2)	0.0394(10)	1
C9	-0.3005(4)	0.2239(4)	0.2635(3)	0.0507(12)	1
F1	0.0566(3)	0.8700(3)	0.3228(2)	0.0804(11)	1
F2	0.0912(3)	0.7240(3)	0.4189(2)	0.0755(10)	1
F3	0.2263(4)	0.7475(3)	0.3160(3)	0.1167(18)	1
F4	0.0683(6)	0.7029(4)	0.3139(3)	0.139(2)	1
F5	0.4336(4)	0.6461(4)	0.6088(2)	0.0959(13)	1
F6	0.5619(3)	0.7339(3)	0.60185(18)	0.0632(8)	1
F7	0.5686(3)	0.6632(4)	0.5068(3)	0.1085(16)	1
F8	0.4236(4)	0.8066(4)	0.5344(3)	0.1217(18)	1
N1	0.1500(3)	0.3940(3)	0.16451(18)	0.0305(7)	1
N2	0.1979(3)	0.1652(3)	0.20482(18)	0.0312(7)	1
N3	0.3288(3)	0.1576(3)	0.30868(19)	0.0316(7)	1

Table A9 continued.

N4	0.2791(3)	0.3842(3)	0.26836(18)	0.0300(7)	1
N5	0.0873(3)	0.1417(3)	0.39345(17)	0.0282(7)	1
N6	0.0814(3)	0.3380(3)	0.39750(17)	0.0273(7)	1
N7	0.0015(3)	0.2212(3)	0.24888(18)	0.0301(7)	1
N8	-0.0176(3)	0.4353(3)	0.25142(18)	0.0307(7)	1
N9	-0.1289(3)	0.3053(3)	0.39976(19)	0.0315(7)	1
O1	0.9011(9)	-0.0306(11)	0.2048(8)	0.260(7)	1
O2	0.226(2)	-0.3260(15)	0.1175(9)	0.372(12)	1
O3	0.7737(15)	-0.0218(13)	0.1393(8)	0.408(13)	1
O4	1.0752(15)	-0.2361(15)	0.0624(9)	0.445(16)	1
O6	0.9089(15)	-0.192(2)	0.0235(9)	0.426(14)	1
O7	0.2621(17)	-0.181(2)	0.0496(10)	0.393(12)	1
Rh1	0.03127(2)	0.28777(2)	0.323314(15)	0.02484(9)	1
Rh2	0.23252(2)	0.27490(2)	0.239181(16)	0.02557(9)	1

U(eq) is defined as one third of the trace of the orthogonalized Uij tensor.

Table A9 continued.

Bond lengths [Å] and angles [°].

Rh1	N5	2.054(3)
Rh1	N6	2.060(3)
Rh1	N8	2.064(3)
Rh1	N7	2.070(3)
Rh1	N9	2.126(3)
Rh1	Rh2	2.5804(4)
Rh2	N2	2.006(3)
Rh2	N1	2.015(3)
Rh2	N4	2.029(3)
Rh2	N3	2.034(3)
N1	C30	1.307(5)
N1	C32	1.426(5)
N2	C17	1.328(5)
N2	C13	1.427(5)
N3	C2	1.143(5)
N4	C26	1.145(5)
N5	C23	1.332(5)
N5	C21	1.374(5)
N6	C34	1.338(5)
N6	C33	1.365(5)
N7	C17	1.324(5)
N7	C18	1.429(5)
N8	C30	1.327(5)
N8	C27	1.426(5)
N9	C14	1.152(5)
C1	C43	1.377(7)
C1	C10	1.402(7)
C1	C42	1.532(7)
C2	C51	1.468(6)
C3	C14	1.459(6)
C4	C52	1.351(7)
C4	C28	1.441(6)
C5	C27	1.392(6)
C5	C10	1.397(6)
C6	C26	1.467(6)

Table A9 continued.

C7	C15	1.378(6)
C7	C16	1.405(6)
C8	C43	1.393(6)
C8	C27	1.399(6)
C9	C45	1.387(7)
C9	C22	1.391(6)
C11	C38	1.371(8)
C11	C35	1.390(7)
C12	C19	1.372(6)
C12	C28	1.415(6)
C13	C36	1.388(6)
C13	C35	1.393(6)
C15	C23	1.399(6)
C16	C21	1.404(5)
C16	C52	1.435(6)
C18	C22	1.389(6)
C18	C20	1.398(6)
C19	C34	1.405(6)
C20	C44	1.397(6)
C21	C33	1.439(6)
C24	C40	1.385(8)
C24	C29	1.387(7)
C24	C41	1.520(7)
C25	C40	1.389(7)
C25	C32	1.394(6)
C28	C33	1.403(5)
C29	C31	1.395(6)
C31	C32	1.383(6)
C36	C37	1.384(7)
C37	C38	1.404(8)
C38	C39	1.507(7)
C44	C45	1.394(7)
C45	C46	1.520(7)
B1	F4	1.349(6)
B1	F3	1.388(7)
B1	F2	1.392(7)
B1	F1	1.393(7)
F5	B2	1.426(7)

Table A9 continued.

F6	B2	1.376(6)	
F7	B2	1.357(7)	
F8	B2	1.343(7)	
C54	C53	1.304(11)	
C54	O3	1.324(12)	
C54	O1	1.378(13)	
C56	O1	1.51(3)	
C56	C57	1.52(3)	
N5	Rh1	N6	80.86(13)
N5	Rh1	N8	177.41(13)
N6	Rh1	N8	98.01(13)
N5	Rh1	N7	93.54(13)
N6	Rh1	N7	172.20(13)
N8	Rh1	N7	87.36(13)
N5	Rh1	N9	88.56(12)
N6	Rh1	N9	84.57(12)
N8	Rh1	N9	93.66(13)
N7	Rh1	N9	100.79(13)
N5	Rh1	Rh2	91.02(9)
N6	Rh1	Rh2	89.42(9)
N8	Rh1	Rh2	86.63(9)
N7	Rh1	Rh2	85.24(9)
N9	Rh1	Rh2	173.97(9)
N2	Rh2	N1	90.80(13)
N2	Rh2	N4	175.63(13)
N1	Rh2	N4	89.57(13)
N2	Rh2	N3	90.79(13)
N1	Rh2	N3	174.95(13)
N4	Rh2	N3	88.48(13)
N2	Rh2	Rh1	84.66(10)
N1	Rh2	Rh1	83.88(10)
N4	Rh2	Rh1	99.71(9)
N3	Rh2	Rh1	101.04(10)
C30	N1	C32	120.5(3)
C30	N1	Rh2	123.3(3)
C32	N1	Rh2	116.2(3)
C17	N2	C13	119.1(3)
C17	N2	Rh2	121.0(3)

Table A9 continued.

C13	N2	Rh2	119.8(3)
C2	N3	Rh2	172.8(3)
C26	N4	Rh2	173.7(3)
C23	N5	C21	118.3(3)
C23	N5	Rh1	128.8(3)
C21	N5	Rh1	112.9(3)
C34	N6	C33	118.1(3)
C34	N6	Rh1	129.0(3)
C33	N6	Rh1	112.9(2)
C17	N7	C18	115.1(3)
C17	N7	Rh1	117.6(3)
C18	N7	Rh1	127.0(3)
C30	N8	C27	116.9(3)
C30	N8	Rh1	117.3(3)
C27	N8	Rh1	125.7(3)
C14	N9	Rh1	162.6(3)
C43	C1	C10	118.1(4)
C43	C1	C42	122.0(5)
C10	C1	C42	119.9(5)
N3	C2	C51	179.1(5)
C52	C4	C28	121.1(4)
C27	C5	C10	121.3(4)
C15	C7	C16	120.0(4)
C43	C8	C27	120.5(4)
C45	C9	C22	121.3(4)
C5	C10	C1	120.4(5)
C38	C11	C35	122.4(5)
C19	C12	C28	118.8(4)
C36	C13	C35	118.5(4)
C36	C13	N2	120.3(4)
C35	C13	N2	121.2(4)
N9	C14	C3	178.5(5)
C7	C15	C23	119.6(4)
C21	C16	C7	116.9(4)
C21	C16	C52	118.4(4)
C7	C16	C52	124.7(4)
N7	C17	N2	123.5(4)
C22	C18	C20	118.4(4)

Table A9 continued.

C22	C18	N7	122.2(4)
C20	C18	N7	119.4(4)
C12	C19	C34	120.5(4)
C44	C20	C18	120.4(4)
N5	C21	C16	123.0(4)
N5	C21	C33	116.6(3)
C16	C21	C33	120.4(4)
C18	C22	C9	120.8(4)
N5	C23	C15	122.2(4)
C40	C24	C29	117.3(4)
C40	C24	C41	122.7(5)
C29	C24	C41	120.0(5)
C40	C25	C32	120.9(5)
N4	C26	C6	178.5(5)
C5	C27	C8	117.8(4)
C5	C27	N8	121.3(4)
C8	C27	N8	120.8(4)
C33	C28	C12	117.4(4)
C33	C28	C4	118.7(4)
C12	C28	C4	123.9(4)
C24	C29	C31	121.5(5)
N1	C30	N8	123.5(4)
C32	C31	C29	120.9(4)
C31	C32	C25	117.8(4)
C31	C32	N1	119.5(4)
C25	C32	N1	122.6(4)
N6	C33	C28	123.4(4)
N6	C33	C21	116.8(3)
C28	C33	C21	119.9(4)
N6	C34	C19	121.8(4)
C11	C35	C13	119.8(5)
C37	C36	C13	121.0(5)
C36	C37	C38	120.8(5)
C11	C38	C37	117.5(5)
C11	C38	C39	121.8(6)
C37	C38	C39	120.6(6)
C24	C40	C25	121.5(5)
C1	C43	C8	121.8(4)

Table A9 continued.

C45	C44	C20	121.1(5)
C9	C45	C44	118.0(4)
C9	C45	C46	120.8(5)
C44	C45	C46	121.2(5)
C4	C52	C16	121.6(4)
F4	B1	F3	112.6(6)
F4	B1	F2	107.8(5)
F3	B1	F2	106.1(5)
F4	B1	F1	112.8(5)
F3	B1	F1	108.4(5)
F2	B1	F1	108.8(5)
F8	B2	F7	115.9(5)
F8	B2	F6	111.7(5)
F7	B2	F6	112.3(4)
F8	B2	F5	104.4(5)
F7	B2	F5	104.5(5)
F6	B2	F5	107.1(5)
C53	C54	O3	123.2(13)
C53	C54	O1	123.2(11)
O3	C54	O1	112.9(11)
O1	C56	C57	80(2)
C54	O1	C56	64.9(15)

Symmetry transformations used to generate equivalent atoms:
#1 -x-1,-y+1,-z+1

Table A9 continued.

Anisotropic displacement parameters ($Å^2 \times 10^3$).

	U11	U22	U33	U23	U13	U12
Rh1	0.02510(16)	0.02494(16)	0.02429(15)	-0.00359(11)	-0.00662(11)	-0.00698(12)
Rh2	0.02416(16)	0.02751(16)	0.02478(15)	-0.00423(12)	-0.00714(11)	-0.00634(12)
N1	0.0307(17)	0.0316(17)	0.0278(16)	-0.0034(13)	-0.0080(13)	-0.0080(14)
N2	0.0304(17)	0.0321(17)	0.0311(17)	-0.0074(14)	-0.0081(14)	-0.0062(14)
N3	0.0273(17)	0.0343(18)	0.0331(17)	-0.0057(14)	-0.0090(14)	-0.0077(14)
N4	0.0285(17)	0.0339(17)	0.0274(16)	-0.0058(14)	-0.0029(13)	-0.0116(14)
N5	0.0283(16)	0.0284(16)	0.0250(15)	-0.0025(13)	-0.0043(13)	-0.0082(13)
N6	0.0252(16)	0.0319(17)	0.0236(15)	-0.0056(13)	-0.0015(12)	-0.0097(13)
N7	0.0299(17)	0.0319(17)	0.0311(17)	-0.0072(14)	-0.0092(14)	-0.0091(14)
N8	0.0335(18)	0.0278(16)	0.0275(16)	-0.0015(13)	-0.0086(14)	-0.0063(14)
N9	0.0293(17)	0.0307(17)	0.0322(17)	-0.0056(14)	-0.0075(14)	-0.0054(14)
C1	0.043(3)	0.046(3)	0.039(2)	-0.013(2)	-0.011(2)	0.008(2)
C2	0.034(2)	0.040(2)	0.039(2)	-0.0087(19)	-0.0100(19)	-0.0087(19)
C3	0.034(2)	0.084(4)	0.058(3)	-0.034(3)	0.000(2)	-0.012(3)
C4	0.048(3)	0.059(3)	0.035(2)	-0.008(2)	-0.018(2)	-0.013(2)
C5	0.036(2)	0.034(2)	0.047(3)	-0.0032(19)	-0.014(2)	-0.0059(18)
C6	0.058(3)	0.052(3)	0.053(3)	-0.021(2)	-0.001(2)	-0.029(2)
C7	0.045(3)	0.036(2)	0.041(2)	0.0056(19)	-0.015(2)	-0.008(2)
C8	0.042(2)	0.037(2)	0.039(2)	-0.0079(18)	-0.0082(19)	-0.0094(19)
C9	0.034(2)	0.070(3)	0.058(3)	-0.030(3)	0.003(2)	-0.023(2)
C10	0.031(2)	0.051(3)	0.048(3)	-0.005(2)	-0.012(2)	0.001(2)
C11	0.057(3)	0.032(2)	0.072(4)	-0.016(2)	-0.012(3)	-0.001(2)
C12	0.031(2)	0.051(3)	0.036(2)	-0.019(2)	-0.0024(17)	-0.0136(19)
C13	0.032(2)	0.035(2)	0.035(2)	-0.0091(17)	-0.0110(17)	-0.0045(17)
C14	0.034(2)	0.045(2)	0.038(2)	-0.0074(19)	-0.0124(19)	-0.0123(19)
C15	0.045(3)	0.027(2)	0.044(2)	-0.0035(18)	-0.009(2)	-0.0111(18)
C16	0.033(2)	0.038(2)	0.032(2)	-0.0009(17)	-0.0089(17)	-0.0078(18)
C17	0.034(2)	0.030(2)	0.0291(19)	-0.0072(16)	-0.0099(16)	-0.0089(17)
C18	0.030(2)	0.0306(19)	0.035(2)	-0.0089(16)	-0.0087(16)	-0.0098(16)
C19	0.033(2)	0.041(2)	0.038(2)	-0.0191(19)	0.0016(18)	-0.0128(18)
C20	0.032(2)	0.049(3)	0.038(2)	-0.007(2)	-0.0104(18)	-0.0107(19)
C21	0.0264(19)	0.034(2)	0.0254(18)	-0.0039(16)	-0.0037(15)	-0.0094(16)

Table A9 continued.

C22	0.041(2)	0.060(3)	0.035(2)	-0.014(2)	-0.0047(19)	-0.024(2)
C23	0.037(2)	0.030(2)	0.033(2)	-0.0052(16)	-0.0075(17)	-0.0107(17)
C24	0.063(3)	0.048(3)	0.030(2)	-0.004(2)	-0.001(2)	-0.012(2)
C25	0.040(2)	0.062(3)	0.034(2)	-0.005(2)	-0.0134(19)	-0.012(2)
C26	0.035(2)	0.037(2)	0.032(2)	-0.0091(18)	0.0007(17)	-0.0111(18)
C27	0.032(2)	0.030(2)	0.032(2)	-0.0036(16)	-0.0100(17)	-0.0052(17)
C28	0.030(2)	0.041(2)	0.030(2)	-0.0098(17)	-0.0047(16)	-0.0069(17)
C29	0.039(2)	0.050(3)	0.037(2)	-0.008(2)	0.0025(19)	-0.014(2)
C30	0.031(2)	0.0279(19)	0.0291(19)	-0.0016(15)	-0.0113(16)	-0.0063(16)
C31	0.042(2)	0.051(3)	0.030(2)	-0.0059(19)	-0.0076(18)	-0.015(2)
C32	0.034(2)	0.0265(19)	0.0263(19)	-0.0013(15)	-0.0058(16)	-0.0071(16)
C33	0.0259(19)	0.035(2)	0.0237(18)	-0.0046(15)	-0.0021(15)	-0.0104(16)
C34	0.030(2)	0.031(2)	0.0303(19)	-0.0094(16)	-0.0004(16)	-0.0094(16)
C35	0.051(3)	0.038(2)	0.052(3)	-0.011(2)	-0.005(2)	-0.012(2)
C36	0.041(3)	0.041(3)	0.059(3)	-0.016(2)	0.002(2)	-0.008(2)
C37	0.048(3)	0.052(3)	0.073(4)	-0.020(3)	0.013(3)	-0.010(3)
C38	0.059(3)	0.050(3)	0.057(3)	-0.023(3)	-0.011(3)	0.008(3)
C39	0.071(4)	0.066(4)	0.095(5)	-0.037(4)	-0.006(4)	0.019(3)
C40	0.064(4)	0.082(4)	0.034(2)	-0.006(3)	-0.016(2)	-0.021(3)
C41	0.076(4)	0.094(5)	0.031(3)	-0.010(3)	0.006(3)	-0.018(4)
C42	0.054(3)	0.062(3)	0.064(4)	-0.024(3)	-0.013(3)	0.018(3)
C43	0.055(3)	0.031(2)	0.048(3)	-0.012(2)	-0.012(2)	-0.003(2)
C44	0.044(3)	0.070(3)	0.047(3)	-0.011(2)	-0.021(2)	-0.011(2)
C45	0.028(2)	0.078(4)	0.060(3)	-0.030(3)	-0.011(2)	-0.011(2)
C46	0.037(3)	0.129(6)	0.102(5)	-0.049(5)	-0.026(3)	-0.016(3)
C51	0.055(3)	0.051(3)	0.069(4)	-0.003(3)	-0.036(3)	0.005(2)
C52	0.052(3)	0.048(3)	0.034(2)	0.002(2)	-0.019(2)	-0.012(2)
B1	0.078(5)	0.048(3)	0.064(4)	-0.010(3)	-0.015(4)	-0.029(3)
F1	0.090(3)	0.055(2)	0.101(3)	-0.0069(19)	-0.040(2)	-0.0184(19)
F2	0.090(3)	0.072(2)	0.072(2)	-0.0062(18)	-0.024(2)	-0.034(2)
F3	0.094(3)	0.069(3)	0.149(4)	-0.020(3)	0.033(3)	-0.026(2)
F4	0.253(7)	0.107(4)	0.122(4)	-0.015(3)	-0.092(4)	-0.097(4)
F5	0.100(3)	0.119(3)	0.089(3)	-0.018(2)	-0.019(2)	-0.062(3)
F6	0.0608(19)	0.070(2)	0.071(2)	-0.0175(16)	-0.0265(16)	-0.0211(16)
F7	0.066(3)	0.177(5)	0.105(3)	-0.086(3)	-0.010(2)	-0.017(3)
F8	0.094(3)	0.103(3)	0.159(5)	-0.011(3)	-0.077(3)	0.012(3)
B2	0.039(3)	0.076(4)	0.058(4)	-0.017(3)	-0.014(3)	-0.012(3)
C54	0.54(3)	0.033(4)	0.087(8)	-0.002(4)	-0.006(13)	-0.041(10)
O3	0.76(4)	0.292(17)	0.327(19)	0.040(15)	-0.28(3)	-0.30(2)
C56	2.0(2)	2.0(3)	2.0(3)	-0.50(11)	-0.56(11)	-0.78(12)
O1	0.156(9)	0.251(13)	0.42(2)	-0.059(12)	-0.142(11)	-0.055(9)
C57	1.21(11)	1.02(10)	0.86(9)	0.35(7)	0.05(8)	-0.38(8)
O2	0.56(3)	0.37(2)	0.215(15)	-0.093(15)	-0.16(2)	-0.05(2)
O4	0.60(4)	0.43(3)	0.31(2)	-0.28(2)	0.25(2)	-0.25(3)

Table A9 continued.

O6	0.317(19)	0.82(4)	0.306(17)	-0.38(2)	0.056(15)	-0.23(2)
O7	0.40(2)	0.63(4)	0.279(18)	-0.13(2)	-0.142(18)	-0.23(2)

The anisotropic displacement factor exponent takes the form:
$-2\pi^2 [h^2 a^{*2} U11 + ... + 2 h k a^* b^* U12]$

Table A9 continued.

Hydrogen coordinates (x 10^4) and isotropic displacement parameters ($Å^2$ x 10^3).

	x	y	z	U(eq)	Occ.
H10	-0.3965	0.5588	0.3142	0.056	1
H11	0.3735	-0.1703	0.1871	0.067	1
H12	0.1999	0.3881	0.5384	0.045	1
H15	0.1354	-0.1150	0.4360	0.048	1
H17	0.0785	0.1242	0.1829	0.036	1
H19	0.1183	0.5277	0.4486	0.043	1
H20	-0.0531	0.2889	0.1172	0.048	1
H22	-0.1964	0.1944	0.3349	0.051	1
H23	0.0563	0.0393	0.3536	0.040	1
H25	0.0839	0.4317	0.0364	0.055	1
H29	0.4655	0.4198	-0.0096	0.053	1
H30	0.0211	0.5153	0.1477	0.036	1
H31	0.3605	0.4000	0.1123	0.049	1
H34	0.0416	0.4950	0.3635	0.037	1
H35	0.2227	-0.0423	0.2331	0.058	1
H36	0.3880	0.1825	0.1095	0.059	1
H37	0.5378	0.0535	0.0643	0.075	1
H39A	0.6287	-0.1254	0.0580	0.127	1
H39B	0.5452	-0.1943	0.0665	0.127	1
H39C	0.6017	-0.2094	0.1338	0.127	1
H3A	-0.3359	0.4455	0.4832	0.086	1
H3B	-0.2779	0.3602	0.5473	0.086	1
H3C	-0.3587	0.3314	0.5119	0.086	1
H4	0.2528	0.1838	0.5953	0.055	1
H40	0.1879	0.4571	-0.0853	0.072	1
H41A	0.4871	0.4498	-0.1394	0.109	1

H41B	0.3789	0.5246	-0.1708	0.109	1

Table A9 continued.

H41C	0.4093	0.4009	-0.1629	0.109	1
H42A	-0.4948	0.7336	0.3281	0.099	1
H42B	-0.4365	0.8229	0.2733	0.099	1
H42C	-0.4286	0.7861	0.3586	0.099	1
H43	-0.2095	0.7654	0.2765	0.055	1
H44	-0.2200	0.3006	0.0834	0.063	1
H46A	-0.4098	0.2834	0.1128	0.125	1
H46B	-0.4806	0.3122	0.1890	0.125	1
H46C	-0.4351	0.1922	0.1844	0.125	1
H5	-0.2317	0.4292	0.2851	0.049	1
H51A	0.4819	0.0578	0.4250	0.091	1
H51B	0.5435	-0.0010	0.3599	0.091	1
H51C	0.4418	-0.0378	0.4208	0.091	1
H52	0.2560	0.0176	0.5924	0.054	1
H53A	0.7401	-0.0273	0.3074	0.203	1
H53B	0.6771	-0.0801	0.2748	0.203	1
H53C	0.6497	0.0449	0.2584	0.203	1
H56A	0.8389	0.0439	0.1040	2.277	1
H56B	0.8464	-0.0824	0.1303	2.277	1
H57A	1.0313	-0.0033	0.0634	1.801	1
H57B	1.0388	-0.1233	0.1066	1.801	1
H57C	1.0347	-0.0401	0.1495	1.801	1
H6A	0.3500	0.4935	0.3596	0.076	1
H6B	0.3233	0.5833	0.2873	0.076	1
H6C	0.4418	0.4988	0.2844	0.076	1
H7	0.2133	-0.1031	0.5283	0.052	1
H8	-0.0443	0.6339	0.2539	0.047	1
H9	-0.3630	0.2092	0.3008	0.061	1

Symmetry transformations used to generate equivalent atoms:
#1 -x-1,-y+1,-z+1

Table A9 continued.

Torsion angles [°].

N5	Rh1	Rh2	N2	73.06(13)
N6	Rh1	Rh2	N2	153.90(13)
N8	Rh1	Rh2	N2	-108.04(13)
N7	Rh1	Rh2	N2	-20.41(13)
N9	Rh1	Rh2	N2	159.0(8)
N5	Rh1	Rh2	N1	164.44(13)
N6	Rh1	Rh2	N1	-114.72(13)
N8	Rh1	Rh2	N1	-16.65(13)
N7	Rh1	Rh2	N1	70.98(13)
N9	Rh1	Rh2	N1	-109.6(8)
N5	Rh1	Rh2	N4	-107.05(13)
N6	Rh1	Rh2	N4	-26.21(13)
N8	Rh1	Rh2	N4	71.85(13)
N7	Rh1	Rh2	N4	159.48(13)
N9	Rh1	Rh2	N4	-21.1(8)
N5	Rh1	Rh2	N3	-16.70(13)
N6	Rh1	Rh2	N3	64.14(13)
N8	Rh1	Rh2	N3	162.20(13)
N7	Rh1	Rh2	N3	-110.17(13)
N9	Rh1	Rh2	N3	69.3(8)
N2	Rh2	N1	C30	104.3(3)
N4	Rh2	N1	C30	-80.1(3)
N3	Rh2	N1	C30	-147.4(14)
Rh1	Rh2	N1	C30	19.8(3)
N2	Rh2	N1	C32	-78.5(3)
N4	Rh2	N1	C32	97.2(3)
N3	Rh2	N1	C32	29.9(16)
Rh1	Rh2	N1	C32	-163.0(3)
N1	Rh2	N2	C17	-59.2(3)
N4	Rh2	N2	C17	-154.1(16)
N3	Rh2	N2	C17	125.5(3)
Rh1	Rh2	N2	C17	24.5(3)
N1	Rh2	N2	C13	121.5(3)
N4	Rh2	N2	C13	26.7(18)
N3	Rh2	N2	C13	-53.7(3)
Rh1	Rh2	N2	C13	-154.7(3)

Table A9 continued.

N2	Rh2	N3	C2	135(3)
N1	Rh2	N3	C2	27(4)
N4	Rh2	N3	C2	-41(3)
Rh1	Rh2	N3	C2	-140(3)
N2	Rh2	N4	C26	-34(4)
N1	Rh2	N4	C26	-129(3)
N3	Rh2	N4	C26	46(3)
Rh1	Rh2	N4	C26	147(3)
N6	Rh1	N5	C23	179.3(4)
N8	Rh1	N5	C23	-116(3)
N7	Rh1	N5	C23	-6.2(4)
N9	Rh1	N5	C23	94.5(3)
Rh2	Rh1	N5	C23	-91.5(3)
N6	Rh1	N5	C21	-2.0(3)
N8	Rh1	N5	C21	62(3)
N7	Rh1	N5	C21	172.5(3)
N9	Rh1	N5	C21	-86.7(3)
Rh2	Rh1	N5	C21	87.2(3)
N5	Rh1	N6	C34	-179.2(3)
N8	Rh1	N6	C34	3.1(3)
N7	Rh1	N6	C34	136.4(8)
N9	Rh1	N6	C34	-89.8(3)
Rh2	Rh1	N6	C34	89.6(3)
N5	Rh1	N6	C33	2.7(2)
N8	Rh1	N6	C33	-174.9(3)
N7	Rh1	N6	C33	-41.7(10)
N9	Rh1	N6	C33	92.1(3)
Rh2	Rh1	N6	C33	-88.4(2)
N5	Rh1	N7	C17	-67.8(3)
N6	Rh1	N7	C17	-24.0(11)
N8	Rh1	N7	C17	109.8(3)
N9	Rh1	N7	C17	-157.0(3)
Rh2	Rh1	N7	C17	23.0(3)
N5	Rh1	N7	C18	118.5(3)
N6	Rh1	N7	C18	162.3(8)
N8	Rh1	N7	C18	-63.9(3)
N9	Rh1	N7	C18	29.3(3)
Rh2	Rh1	N7	C18	-150.7(3)

Table A9 continued.

N5	Rh1	N8	C30	45(3)
N6	Rh1	N8	C30	108.4(3)
N7	Rh1	N8	C30	-65.9(3)
N9	Rh1	N8	C30	-166.5(3)
Rh2	Rh1	N8	C30	19.5(3)
N5	Rh1	N8	C27	-139(3)
N6	Rh1	N8	C27	-75.0(3)
N7	Rh1	N8	C27	110.7(3)
N9	Rh1	N8	C27	10.1(3)
Rh2	Rh1	N8	C27	-163.9(3)
N5	Rh1	N9	C14	106.2(11)
N6	Rh1	N9	C14	25.3(11)
N8	Rh1	N9	C14	-72.4(11)
N7	Rh1	N9	C14	-160.4(11)
Rh2	Rh1	N9	C14	20.1(18)
Rh2	N3	C2	C51	44(39)
C27	C5	C10	C1	1.9(7)
C43	C1	C10	C5	-0.7(7)
C42	C1	C10	C5	179.6(4)
C17	N2	C13	C36	136.4(4)
Rh2	N2	C13	C36	-44.3(5)
C17	N2	C13	C35	-45.2(5)
Rh2	N2	C13	C35	134.1(4)
Rh1	N9	C14	C3	62(19)
C16	C7	C15	C23	0.9(7)
C15	C7	C16	C21	-1.4(7)
C15	C7	C16	C52	-179.7(4)
C18	N7	C17	N2	162.5(4)
Rh1	N7	C17	N2	-11.9(5)
C13	N2	C17	N7	165.3(4)
Rh2	N2	C17	N7	-14.0(5)
C17	N7	C18	C22	129.9(4)
Rh1	N7	C18	C22	-56.2(5)
C17	N7	C18	C20	-47.6(5)
Rh1	N7	C18	C20	126.2(4)
C28	C12	C19	C34	0.4(6)
C22	C18	C20	C44	-2.6(7)
N7	C18	C20	C44	175.0(4)

Table A9 continued.

C23	N5	C21	C16	1.7(6)
Rh1	N5	C21	C16	-177.2(3)
C23	N5	C21	C33	179.9(3)
Rh1	N5	C21	C33	1.0(4)
C7	C16	C21	N5	0.1(6)
C52	C16	C21	N5	178.5(4)
C7	C16	C21	C33	-178.0(4)
C52	C16	C21	C33	0.4(6)
C20	C18	C22	C9	2.1(7)
N7	C18	C22	C9	-175.5(4)
C45	C9	C22	C18	0.2(8)
C21	N5	C23	C15	-2.2(6)
Rh1	N5	C23	C15	176.4(3)
C7	C15	C23	N5	1.0(7)
Rh2	N4	C26	C6	-91(18)
C10	C5	C27	C8	-1.1(6)
C10	C5	C27	N8	178.5(4)
C43	C8	C27	C5	-0.8(6)
C43	C8	C27	N8	179.6(4)
C30	N8	C27	C5	119.0(4)
Rh1	N8	C27	C5	-57.6(5)
C30	N8	C27	C8	-61.3(5)
Rh1	N8	C27	C8	122.0(4)
C19	C12	C28	C33	0.3(6)
C19	C12	C28	C4	-179.3(4)
C52	C4	C28	C33	0.5(7)
C52	C4	C28	C12	-180.0(4)
C40	C24	C29	C31	-0.4(8)
C41	C24	C29	C31	179.5(5)
C32	N1	C30	N8	172.5(4)
Rh2	N1	C30	N8	-10.4(5)
C27	N8	C30	N1	172.0(4)
Rh1	N8	C30	N1	-11.1(5)
C24	C29	C31	C32	1.3(7)
C29	C31	C32	C25	-1.0(7)
C29	C31	C32	N1	177.0(4)
C40	C25	C32	C31	-0.1(7)
C40	C25	C32	N1	-178.0(5)

Table A9 continued.

C30	N1	C32	C31	135.3(4)
Rh2	N1	C32	C31	-42.0(5)
C30	N1	C32	C25	-46.8(6)
Rh2	N1	C32	C25	135.9(4)
C34	N6	C33	C28	-1.7(5)
Rh1	N6	C33	C28	176.6(3)
C34	N6	C33	C21	178.7(3)
Rh1	N6	C33	C21	-3.0(4)
C12	C28	C33	N6	0.4(6)
C4	C28	C33	N6	179.9(4)
C12	C28	C33	C21	180.0(4)
C4	C28	C33	C21	-0.5(6)
N5	C21	C33	N6	1.4(5)
C16	C21	C33	N6	179.6(3)
N5	C21	C33	C28	-178.2(3)
C16	C21	C33	C28	0.0(6)
C33	N6	C34	C19	2.3(5)
Rh1	N6	C34	C19	-175.6(3)
C12	C19	C34	N6	-1.7(6)
C38	C11	C35	C13	0.1(9)
C36	C13	C35	C11	-0.2(7)
N2	C13	C35	C11	-178.6(4)
C35	C13	C36	C37	0.1(8)
N2	C13	C36	C37	178.6(5)
C13	C36	C37	C38	0.0(9)
C35	C11	C38	C37	0.0(9)
C35	C11	C38	C39	179.0(5)
C36	C37	C38	C11	-0.1(9)
C36	C37	C38	C39	-179.1(6)
C29	C24	C40	C25	-0.8(9)
C41	C24	C40	C25	179.4(5)
C32	C25	C40	C24	1.0(9)
C10	C1	C43	C8	-1.2(7)
C42	C1	C43	C8	178.5(5)
C27	C8	C43	C1	2.0(7)
C18	C20	C44	C45	1.0(8)
C22	C9	C45	C44	-1.9(8)
C22	C9	C45	C46	178.7(5)

Table A9 continued.

C20	C44	C45	C9	1.3(8)
C20	C44	C45	C46	-179.3(5)
C28	C4	C52	C16	-0.1(8)
C21	C16	C52	C4	-0.3(7)
C7	C16	C52	C4	177.9(5)
C53	C54	O1	C56	175(3)
O3	C54	O1	C56	4(3)
C57	C56	O1	C54	-174(4)

Table A10. Crystal data and structure refinement for $[Rh_2(DTolF)_2(phen)_2(H_2O)][BF_4]_2$ (10).

Identification code	$[Rh_2(DTolF)_2(phen)_2(H_2O)][BF_4]_2$
Empirical formula	C54 H50 B2 F8 N10 Rh2
Formula weight	1132.41 g/mol
Temperature	293(2) K
Wavelength	0.71073 Å
Crystal system	orthorhombic
Space group	$P2_12_12$
Unit cell dimensions	a = 19.6939(3) Å
	b = 38.7660(1) Å
	c = 13.7938(2) Å
	$\alpha = 90^\circ$
	$\beta = 90^\circ$
	$\gamma = 90^\circ$
Volume	10530.8(2) $Å^3$
Z	8
ρ_{calc}	1.429 g/cm^3

Table A10 continued.

μ	0.696 cm^{-3}
F(000)	na
Crystal size	0.26 x 0.21 x 0.10 mm^3
Theta range for data collection	na
Index ranges	na
Reflections collected	23860
Independent reflections	9028 [R(int) = 0.1624]
Refinement method	na
Data / restraints / parameters	na
Goodness-of-fit on F^2	na
Final R indices [$I>2\sigma(I)$]	na
R indices (all data)	na
Largest diff. peak and hole	na


MICHIGAN STATE UNIVERSITY LIBRARIES
3 1293 02112 6457